To the Graduate Council:

I am submitting herewith a thesis written by Sean Justin Coffelt entitled "Stability Analysis of Single and Double Steel Girders during Construction." I have examined the final electronic copy of this thesis for form and content and recommend that it be accepted in partial fulfillment of the requirements for the degree of Master of Science with a major in Civil Engineering.

Qiuhong Zhao, Major Professor

We have read this thesis and recommend its acceptance:

Edwin G. Burdette

John Ma

Accepted for the Council:

Carolyn R. Hodges

Vice Provost and Dean of the Graduate School

Stability Analysis of Single and Double Steel Girders during Construction

A Thesis Presented for the

Master of Science Degree

The University of Tennessee, Knoxville

Sean Justin Coffelt

December 2010

ACKNOWLEDGEMENTS

I would like to thank my committee Dr. Zhao, Dr. Burdette, and Dr. Ma for teaching me so much throughout my time at UT and preparing me for whatever career is in my soon to be future. I am truly going to miss having classes with you. I have greatly improved my understanding of steel behavior through my research with my advisor Dr. Zhao. Thanks to her I have learned to use FEA software, became more familiar with AASHTO and AISC codes, and submitted papers reflecting our research findings. I would also like to thank Nancy Roberts for her advice and for having me as a TA throughout graduate school. And of course, much appreciation to my family and Heather for always supporting and being there for me.

ABSTRACT

Built-up steel I-girders are very commonly used in bridge construction. Their spans are typically very long, and they are susceptible to lateral torsional buckling if not enough lateral support is provided. This thesis includes guidelines for preventing lateral torsional buckling of steel I-girders under dead and wind load, accompanied with finite element analysis of double girder systems. The first portion includes capacity envelopes for single girders with single and double symmetric cross sections under various loading conditions and boundary conditions for double and single symmetric cross sections with double girders subjected to dead loads only. The second portion is dedicated to finite element analysis of double girders. Buckling analyses have been conducted on single symmetric double girders to verify their capacity equations and investigate the behavior of double girders subjected to wind load. The analyses focus on the weak axis bending of the double girder system as a whole and an evaluation of whether buckling of cross-bracing is an issue when lateral loads are present.

TABLE OF CONTENTS

LIST OF TABLES

LIST OF FIGURES

CHAPTER I: INTRODUCTION

Built-up steel I-girders have been used in bridge construction for decades. Bridge girders typically a long span and therefore are prone to instability when there is not enough lateral support for the compression flanges. Generally, the top girder flange is connected to the concrete deck. The finished deck provides continuous bracing throughout the span, which prevents lateral torsional buckling. During construction, however, the girders are at very high risk of buckling under their self-weight, wind, construction loading, etc. when the deck has not hardened or been attached.

In October 2002, the Marcy Pedestrian Bridge in Marcy, NY collapsed during construction and resulted in a fatality and several injuries. The bridge consisted of a U-shaped 'tub' girder with 8 evenly spaced internal k-frames that spanned approximately 170 feet. The concrete bridge deck was being poured at the time of collapse. The pouring began at the end of the span and moved inward. When the pouring reached the girder's midspan, a global buckling failure was observed and the girder twisted off of its abutments and fell to the ground.

Several techniques can be used by erectors to increase the girder's lateral torsional buckling capacity during construction (i.e. before the deck is in place and hardened). One common technique is to add temporary supports (falsework) until the system is able to support itself. Another common technique is to brace parallel girders to one another at points along their span. This increases the girders' resistance to lateral torsional buckling, and theoretically, the two girders are now acting as one equivalent girder with an effective flange width equal to the girder center-to-center spacing (1). Research has been conducted on single girder systems to determine their stability during erection, but very little research has been conducted on double girder systems and the main factors that affect their lateral torsional buckling capacity. The number of cross-bracings makes a contribution to the overall capacity of the system. The cross-bracings play an important role because they transfer forces from one girder to another and provide top flange stability. If there are too few cross-braced points, the length of the unbraced top flange will be too large and buckling may occur.

The number of cross-braced points may be even more critical for single symmetric girders. Single symmetric girders are commonly used in bridge design and can be very economical. They can decrease material cost as well as the self-weight of the structure. Typically, the bottom flange will be larger because it provides the necessary tension forces caused by positive bending. When the deck is hardened and completed, it will be permanently joined to the top flange, and they will act together in bending, creating less need for a large top flange. Before the deck is completed during construction, the smaller top flange may be more susceptible to lateral torsional buckling because it is the main contributor to lateral torsional buckling capacity in positive bending. This decrease in lateral torsional buckling capacity may indicate that a simply supported system will require more cross-braces throughout its span to achieve stability. On the other hand, a cantilever system will have negative bending which relies on the bottom flange for lateral torsional buckling capacity. Because the bottom flange is larger than the top, lateral torsional buckling will be less likely to occur. This case may require fewer cross-braced points throughout its span to achieve stability.

The spacing between the girders plays an important role. If the spacing is small, the effective flange width will also be small which could mean that they may be more inclined to act as one and achieve stability. Also, in double girder systems with smaller girder spacing, the cross-braces are shorter with greater stiffness than the ones in systems with larger spacing and identical cross section, which means that there is less risk of the bracebuckling when transverse forces become large. If the girder spacing becomes large, the effective flange width will be much greater than the width of a single girder. This should give a higher system capacity in comparison to smaller spacing assuming that the longer braces provide adequate support. Because of the larger distance between girders, the braces will be longer and have less stiffness in relation to shorter spacing. This may decrease the bracing's effectiveness to transfer loading between the girders if the transverse forces become large enough to cause buckling of the bracing.

Another questionable topic about double girder stability is directed toward wind loading. Would the wind load add to the instability of the double girder system? When gravity loading is the only influence on the system, the cross-braces provide flange stability that increases lateral torsional buckling capacity. Because the gravity load acts perpendicular to the brace orientation a great amount of force is not transmitted to the adjoined girders. With the addition of wind load, the cross-braces are the only means for transferring horizontal forces from the windward girder to the leeward girder and may have a greater influence on the overall capacity of the system. In this case, more braces may be required or the braces may need additional stiffness to counteract the increase of force being transferred.

CHAPTER II: LITERATURE REVIEW

The literature for the topic at hand is quite limited because of its specificity. This paper addresses the lateral torsional buckling capacity of single symmetric girders, as well as the influence of wind on girder systems. There are literally no previous works (that the author has found) that explain in full the influence that the biaxial bending will have on the girder systems. Due to the lack of specific literature, several different papers on the individual topics have been selected to build a greater understanding of what the expected results should be and how the models should be analyzed.

When examining literature on the lateral torsional buckling of single symmetric girders, many of the papers on this topic are written by European researchers. Eurocode 3 has incorporated variables into their lateral torsional buckling equation that are specific to single symmetric cross sections (2). These variables include the 'measure of monosymmetry' (β_f), and the monosymmetry parameter (r_z). The measure of monosymmetry is the proportion of the weak axis moment of inertia of the compression flange to the total weak axis moment of inertia of both tension and compression flanges and ranges from 0 to 1. Roberts and Burt (3) and Wang and Kitipornchai (4) performed extensive buckling analyses to confirm elastic lateral torsional buckling formula and determine the influence of the measure of monosymmetry. It was proven that a β_f value approaching 1 would mean that lateral torsional buckling is highly unlikely. Roberts and Narayanan (5) tested small scale models of single symmetric beams and concluded that, for all cases, the ultimate limit state design curves are conservative in comparison to test results.

As for the American Association of State and Highway Transportation Officials (AASHTO) (6) and the American Institute of Steel Construction (AISC) (7) elastic lateral torsional buckling equations, the effective radius of gyration for lateral torsional buckling (r_t) incorporates the size of the compression flange and approximately one third of the web to the elastic lateral torsional buckling equation. When comparing critical buckling stresses found using Eurocode 3 (2) and AASHTO (6), every single symmetric and double symmetric cross section examined showed AASHTO (6) to be more conservative, especially for cases with high measures of monosymmetry

After the Marcy Bridge collapse, Yura published a paper addressing the "no buckling" concept when $I_y>I_x$. The Marcy Bridge consisted of a tub girder with a "U" shape section that had $I_y>I_x$. Theoretically, lateral torsional buckling will only happen if the loading is about the strong primary axis. Weak axis loading will typically result in the yielding of the material before buckling behavior can be observed. For the Marcy Bridge, loading was due to gravity and bent the girder about the "weaker" I_x axis which should fail due to yielding the cross section before buckling can occur. This was not the case; the girder buckled due to an increase of load from the concrete pour for the deck. This section had an I_y/I_x value of 1.75. Therefore, lateral torsional buckling was not believed to be a concern and the girder was designed to hold the applied dead and service loads. Although the failed girder was a "U" shape girder, it is comparable to a double I girder system with continuous bottom flange bracing (8). When a double I girder system displaces laterally, the cross frames provide no out-of-plane rigidity (Vierendeel action) because of their size and end connections (considered pinned) (9). This means that the girders do not act as a rigid system, and each girder will bend individually while sharing applied load. The out-of-plane moment of inertia for the double girder system is $2I_{yo}$ where the subscript, o, denotes the property from a single girder. This means that for this case $I_y < I_x$ and global buckling should be considered (8).

Soon after, Yura published another paper in which a method was developed for determining the global lateral buckling capacity of multigirder systems interconnected by cross frames suitable for use in design specifications (1). For years the solution for lateral torsional buckling for a simply supported girder under uniform moment and bent about the strong axis, given as EQ. 1, was the primary way for determining the capacity of single girder systems (10).

$$M_o = \frac{\pi}{L_b}\sqrt{EI_yGJ + \frac{\pi^2E^2I_yC_w}{L_b^2}} \tag{1}$$

This is very useful for the single girders, but the common practice is to use cross-braces between girders during the erection process. Yura adjusted this equation and developed it to calculate the buckling capacity of multiple girder systems. This equation was then further simplified by combining the dominant parameters to give an equation that is directly proportional to the spacing of the girder system (EQ. 2). When compared to finite element analysis (FEA) results and EQ. 1, EQ. 2 was on average, 1.2% conservative (1). Zhao et al. (10) confirmed extended EQ. 2 through buckling analyses of simply supported and cantilever double symmetric double girders.

$$M_{gs} = \mathrm{C_b}\,\frac{\pi^2 sE}{L_g^2}\sqrt{I_yI_x} \tag{2}$$

Determining the importance of the cross frame stiffness was the next task. This was done by examining the same simply supported girder system with three equally spaced cross frames and varying the stiffnesses of the cross frames. The results show that very small sections used for cross frames can achieve close to (if not the maximum) stiffness required. It was also noted that an increase in cross frame stiffness is more apparent in girder systems with larger spacings. The number of cross frames used was also under investigation. The same double girder section was used with 3, 4, and 5 equally spaced cross frames and the moment capacity was found by FEA. Graphically the three systems were nearly identical, which leads to the conclusion that the addition of cross frames will not always increase capacity, and the double girder with 3 cross frames provided sufficient bracing (1).

From another study by Zhao et al., double girders were analyzed using FEA software ABAQUS to determine the effects of cross-braces and number of cross-braces required throughout the span to achieve enough bracing for the double girders under dead. Given girder spacings were analyzed with 2, 3, 4, and 9 braces throughout the span. It turned out that 3 or more braces provided over 90% of the theoretical capacity. Any additional bracing has very little strength contribution while 2 braces only provided between 70 and 85 percent of the theoretical capacity. This concluded that a minimum of 3 braces are required to provide adequate stability for double symmetric double girders subjected to dead load only (11).

Kozy described a twin I girder system being constructed and explained that it has adequate strength to resist lateral torsional buckling under construction loading and self-weight, but is susceptible to global buckling during the pouring of the concrete deck. Because the girders were already in place and the timber forms were on top of the girders, a simple cross bracing scheme was needed to increase the system capacity. He noted that AASHTO's specifications for lateral bracing are limited and implied that they are used for the purpose of resisting lateral loads when lateral bracing is vital to the prevention of buckling under vertical loads. He also argued that AISC gives requirements for strength and stiffness of bracing for developing buckling strength of the primary member but is limited in the fact that they are developed based on the unbraced length between braces in simple cases and with an effective length factor, K, equal to 1.0. No guidance is given for the cases where the bracing strength and/or stiffness requirements are not met. AASHTO describes that the most efficient method to increase lateral and torsional rigidity is to add bracing to the top and bottom flanges in the vicinity of the support locations. Because the timber forms were already in place on top of the girders, top bracing will be complicated. Because of this, a number of bracing schemes were analyzed with bottom only bracing to both top and bottom bracing until a scheme was found that minimizes the impact of the top flanges. He concluded that AISC's method of using 1% or 2% of the beam flange force to design the bracing members can be unconservative for the design of bracing for system buckling (12).

The papers discussed previously give insight on the processes for analyzing double girder systems under vertical loading, but there are also horizontal wind loads that apply in the following paper. Cheng (13) conducted research on the Lu Pu steel arch bridge in China that was in the construction phase; questions arose about the influence of wind loading. From their studies, it was found that the variation of wind pressures with height should be included in the calculations as these pressures had significant influence on the horizontal and vertical deflections of the bridge. The three components of wind load,: the drag force, lift force, and pitch moment, were compared to determine how each would contribute to the bridge response. It was concluded that the lift force and pitch moment had minimal influence on the deflections of the bridge when added to the drag force, implying that it will suffice to consider only the drag force for the analysis.

AASHTO LRFD bridge design specifications have guidelines for calculating wind pressures on structures. The procedures are not necessarily for computing erection loads, but give some insight into calculating wind pressures. Based on the height of the structure above ground, corresponding wind velocities are to be determined either by site-specific wind surveys, fastest-mile-of-wind charts available in ASCE 7-88 (14) or, with the absence of a better criterion, the assumption of 100 mph. A given wind velocity can be converted to a design wind pressure with the following equation:

$$P_D = P_B \left(\frac{V_{DZ}}{V_B}\right)^2 \qquad (3)$$

Here, P_B and V_B are the base wind pressure and velocity respectively. P_D is the design wind pressure and V_{DZ} is the wind velocity at design elevation Z (mph). The stagnation pressure associated with 100 mph wind is 25.6 psf, which is significantly less than the values given for design (50 psf for beams). This is because the design base pressure includes the effect of gusting combined with “some tradition of long-time usage” (6). Because the girders in question are in the erection stage and will not be exposed for a long period, the stagnation pressure was used for calculations.

CHAPTER III: SINGLE GIRDER CAPACITY EQUATIONS

AASHTO guidelines have been used as a basis for the girder dimensions and proportions for all calculations. Simply supported and cantilever girders were studied with web depths (D) between 40 and 96 inches, and flange widths (b) between 12 and 48 inches. Minimum web and flange thicknesses allowed were also used, as increasing the flange thickness will only increase capacity. Increasing web thickness will slightly decrease capacity from added self-weight, but for simplicity and practical reasons a minimum thickness of 0.5" is used because in practice it is more economical and web stiffeners can be utilized for increasing web strength. Additional requirements from AASHTO are as follows:

$b_f/2t_f \leq 12$ $\quad$ $t_f/t_w > 1.1$ $\quad$ $1.5 \leq D/b \leq 6$ $\quad$ $d/t_w < 150$ $\quad$ $0.1 \leq I_{yc}/I_{yt} \leq 10$

AASHTO gives a maximum D/b ratio of 6.0, while the lower D/b value of 1.5 was adopted as common practice and gives a wider spectrum of calculations. The first two requirements given above give limits used for minimum flange thicknesses to ensure local buckling will not be an issue. The last limits are in regard to single symmetric sections and their flange proportions. I_{yc} and I_{yt} are the moments of inertia of the compression and tension flanges about the weak axis respectively. AASHTO load combinations IV (1.5*Dead load) and III (1.25*Dead load + 1.4*Wind load) were used in calculations (6).

AASHTO EQ. 6.10.8.2.3-8 is the basis for all single girder elastic LTB calculations.

$$F_{cr} = \frac{C_b R_b \pi^2 E}{(\frac{L_b}{r_t})^2} \quad (4)$$

3.1 Double Symmetric Girders: Load Combo IV

When EQ. (4) is set equal to the maximum normal stress due to self-weight and solve for L, the maximum unbraced length for a single girder can be found (15) (calculations can be found in appendix).

$$L_{max}^{Simple} = \sqrt[4]{\frac{C_b R_b \pi^2 E r_t^2}{\frac{1.5 d w_d}{16 I_x}}} = 2 * \sqrt[4]{\frac{C_b R_b \pi^2 E r_t^2}{\frac{1.5 d w_d}{I_x}}} \quad (5)$$

$$L_{max}^{Cantilever} = \sqrt[4]{\frac{C_b R_b \pi^2 E r_t^2}{\frac{1.5 d w_d}{4 I_x}}} = \sqrt{2} \sqrt[4]{\frac{C_b R_b \pi^2 E r_t^2}{\frac{1.5 d w_d}{I_x}}} \quad (6)$$

When looking over the Lmax equations, it is noticeable that the r_t^2 (effective radius of gyration for LTB) term is one of the most dominant variables for LTB capacity. The rt equation is (6) : $r_t = \frac{b_{fc}}{\sqrt{12\left(1+\frac{1}{3}\frac{D_c t_w}{b_{fc} t_{fc}}\right)}}$ (7)

This shows the importance of the compression flange size when considering LTB. An increase in compression flange size will be accompanied with an increase in capacity.

3.1.1 Simply Supported Girders: Load Combo IV

Using EQ. (5) maximum unbraced lengths of simply supported girders were found by creating an excel spreadsheet that calculates all needed parameters. Web depths were held constant while changing flange widths, and vice versa. First plots were created that show L_{max} vs. D, then $(L/b)_{max}$ vs. D, and finally $(L/b)_{max}$ vs. D/b. The $(L/b)_{max}$ vs. D/b plot is shown below with corresponding envelope equations. The other plots for simply supported double symmetric sections under dead load only can be found in Appendix A.

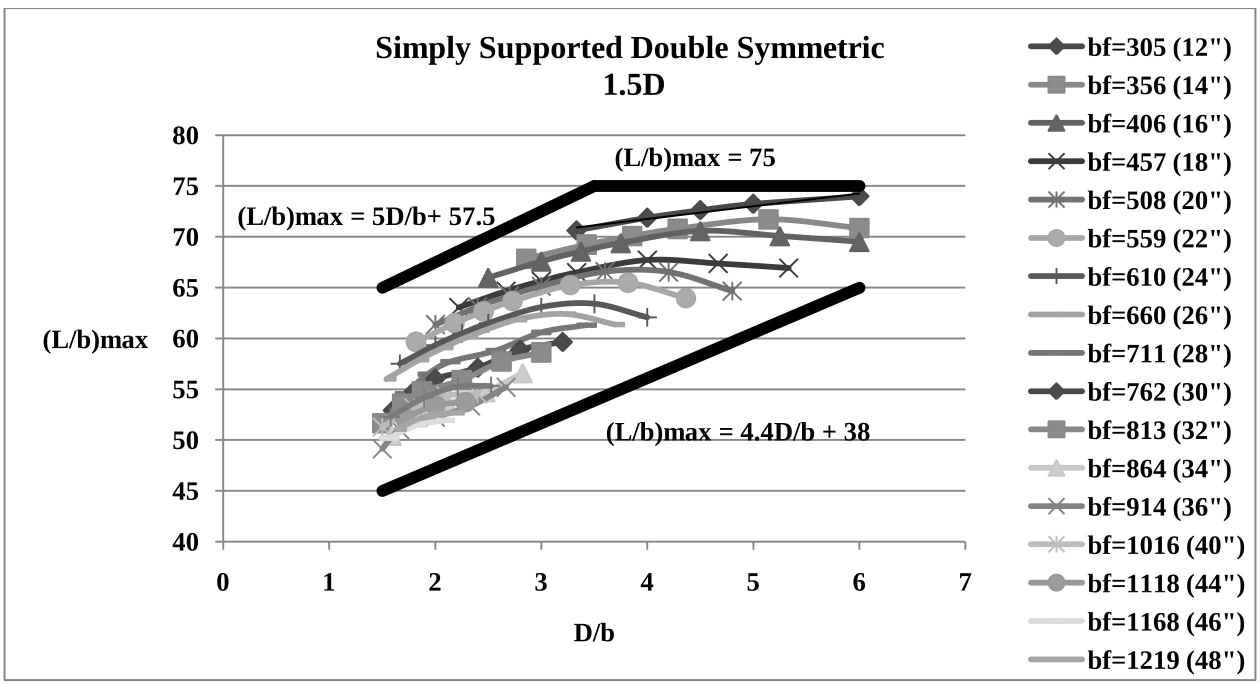

Figure 1 L/b vs. D/b for simply supported double symmetric girders (load combo IV)

In Figure 1, flange widths are held constant while the web depths are varied. While sections with larger flanges may have a higher capacity, the sections with smaller flanges form the upper bound because they give a higher L/b ratio. The lower bound equation gives the maximum (L/b)max that will be safe during erection and will not require any falsework to achieve stability. Anything between the upper and lower bounds is in a gray area and may or may not need temporary support. If an L/b ratio exceeds the upper limit it will be unstable.

3.1.2 Cantilever Girders: Load Combo IV

The $(L/b)_{max}$ vs. D/b are shown below with their corresponding envelope equations. The other plots for cantilever double symmetric sections under dead load only can be found in Appendix A.

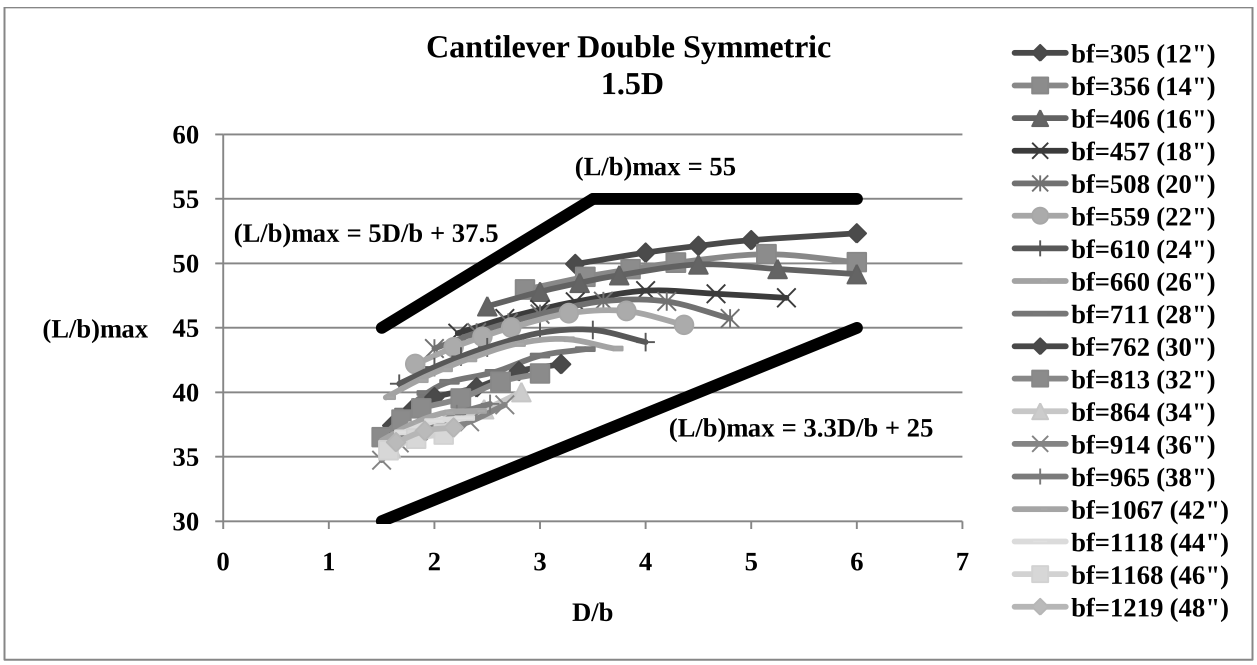

Figure 2 L/b vs. D/b for cantilever double symmetric girders (load combo IV)

The cantilever sections follow the same trend as the simply supported sections, but have a slightly lower capacity.

3.2 Double Symmetric Girders: Load Combo III

Load combo III combines wind loading with gravity loading (1.25D + 1.4W). The biaxial bending creates an additional stress in the compression flange which in turn will further decrease capacity. For a girder under both horizontal wind loads and self-weight, AASHTO/LRFD requires (6):

$$f_{bu} + \frac{1}{3} f_l \leq \phi \, F_{cr} \qquad \phi = 1.0 \tag{8}$$

Where f_{bu} is the flange stress due to dead load and f_l corresponds to the flange lateral bending stress. When these stresses are substituted for F_{cr} and the equation is solved for L, the maximum unbraced length for a single girder under dead load and wind is:

$$L_{max}^{Simple} = \sqrt[4]{\frac{C_b R_b \pi^2 E r_t^2}{\frac{1.25 d w_d}{16 I_x} + \frac{1}{3}\frac{1.4 b w_w}{16 I_y}}} = 2 * \sqrt[4]{\frac{C_b R_b \pi^2 E r_t^2}{\frac{1.25 d w_d}{I_x} + \frac{1}{3}\frac{1.4 b w_w}{I_y}}} \tag{9}$$

$$L_{max}^{Cantilever} = \sqrt[4]{\frac{C_b R_b \pi^2 E r_t^2}{\frac{1.25 d w_d}{4 I_x} + \frac{1}{3}\frac{1.4 b w_w}{4 I_y}}} = \sqrt{2} \sqrt[4]{\frac{C_b R_b \pi^2 E r_t^2}{\frac{1.25 d w_d}{I_x} + \frac{1}{3}\frac{1.4 b w_w}{I_y}}} \tag{10}$$

3.2.1 Simply Supported Girders: Load Combo III

Using EQ. (9) to find the maximum unbraced lengths for all of the girder cross sections, .plots were created that show $(L/b)_{max}$ vs. D, and $(L/b)_{max}$ vs. D/b. The $(L/b)_{max}$ vs. D/b plot for a simply supported girder subjected to a wind velocity of 45 mph is shown below along with the $(L/b)_{max}$ envelopes. All other plots for simply supported double symmetric girders subjected to dead load and wind can be found in Appendix A.

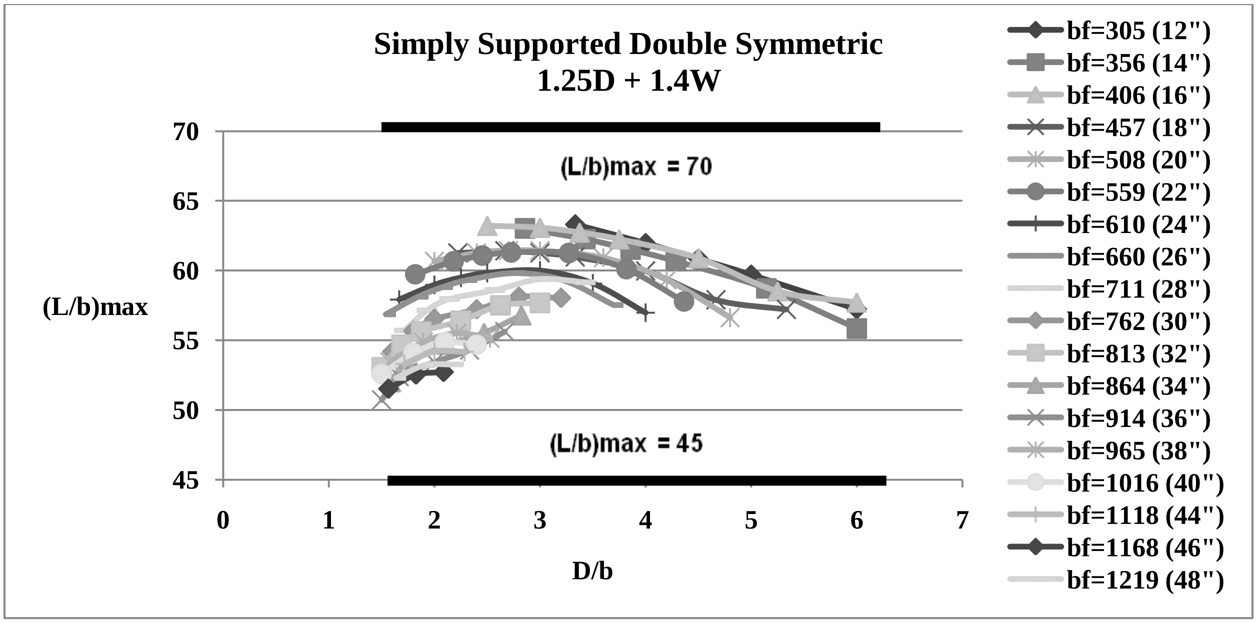

Figure 3 L/b vs. D/b for simply supported double symmetric girders (load combo III)

The addition of wind loading gives a completely different L/b vs. D/b trend than before with dead loading only. This shows that the girders with the smaller flange widths still form the upper bound, but when the D/b ratio exceeds a ratio of 3, there is a steady decline in L/b capacity. This is because as the web depth increases, so do the lateral forces due to wind loading. The sections with the smallest flange widths have a continuous decrease in L/b capacity as the web depth increases, while the larger flanges have an increase in L/b capacity to a certain point before they begin to decline due to the increase of lateral load.

3.2.2 Cantilever Girders: Load Combo III

Using EQ. 10 to find the maximum unbraced lengths for all of the girder cross sections, .plots were created that show $(L/b)_{max}$ vs. D, and $(L/b)_{max}$ vs. D/b. The $(L/b)_{max}$ vs. D/b plot for a cantilever girder subjected to a wind velocity of 45 mph is shown below along with the $(L/b)_{max}$ envelopes. All other plots for cantilever double symmetric sections subjected to dead load and wind can be found in Appendix A.

The cantilever sections show the same trend as before with the simply supported sections.

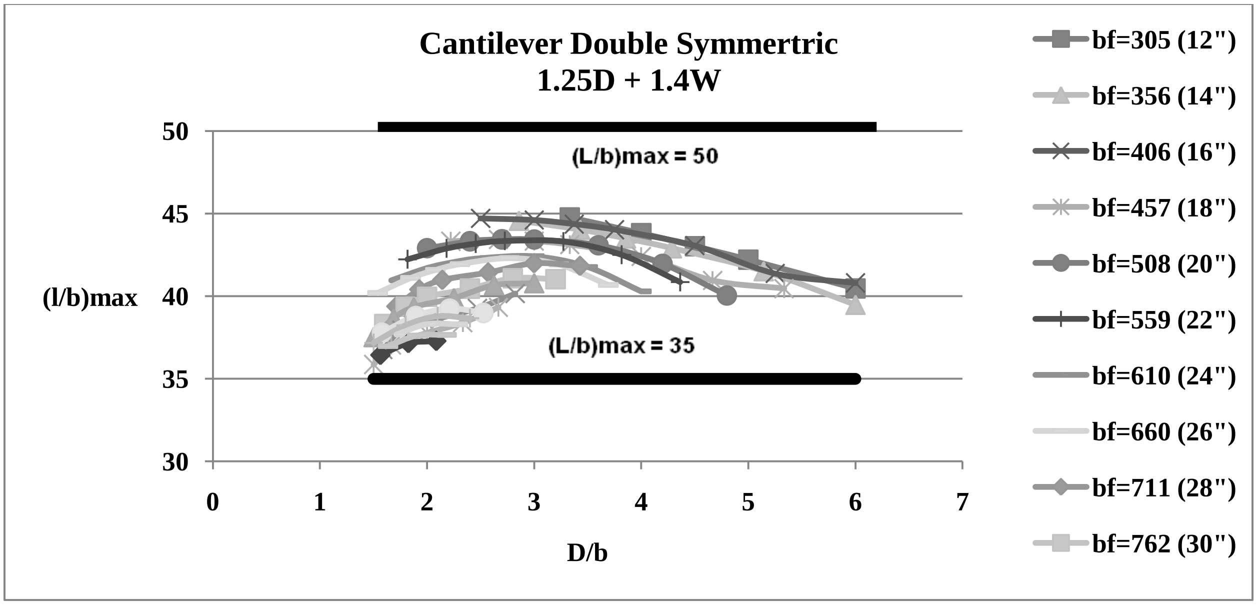

Figure 4 L/b vs. D/b for cantilever double symmetric girders (load combo III)

3.3 Single Symmetric Girders: Load Combo IV

When examining the single symmetric sections, both simply supported and cantilever girders have the smaller flange on top and larger flange on the bottom. This approach in bridge design has been shown to save money by reducing the cost of materials and can reduce the self-weight of the structure. The same capacity equations were used for the single symmetric sections as before with the double symmetric sections in EQs. 5, 6, 9, and 10. Once again, the capacities will rely heavily on the r_t^2 term which emphasizes the size of the compression flange.

The maximum unbraced lengths for the single symmetric sections were found by selecting different tension flange sizes and varying the compression flange from the smallest allowable size until it reaches the size of the tension flange. These flange proportions were governed by AASHTO's flange restrictions $0.1 \leq I_{yc}/I_{yt} \leq 10$, and also maintain a D/b ratio between 1.5 and 6. The flange sizes for single symmetric sections are summarized in Table 1.

Table 1 Single symmetric flange sizes

	Flange Width (inches)	
Boundary Condition	**Top Flange**	**Bottom Flange**
Simply Supported	12 to 24	24
	20 to 36	36
	28 to 48	48
Cantilever	12	12 to 20
	18	18 to 30
	24	24 to 42
	30	30 to 48
	40	40 to 48

3.3.1 Simply Supported Single Symmetric Girders: Load Combo IV

Using EQ. 5 and the cross sections given in Table 1, the maximum unbraced lengths were found for simply supported girders under dead load only. In Figure 5 below, an example is shown for simply supported single symmetric girders. For this particular case web depths were varied from 40” to 96” and the top (compression) flange is varied from 14” to 24”. The bottom (tension) flange is held constant at 24”. The L/b and D/b values correspond to the top (compression) flange size, and show a gradual increase in L/b capacity as the flange becomes smaller. The bold curve shown denotes the capacity for a double symmetric girder with flanges of 24” and various web depths. It forms the lower bound for the single symmetric sections. Even though these L/b capacities show a gradual increase, the actual capacity of the single symmetric sections will be smaller than the double symmetric case because of their smaller compression flange size

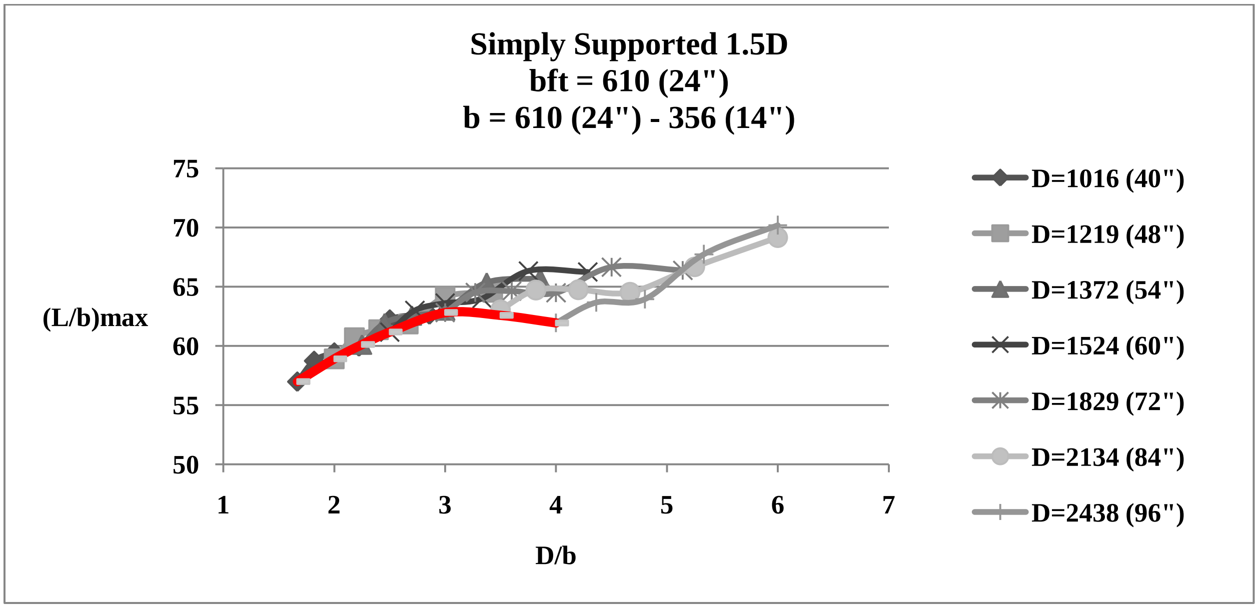

Figure 5 L/b vs. D/b example for simply supported double symmetric girders (load combo IV)

Figure 6 shows the L/b capacities for all of the single symmetric simply supported girders. The envelope equations are the same as before with the double symmetric simply supported girders. Other graphs for simply supported single symmetric girders under dead load only can be found in Appendix B.

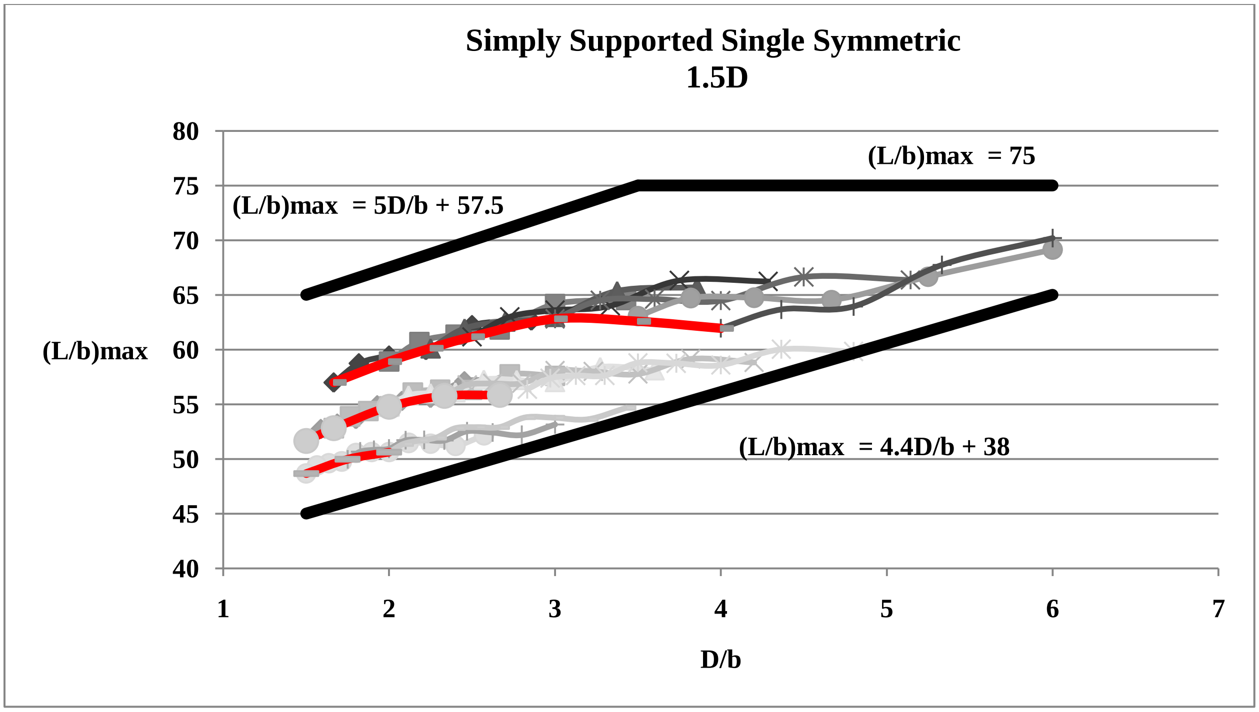

Figure 6 L/b vs. D/b for simply supported single symmetric girders (load combo IV)

3.3.2 Cantilever Single Symmetric Girders: Load Combo IV

Using EQ. 6 and the cross sections given in Table 1, the maximum unbraced lengths were found for single symmetric cantilever girders under dead load only. In Figure 7 below, an example is shown for cantilever single symmetric girders. In this case, the bottom (compression) flange is varied from 24” to 42”. The top (tension) flange is held constant at 24”. The bold red curve shown denotes the capacity for a double symmetric girder with flanges of 24” and various web depths. It forms the upper bound for the single symmetric sections. Even though the L/b capacities for the single symmetric cantilever are less than the double symmetric case shown, their actual capacity for unbraced length will be larger because of the increased bottom (compression) flange size.

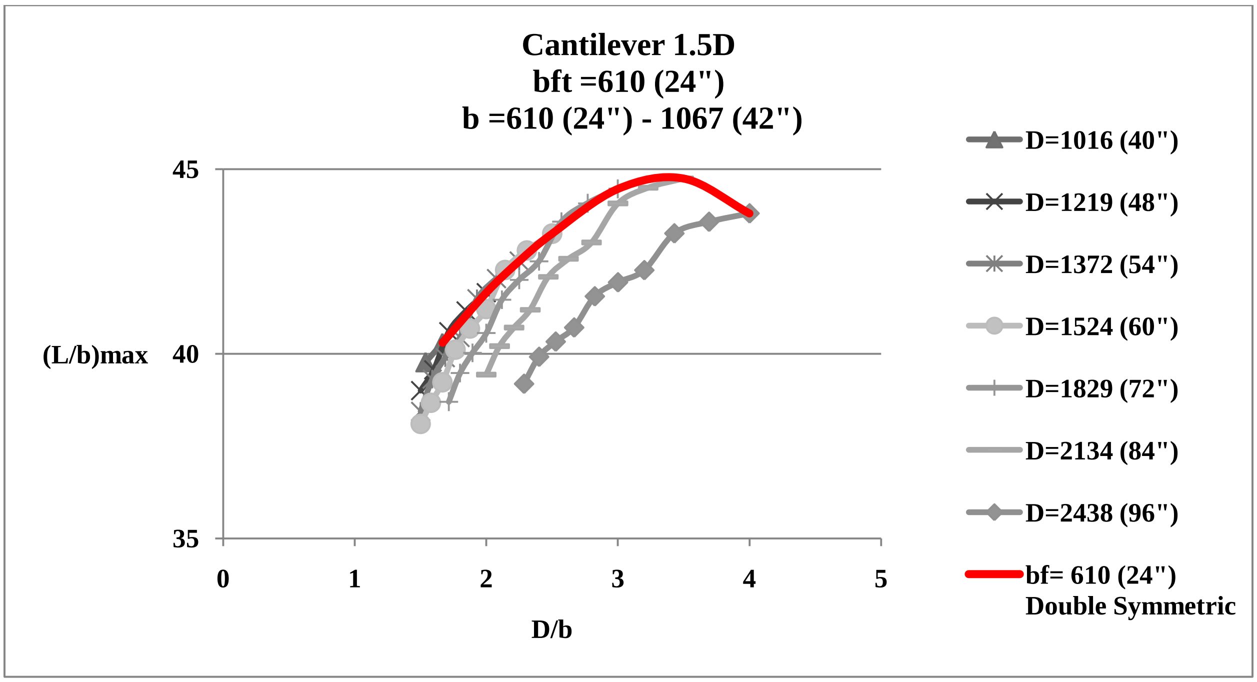

Figure 7 L/b vs. D/b example for cantilever single symmetric girders (load combo IV)

Figure 8 shows the L/b capacities for all of the single symmetric cantilever girders. The envelope equations are the same as before with the double symmetric cantilever girders. All other graphs for cantilever single symmetric girders under dead load only can be found in Appendix B.

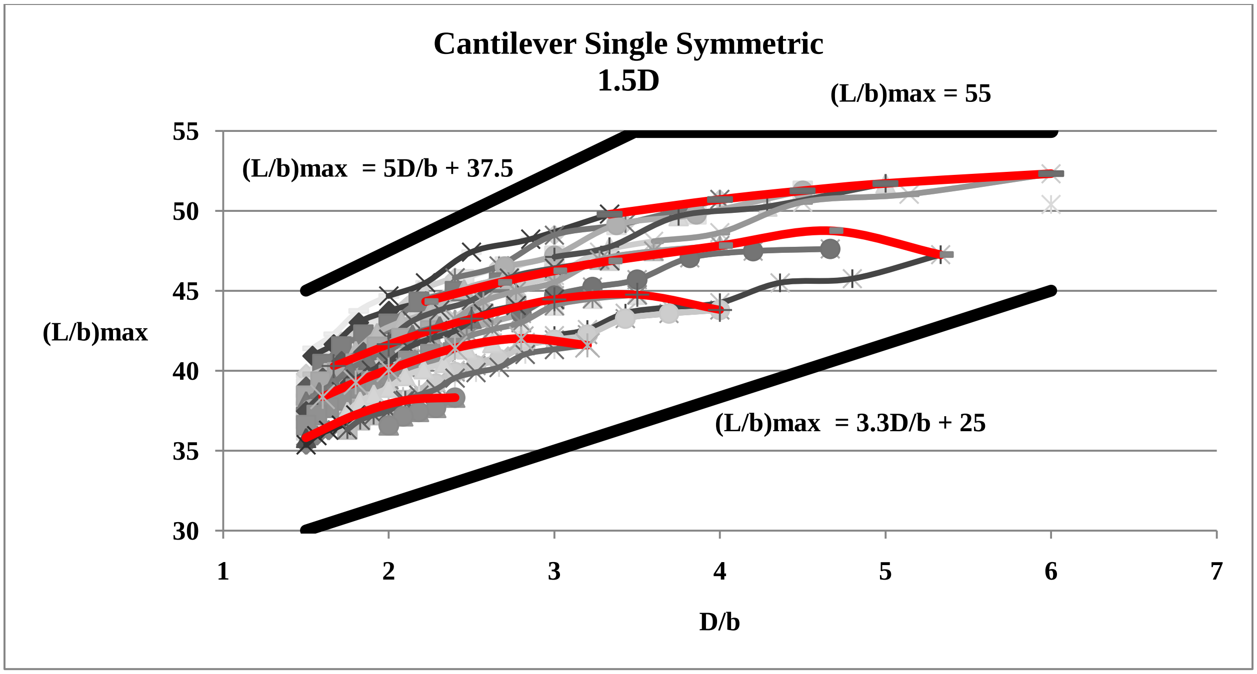

Figure 8 L/b vs. D/b for cantilever single symmetric girders (load combo IV)

3.4 Single Symmetric Girders: Load Combo III

Capacity EQs. 9 and 10 were also used for the single symmetric sections under dead load and wind. The same cross sections were used as before with Load Combo IV. A wind velocity of 45 mph was used for all plots.

3.4.1 Simply Supported Single Symmetric Girders: Load Combo III

As seen before with Load Combo IV, the double symmetric sections, denoted by the red curves, form the lower bounds for the single symmetric sections with the same size tension flange. The same upper and lower bounds as before with the double symmetric simply supported sections apply for the single symmetric sections under dead and wind load. All other plots for single symmetric simply supported girders under dead and wind load are found in Appendix B.

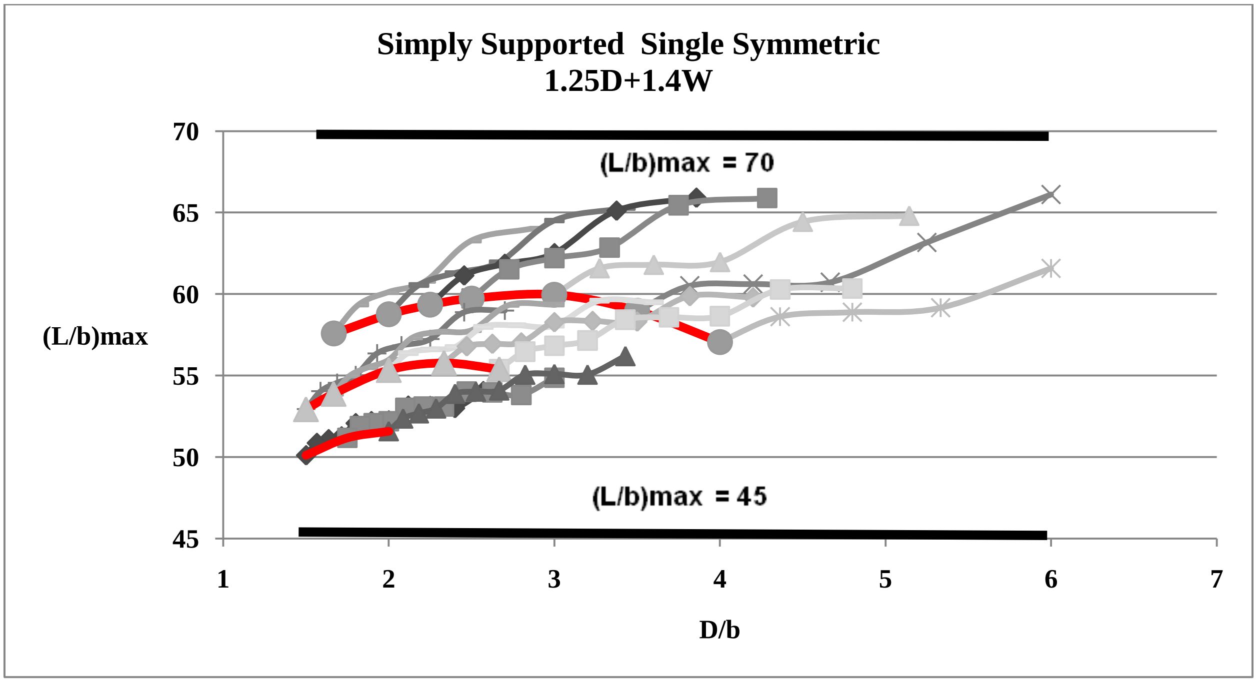

Figure 9 L/b vs. D/b for simply supported single symmetric girders (load combo III)

3.4.2 Cantilever Single Symmetric Girders: Load Combo III

The same trend as before with Load Combo IV is observed below in Figure 10. The double symmetric cantilevers form the upper bound for the single symmetric cantilevers with the same size tension flange. The upper and lower bound envelopes shown for the single symmetric cantilevers are the same as the double symmetric cantilevers. All other plots for single symmetric cantilevers under dead and wind load can be found in Appendix B.

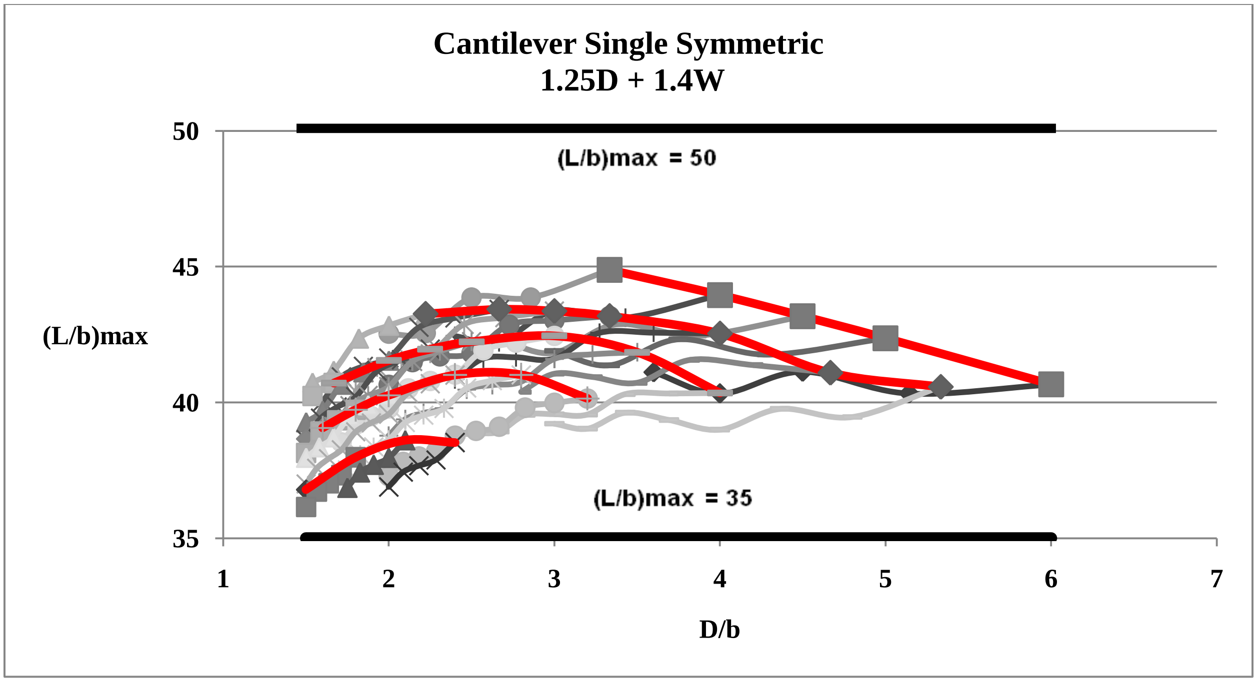

Figure 10 L/b vs. D/b for cantilever single symmetric girders (load combo III)

CHAPTER IV: DOUBLE GIRDER CAPACITY EQUATIONS

4.1 Double Symmetric Double Girders: Load Combo IV

By modifying Yura's equation (EQ. 2) for the global buckling capacity of a double girder system, the maximum unbraced length can be found (1). The equations for maximum unbraced length of a simply supported and cantilever double girder system are shown below as EQs. 11 and 12 respectively. In EQs. 11 and 12, Ix and Iy denote the strong and weak axis moment of inertia of a single girder, 's' is the center to center spacing between the girders, and the $1.5w_d$ corresponds to using AASHTO's Load Combo IV (6) where w_d is the total uniform distributed load from the self-weight of the double girder system. The Cb value used for simply supported girders was 1.12. Cantilever girders had a Cb value of 2.04 with a multiplier of 1.37 from previous parametric studies by Zhao et. al(16) making the effective Cb value 2.79.

$$L_{max}^{Simple} = \sqrt[4]{\frac{8C_b\pi^2 sE}{1.5w_d}\sqrt{I_x I_y}} \tag{11}$$

$$L_{max}^{Cantilever} = \sqrt[4]{\frac{2C_b\pi^2 sE}{1.5w_d}\sqrt{I_x I_y}} \tag{12}$$

For analyzing the double girder systems, an equivalent flange width 's' is used which represents the spacing between the girders in the horizontal direction from y-axis to y-axis. The spacings used in calculations were 72, 96, 120, 144, and 168 inches. The cross sections of the girders used are the same as before with single girders and followed the same flange and web proportion guidelines given by AASHTO (6).

(L/b)max vs D/b plots have been developed to show the relationship between the flange size and capacity. (L/s)max vs. D/s plots have also been developed to show the relationship between the equivalent flange width 's' and capacity.

4.1.1 Simply Supported Double Symmetric Double Girders: Load Combo IV

To develop (L/s)max vs D/s plots, girder depths are held constant while flange widths and the spacing 's' between the girders are varied. Figure 11 below corresponds to a double girder system with web depth of 60" and flange sizes shown on the legend of the plot. It is observed that the larger flange widths correspond to a higher (L/s)max value. An increase in girder spacing will increase the system capacity, but from Figure 11 it is noticed that (L/s)max values have an opposite tendency.

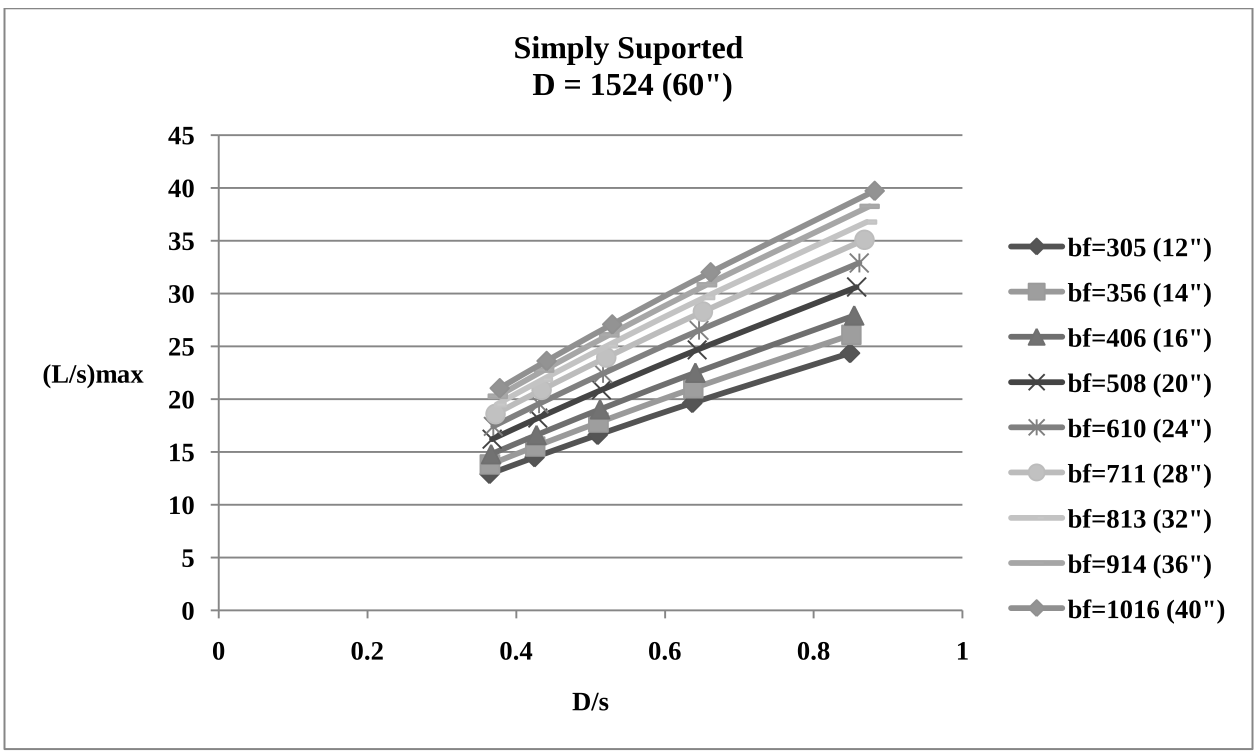

Figure 11 (L/s)max vs. D/s example of simply supported double girders (load combo IV)

(L/s)max plots for all cross sections and spacings for simply supported double girders have been condensed below into Figure 12. The corresponding lower and upper bound capacity envelope equations are also shown. All other plots for simply supported double girders can be found in Appendix C.

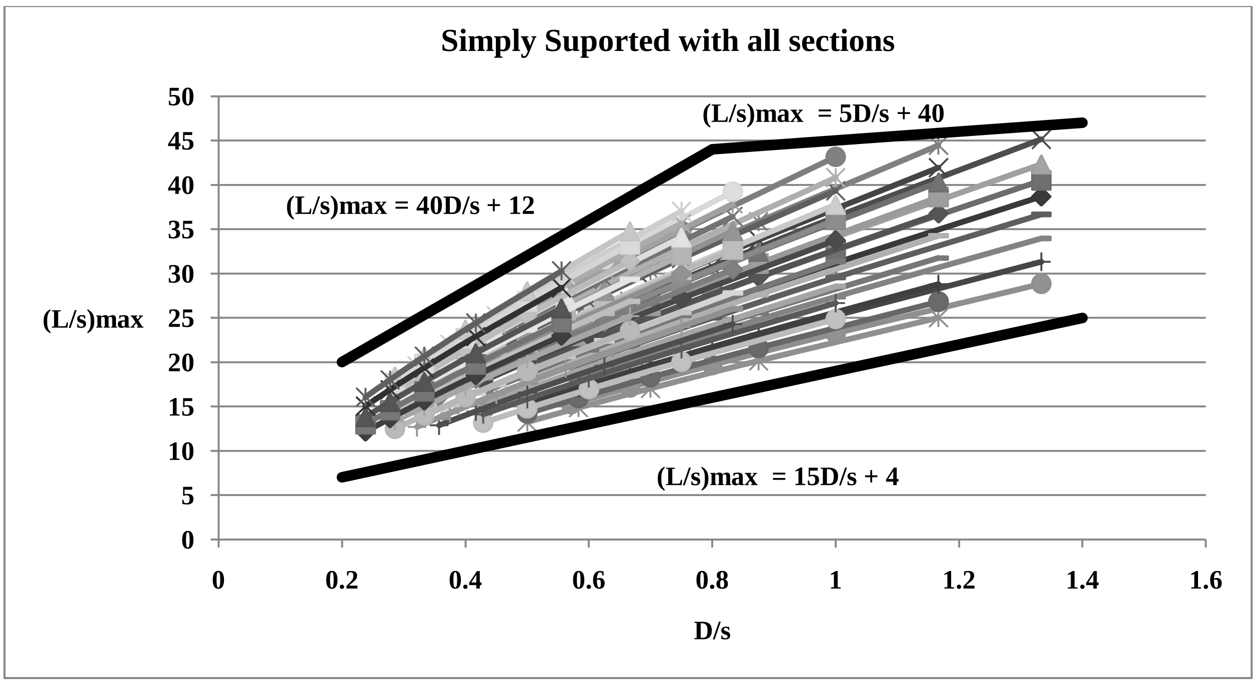

Figure 12 (L/s)max vs. D/s for simply supported double girders (load combo IV)

To further examine the behavior of simply supported double girder systems, (L/b)max vs. D/b plots have been developed. The girder spacings are held constant while the web depths and flange widths are varied. Figure 13 shows the (L/b)max capacities for simply supported double girders that have a spacing 's' of 96".

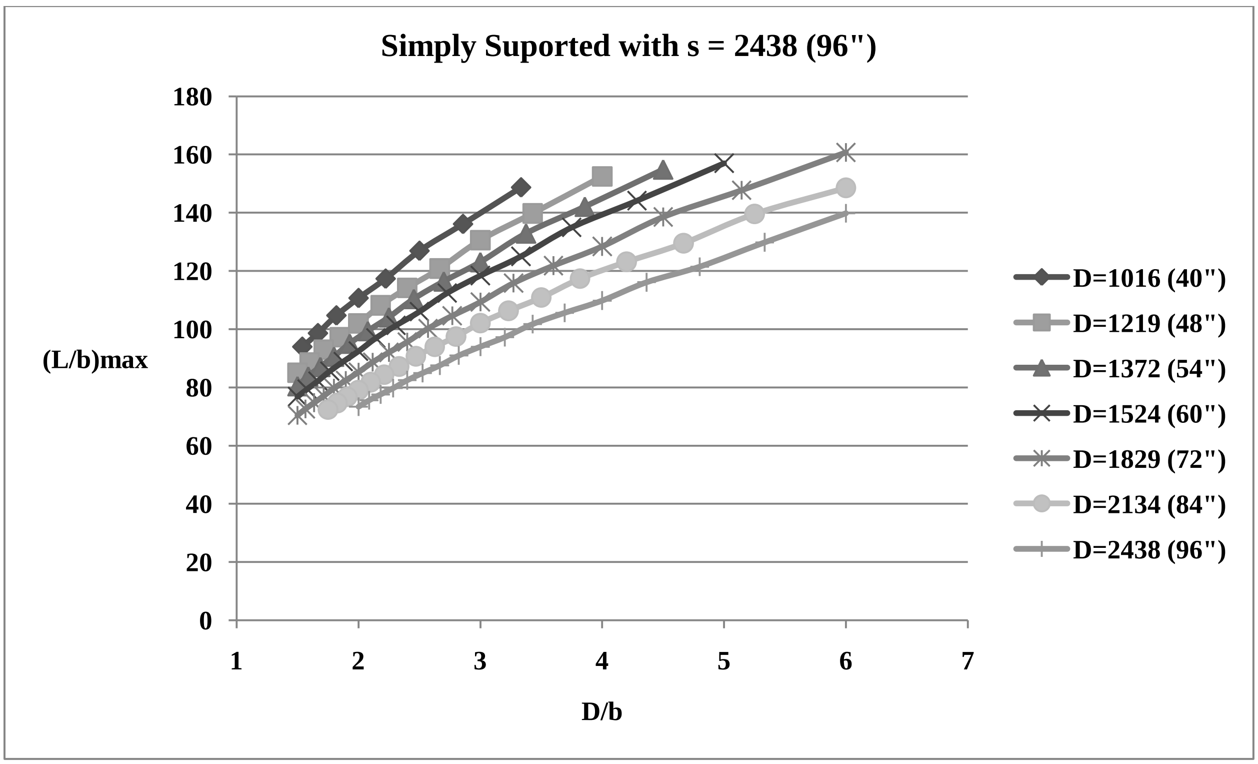

Figure 13 (L/b)max vs. D/b example for simply supported double girders (load combo IV)

All simply supported double girder (L/b)max plots have been condensed below into Figure 14, which shows the corresponding capacity envelope equations. All other plots for simply supported double girders can be found in Appendix C.

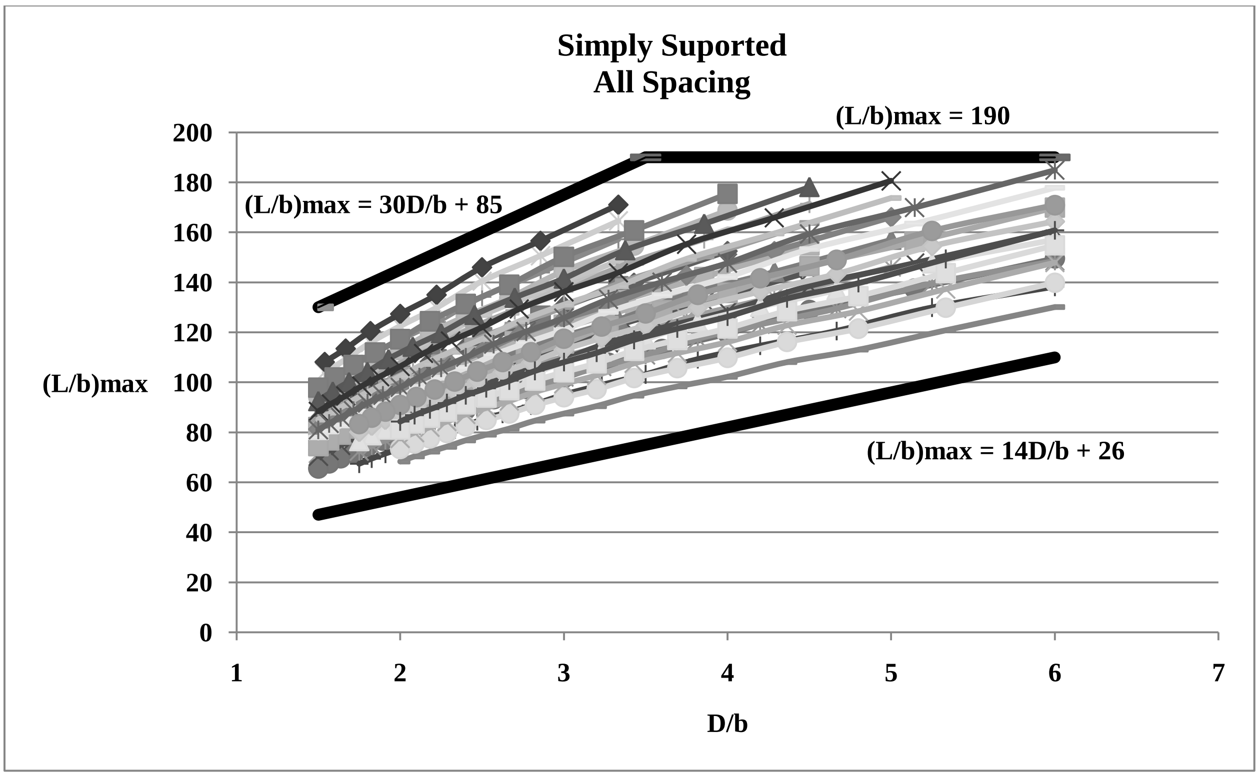

Figure 14 (L/b)max vs. D/b for simply supported double girders (load combo IV)

4.1.2 Cantilever Double Symmetric Double Girders: Load Combo IV

Using EQ. 12 to find the maximum unbraced length of a cantilever double girder system, (L/s)max and (L/b)max plots have been developed. The same procedure has been used as before with simply supported double girders. Figure 15 below shows the combination of all (L/s)max plots for cantilever double girder systems under dead load only. Lower and upper bound capacity equations are also shown. All other plots for cantilever double girder systems can be found in Appendix C.

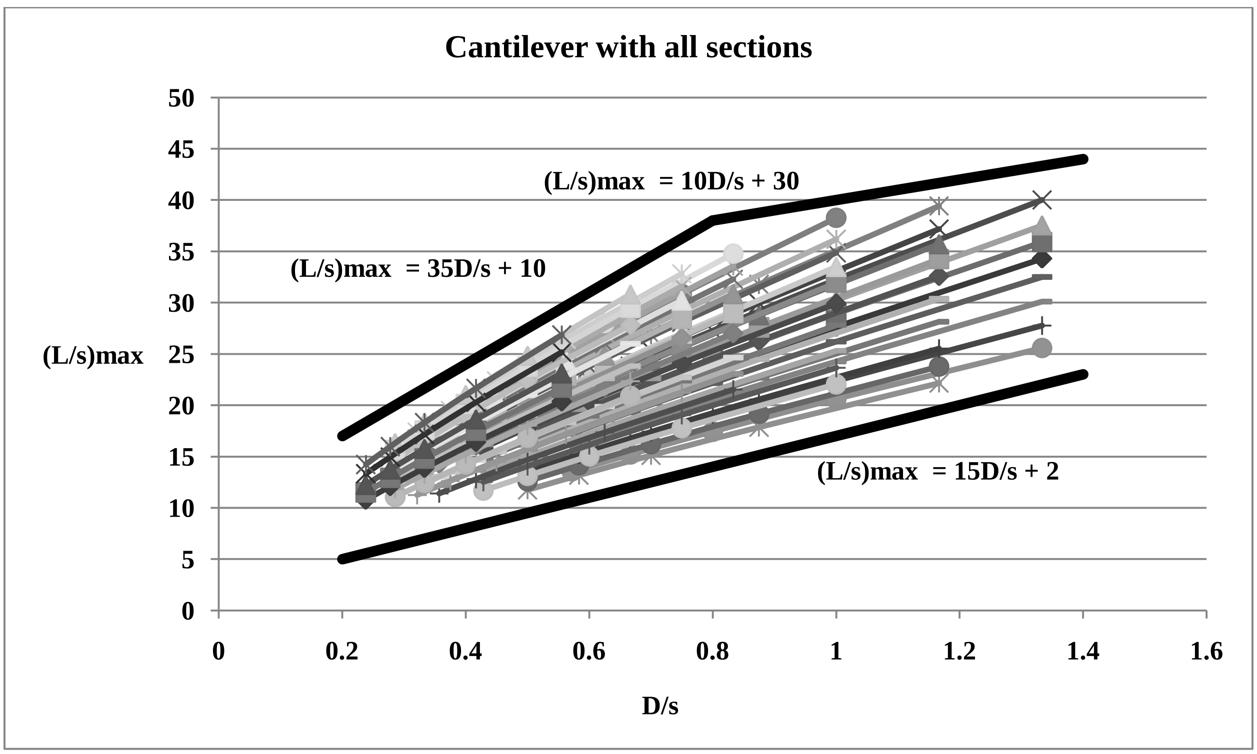

Figure 15 (L/s)max vs. D/s for cantilever double girders (load combo IV)

Figure 16 below is the combination of all cantilever double girder cross sections and spacing with corresponding (L/b)max envelope equations. All other cantilever double girder plots can be found in Appendix C.

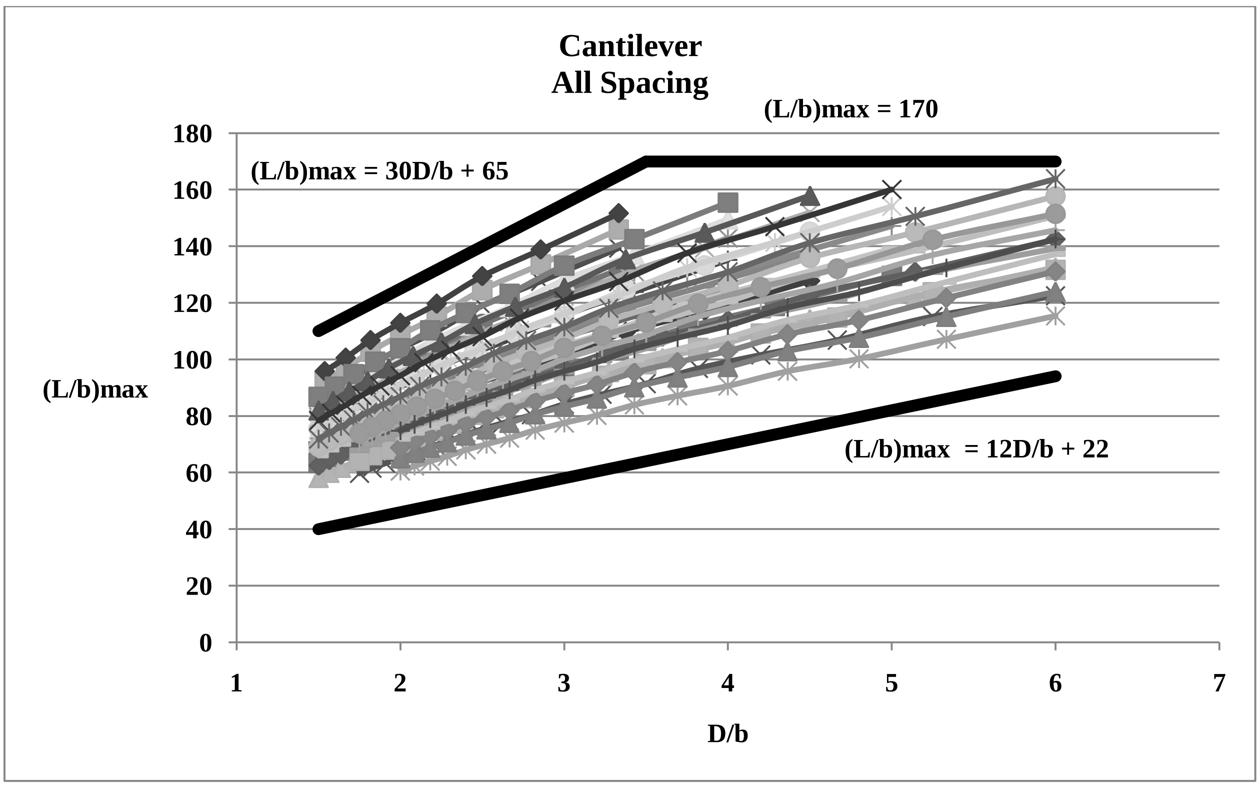

Figure 16 (L/b)max vs. D/b for cantilever double girders (load combo IV)

4.2 Single Symmetric Double Girders: Load Combo IV

In addition to the double symmetric double girders, single symmetric double girder systems have also been investigated. To determine the maximum unbraced length for a single symmetric double girder system, Yura's equation (EQ. 2) must be modified by substituting an effective moment of inertia, $I_{eff} = I_{yc} + (b/c)I_{yt}$, in place of I_y where I_{yc} and I_{yt} are the weak axis moment of inertias of the compression and tension flanges respectively and b and c are the distances from the neutral axis to the center of the tension and compression flanges respectively. The maximum unbraced lengths of simply supported and cantilever single symmetric double girders can be found by using EQs. 14 and 15. These equations are verified using buckling analysis in Chapter 5. Through the buckling analyses, Cb values of 2.14 and 3.0 were selected for simply supported and cantilever single symmetric double girders.

$$M_{gs} = C_b \frac{\pi^2 sE}{L_g^2}\sqrt{I_x I_{eff}} \tag{13}$$

$$L_{max}^{Simple} = \sqrt[4]{\frac{8C_b\pi^2 sE}{1.5w_d}\sqrt{I_x I_{eff}}} \tag{14}$$

$$L_{max}^{Cantilever} = \sqrt[4]{\frac{2C_b\pi^2 sE}{1.5w_d}\sqrt{I_x I_{eff}}} \tag{15}$$

The same cross sections have been used for the single symmetric double girders as before with single symmetric single girders. The top flange is smaller than the bottom flange for both simply supported and cantilever single symmetric double girders. All plots for single symmetric double girders can be found in Appendix D.

4.2.1 Simply Supported Single Symmetric Double Girders: Load Combo IV

Using EQ. 14, (L/b)max and (L/s)max plots have been developed for simply supported single symmetric double girders. For both cases, each spacing 's' is held constant while the top (compression) flange is varied. With the maximum unbraced lengths of all girder spacings and cross sections calculated, the data is condensed into Figures 17 and 18. The L/b and D/b ratios are calculated using the top (compression) flange.

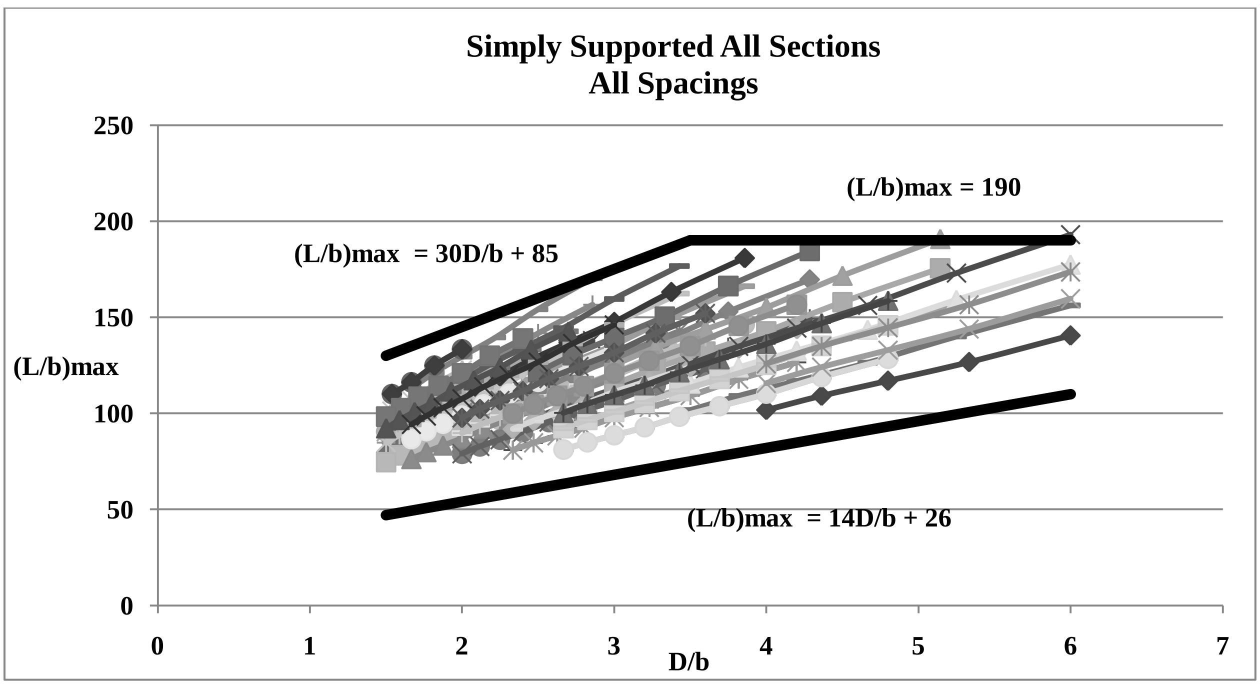

Figure 17 (L/b)max vs. D/b for simply supported single symmetric double girders (load combo IV)

Figure 17 above shows the (L/b)max values for all simply supported single symmetric double girders. The envelope equation shown on the figure is the same that is used for simply supported double symmetric double girders.

Figure 18 below shows the (L/s)max vs. D/s relationship for the simply supported single symmetric double girders. The data in the figure is a series of vertical curves. This is because the spacing ‘s’ is held constant for each case while the compression flange is varied. With the spacing constant, each web depth will have a change in (L/s)max value as the compression flange is changed while the D/s ratio stays the same. The envelope equations shown are the same as for the simply supported double symmetric double girders.

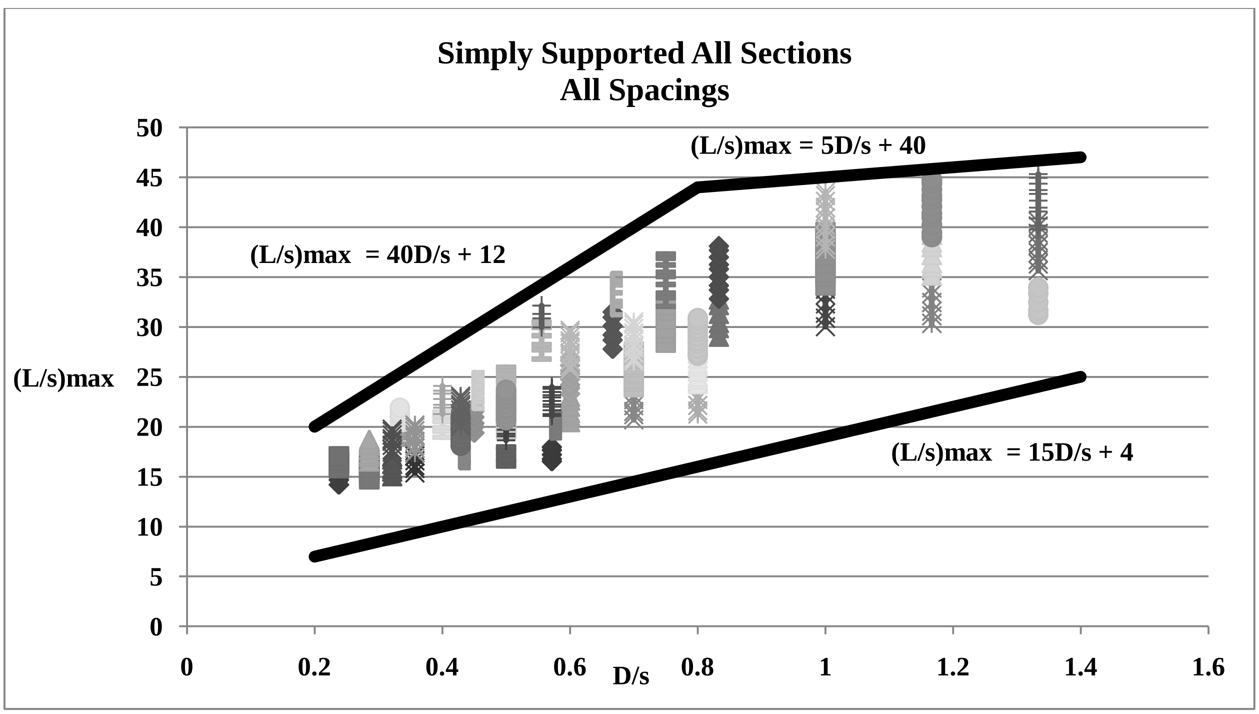

Figure 18 (L/s)max vs. D/s for simply supported single symmetric double girders (load combo IV)

4.2.2 Cantilever Single Symmetric Double Girders: Load Combo IV

Similar to the previous section, plots have been created for cantilever single symmetric double girders showing (L/b)max and (L/s)max relationships. Figure 19 below shows the (L/b)max vs. D/b relationship for Cantilever Single Symmetric Double Girders under dead load. The envelope equations cantilever double symmetric double girders is plotted in black. The upper bound is exceeded due to a capacity increase for the single symmetric cantilevers, so a new upper bound is created that contains the curves. This is due to the reduction in self weight by decreasing the tension flange

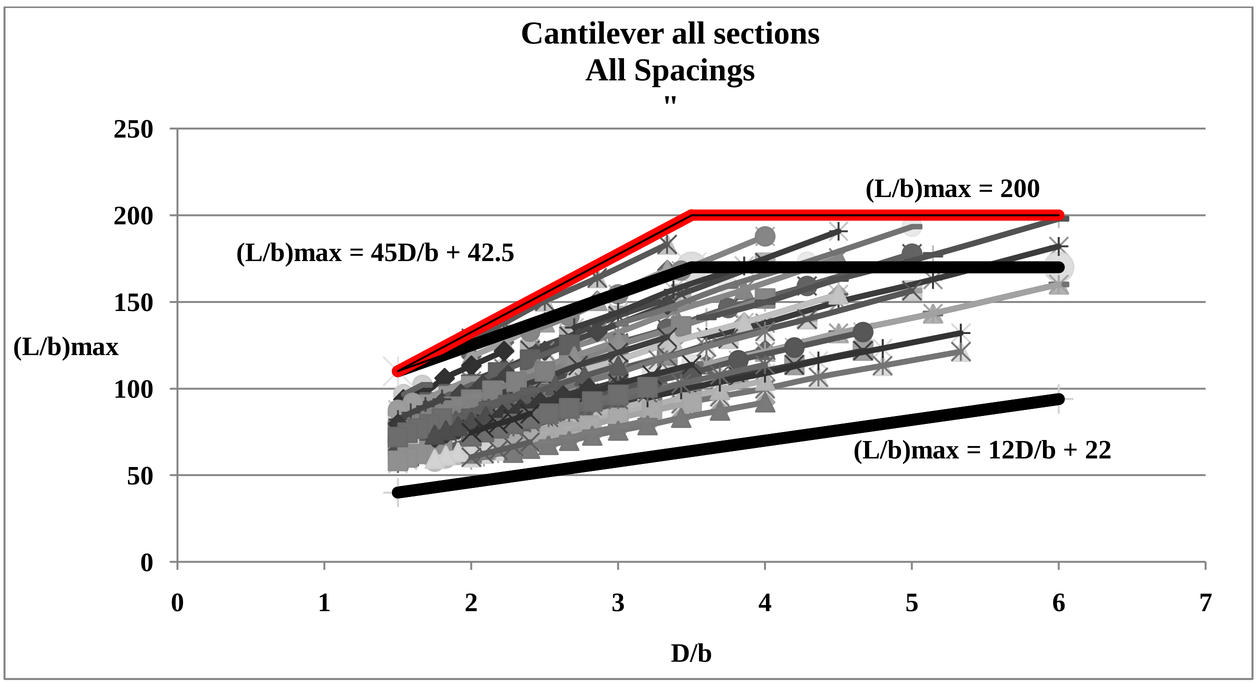

Figure 19 (L/b)max vs. D/b for cantilever single symmetric double girders (load combo IV)

Figure 20 shows the (L/s)max vs. D/s relationship for cantilever single symmetric double girders. The envelope equations shown are the same as before with the cantilever double symmetric double girders. The envelope equations for the cantilever double symmetric double girders still may be applied to the single symmetric cantilevers, but the lower bound will be more conservative.

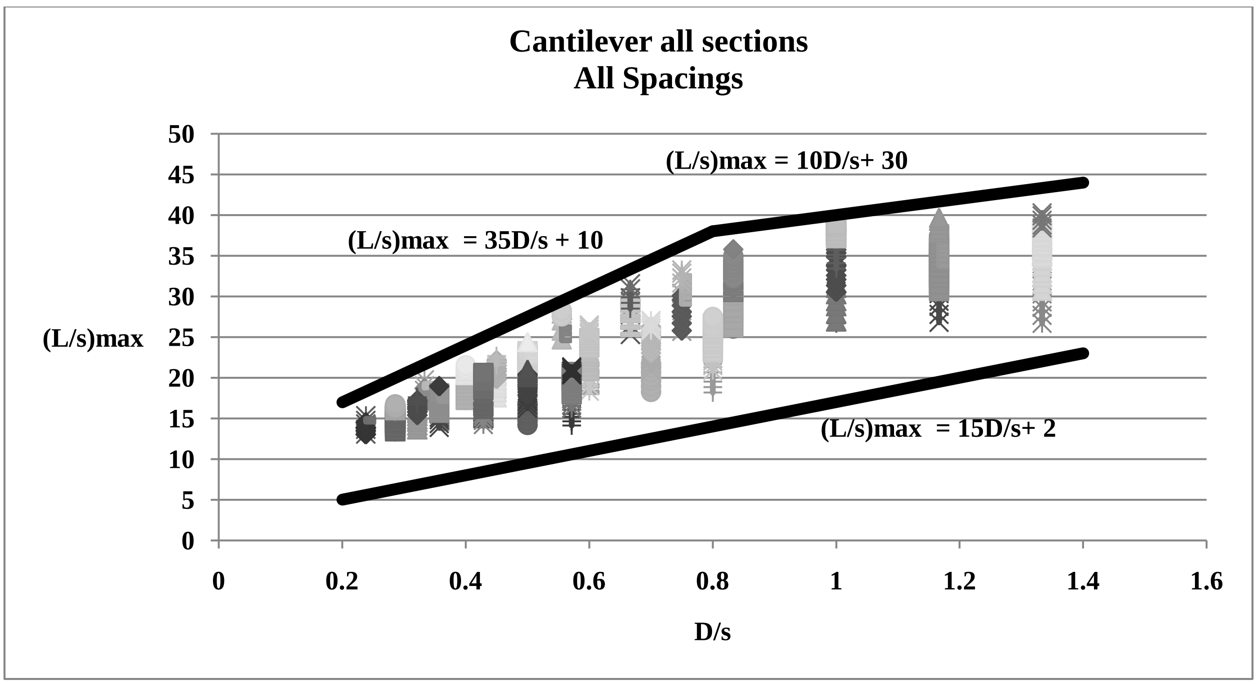

Figure 20 (L/s)max vs. D/s for cantilever single symmetric double girders (load combo IV)

CHAPTER V: FINITE ELEMENT ANALYSIS

5.1 Buckling Analyses on Single Symmetric Double Girders

Buckling analyses have been conducted to investigate the lateral torsional buckling capacity of simply supported and cantilever single symmetric double girders. For each double girder span, the center-to-center spacing between the girders is varied from 72" to 168". For both spacings, the number of cross-braced points throughout the span is also varied using 3, 4, and 8 cross-braced points. This will help to determine the minimum number of braces that are necessary to achieve global lateral torsional buckling. Results from finite element analysis are then compared to Yura's global lateral torsional buckling equation for single symmetric girders shown below as EQ. 13 (1).

$$M_{gs} = \mathrm{C_b}\ \frac{\pi^2 sE}{L_g^2}\sqrt{I_x I_{eff}} \tag{13}$$

5.1.1 Model Description

A wide range of girder cross sections has been chosen to ensure that the results from buckling analysis are valid for all sizes of single symmetric double girders. Girder web depths vary from 40" to 96", top flanges from 14" to 28", and bottom flanges from 24" to 48". Girder spacings of 72" and 168" are also investigated with 3, 4, and 8 cross-braced points evenly spaced throughout the span. Table 2 shows the list of models used for simply supported and cantilever single symmetric double girder analyses.

Finite element analysis software PATRAN was used to model the double girder systems, and MD NASTRAN was used to conduct buckling analyses and static analysis for model verification. The girder web and flanges were modeled using 4-node shell elements, and the cross-braces were modeled using 2-node rod elements with pinned end conditions. A z-frame cross-brace configuration was used for all models with the nodes of the braces connecting to the girders at the web/flange interfaces. Actual cross-braces would connect to web stiffeners located throughout the span. This connection detail was used for simplicity and is further discussed in the model verification section. The grade 50 steel material properties were input as elasto-plastic perfectly plastic with a Young's Modulus of 29000 ksi, yield stress of 50 ksi, and Poisson's ratio of 0.3. All double girders were modeled with the span parallel to the x-axis and girder webs parallel to the y-axis. The loading on the double girder systems was applied by assigning an inertial load (gravity) of 386.4 in/s^2 in the negative y direction that acted on a specified density given in the material property definition. AASHTO LRFD Load Combo IV was used to define the density of the material by multiplying 1.5 times the density (6). With an unfactored density of 0.000734 lb_{mass}/in^3, the factored density became 0.001101 lb_{mass}/in^3.

The end conditions of the simply supported double girders were modeled by restricting the torsional rotations and lateral displacements normal to the web for all nodes at each end of the spans. Vertical displacements were restrained at the node closest to the neutral axis for both ends, and the longitudinal displacement was restrained at the node closest to the neutral axis at one end of the span while free to displace at the other end. The end condition for the cantilever double girders was modeled by restricting all translations and rotations at all nodes at one end of the girder span.

Table 2 List of single symmetric models

model #	D (in)	t_w (in)	$b_{top\ flange}$ (in)	t_f (in)	$b_{bottom\ flange}$ (in)	t_f (in)	Spacing between girders (in)	D/s	Length (ft)
1	40	0.5	14	0.625	24	1	72	0.56	150
2	40	0.5	14	0.625	24	1	168	0.24	150
3	40	0.5	14	0.625	24	1	72	0.56	200
4	40	0.5	14	0.625	24	1	168	0.24	200
5	48	0.5	14	0.625	24	1	72	0.67	200
6	48	0.5	14	0.625	24	1	168	0.29	200
7	60	0.5	20	0.825	36	1.5	72	0.83	180
8	60	0.5	20	0.825	36	1.5	168	0.36	180
9	60	0.5	20	0.825	36	1.5	168	0.36	240
10	72	0.5	20	0.825	36	1.5	72	1	190
11	72	0.5	20	0.825	36	1.5	168	0.43	190
12	72	0.5	20	0.825	36	1.5	168	0.43	280
13	96	0.75	28	1.25	48	2	72	1.33	280
14	96	0.75	28	1.25	48	2	168	0.57	280
15	96	0.75	28	1.25	48	2	72	1.33	320
16	96	0.75	28	1.25	48	2	168	0.57	320

5.1.2 Model Verification

Static linear elastic analyses were conducted on 5 different girder models. The models were subjected to an external load of 1.5 times their self-weight, and displacements at midspan were recorded. Table 3 compares the theoretical displacements to displacements from finite element analysis. There is less than 3% difference for all of the models, which shows that the girder models were working properly and can be expected to produce accurate results.

Table 3 Model verification

Model #	Model Verification Maximum Vertical Displacement (in)		
	Theoretical	FEA	% Diff.
S1-3	7.3	7.51	2.80
S5-3	16.57	16.9	1.95
S7-3	6.62	6.77	2.22
S13-2	15.25	15.4	0.97
S15-3	26.02	26.3	1.06

Another necessary verification is to determine whether the bracing connections to the girders will give accurate enough results when compared to a more realistic model. Two single symmetric double girder models were created using finite element software PATRAN. The models had identical cross sections and the same span length with 3 equally spaced cross-braced points (see model #3 in Table 2). One model had the cross-braces connect to web stiffeners while the other model had cross-braces connect to the web/flange interface. Buckling analyses were conducted to determine if simplifying the double girder model by excluding web stiffeners would provide accurate results in comparison to the more realistic model with web stiffeners. The first three eigenvalues were recorded for both simply supported and cantilever models with and without web stiffeners and compared in Table 4. The percent difference was below 0.2 for every case but the third eigenvalue of the cantilever section which had a percent difference of 1.01. This shows that the simplification of the double girder models by excluding web stiffeners is acceptable and will provide accurate results.

Table 4 Verification of simplified model without web stiffeners

Model #3	Eigenvalue	Without Stiffeners	With Stiffeners	% Diff.
Simply Supported	1	0.48427	0.4845	0.05
	2	0.57336	0.57443	0.19
	3	0.59307	0.59416	0.18
Cantilever	1	0.40459	0.40402	0.14
	2	0.91502	0.91644	0.16
	3	1.5768	1.5609	1.01

When modeling the end conditions for the simply supported single symmetric double girder models, it is important that the nodes selected to restrict translation in the vertical and longitudinal directions (imitating the pin and roller) are as close to the neutral axis as possible. If the restricted node is above the neutral axis, the buckling capacity of the system will increase due to the added stability by restricting top flange rotation. However, if it is lower than the neutral axis the buckling capacity is reduced. It is difficult to create a finite element model with a node that perfectly coincides with the neutral axis, so it is important to determine the impact of selecting a node that is the closest and if it will be accurate enough in comparison. To verify this, buckling analyses were conducted on model 7. The first eigenvalue was recorded for three different cases: pinned at the node at the neutral axis, the node above the neutral axis, and the node below the neutral axis. Table 5 shows the eigenvalues that correspond to these cases. For the nodes above and below the neutral axis, the eigenvalue was less than 0.02% different than the eigenvalue with the node located at the neutral axis. This confirms that it will suffice to choose the node closest to the neutral axis to achieve accurate buckling results.

Table 5 Verification of simply supported end conditions.

	Node Location	Eigenvalue	% Diff.
Node Location	Above N.A.	1.7039	0.018
	At N.A.	1.7036	0.000
	Below N.A.	1.7034	0.012

5.1.3 Analysis Results

Eigenvalue buckling analyses were conducted on a total of 96 different finite element models to determine the lateral torsional buckling capacity of the double girder system. The critical buckling moment was calculated by multiplying the theoretical maximum moment (i.e. $wL^2/8$ and $wL^2/2$) in the girder system by the first eigenvalue that corresponded to the global buckling of the system. For all cantilever cases analyzed, the first buckled shape was global. For the simply supported cases, global buckling was observed as the first mode in most cases, while a few cases had local buckling modes for their primary buckled shape. The Cb value used for simply supported single symmetric double girders was 1.12.

Tables 6 and 7 show the buckling results for the simply supported and cantilever girders respectively. λ_1 refers to the first mode's eigenvalue, λ_1 buckle describes the buckled shape of the first mode, and λ_{global} is the eigenvalue that corresponds to the first mode resembling global buckling. Tables 6 and 7 give these values for all models with 3, 4, and 8 cross braces along the span.

The λ_{global} for models 8 and 11 say "none". This is because the span was not long enough for global buckling to occur. Local buckling was the only observed failure mode.

Table 6 Simply supported buckling results

Simply Supported Models									
model #	3 Braces			4 Braces			8 braces		
	λ_1	λ_1 Buckle	λ_{global}	λ_1	λ_1 Buckle	λ_{global}	λ_1	λ_1 Buckle	λ_{global}
1	1.46	global	1.46	1.52	global	1.52	1.51	global	1.51
2	1.51	b/w braces	2.1	2.06	b/w braces	3.07	3.32	global	3.32
3	0.48	global	0.48	0.5	global	0.5	0.5	global	0.5
4	0.59	b/w braces	0.79	0.75	b/w braces	1.02	1.09	global	1.09
5	0.54	global	0.536	0.56	global	0.56	0.56	global	0.56
6	0.58	b/w braces	0.81	0.78	b/w braces	1.14	1.25	global	1.25
7	1.7	global	1.7	1.75	global	1.75	1.74	global	1.74
8	2.1	local	none	2.12	local	none	2.07	local	none
9	0.76	b/w braces	1.03	1.04	b/w braces	1.27	1.15	local	none
10	1.55	global	1.55	1.6	global	1.6	1.6	global	1.6
11	1.62	local	none	1.61	local	none	1.57	local	none
12	0.47	b/w braces	0.64	0.64	b/w braces	0.79	0.74	local	0.83
13	0.61	global	0.61	0.62	global	0.62	0.62	global	0.62
14	1.13	b/w braces	1.31	1.37	local	1.42	1.36	local	1.46
15	0.37	global	0.37	0.37	global	0.37	0.37	global	0.37
16	0.7	b/w braces	0.78	0.84	global	0.84	0.86	global	0.86

Table 7 Cantilever buckling results

Cantilever Models						
model #	3 Braces		4 Braces		8 braces	
	λ_1	λ_1 Buckle	λ_1	λ_1 Buckle	λ_1	λ_1 Buckle
1	1.22	global	1.23	global	1.22	global
2	2.32	global	2.46	global	2.44	global
3	0.4	global	0.41	global	0.41	global
4	0.78	global	0.81	global	0.81	global
5	0.44	global	0.45	global	0.45	global
6	0.85	global	0.91	global	0.91	global
7	1.56	global	1.57	global	1.56	global
8	3	global	3.07	global	3.1	global
9	0.98	global	1.01	global	1.02	global
10	1.4	global	1.41	global	1.41	global
11	2.75	global	2.84	global	2.85	global
12	0.61	global	0.63	global	0.64	global
13	0.57	global	0.58	global	0.58	global
14	1.1	global	1.12	global	1.13	global
15	0.35	global	0.35	global	0.35	global
16	0.65	global	0.67	global	0.67	global

When compared to the critical moment from EQ. 13, the critical moment from buckling analysis was very accurate. Figure 21 shows the ratio of the critical buckling moment to the theoretical capacity. The points shown in the plot correspond to the first mode that shows global buckling, even if it is not the first mode.

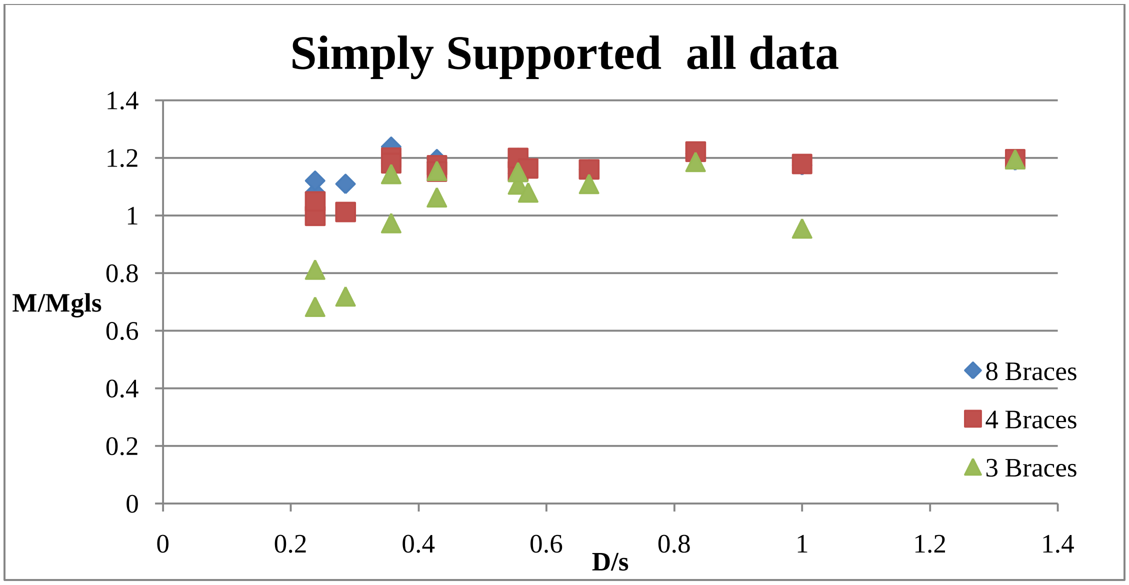

Figure 21 Simply supported FEA buckling results

Figure 22 shows the ratio of the critical buckling moment from buckling analysis to the capacity. The data points shown in the figure are only from the simply supported girders that have global buckling as the first mode.

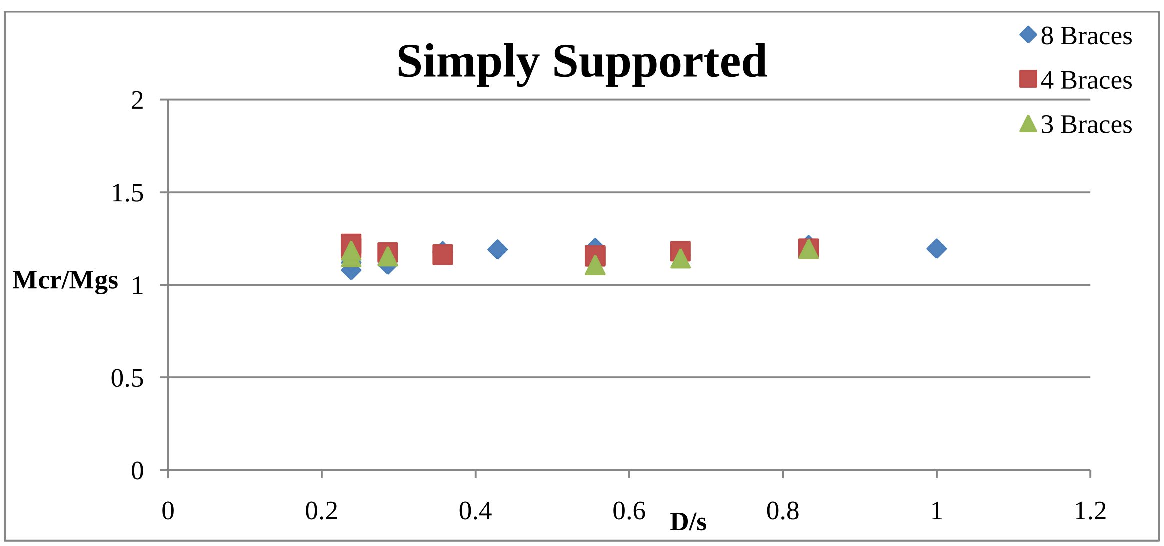

Figure 22 Simply supported reduced FEA buckling results

The cantilever single symmetric double girder results show that the theoretical buckling capacity given by EQ. 13 is very conservative. When the Cb value is increased to 3.0, the maximum allowed by AISC, the results are very accurate (7). They are shown in Figure 23.

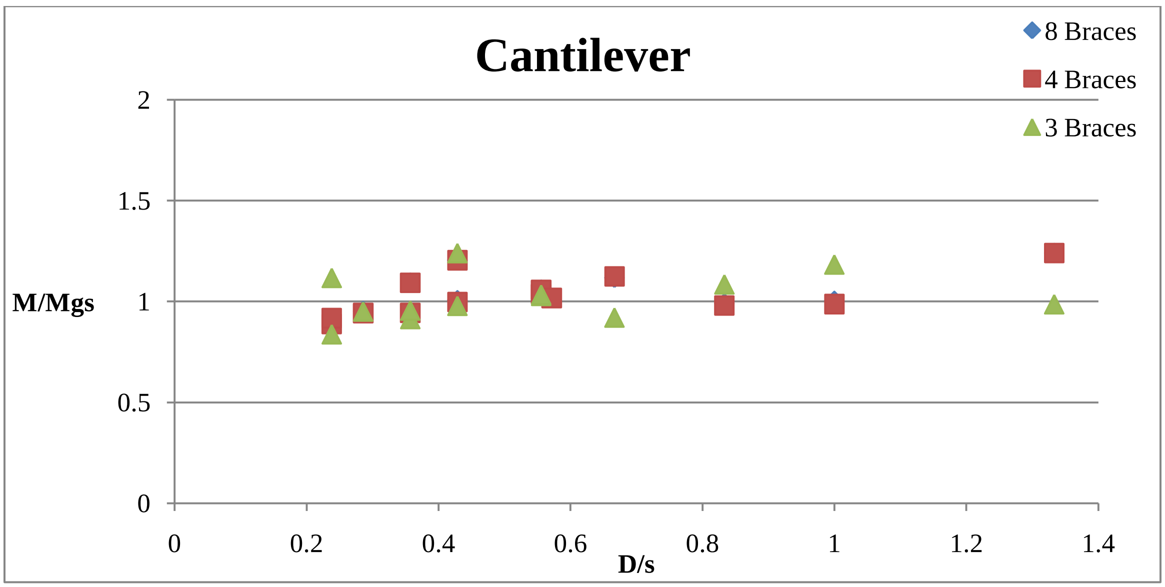

Figure 23 Cantilever FEA buckling results

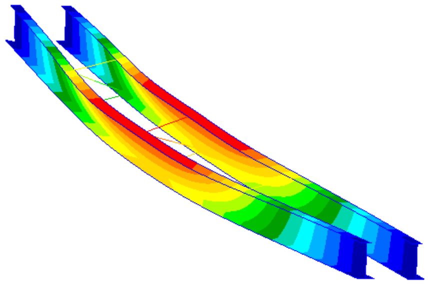

Mode 1 (λ=0.536)

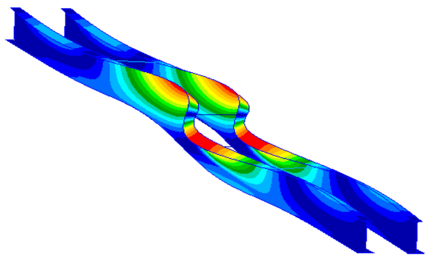

Mode 2 (λ=0.585)

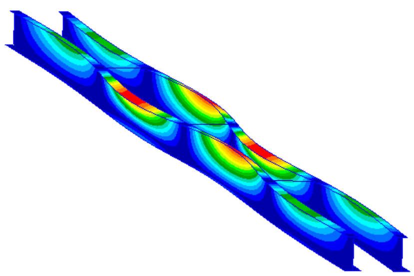

Mode 3 (λ=0.603)

Simply Supported Case

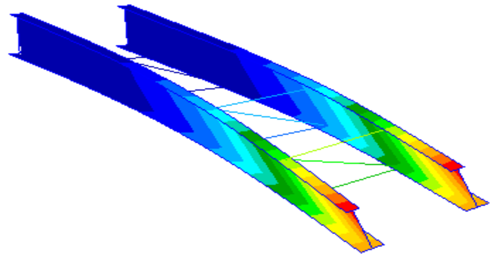

Mode 1 (λ=0.610)

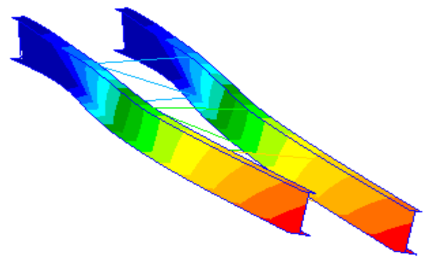

Mode 2 (λ=1.023)

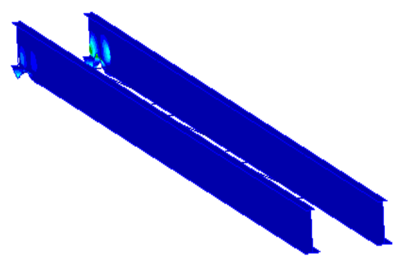

Mode 3 (λ=1.392)

Cantilever Case

Figure 24 Dominant mode shapes and eigenvalues for single symmetric double girder systems.

Figure 24 shows the main buckling modes for simply supported and cantilever single symmetric double girder systems. Mode 1 for the cantilever case was the same for all models examined with 3, 4 and 8 braces. This means that 3 cross-braced points provide enough stability for the system to buckle globally. Mode 3 for the cantilever case shows local buckling at the fixed end. All modes greater than mode 3 have similar buckled shapes that imply that the loads cause local buckling, but they have eigenvalues much greater that mode 1 so they are unlikely to occur.

The simply supported girders showed more variability than the cantilever girders. The models with larger spacing between girders, especially when D/s was less than 0.5, required the maximum bracing to achieve a mode 1 of global bucking. When the number of cross-braced points was 3 or 4 and the spacing was 168”, buckling between braces was the primary buckling mode. Figure 25 shows the primary buckling mode for the girders with large spacings. Mode 3, shown below is the closest mode shape to global buckling for the girders with large spacings. Even though the girders move laterally together, there is still some buckling between the braces observed. The girders with this behavior were excluded from Figure 22 because a ‘true’ global buckling was not observed. This was not the case for simply supported double symmetric double girders where global buckling stability was achieved with a minimum of 3 cross-braces (16). The simply supported single symmetric double girders have a need for more bracing to achieve stability and make global buckling the primary mode, especially when the spacing between girders is large.

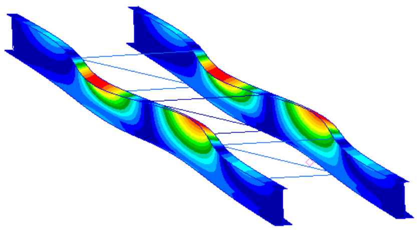

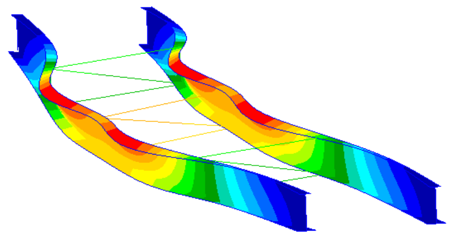

Mode 1 (λ=0.577) Mode 3 (λ=0.812)

Figure 25 Mode shapes and eigenvalues for simply supported single symmetric double girders with large spacing between girders

5.2 Effects of Wind Loading

5.2.1 Investigating the "no buckle" concept

In Chapter II, the "no buckling" concept was discussed concerning sections with $I_y > I_x$. If a double girder system were thought to be rigid with very stiff cross-braces, the stress distribution from wind loading would have the windward girder in tension and leeward girder in compression. This would mean that I_y for the double girder system would be $2I_{yo} + 2Ad^2$. Where Iyo is the weak axis moment of inertia for a single girder, A is the cross sectional area of a single girder, and d is half of the center-to-center spacing between the girders. If this were true, I_y would be very close to if not greater than I_x for the double girder system, and yielding would be a greater concern than lateral torsional buckling.

To investigate the "no buckling" concept for the case of double girders, FEA was conducted on a cantilever double girder system to observe its behavior under dead and wind load. Linear static and nonlinear analyses were both conducted, and no visible difference in behavior was observed. Figure 26 shows the stress distribution for a cantilever double girder system under dead and wind load. The wind pressure is being applied from left to right on the point of view given. Both girders have nearly identical stresses throughout their cross sections, and are deflecting laterally together. Because the wind and dead load are applied, there are tensile stresses concentrated at the windward side of both top flanges. Conversely, the leeward sides of both bottom flanges have large compressive stresses. These stress locations show that the system is "rolling over" due to the loading conditions. Based on these observations it seems that the girders are acting individually, but transferring loads via the cross-braces to achieve stability. Because the girders are not acting rigidly, the "no buckling" concept does not apply to the system.

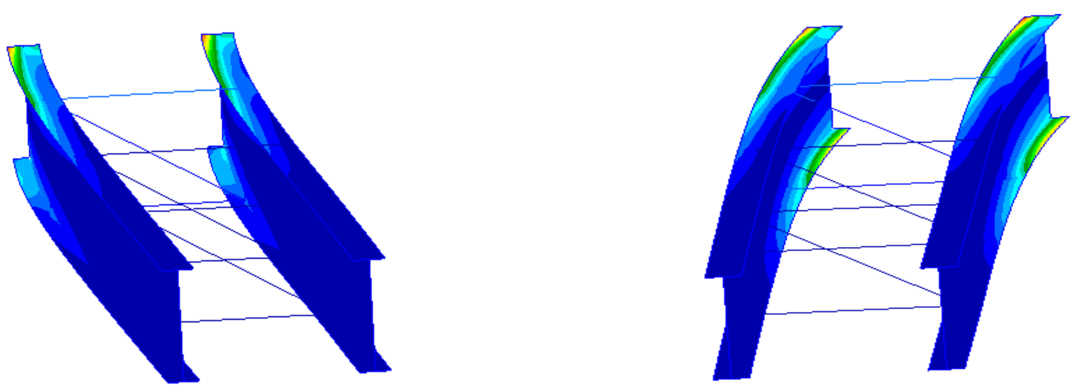

Figure 26 Double girder under wind and dead load

. Another analysis was conducted to determine if the simplification of using $I_y = 2* I_{yo}$ (mentioned in Chapter II) for the double girders system is indeed accurate. A nonlinear analysis was conducted on the double girder system under wind load to compare FEA deflections and stresses with hand calculated values. For the analysis a uniform pressure of 0.05 psi was applied to the web of one girder in the lateral direction to simulate wind. This pressure was chosen to ensure that the material would still be in the linear elastic range and the equations used would still apply (7). Table 8 gives a summary of the double girder section properties along with FEA and calculated deflections and stresses. The results confirm that the minor axis moment of inertia for double girder systems can be assumed to be the summation of the individual girder's minor axis moment of inertia.

Table 8 Double girder minor axis bending results

Cantilever Double Girder Properties								Calculated using $2*I_{yo}$		FEA Results	
D (in)	t_w (in)	b (in)	t_f (in)	I_{yo} (in^4)	$2*I_{yo}$ (in^4)	Spacing (in)	Length (ft)	Deflection (in)	Max stress (ksi)	Deflection (in)	Max stress (ksi)
40	0.5	12	0.563	162.42	324.84	72	87	31.5	20.1	31.4	19.3

5.2.2 Brace Forces Due to Wind Loading

Double girders have been analyzed under gravity and wind loading using nonlinear analysis to determine if the brace forces would exceed their buckling capacity. The wind load was applied to one of the webs in increments until failure of the girder system occurred, and the brace forces were recorded for all load increments. The span lengths of the double girders analyzed were kept under their maximum length calculated using EQ. 2.

The section properties of double girder models analyzed are summarized in Table 9, and have the same material properties described earlier in section 5.1.1. Both models had three evenly spaced z-frame cross-braces along the span, and were analyzed as cantilever and simply supported double girders.

Table 9 Double girder models with wind loading

	D (in)	t_w (in)	b (in)	t_f (in)	Spacing (in)	Length (ft)
Model 1	40	0.5	12	0.5625	72	100
Model 2	96	0.75	16	0.75	168	140

Table 10 shows the brace forces for model 1 as a cantilever. All braces in Table 8 are connected to the top flange/web interface. The braces located at the bottom flange/web interface sustained nearly identical forces for every increment as the braces in Table 10. Brace 1 is closest to the free end, 2 is at midspan, and 3 is closest to the free end. The wind velocity and pressure for each increment are shown to the left. The force in each brace is shown in its designated column along with the percent of the total force transferred between the girders. The final increment shows that the largest brace force in the analysis is 630 lbs at brace 3. Considering that the smallest size angle listed in the AISC manual (L2x2x1/8) has a buckling capacity of over 3,000 lbs at a length of 15.5 ft, buckling was not an issue for this case.

Table 10 Brace forces for model 1 cantilever

Wind Loading		Brace 1		Brace 2		Brace 3	
V (mph)	**P (psf)**	**Force (lb)**	**% of total Force**	**Force (lb)**	**% of total Force**	**Force (lb)**	**% of total Force**
0.00	0.00	0.00		0.00		0.00	
7.53	0.15	3.67	33.7%	1.00	9.2%	6.22	57.2%
11.17	0.32	8.06	33.7%	2.19	9.2%	13.69	57.2%
14.37	0.53	13.34	33.7%	3.63	9.2%	22.66	57.2%
17.45	0.78	19.67	33.7%	5.34	9.1%	33.42	57.2%
20.54	1.08	27.26	33.7%	7.39	9.1%	46.30	57.2%
23.73	1.44	36.36	33.7%	9.87	9.1%	61.83	57.2%
27.06	1.87	47.29	33.6%	12.83	9.1%	80.44	57.2%
30.59	2.39	60.20	33.8%	16.10	9.0%	101.85	57.2%
34.34	3.02	77.01	33.2%	21.87	9.4%	132.87	57.3%
38.37	3.77	94.83	33.6%	25.73	9.1%	161.70	57.3%
42.70	4.67	117.37	33.6%	31.73	9.1%	200.55	57.4%
47.37	5.75	144.95	33.5%	39.22	9.1%	248.54	57.4%
52.44	7.04	176.03	33.5%	47.11	9.0%	302.52	57.5%
57.93	8.59	214.84	33.4%	57.74	9.0%	370.32	57.6%
63.91	10.46	260.45	33.3%	69.72	8.9%	451.47	57.8%
70.41	12.69	314.67	33.2%	83.87	8.8%	549.60	58.0%
75.30	14.52	358.14	33.0%	95.17	8.8%	630.34	58.2%
		Average:	**33.5%**		**9.1%**		**57.4%**

Model 2 was analyzed as a cantilever using the same procedure as model 1. The results are shown in Table 11. Brace 1 is closest to the fixed end, 2 is at midspan, and 3 is closest to the free end. The brace forces shown in Table 9 are much higher than with model 1 even though the pressure load is smaller. This is due to the larger web depth of model 2 (96") and slightly longer span. Table 11 shows a maximum force at the last increment of 1,258 lbs. This force is much larger than before with model 1, but still is not large enough to consider buckling.

From Tables 10 and 11, the distribution of forces from windward to leeward girder show 57% of the total force being transmitted from brace 3, 33.4% from brace 1, and 9.2% from brace 2. Knowing how the forces are distributed may be useful for bracing design.

Table 11 Brace forces for model 2 cantilever

Wind Loading		Brace 1		Brace 2		Brace 3	
V (mph)	P (psf)	Force (lb)	% of total Force	Force (lb)	% of total Force	Force (lb)	% of total Force
0.00	0.00	0.00		0.00		0.00	
5.83	0.09	7.30	33.5%	2.02	9.3%	12.48	57.2%
8.65	0.19	16.07	33.5%	4.45	9.3%	27.46	57.2%
11.13	0.32	26.59	33.5%	7.35	9.3%	45.44	57.2%
13.51	0.47	39.21	33.5%	10.85	9.3%	67.01	57.2%
15.91	0.65	54.35	33.5%	15.03	9.3%	92.90	57.2%
18.38	0.86	72.52	33.5%	20.06	9.3%	123.97	57.2%
20.96	1.12	94.33	33.5%	26.09	9.3%	161.26	57.3%
23.69	1.44	120.48	33.5%	33.32	9.3%	206.02	57.3%
26.60	1.81	151.84	33.5%	42.00	9.3%	259.74	57.3%
29.72	2.26	189.45	33.5%	52.40	9.3%	324.24	57.3%
33.07	2.80	234.53	33.5%	64.87	9.3%	401.69	57.3%
36.70	3.45	288.53	33.4%	79.79	9.2%	494.73	57.3%
40.62	4.22	353.16	33.4%	97.65	9.2%	606.55	57.4%
44.88	5.16	430.43	33.4%	118.98	9.2%	741.05	57.4%
49.50	6.27	522.64	33.3%	144.39	9.2%	903.01	57.5%
54.54	7.62	632.40	33.2%	174.52	9.2%	1,098.38	57.6%
58.33	8.71	720.96	33.1%	198.70	9.1%	1,258.46	57.8%
		Average:	**33.4%**		**9.2%**		**57.3%**

Models 1 and 2 from Table 9 were also analyzed as simply supported double girders. The same procedure was used for determining the brace forces as before with the cantilever cases. Table 11 shows the results from analysis of model 1 simply supported. Brace 1 and 3 are closest to the supports, and 2 is at midspan. All of the braces in Table 11 are connected to the girders at the top flange/web interface. The braces at the bottom flange/web interface showed nearly identical forces through each increment as the ones shown in Table 12.

Table 12 Brace forces for model 1 simply supported

Wind Loading		**Brace 1**		**Brace 2**		**Brace 3**	
V (mph)	**P (psf)**	**Force (lb)**	**% of total Force**	**Force (lb)**	**% of total Force**	**Force (lb)**	**% of total Force**
0.00	0.00	0.00		0.00		0.00	
23.84	1.45	48.34	35.5%	39.34	28.9%	48.34	35.5%
35.35	3.20	106.21	35.5%	86.58	29.0%	106.21	35.5%
45.47	5.29	175.28	35.5%	143.39	29.0%	175.28	35.5%
55.22	7.81	257.51	35.4%	211.76	29.1%	257.51	35.4%
65.02	10.82	355.27	35.4%	294.04	29.3%	355.27	35.4%
75.11	14.44	471.48	35.3%	392.99	29.4%	471.48	35.3%
85.66	18.79	617.33	35.4%	508.13	29.2%	617.34	35.4%
96.82	24.00	787.93	35.5%	646.75	29.1%	787.94	35.5%
106.60	29.09	953.69	35.5%	780.97	29.0%	953.73	35.5%
	Average:		**35.4%**		**29.1%**		**35.4%**

The maximum force shown in Table 12 of 954 lbs still is not enough force to cause buckling of the braces, even though it was subjected to over 100 mph wind. The brace forces for model 2 simply supported are shown in Table 13. The maximum force observed for model 2 simply supported was 1,763 lbs, which is much larger than model 1 simply supported. This force may be large enough to cause buckling of the braces if the cross sections of the braces are small enough. The brace force distribution was also the same for both simply supported models with 35.4% of the load to each of the outer braces, and 29.1% to the brace at midspan.

Table 13 Brace forces for model 2 simply supported

Wind Loading		Brace 1		Brace 2		Brace 3	
V (mph)	P (psf)	Force (lb)	% of total Force	Force (lb)	% of total Force	Force (lb)	% of total Force
21.74	1.21	0.00		0.00		0.00	
30.74	2.42	17.52	35.5%	14.32	29.0%	17.52	35.5%
37.65	3.63	38.55	35.5%	31.51	29.0%	38.55	35.5%
43.47	4.84	63.78	35.5%	52.13	29.0%	63.78	35.5%
48.61	6.05	94.06	35.5%	76.88	29.0%	94.06	35.5%
53.24	7.26	130.38	35.5%	106.58	29.0%	130.38	35.5%
57.51	8.47	173.96	35.5%	142.22	29.0%	173.96	35.5%
61.48	9.68	226.24	35.5%	184.99	29.0%	226.24	35.5%
65.21	10.89	288.93	35.5%	236.33	29.0%	288.93	35.5%
68.74	12.10	364.10	35.5%	297.95	29.0%	364.10	35.5%
72.09	13.31	454.19	35.5%	371.92	29.0%	454.19	35.5%
75.30	14.52	562.12	35.5%	460.72	29.1%	562.12	35.5%
78.37	15.72	691.33	35.5%	567.35	29.1%	691.33	35.5%
81.33	16.93	845.91	35.4%	695.39	29.1%	845.91	35.4%
84.19	18.14	1030.70	35.4%	849.17	29.2%	1030.69	35.4%
86.95	19.35	1251.42	35.4%	1033.85	29.2%	1251.42	35.4%
89.62	20.56	1515.75	35.4%	1256.13	29.3%	1515.73	35.4%
92.22	21.77	1726.95	35.3%	1438.41	29.4%	1726.93	35.3%
	Average:		**35.5%**		**29.1%**		**35.5%**

CONCLUSIONS

Capacity envelopes have been developed for single girders with both double and single symmetric cross sections under various loading and end conditions. Capacity envelopes have also been created for double girders with double and single symmetric cross sections under dead load only. Finite Element Analyses have also been conducted on double girders under dead and wind load to observe behavior and investigate the impact of the cross-braces. From the girders examined in this thesis, the following conclusions can be drawn.

1. Single symmetric simply supported girders have a greatest risk of lateral torsional buckling. The smaller compression flange greatly reduces lateral torsional buckling capacity, especially for sections with a much larger tension flange.
2. Yura's buckling equation for single symmetric double girders has been verified. The only modification is that a maximum Cb value of 3.0 (from AISC) must be assigned to cantilever systems.
3. Cantilever single symmetric double girders require a minimal amount of bracing to have global buckling as the primary buckling mode.
4. Conversely, simply supported single symmetric double girders require the maximum amount of bracing to enable the system to act globally and eliminate buckling between braces. This is especially true for systems with large spacing between girders.
5. When double girders are subjected to wind loads, the girders deflect laterally together, and have almost identical stress distributions throughout their span. The weak axis moment of inertia for the system is equivalent to the summation of the weak axis moment of inertias for the individual girders. This implies that they

bend individually while achieving stability by sharing the lateral forces, and $I_y = 2I_{yo}$.

6. Buckling of braces in double girder systems due to wind loading is highly unlikely, but possible. Yielding or buckling of the double girders is more likely to occur before the brace forces exceed buckling capacity. Double girders with large center-to-center spacings have the highest risk of buckling the braces, especially when the web depths are large, increasing the wind load.

LIST OF REFERENCES

(1) Yura, Joseph A., T. Helwig, R. Herman and C. Zhou. Global Lateral Buckling of I-shaped Girder Systems. *Journal of Structural Engineering,* ASCE, Vol. 134, No. 9, 2008, pp.1487-1494.

(2) Eurocode 3: Design of steel structures, Part 1-1, 1992

(3) Roberts T.M., Burt C.A. "Instability of Monosymmetric I-beams and Cantilevers" International Journal of Mechanical Science, pg 313-324, 1985

(4) Wang C.M., Kitipornchai S. "On Stability of Monosymmetric Cantilevers" Engineering and Structures, pg. 169-180, 1986

(5) Roberts T.M, Narayanan R. "Strength of Laterally Unrestrained Monosymmetric Beams" Thin Walled Structures. Elsevier Science Publishers Ltd. 1998

(6) American Association of State Highway and Transportation Officials. *LRFD Bridge Design Specifications, Fourth Edition*, Washington, D.C., 2007.

(7) American Institute of Steel Construction (2006), "Steel Construction Manual", Thirteenth Edition, Chicago, Illinois.

(8) Yura, Joseph A., and J. A. Widianto. Lateral Buckling and Bracing of Beams – A Re-evaluation after the Marcy Bridge Collapse. *Proc. Structural Stability Research Council, Montreal*, 2005, pp. 277-294.

(9) Komatsu, S., Nishimura, N., and Ohno, M. "Overall lateral buckling of the ladder-like plate girder bridges and the stiffening design method." Transportation Japan Society of Civil Engineers. 1983

(10) Timoshenko, S., and J. Gere. *Theory of elastic stability,* McGraw-Hill, New York, 1961.

(11) Zhao, Qiuhong, B. Yu and E. G. Burdette. “Investigation on Effects of Cross-frames to Stability of Double Girder System under erection.” *Proceedings of the 89th Annual TRB Meeting,* Washington, D.C. (Submitted in 2008)

(12) Kozy, Brian and S. Tunstall. “Stability analysis and bracing for system buckling in twin I-girder bridges.” *Bridge Structures,* 3(3), 2007, pp. 149-163.

(13) Cheng, Jin. Jiang, J. Xiao, R. Xia, M. “Wind-induced load capacity analysis and parametric study of a long-span arch bridge under construction.” Computers and Structures 81 pg. 2513-2524, 2003.

(14) American Society of Civil Engineers (2005), “Minimum Design Loads for Buildings and Other Structures”.

(15) Zhao, Qiuhong, B. Yu, E. G. Burdette and J. S. Hastings. “Monitoring Steel Girder Stability for a Safer Bridge Erection." *J. of Performance of Constructed Facilities, ASCE.*

(16) Zhao, Qiuhong, B. Yu and E. G. Burdette. “Simplified erection guidelines for double I-girder systems during bridge construction.” Transportation Research Board Annual Meeting 2010

APPENDICES

APPENDIX A: DOUBLE SYMMETRIC SINGLE GIRDERS

Appendix A shows the plots for double symmetric single girders. Lmax vs D, (L/b)max vs. D, and (L/b)max vs. D/b relationships are shown for simply supported and cantilever girders subjected to Load Combos IV (1.5D) and III (1.25D + 1.4W).

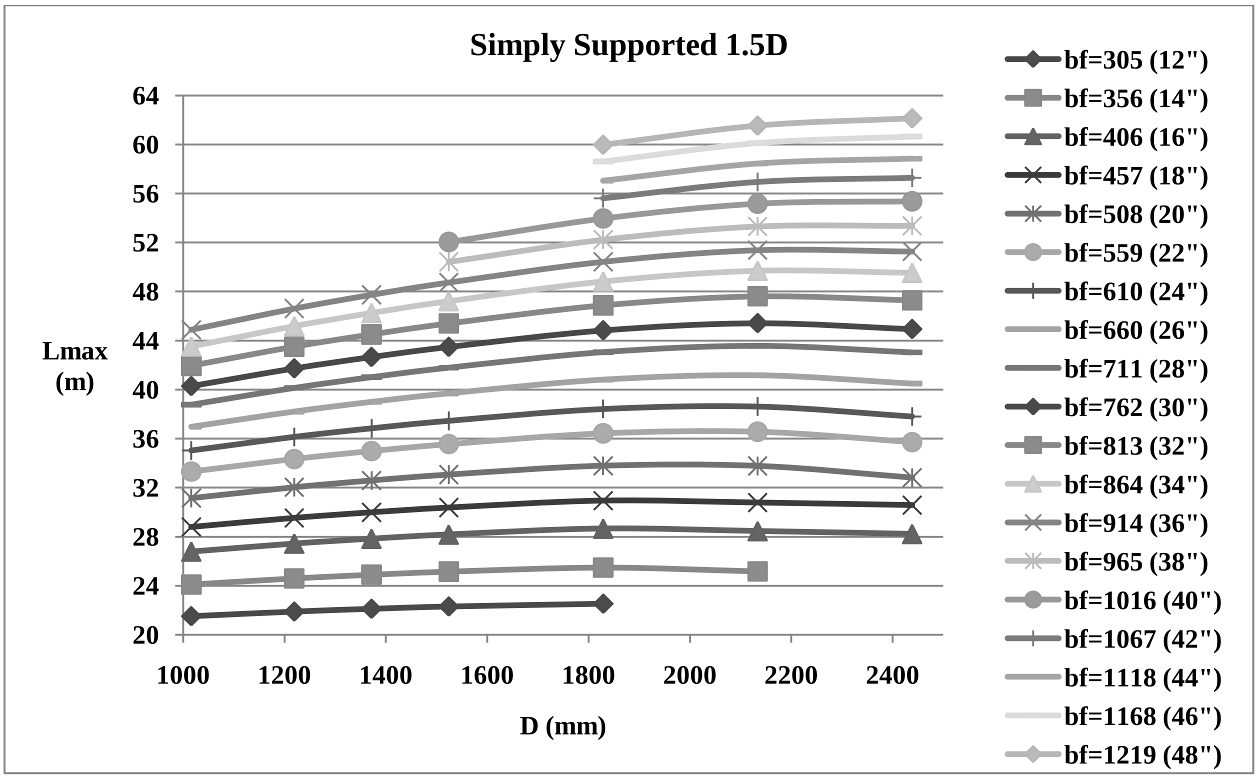

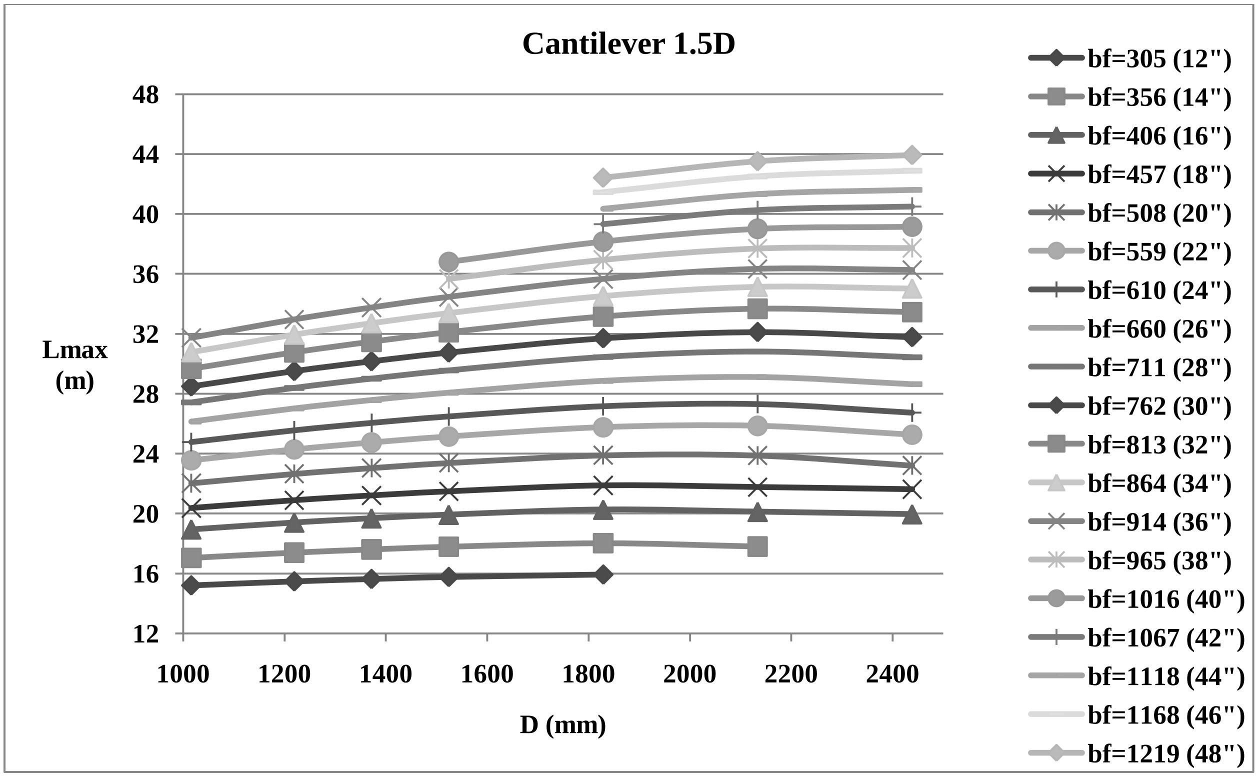
Cantilever 1.5D
Lmax (m)
48
44
40
36
32
28
24
20
16
12
1000
1200
1400
1600
1800
2000
2200
2400
D (mm)
bf=305 (12")
bf=356 (14")
bf=406 (16")
bf=457 (18")
bf=508 (20")
bf=559 (22")
bf=610 (24")
bf=660 (26")
bf=711 (28")
bf=762 (30")
bf=813 (32")
bf=864 (34")
bf=914 (36")
bf=965 (38")
bf=1016 (40")
bf=1067 (42")
bf=1118 (44")
bf=1168 (46")
bf=1219 (48")

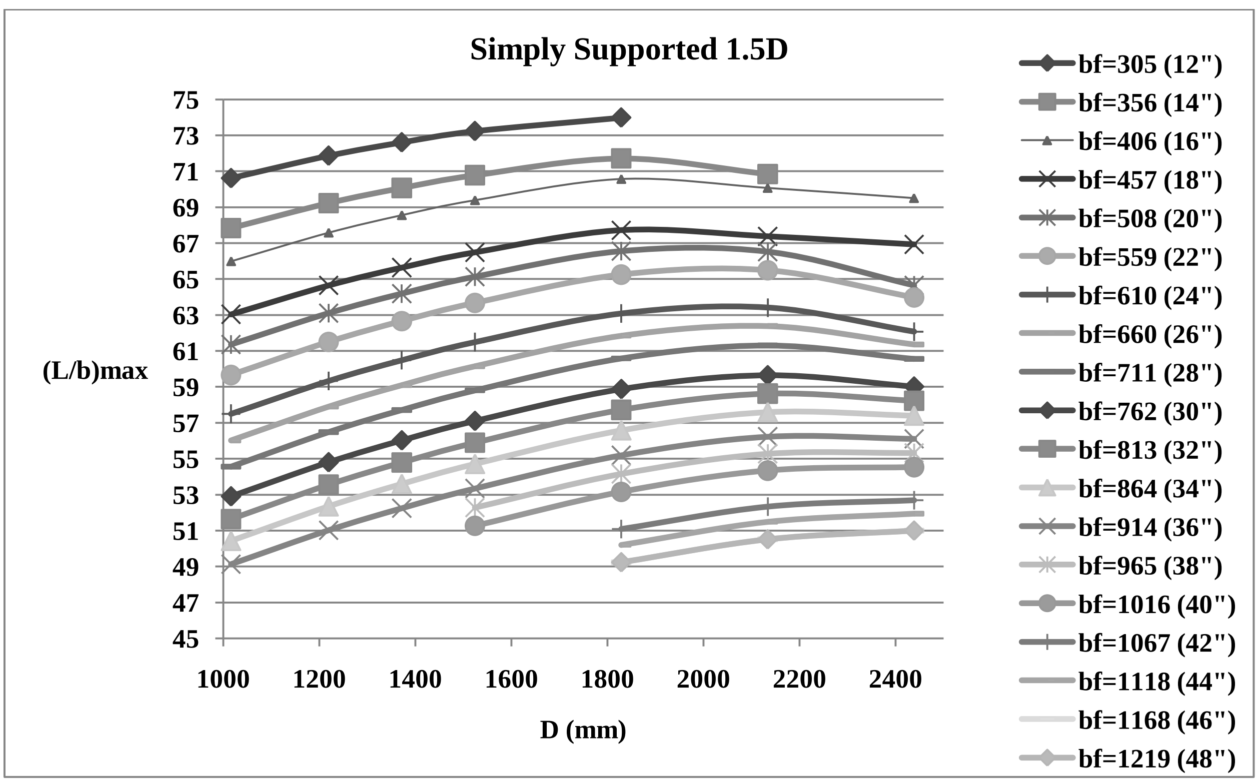
Simply Supported 1.5D
(L/b)max
75
73
71
69
67
65
63
61
59
57
55
53
51
49
47
45
1000
1200
1400
1600
1800
2000
2200
2400
D (mm)
bf=305 (12")
bf=356 (14")
bf=406 (16")
bf=457 (18")
bf=508 (20")
bf=559 (22")
bf=610 (24")
bf=660 (26")
bf=711 (28")
bf=762 (30")
bf=813 (32")
bf=864 (34")
bf=914 (36")
bf=965 (38")
bf=1016 (40")
bf=1067 (42")
bf=1118 (44")
bf=1168 (46")
bf=1219 (48")

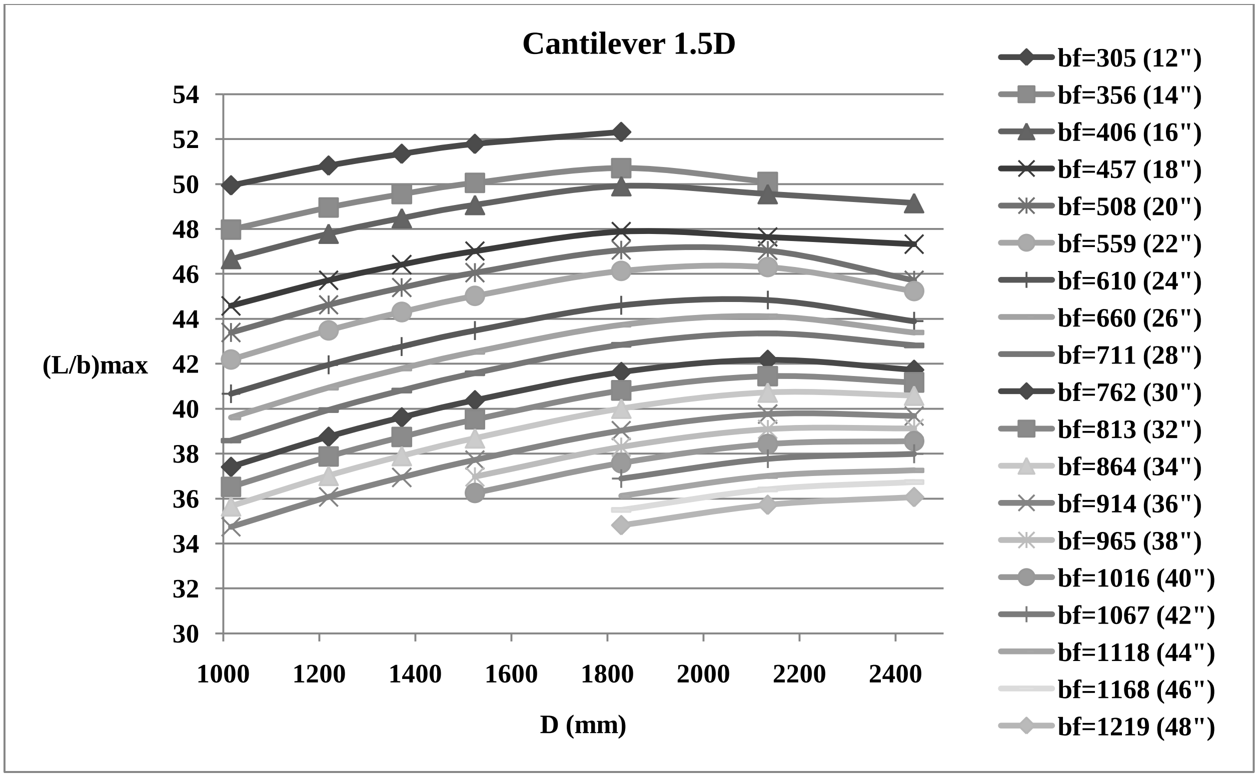
Cantilever 1.5D
(L/b)max
D (mm)
54
52
50
48
46
44
42
40
38
36
34
32
30
1000
1200
1400
1600
1800
2000
2200
2400
bf=305 (12")
bf=356 (14")
bf=406 (16")
bf=457 (18")
bf=508 (20")
bf=559 (22")
bf=610 (24")
bf=660 (26")
bf=711 (28")
bf=762 (30")
bf=813 (32")
bf=864 (34")
bf=914 (36")
bf=965 (38")
bf=1016 (40")
bf=1067 (42")
bf=1118 (44")
bf=1168 (46")
bf=1219 (48")

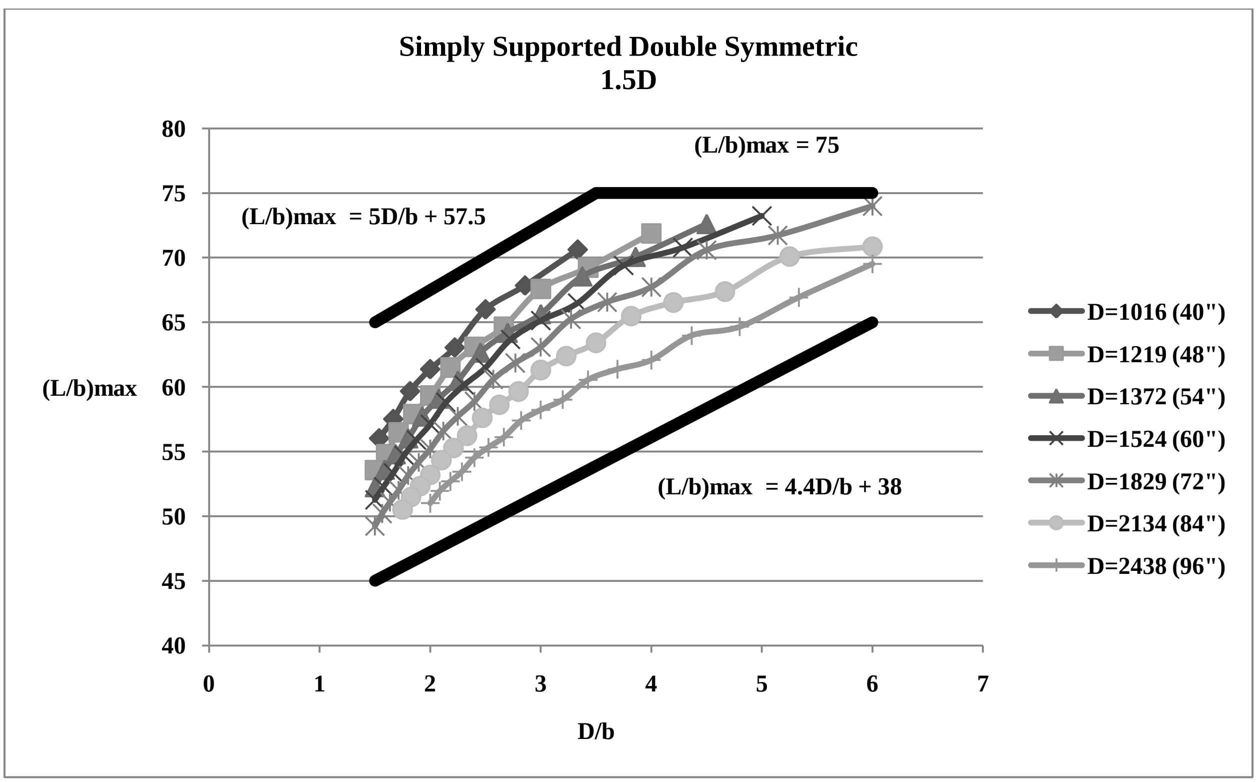
Simply Supported Double Symmetric
1.5D
(L/b)max = 75
(L/b)max = 5D/b + 57.5
(L/b)max = 4.4D/b + 38
(L/b)max
D/b
80
75
70
65
60
55
50
45
40
0
1
2
3
4
5
6
7
D=1016 (40")
D=1219 (48")
D=1372 (54")
D=1524 (60")
D=1829 (72")
D=2134 (84")
D=2438 (96")

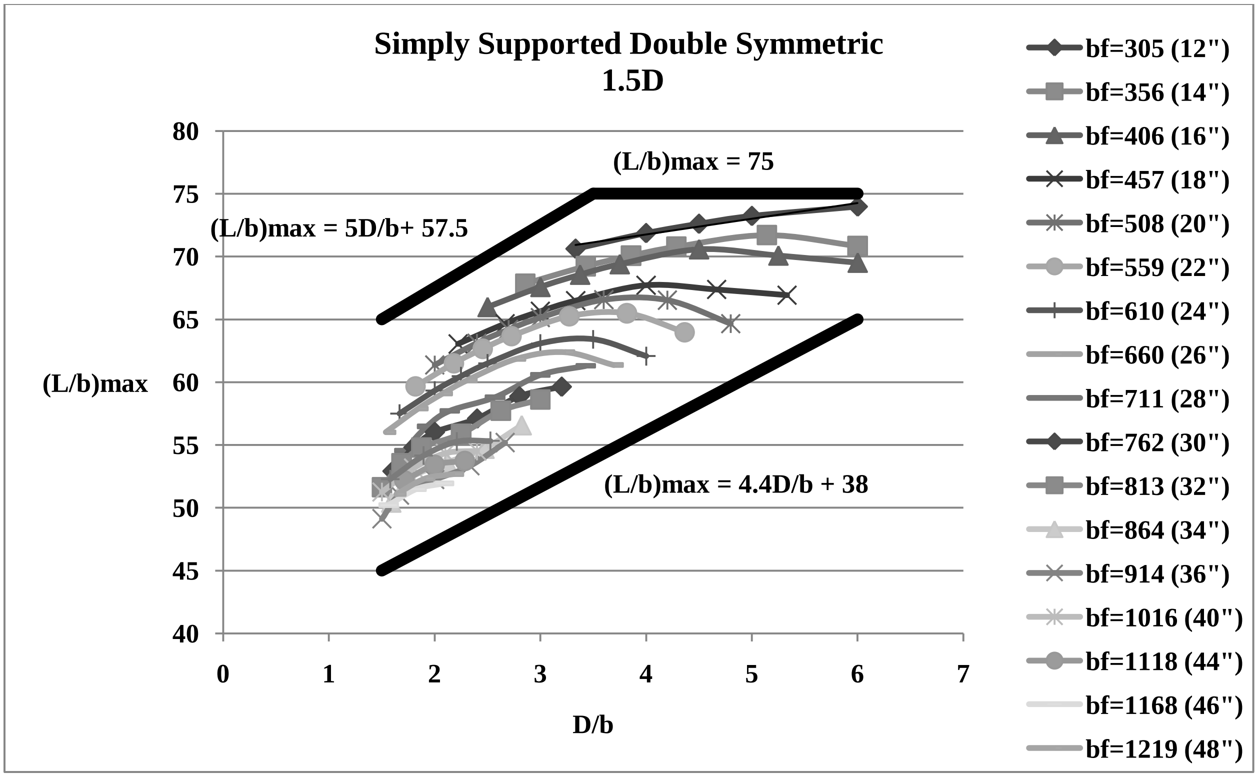
Simply Supported Double Symmetric
1.5D
(L/b)max = 75
(L/b)max = 5D/b+ 57.5
(L/b)max = 4.4D/b + 38
(L/b)max
D/b
80
75
70
65
60
55
50
45
40
0
1
2
3
4
5
6
7
bf=305 (12")
bf=356 (14")
bf=406 (16")
bf=457 (18")
bf=508 (20")
bf=559 (22")
bf=610 (24")
bf=660 (26")
bf=711 (28")
bf=762 (30")
bf=813 (32")
bf=864 (34")
bf=914 (36")
bf=1016 (40")
bf=1118 (44")
bf=1168 (46")
bf=1219 (48")

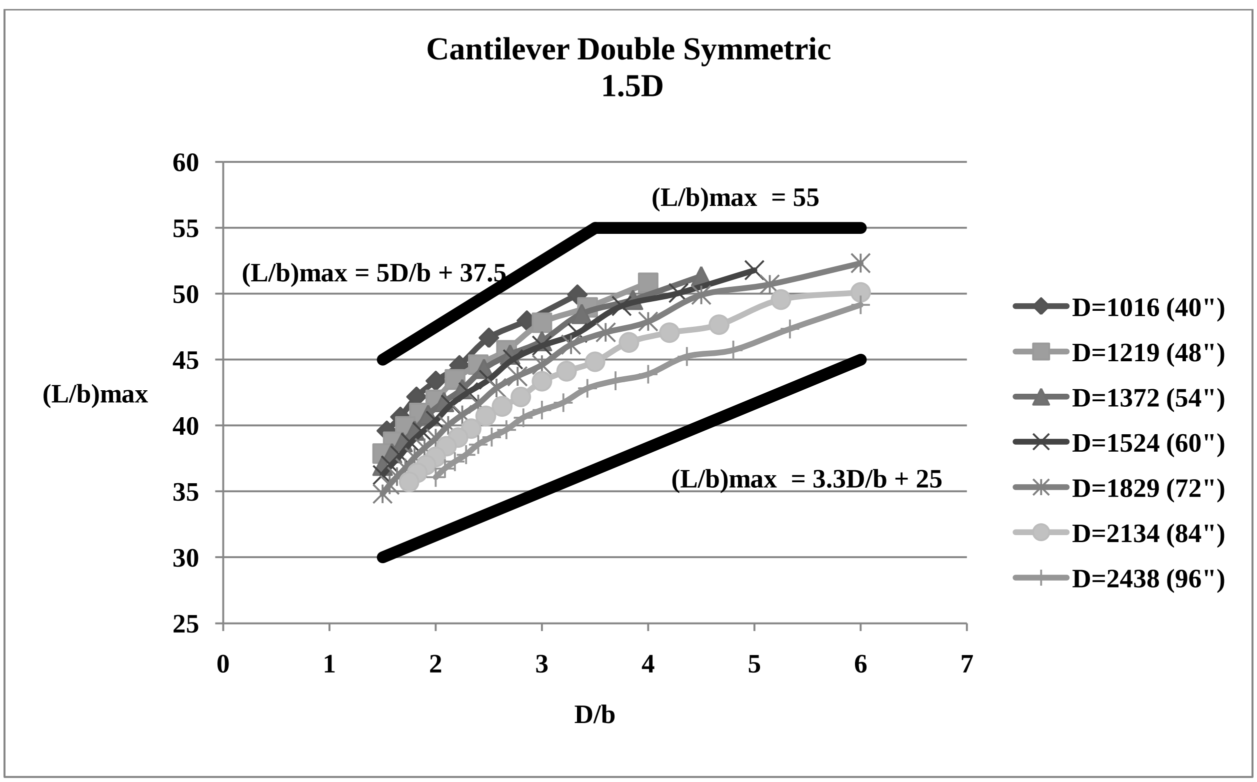
Cantilever Double Symmetric
1.5D
(L/b)max = 55
(L/b)max = 5D/b + 37.5
(L/b)max = 3.3D/b + 25
(L/b)max
D/b
60
55
50
45
40
35
30
25
0
1
2
3
4
5
6
7
D=1016 (40")
D=1219 (48")
D=1372 (54")
D=1524 (60")
D=1829 (72")
D=2134 (84")
D=2438 (96")

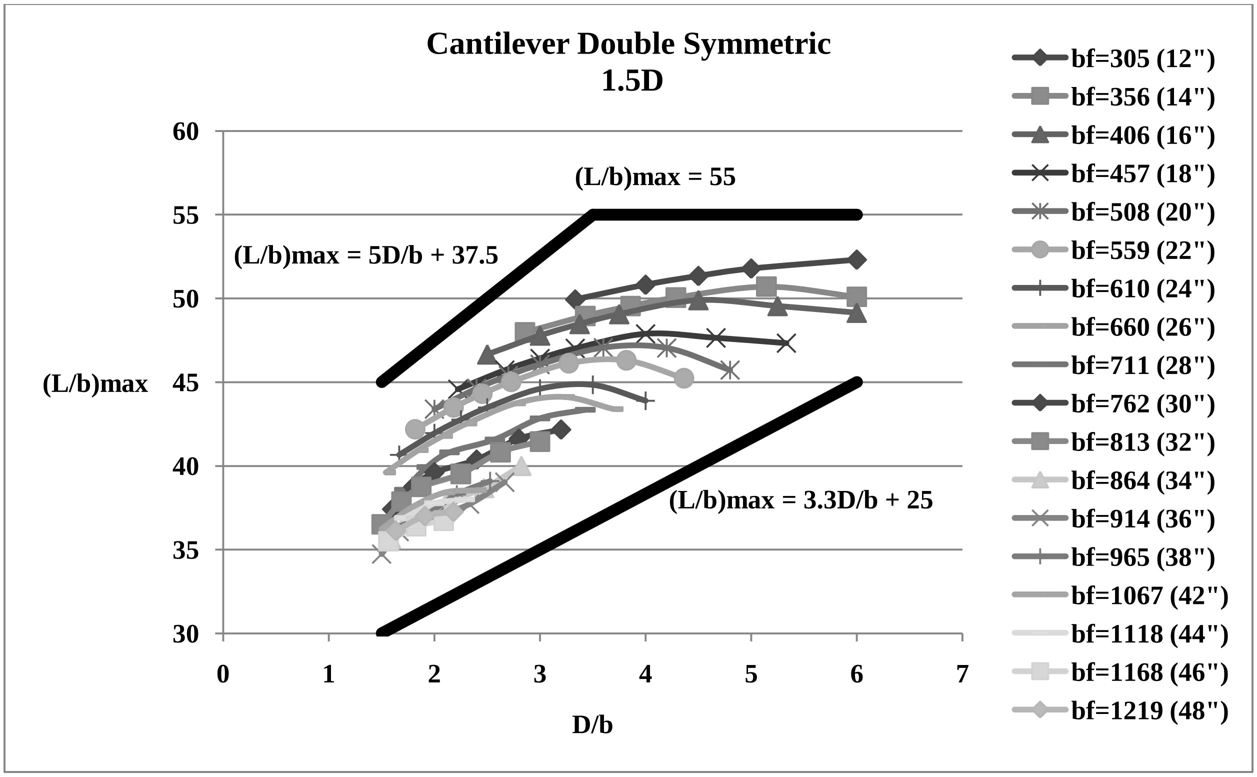
Cantilever Double Symmetric
1.5D
(L/b)max = 55
(L/b)max = 5D/b + 37.5
(L/b)max = 3.3D/b + 25
(L/b)max
D/b
60
55
50
45
40
35
30
0
1
2
3
4
5
6
7
bf=305 (12")
bf=356 (14")
bf=406 (16")
bf=457 (18")
bf=508 (20")
bf=559 (22")
bf=610 (24")
bf=660 (26")
bf=711 (28")
bf=762 (30")
bf=813 (32")
bf=864 (34")
bf=914 (36")
bf=965 (38")
bf=1067 (42")
bf=1118 (44")
bf=1168 (46")
bf=1219 (48")

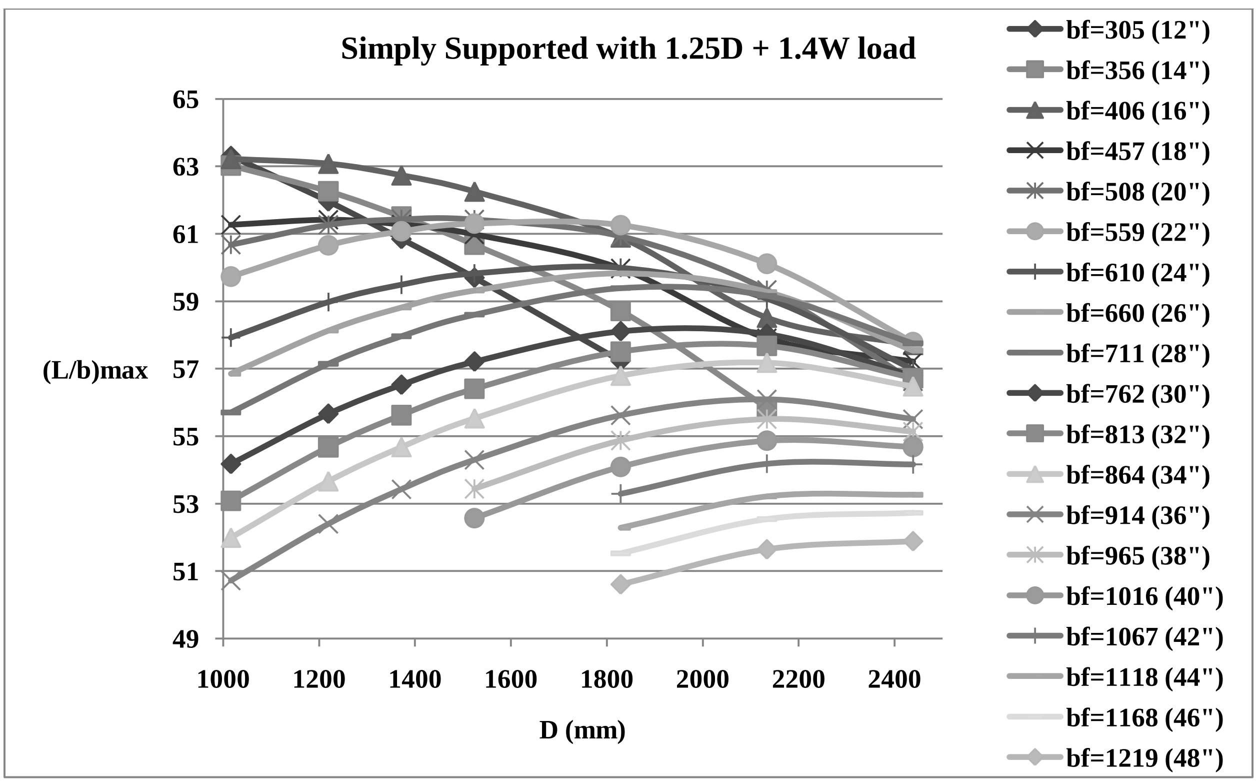
Simply Supported with 1.25D + 1.4W load
(L/b)max
D (mm)
65
63
61
59
57
55
53
51
49
1000
1200
1400
1600
1800
2000
2200
2400
bf=305 (12")
bf=356 (14")
bf=406 (16")
bf=457 (18")
bf=508 (20")
bf=559 (22")
bf=610 (24")
bf=660 (26")
bf=711 (28")
bf=762 (30")
bf=813 (32")
bf=864 (34")
bf=914 (36")
bf=965 (38")
bf=1016 (40")
bf=1067 (42")
bf=1118 (44")
bf=1168 (46")
bf=1219 (48")

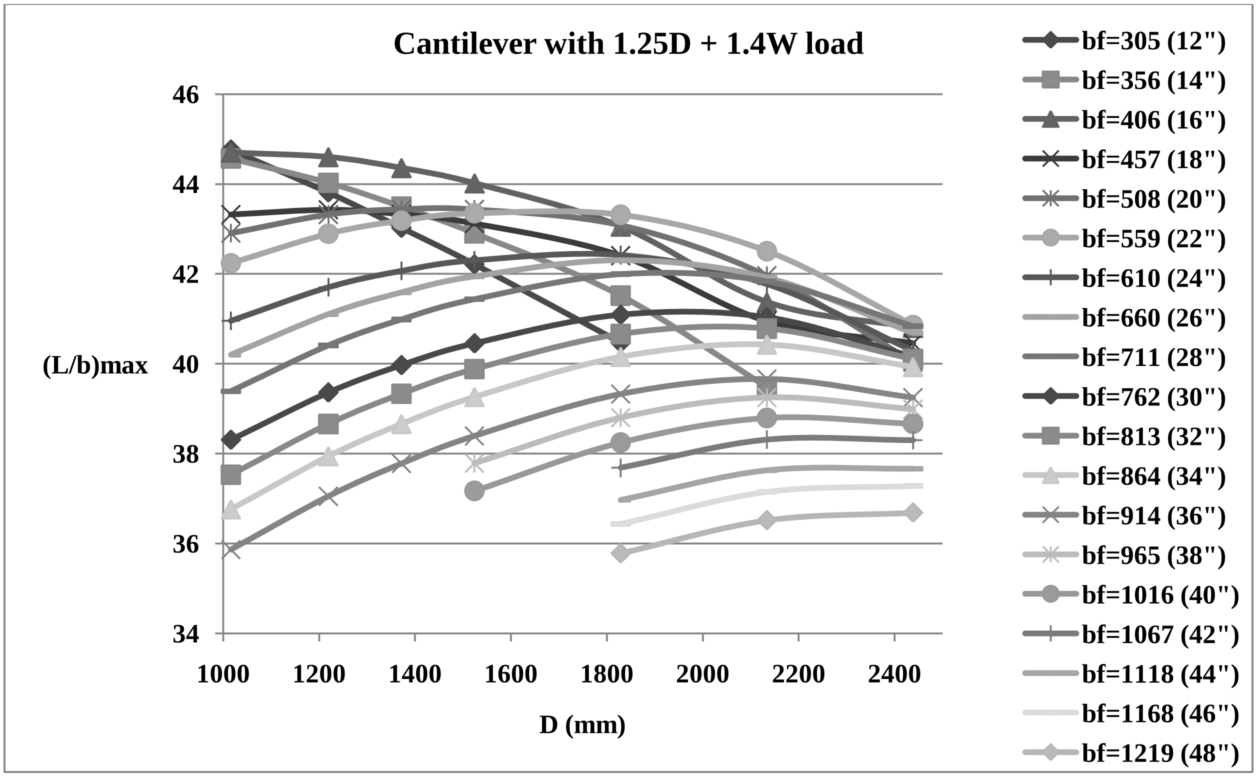
Cantilever with 1.25D + 1.4W load
(L/b)max
D (mm)
46
44
42
40
38
36
34
1000
1200
1400
1600
1800
2000
2200
2400
bf=305 (12")
bf=356 (14")
bf=406 (16")
bf=457 (18")
bf=508 (20")
bf=559 (22")
bf=610 (24")
bf=660 (26")
bf=711 (28")
bf=762 (30")
bf=813 (32")
bf=864 (34")
bf=914 (36")
bf=965 (38")
bf=1016 (40")
bf=1067 (42")
bf=1118 (44")
bf=1168 (46")
bf=1219 (48")

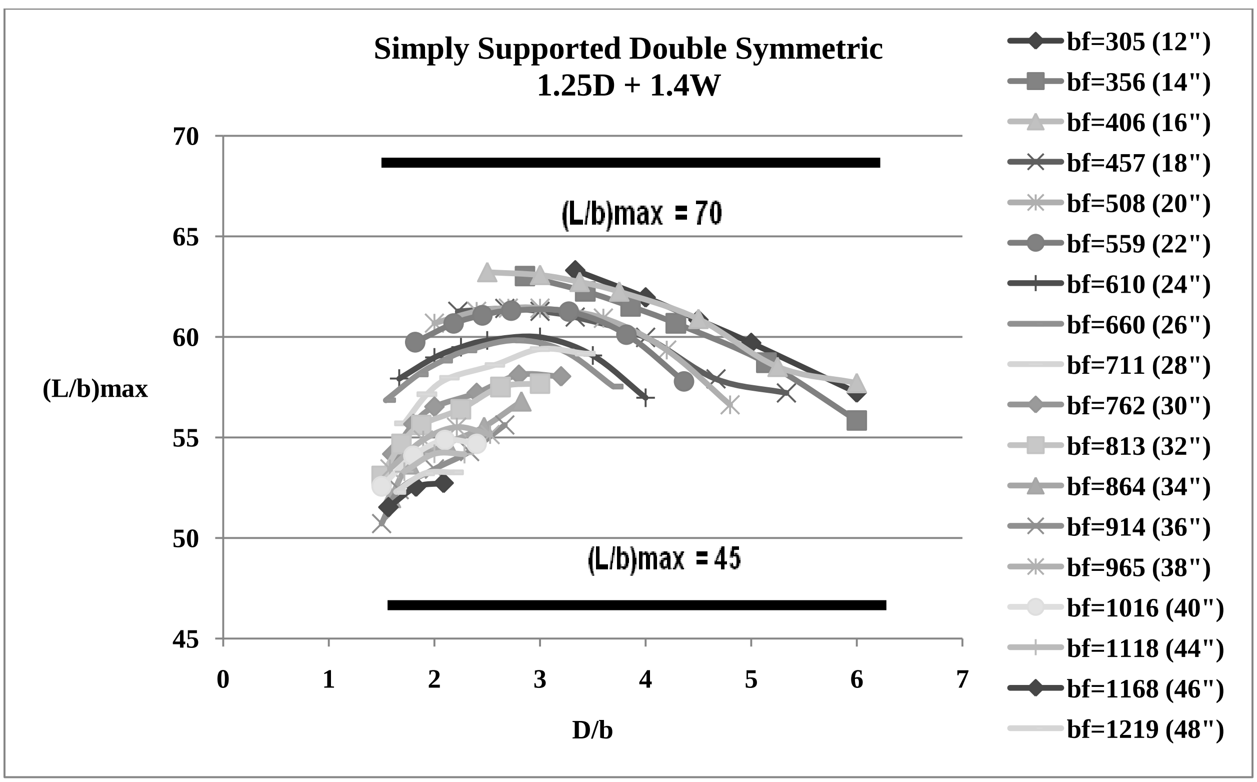
Simply Supported Double Symmetric
1.25D + 1.4W
(L/b)max = 70
(L/b)max = 45
(L/b)max
D/b
70
65
60
55
50
45
0
1
2
3
4
5
6
7
bf=305 (12")
bf=356 (14")
bf=406 (16")
bf=457 (18")
bf=508 (20")
bf=559 (22")
bf=610 (24")
bf=660 (26")
bf=711 (28")
bf=762 (30")
bf=813 (32")
bf=864 (34")
bf=914 (36")
bf=965 (38")
bf=1016 (40")
bf=1118 (44")
bf=1168 (46")
bf=1219 (48")

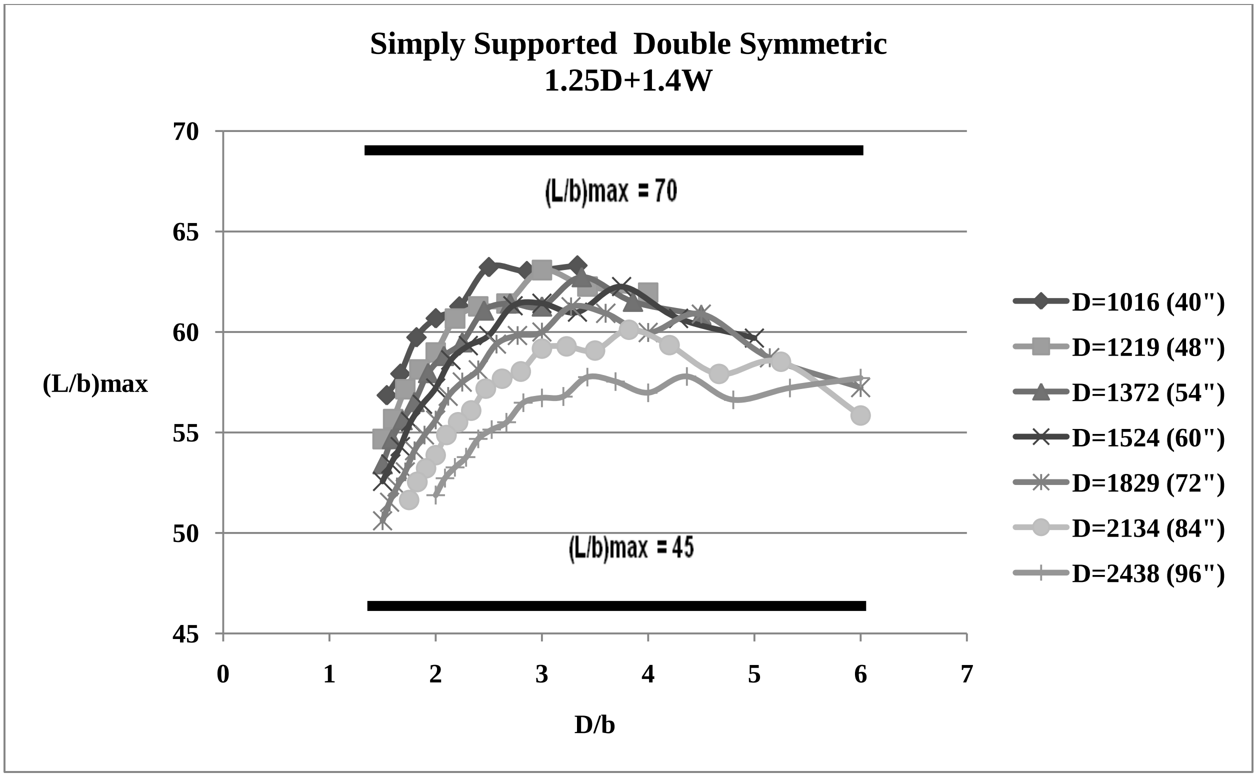
Simply Supported Double Symmetric
1.25D+1.4W
(L/b)max = 70
(L/b)max = 45
(L/b)max
D/b
D=1016 (40")
D=1219 (48")
D=1372 (54")
D=1524 (60")
D=1829 (72")
D=2134 (84")
D=2438 (96")

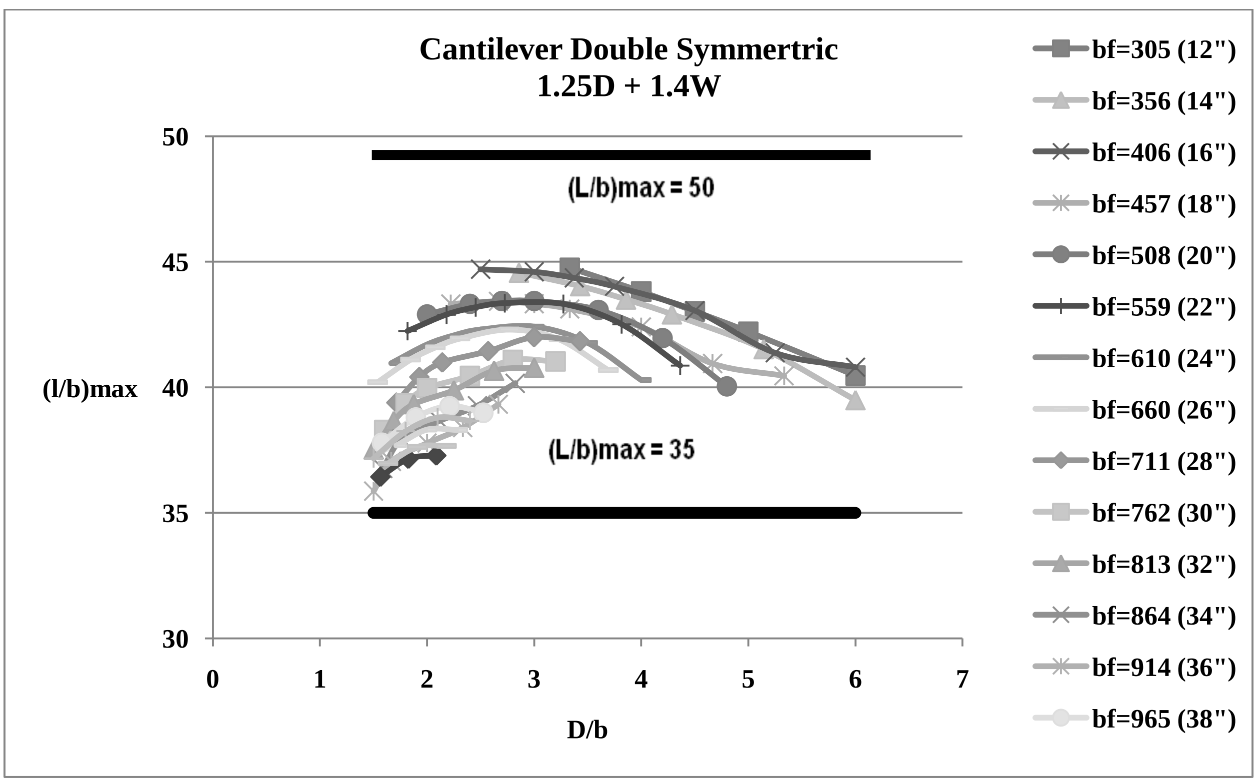
Cantilever Double Symmertric
1.25D + 1.4W
(L/b)max = 50
(L/b)max = 35
(l/b)max
D/b
bf=305 (12")
bf=356 (14")
bf=406 (16")
bf=457 (18")
bf=508 (20")
bf=559 (22")
bf=610 (24")
bf=660 (26")
bf=711 (28")
bf=762 (30")
bf=813 (32")
bf=864 (34")
bf=914 (36")
bf=965 (38")

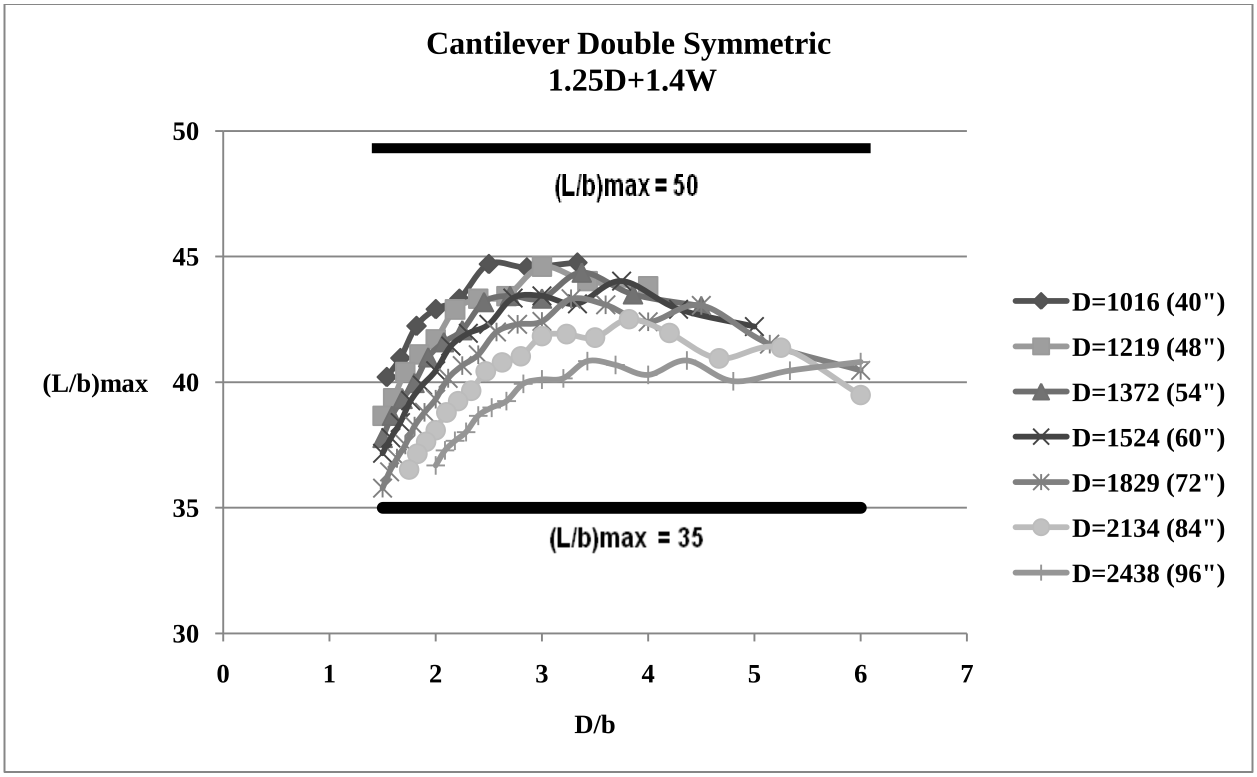
Cantilever Double Symmetric
1.25D+1.4W
(L/b)max = 50
(L/b)max = 35
(L/b)max
50
45
40
35
30
0
1
2
3
4
5
6
7
D/b
D=1016 (40")
D=1219 (48")
D=1372 (54")
D=1524 (60")
D=1829 (72")
D=2134 (84")
D=2438 (96")

APPENDIX B: SINGLE SYMMETRIC SINGLE GIRDERS

Appendix B shows all plots related to single symmetric single girders. Load Combos IV and III are investigated and (L/b)max vs. D/b plots are shown.

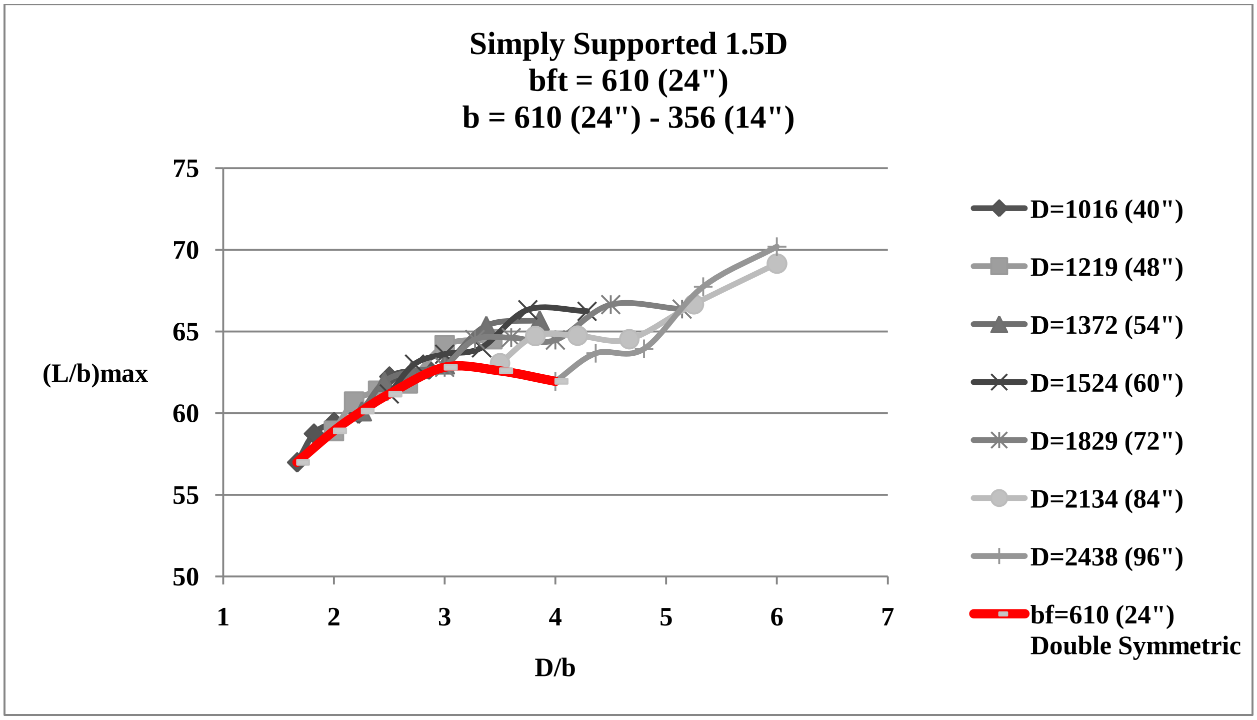

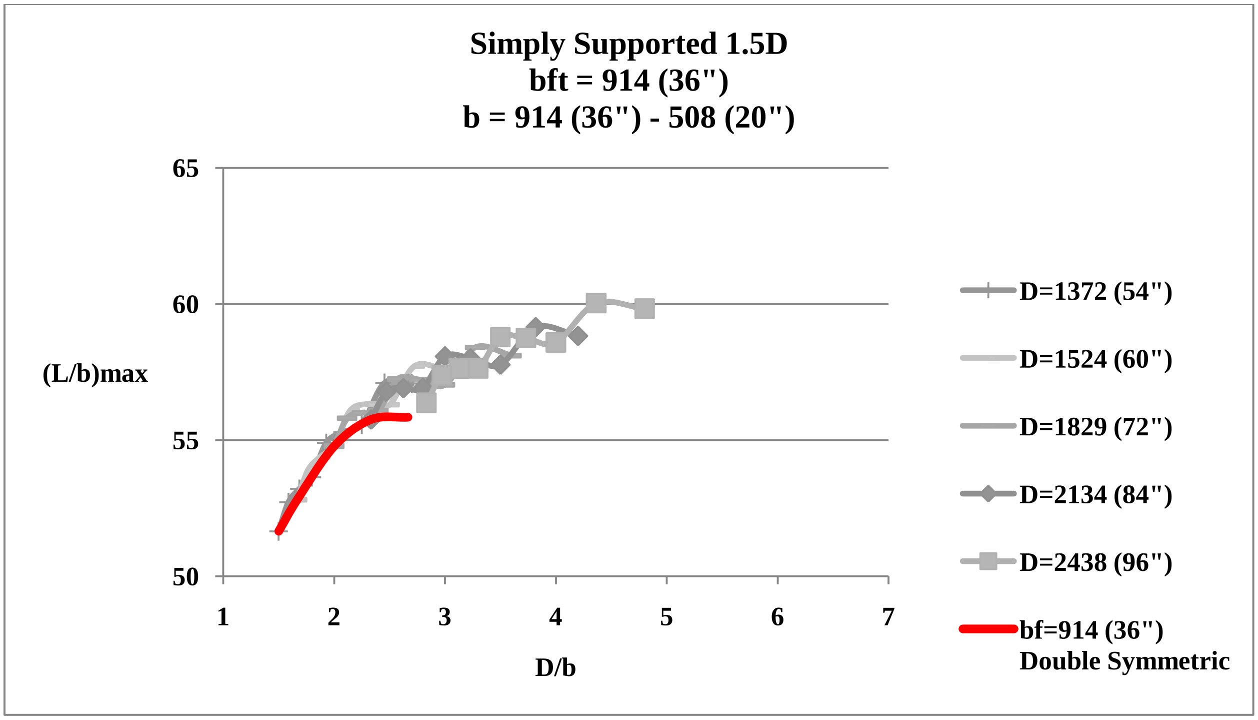
Simply Supported 1.5D
bft = 914 (36")
b = 914 (36") - 508 (20")
(L/b)max
65
60
55
50
1
2
3
4
5
6
7
D/b
D=1372 (54")
D=1524 (60")
D=1829 (72")
D=2134 (84")
D=2438 (96")
bf=914 (36")
Double Symmetric

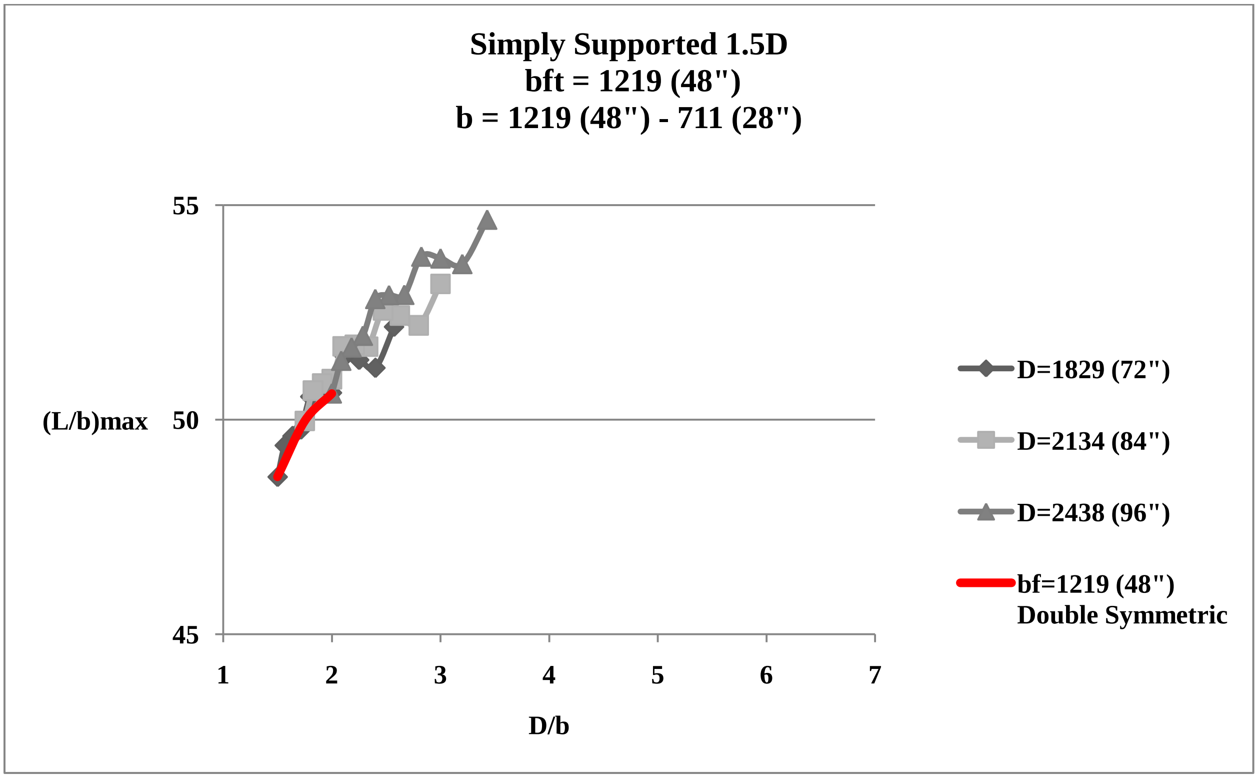
Simply Supported 1.5D
bft = 1219 (48")
b = 1219 (48") - 711 (28")
(L/b)max
55
50
45
1
2
3
4
5
6
7
D/b
D=1829 (72")
D=2134 (84")
D=2438 (96")
bf=1219 (48")
Double Symmetric

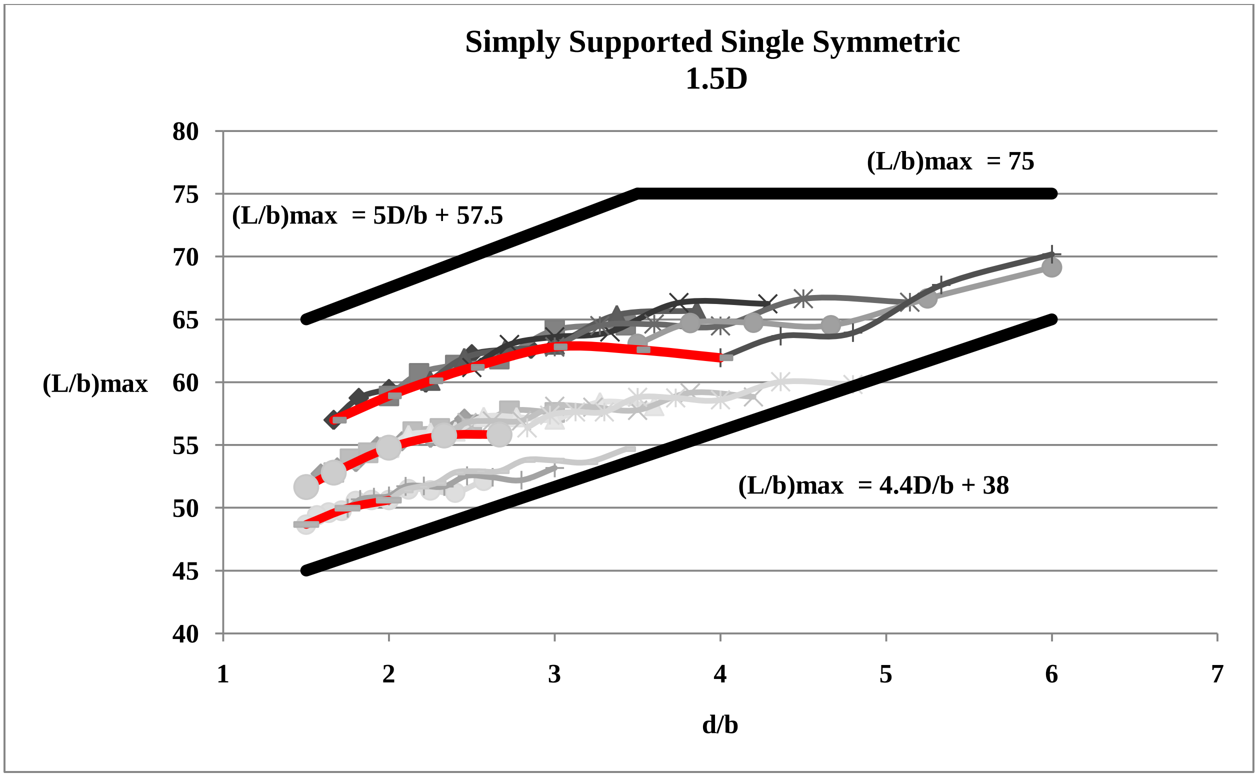
Simply Supported Single Symmetric
1.5D
(L/b)max = 75
(L/b)max = 5D/b + 57.5
(L/b)max = 4.4D/b + 38
(L/b)max
d/b
80
75
70
65
60
55
50
45
40
1
2
3
4
5
6
7

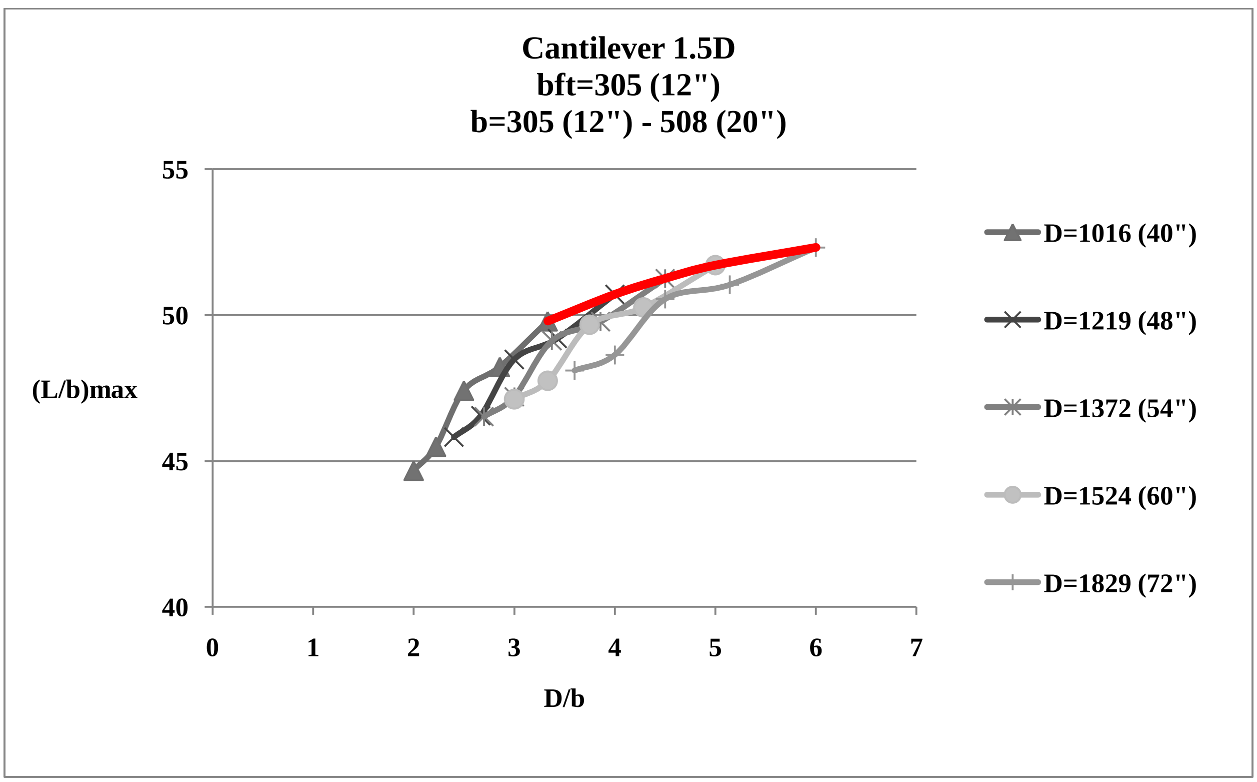
Cantilever 1.5D
bft=305 (12")
b=305 (12") - 508 (20")
(L/b)max
D/b
55
50
45
40
0
1
2
3
4
5
6
7
D=1016 (40")
D=1219 (48")
D=1372 (54")
D=1524 (60")
D=1829 (72")

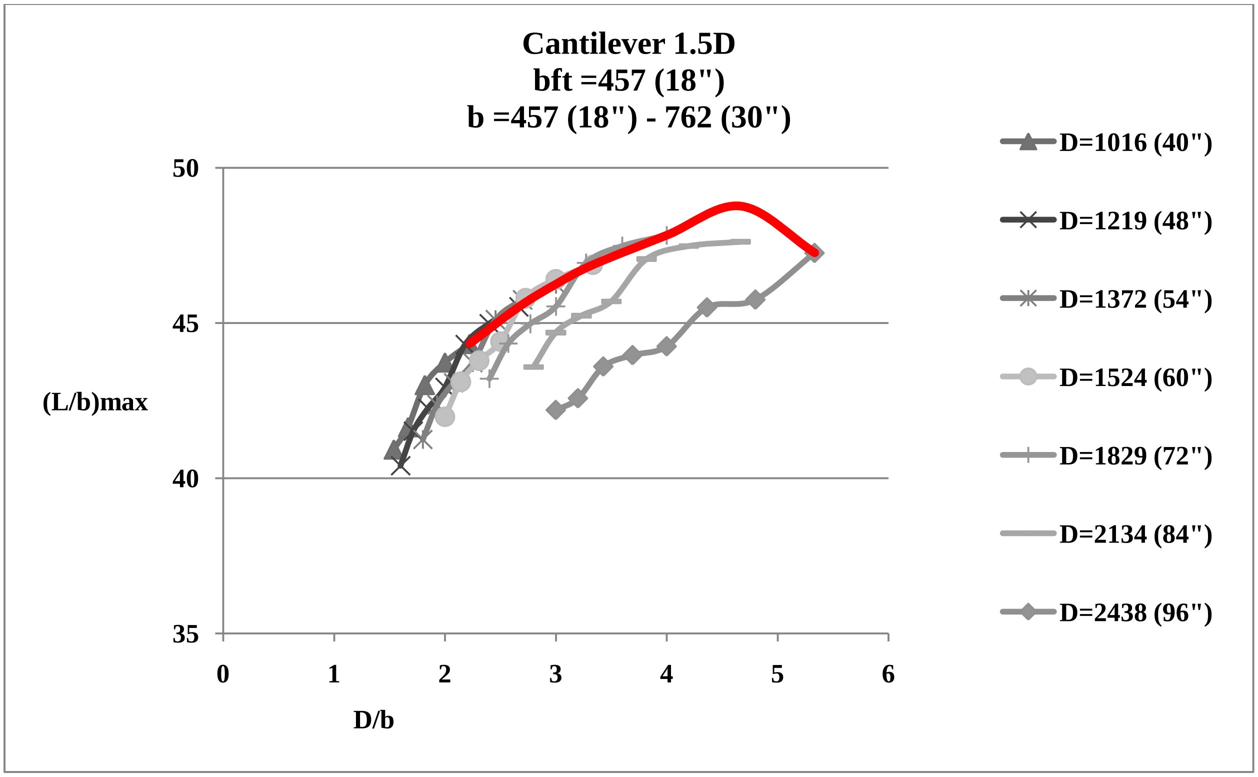
Cantilever 1.5D
bft =457 (18")
b =457 (18") - 762 (30")
50
45
40
35
(L/b)max
0
1
2
3
4
5
6
D/b
D=1016 (40")
D=1219 (48")
D=1372 (54")
D=1524 (60")
D=1829 (72")
D=2134 (84")
D=2438 (96")

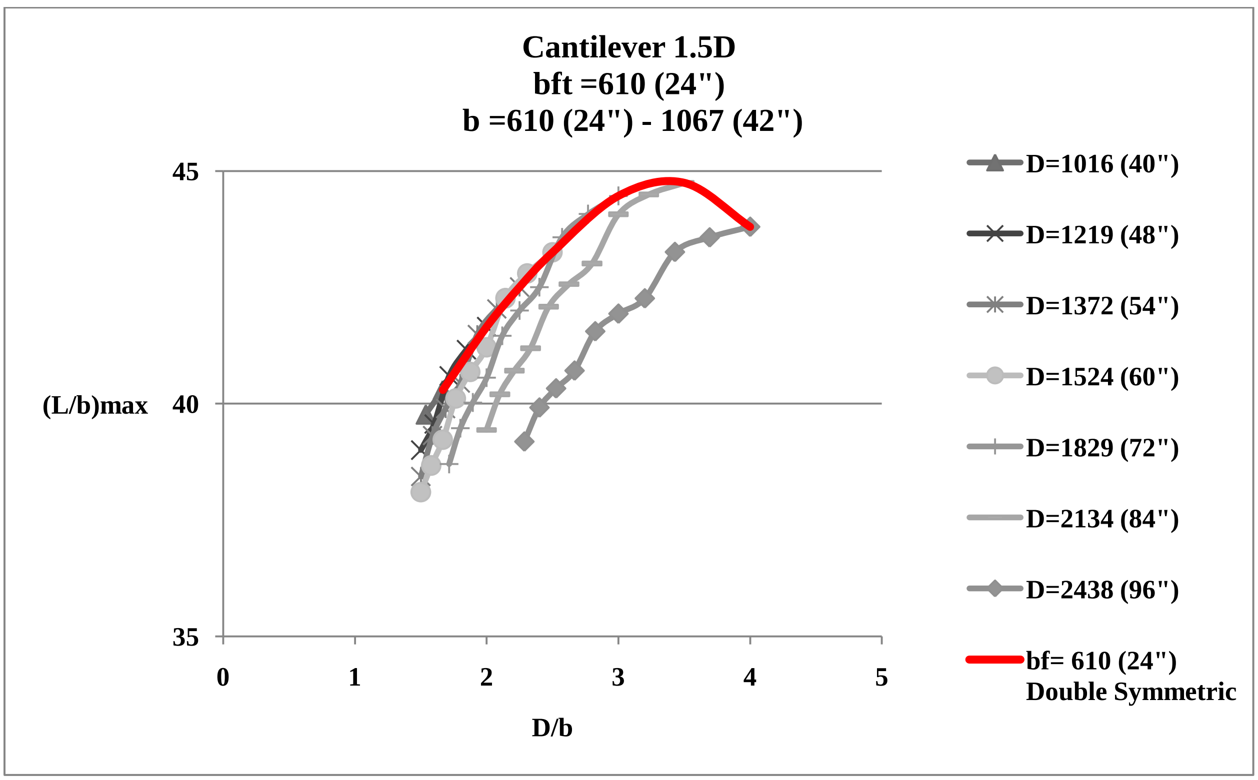
Cantilever 1.5D
bft =610 (24")
b =610 (24") - 1067 (42")
45
40
35
(L/b)max
0
1
2
3
4
5
D/b
D=1016 (40")
D=1219 (48")
D=1372 (54")
D=1524 (60")
D=1829 (72")
D=2134 (84")
D=2438 (96")
bf= 610 (24")
Double Symmetric

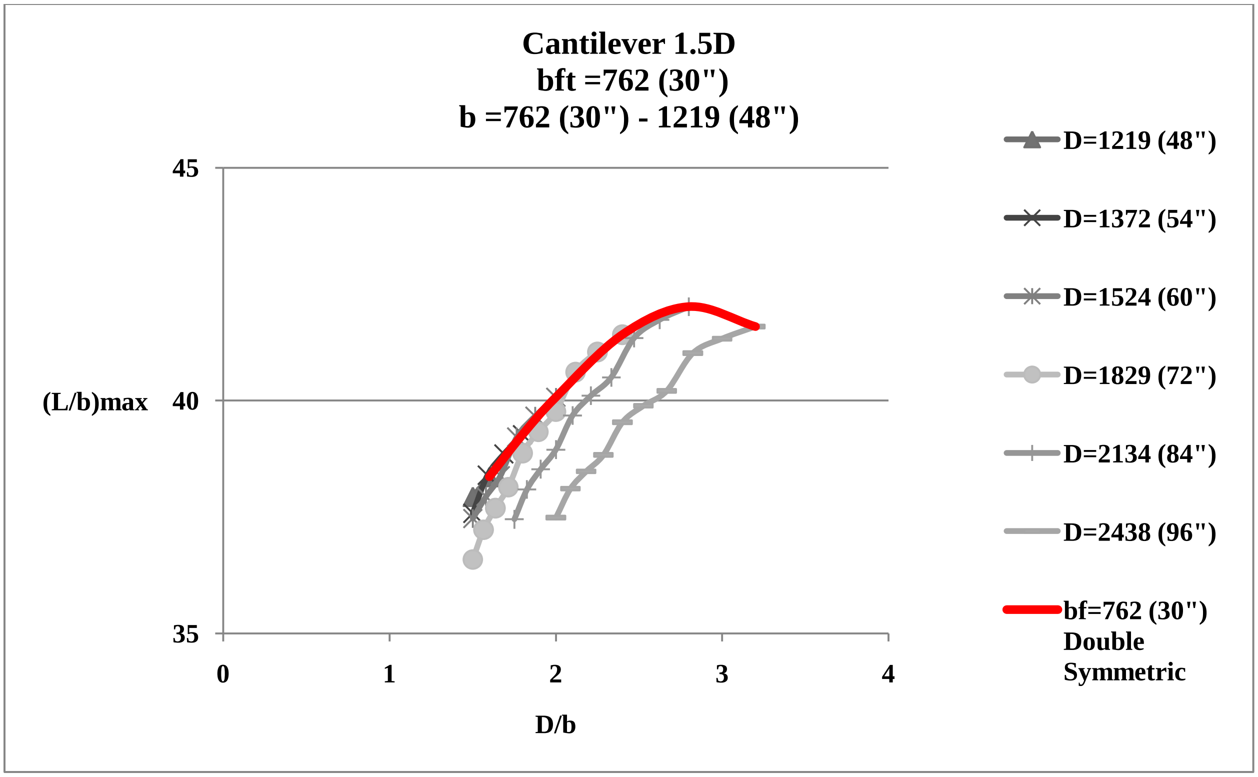
Cantilever 1.5D
bft =762 (30")
b =762 (30") - 1219 (48")
(L/b)max
45
40
35
0
1
2
3
4
D/b
D=1219 (48")
D=1372 (54")
D=1524 (60")
D=1829 (72")
D=2134 (84")
D=2438 (96")
bf=762 (30") Double Symmetric

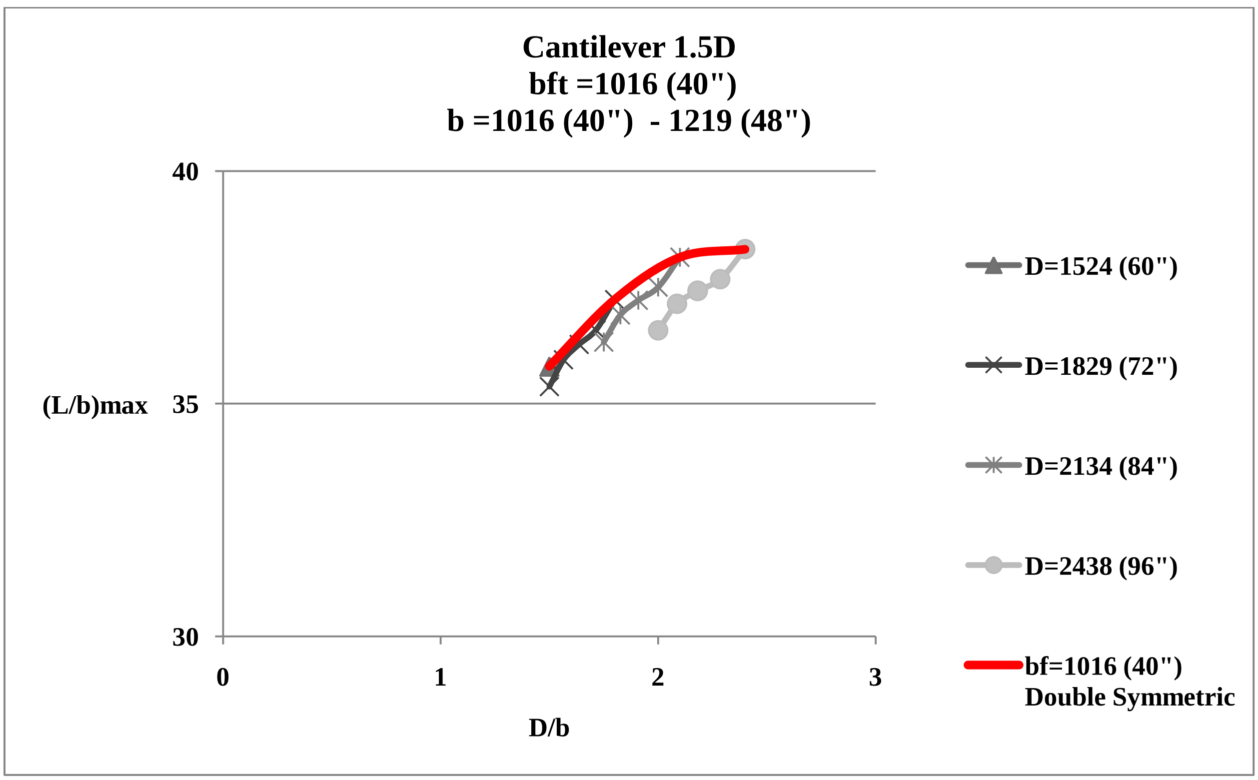
Cantilever 1.5D
bft =1016 (40")
b =1016 (40") - 1219 (48")
(L/b)max
40
35
30
0
1
2
3
D/b
D=1524 (60")
D=1829 (72")
D=2134 (84")
D=2438 (96")
bf=1016 (40") Double Symmetric

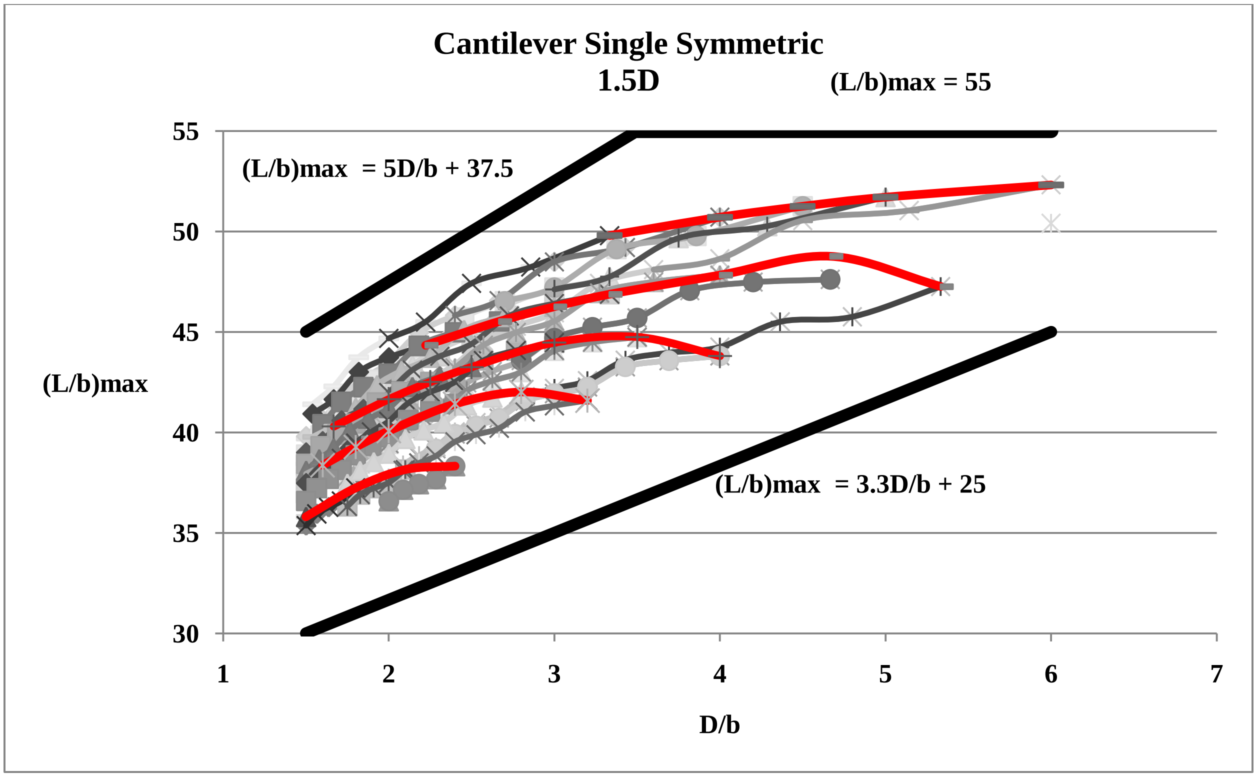

Load Combo III plots.

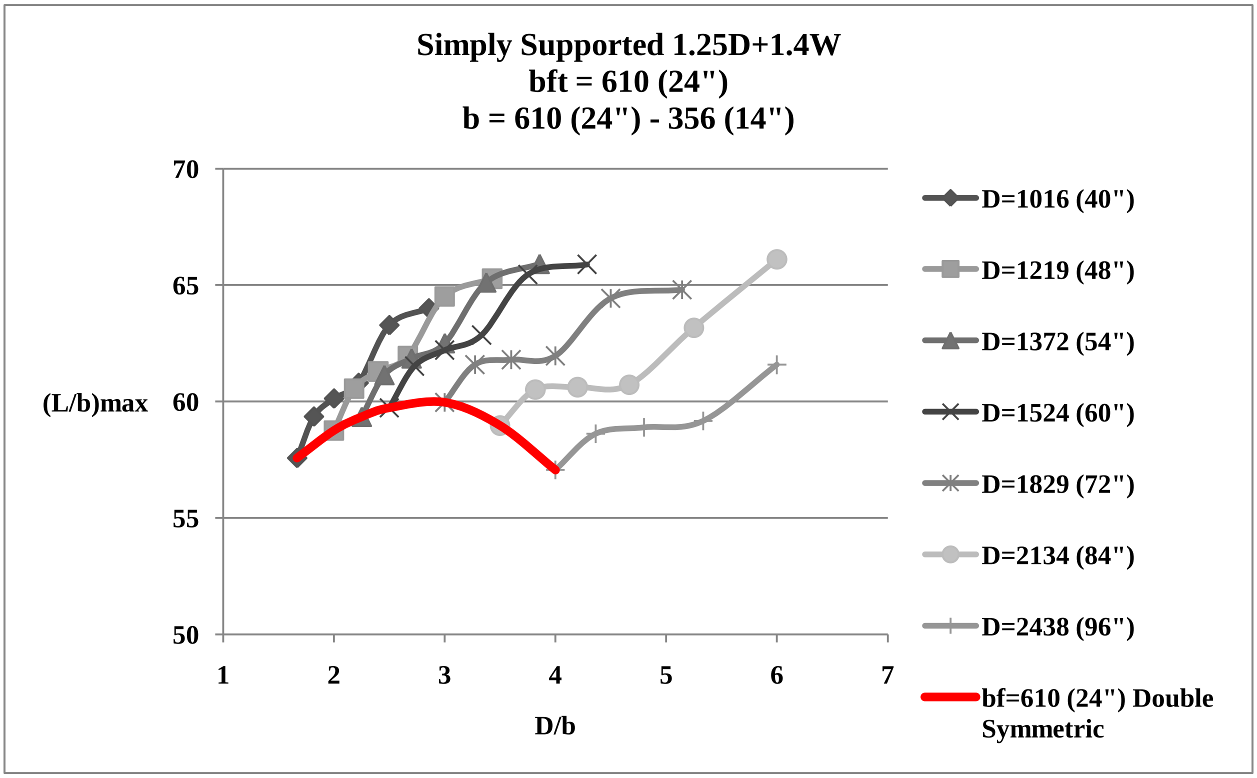

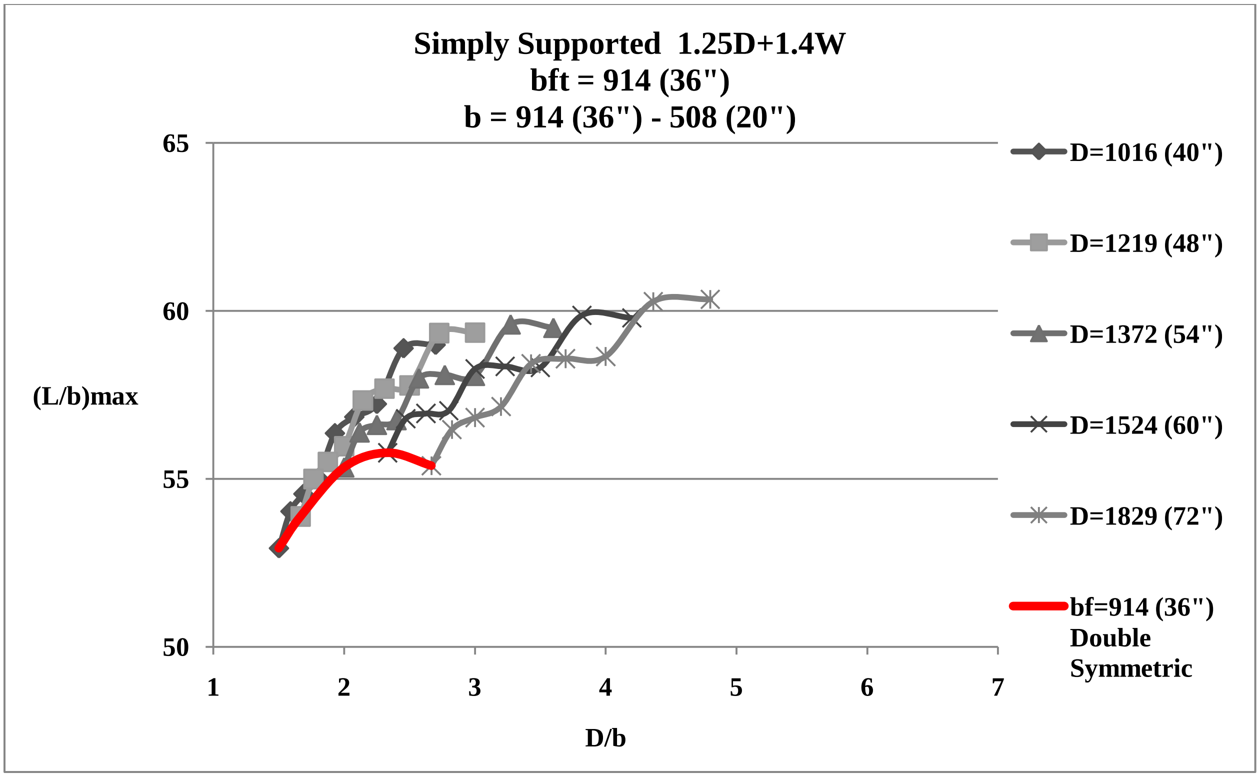

Simply Supported 1.25D+1.4W
bft = 914 (36")
b = 914 (36") - 508 (20")
65
60
55
50
(L/b)max
1
2
3
4
5
6
7
D/b
D=1016 (40")
D=1219 (48")
D=1372 (54")
D=1524 (60")
D=1829 (72")
bf=914 (36") Double Symmetric

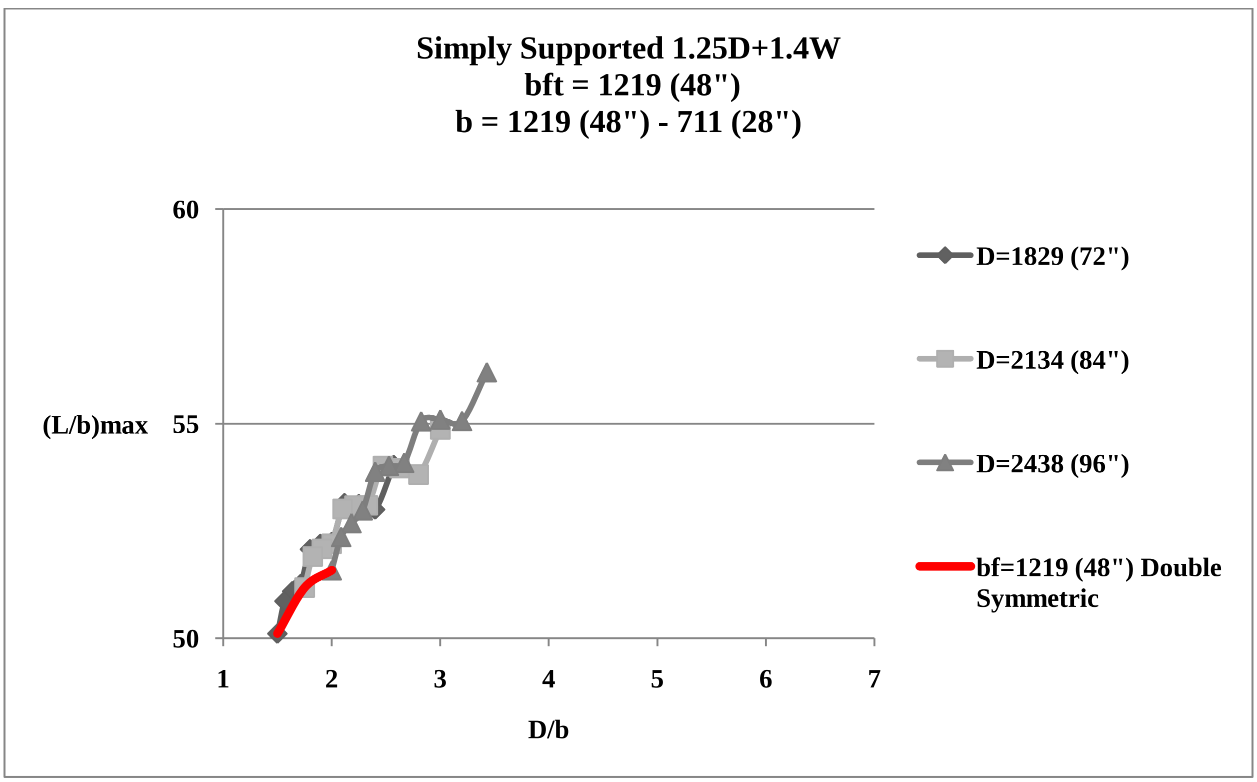

Simply Supported 1.25D+1.4W
bft = 1219 (48")
b = 1219 (48") - 711 (28")
60
55
50
(L/b)max
1
2
3
4
5
6
7
D/b
D=1829 (72")
D=2134 (84")
D=2438 (96")
bf=1219 (48") Double Symmetric

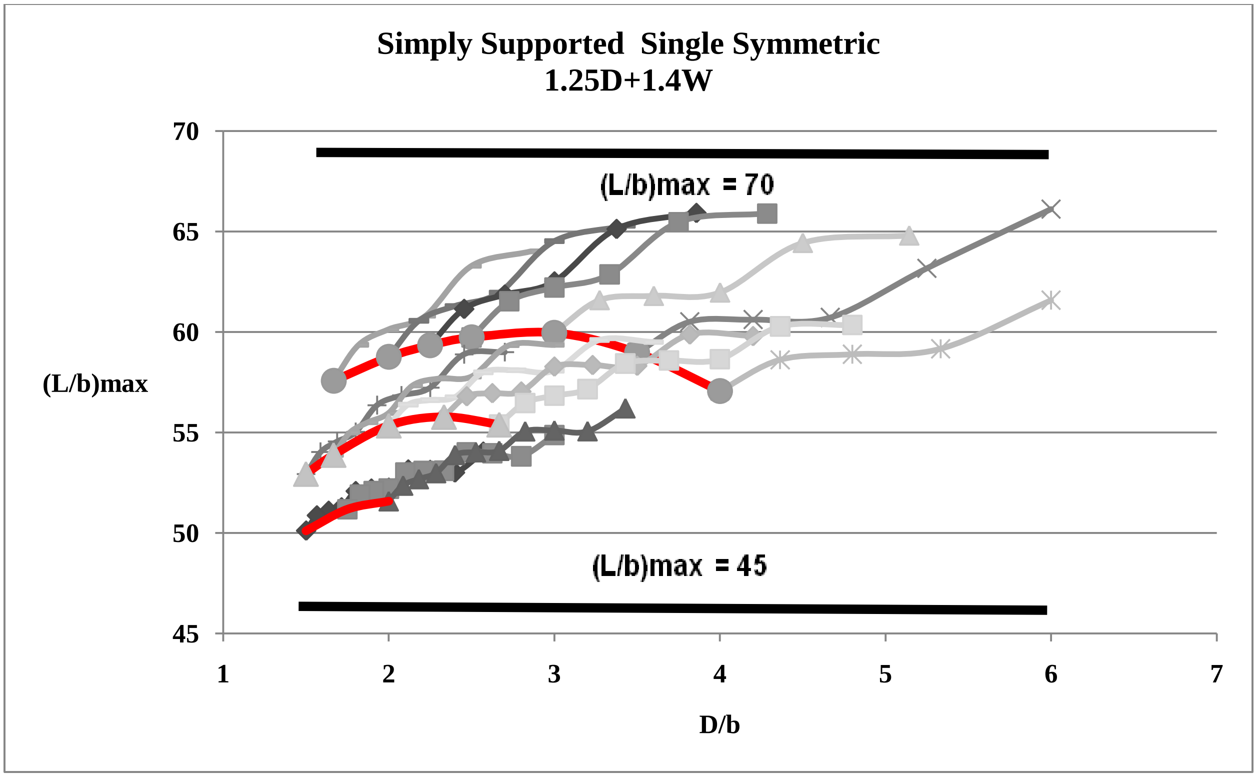
Simply Supported Single Symmetric
1.25D+1.4W
(L/b)max = 70
(L/b)max = 45
(L/b)max
D/b
70
65
60
55
50
45
1
2
3
4
5
6
7

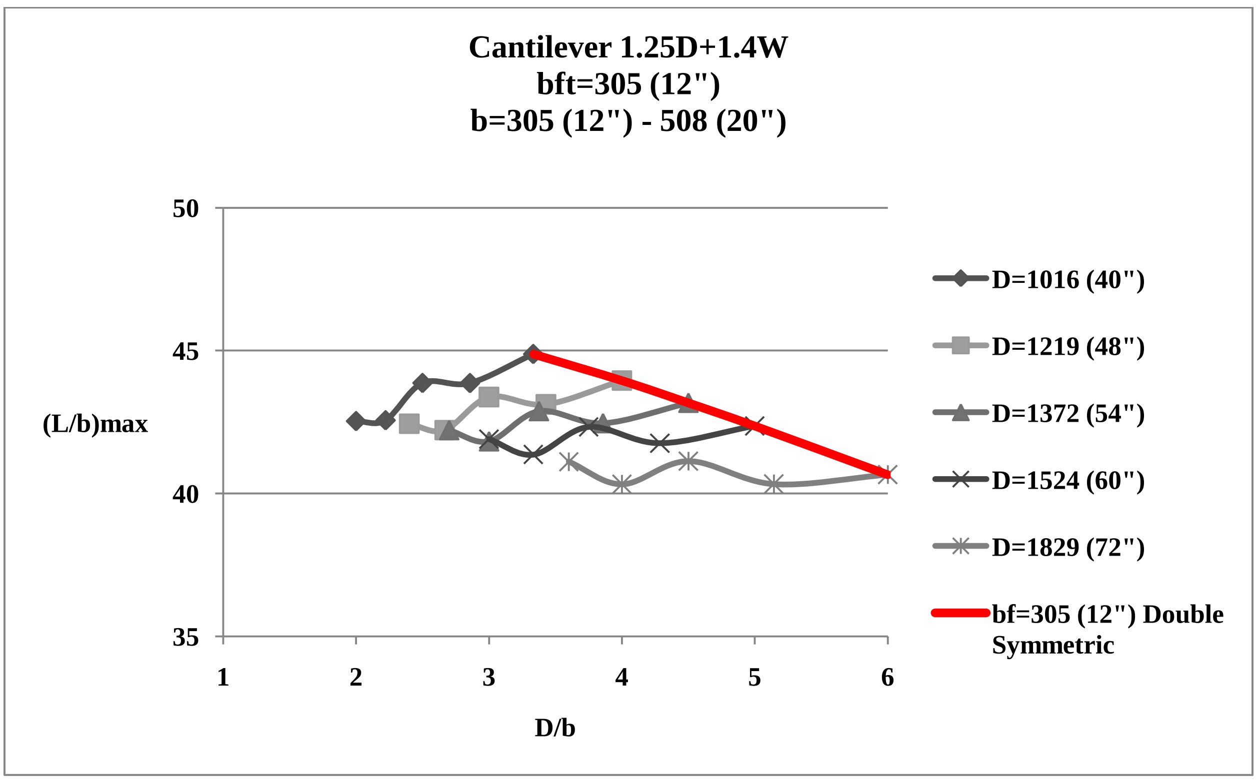
Cantilever 1.25D+1.4W
bft=305 (12")
b=305 (12") - 508 (20")
(L/b)max
D/b
50
45
40
35
1
2
3
4
5
6
D=1016 (40")
D=1219 (48")
D=1372 (54")
D=1524 (60")
D=1829 (72")
bf=305 (12") Double Symmetric

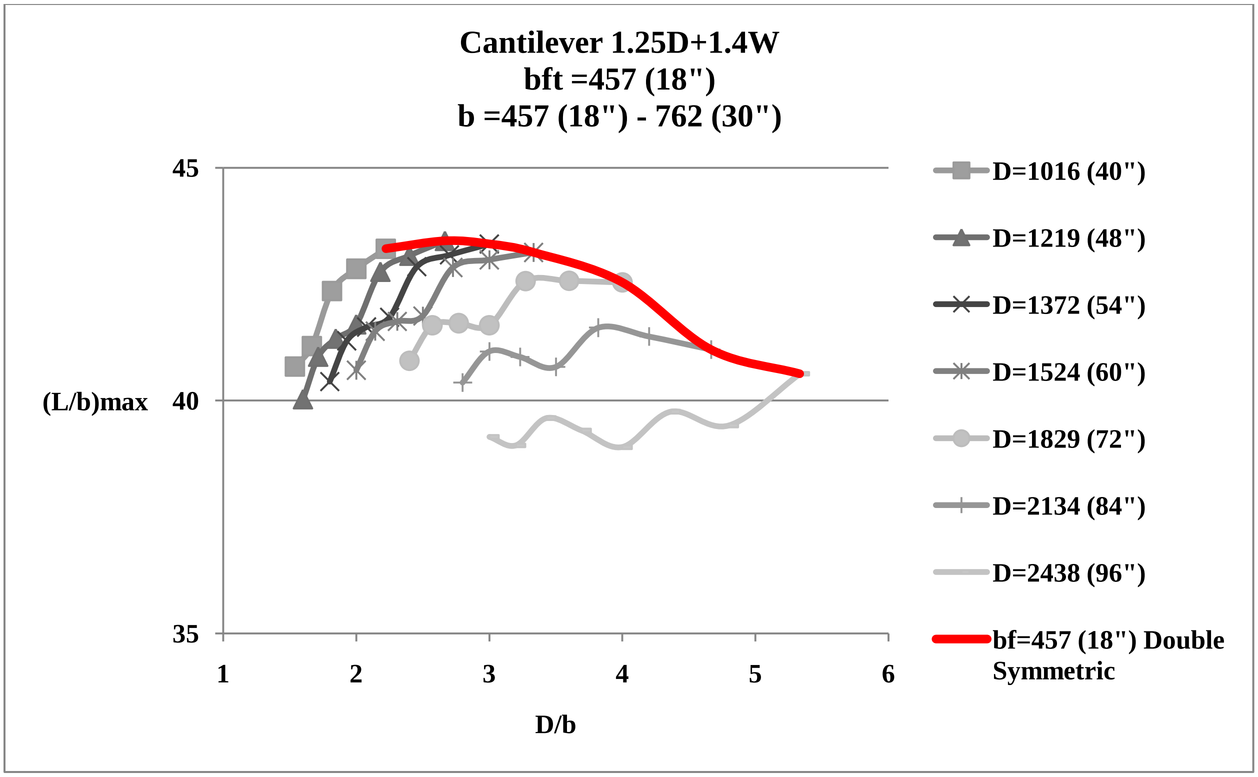
Cantilever 1.25D+1.4W
bft =457 (18")
b =457 (18") - 762 (30")
(L/b)max
45
40
35
1
2
3
4
5
6
D/b
D=1016 (40")
D=1219 (48")
D=1372 (54")
D=1524 (60")
D=1829 (72")
D=2134 (84")
D=2438 (96")
bf=457 (18") Double Symmetric

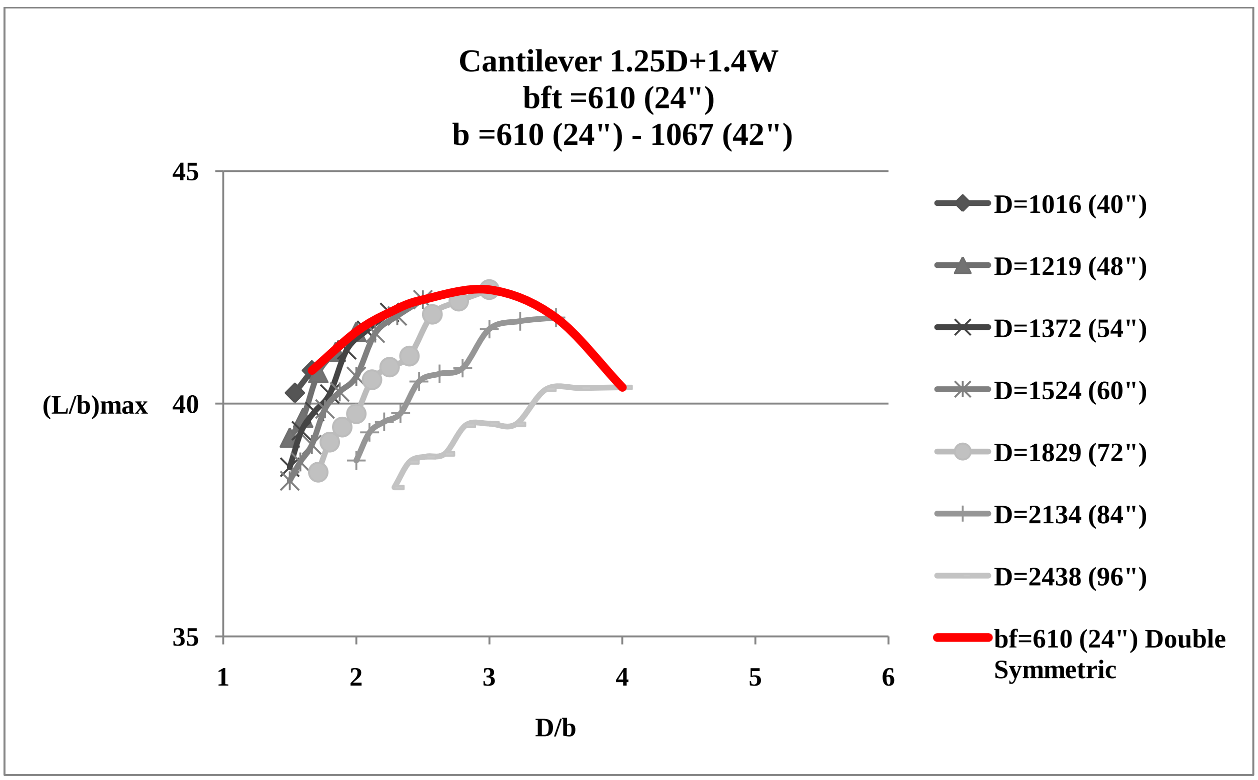
Cantilever 1.25D+1.4W
bft =610 (24")
b =610 (24") - 1067 (42")
(L/b)max
45
40
35
1
2
3
4
5
6
D/b
D=1016 (40")
D=1219 (48")
D=1372 (54")
D=1524 (60")
D=1829 (72")
D=2134 (84")
D=2438 (96")
bf=610 (24") Double Symmetric

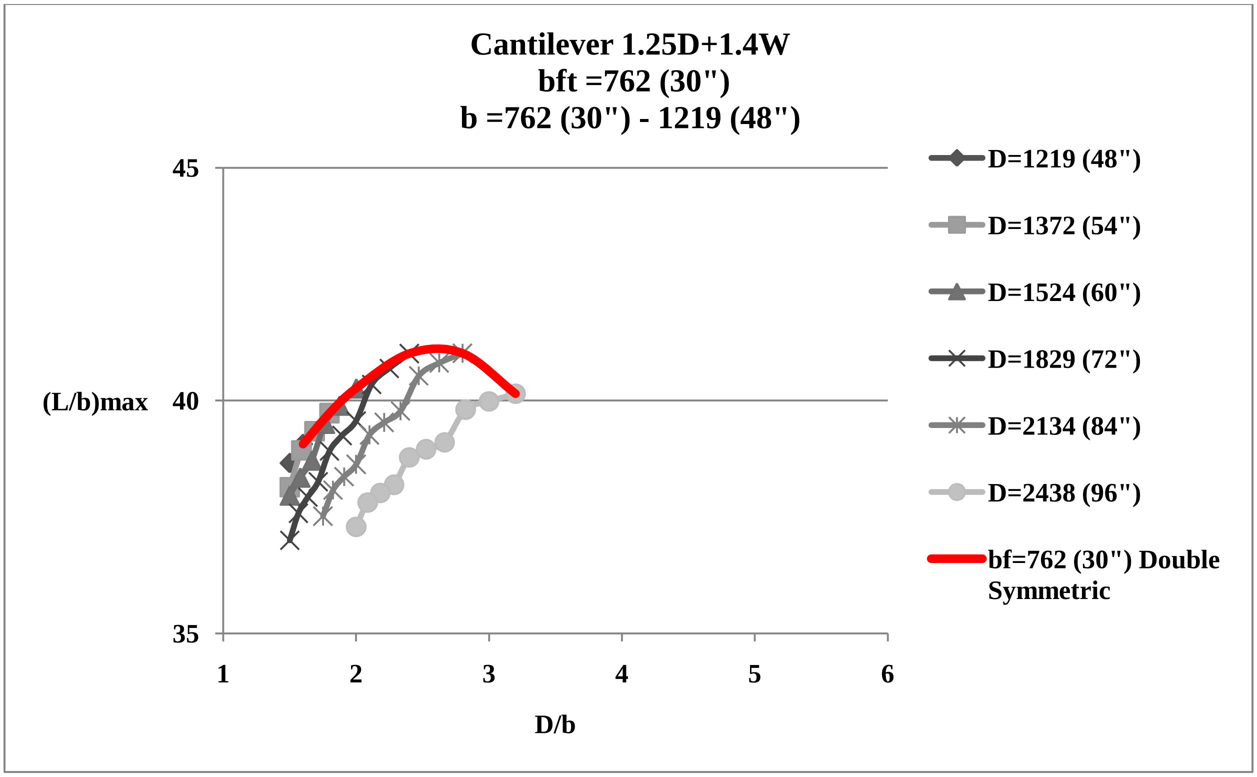
Cantilever 1.25D+1.4W
bft =762 (30")
b =762 (30") - 1219 (48")
45
40
35
(L/b)max
1
2
3
4
5
6
D/b
D=1219 (48")
D=1372 (54")
D=1524 (60")
D=1829 (72")
D=2134 (84")
D=2438 (96")
bf=762 (30") Double Symmetric

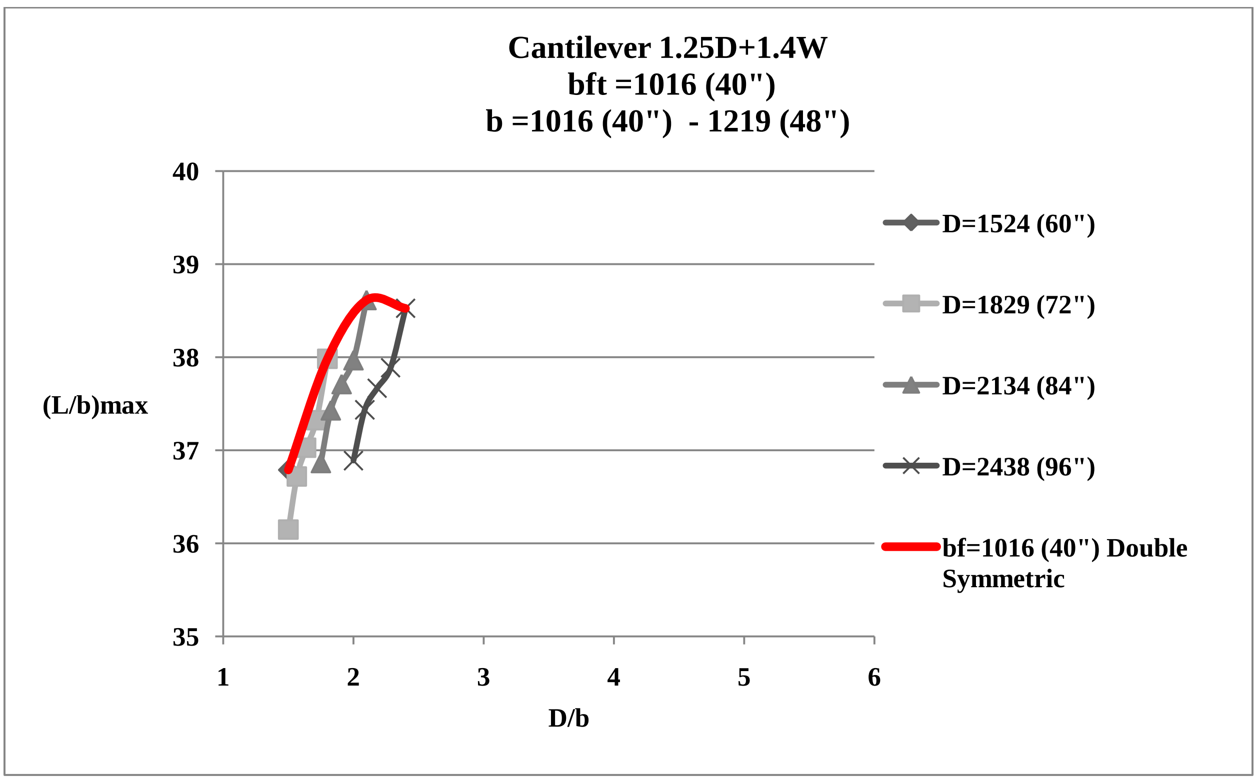
Cantilever 1.25D+1.4W
bft =1016 (40")
b =1016 (40") - 1219 (48")
40
39
38
37
36
35
(L/b)max
1
2
3
4
5
6
D/b
D=1524 (60")
D=1829 (72")
D=2134 (84")
D=2438 (96")
bf=1016 (40") Double Symmetric

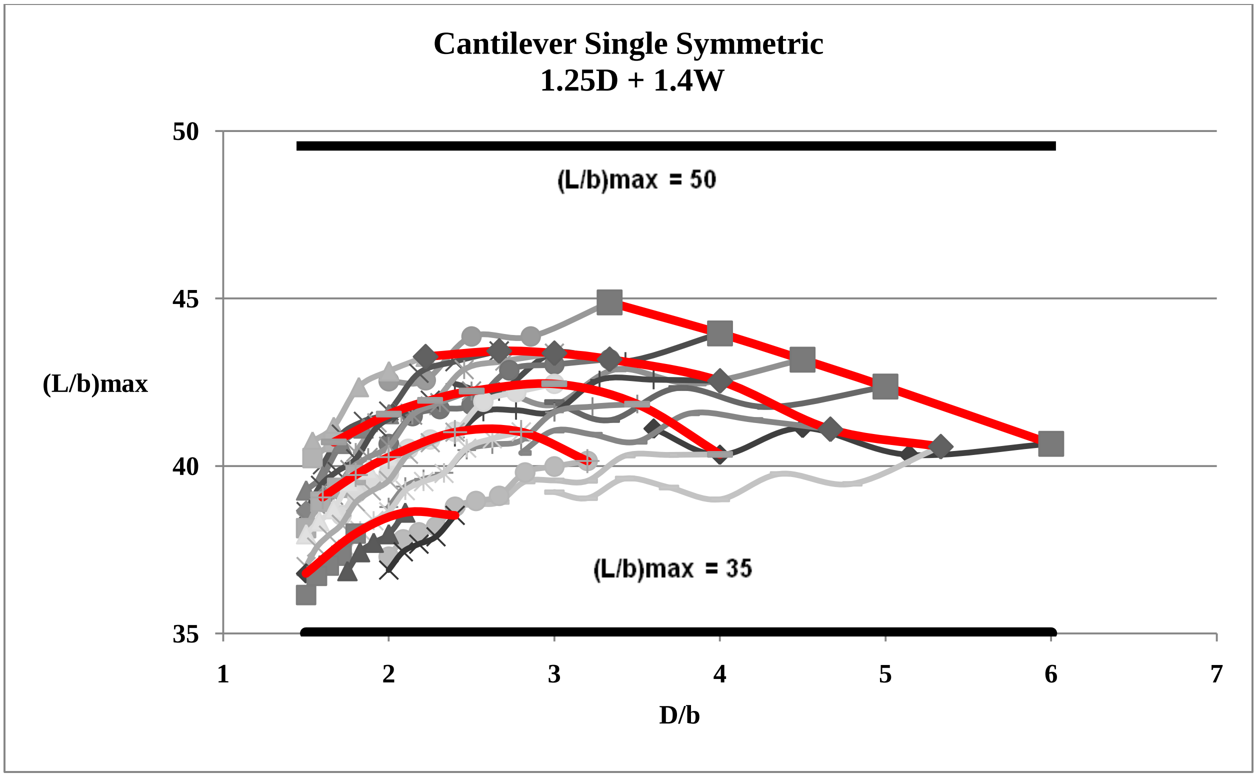
Cantilever Single Symmetric
1.25D + 1.4W
50
45
40
35
(L/b)max = 50
(L/b)max = 35
(L/b)max
1
2
3
4
5
6
7
D/b

APPENDIX C: DOUBLE SYMMETRIC DOUBLE GIRDERS

Appendix C shows L/s vs. D/s, and L/b vs. D/b plots for double symmetric double girders with various spacings between girders. Simply supported and cantilever are investigated with dead load only.

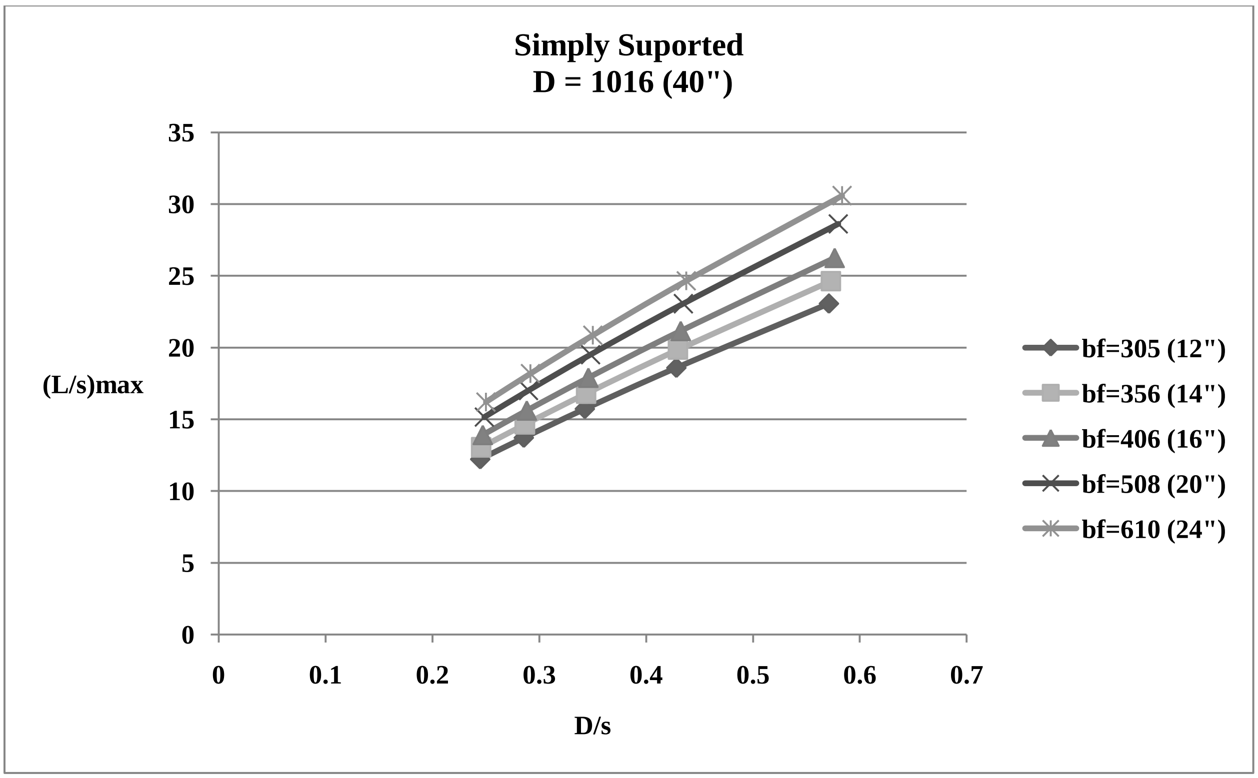

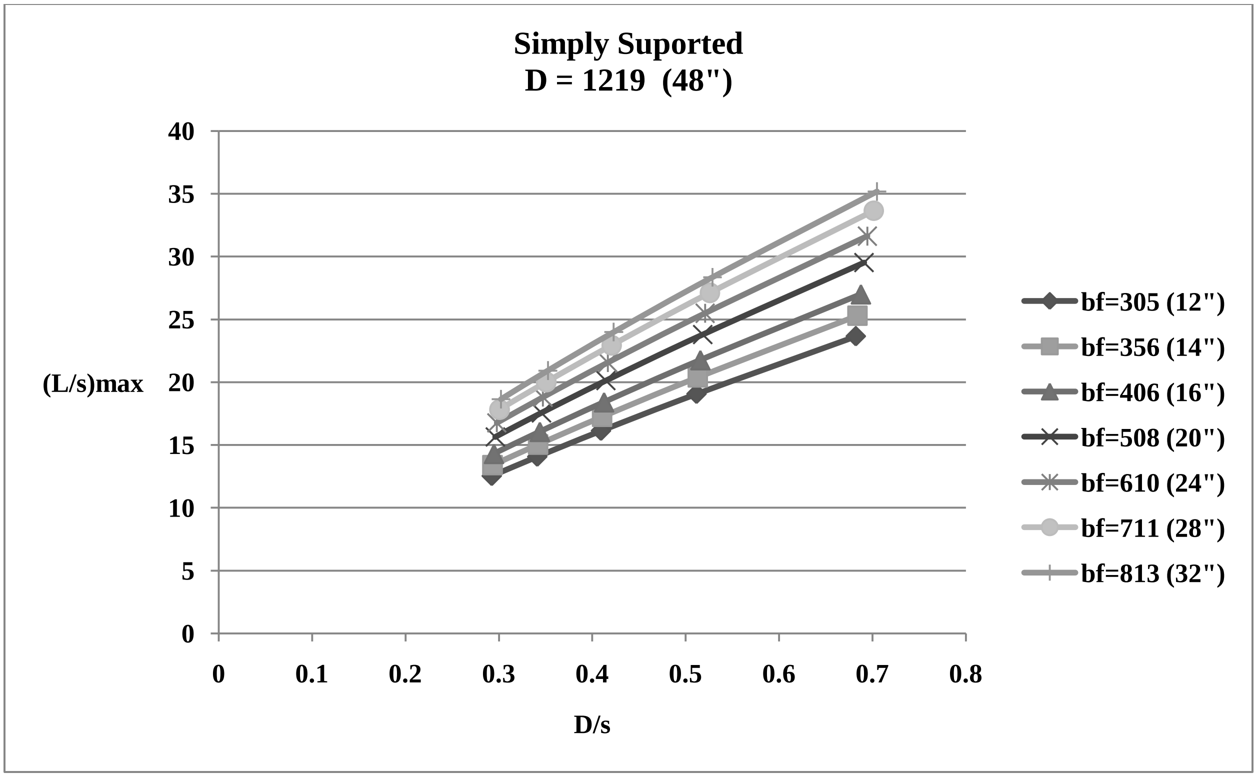
Simply Suported
D = 1219 (48")
(L/s)max
D/s
0
5
10
15
20
25
30
35
40
0
0.1
0.2
0.3
0.4
0.5
0.6
0.7
0.8
bf=305 (12")
bf=356 (14")
bf=406 (16")
bf=508 (20")
bf=610 (24")
bf=711 (28")
bf=813 (32")

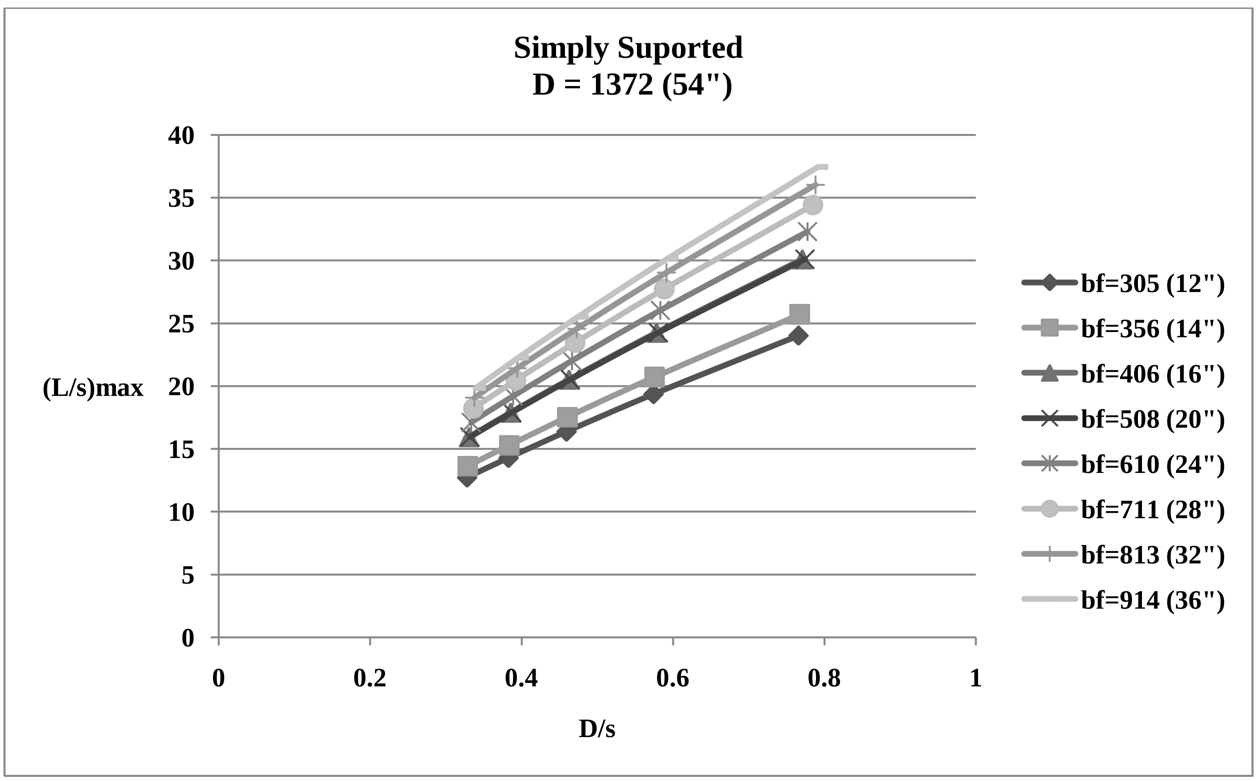
Simply Suported
D = 1372 (54")
(L/s)max
D/s
0
5
10
15
20
25
30
35
40
0
0.2
0.4
0.6
0.8
1
bf=305 (12")
bf=356 (14")
bf=406 (16")
bf=508 (20")
bf=610 (24")
bf=711 (28")
bf=813 (32")
bf=914 (36")

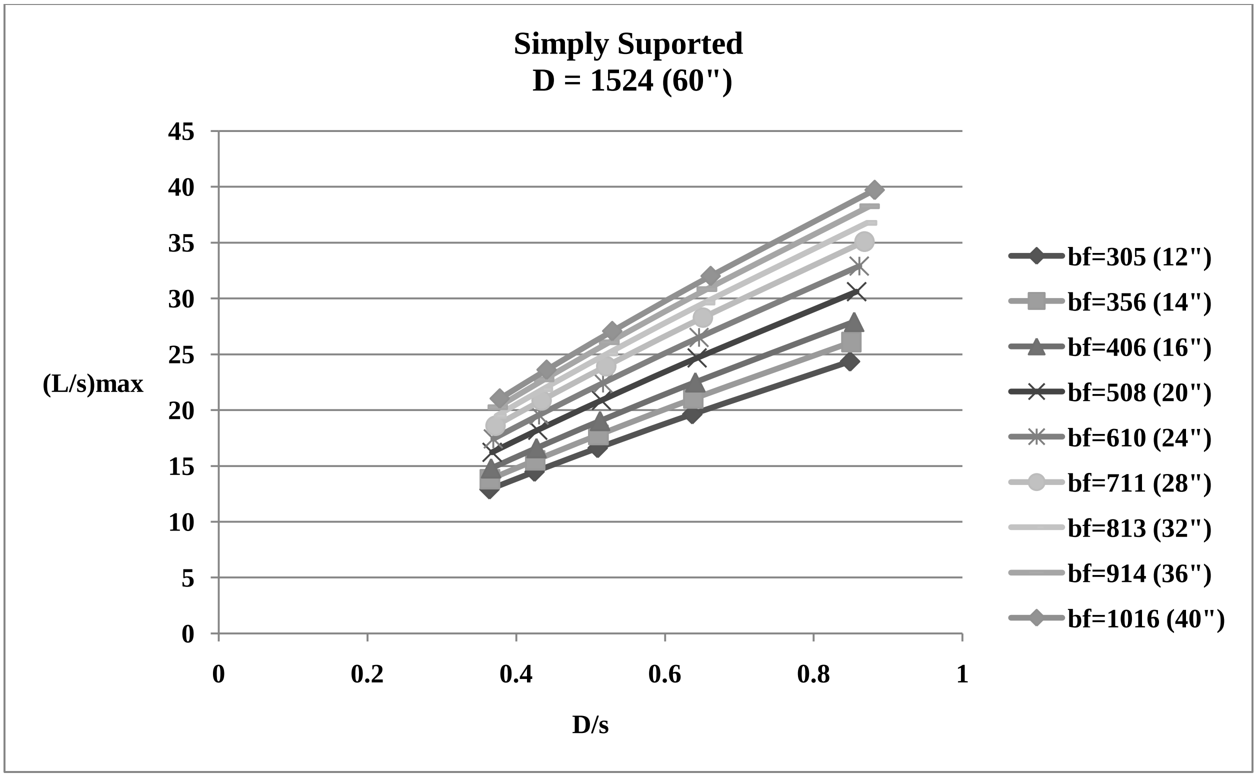
Simply Suported
D = 1524 (60")
(L/s)max
D/s
0
5
10
15
20
25
30
35
40
45
0
0.2
0.4
0.6
0.8
1
bf=305 (12")
bf=356 (14")
bf=406 (16")
bf=508 (20")
bf=610 (24")
bf=711 (28")
bf=813 (32")
bf=914 (36")
bf=1016 (40")

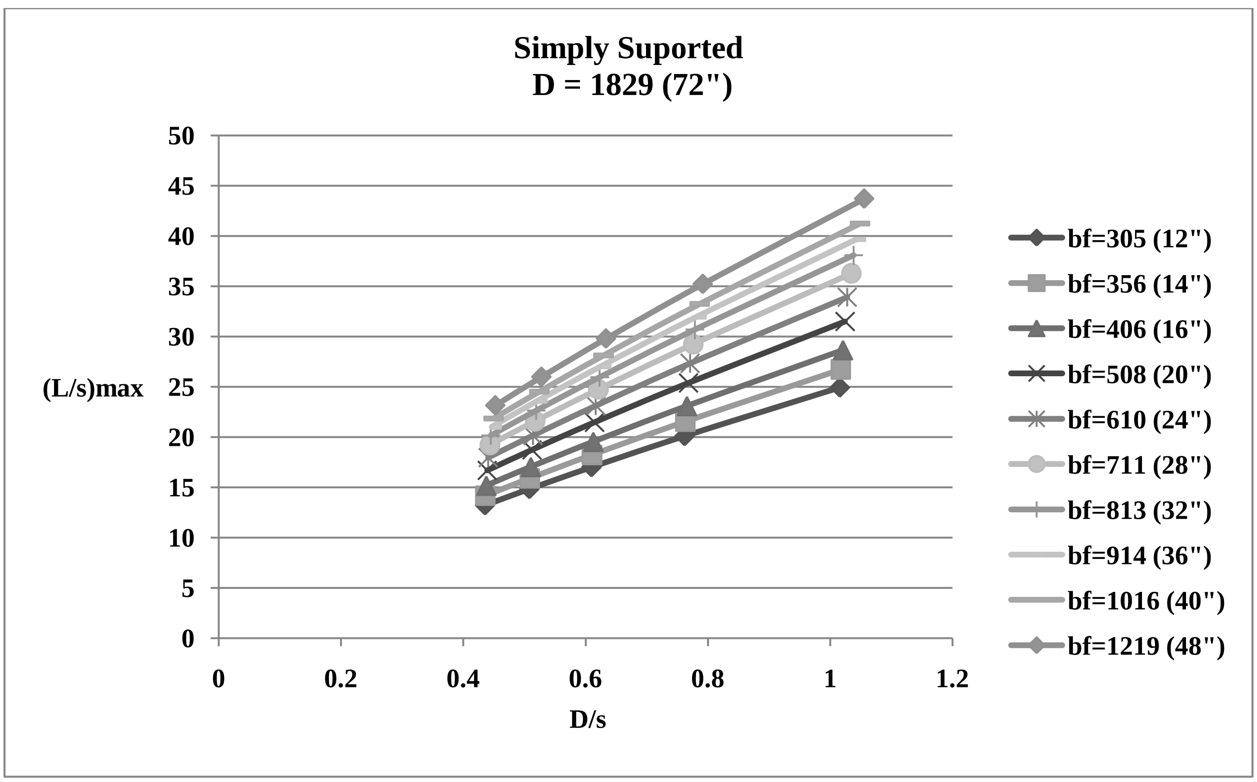
Simply Suported
D = 1829 (72")
(L/s)max
D/s
0
5
10
15
20
25
30
35
40
45
50
0
0.2
0.4
0.6
0.8
1
1.2
bf=305 (12")
bf=356 (14")
bf=406 (16")
bf=508 (20")
bf=610 (24")
bf=711 (28")
bf=813 (32")
bf=914 (36")
bf=1016 (40")
bf=1219 (48")

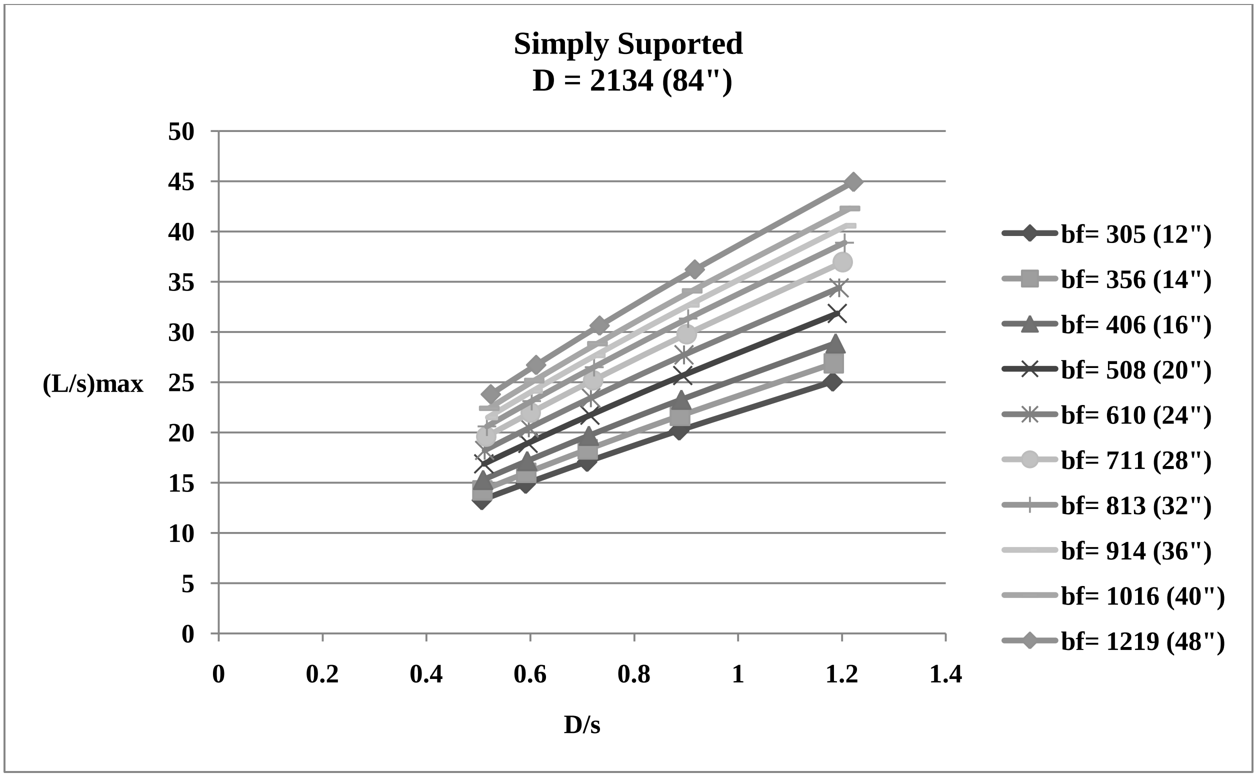
Simply Suported
D = 2134 (84")
(L/s)max
50
45
40
35
30
25
20
15
10
5
0
0
0.2
0.4
0.6
0.8
1
1.2
1.4
D/s
bf= 305 (12")
bf= 356 (14")
bf= 406 (16")
bf= 508 (20")
bf= 610 (24")
bf= 711 (28")
bf= 813 (32")
bf= 914 (36")
bf= 1016 (40")
bf= 1219 (48")

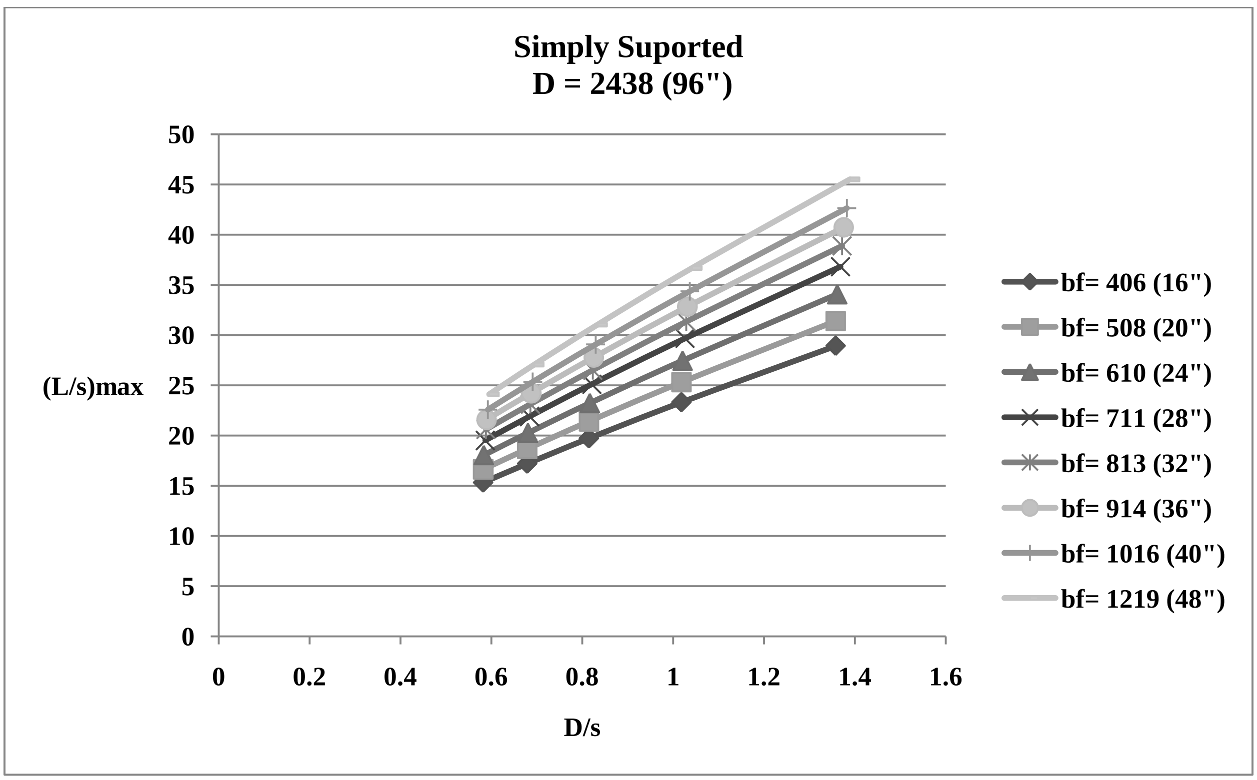
Simply Suported
D = 2438 (96")
(L/s)max
50
45
40
35
30
25
20
15
10
5
0
0
0.2
0.4
0.6
0.8
1
1.2
1.4
1.6
D/s
bf= 406 (16")
bf= 508 (20")
bf= 610 (24")
bf= 711 (28")
bf= 813 (32")
bf= 914 (36")
bf= 1016 (40")
bf= 1219 (48")

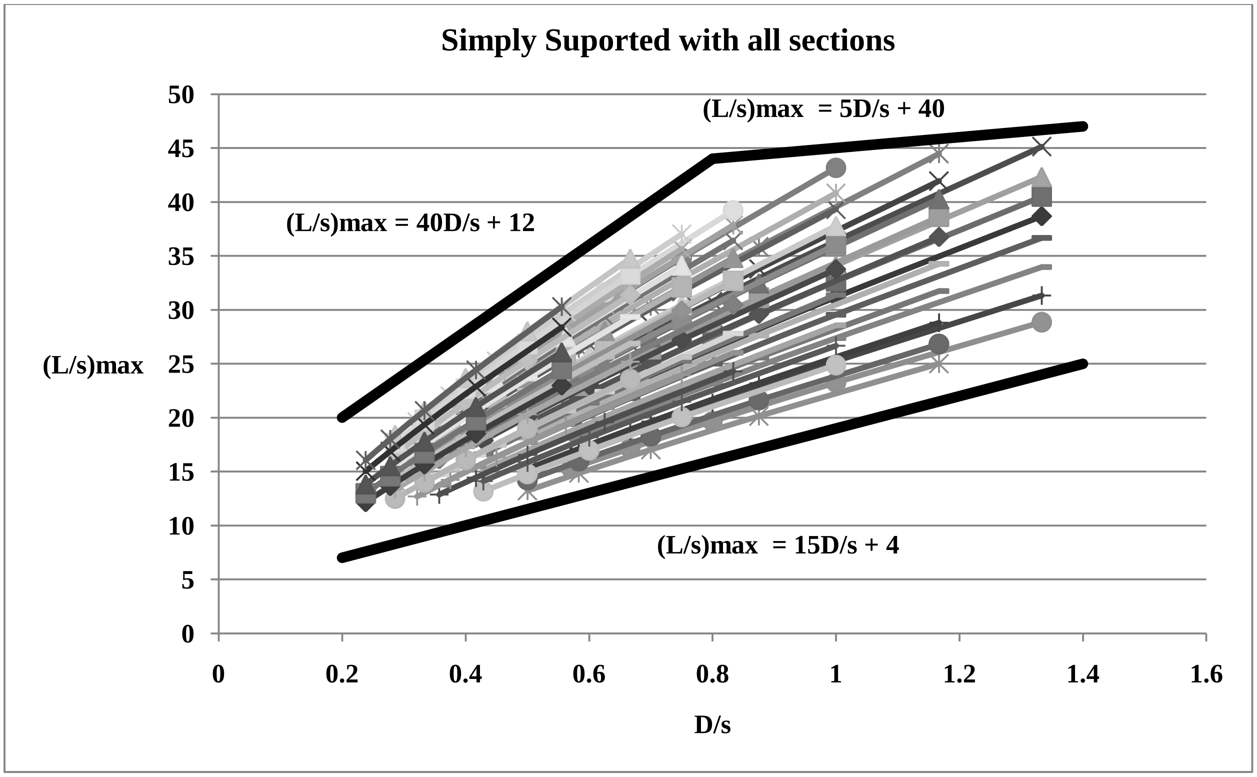
Simply Suported with all sections
(L/s)max = 5D/s + 40
(L/s)max = 40D/s + 12
(L/s)max = 15D/s + 4
(L/s)max
D/s
0
5
10
15
20
25
30
35
40
45
50
0
0.2
0.4
0.6
0.8
1
1.2
1.4
1.6

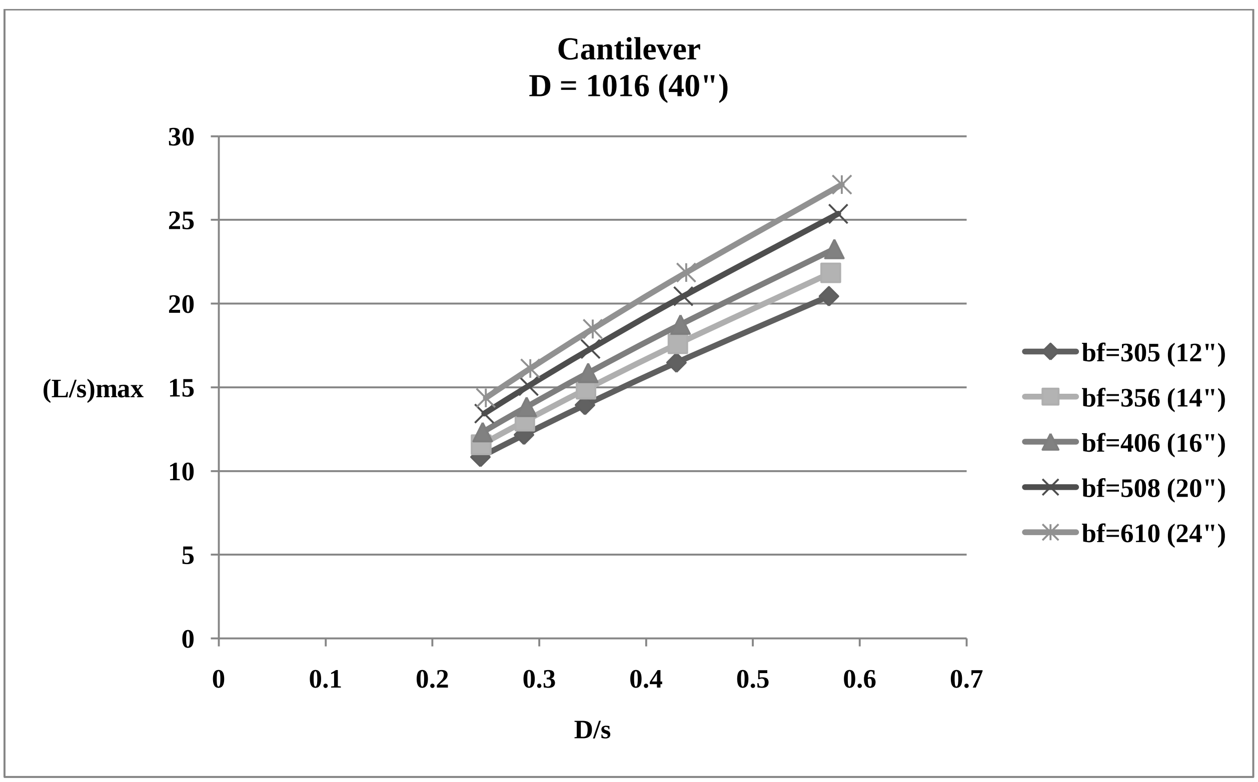
Cantilever
D = 1016 (40")
(L/s)max
D/s
0
5
10
15
20
25
30
0
0.1
0.2
0.3
0.4
0.5
0.6
0.7
bf=305 (12")
bf=356 (14")
bf=406 (16")
bf=508 (20")
bf=610 (24")

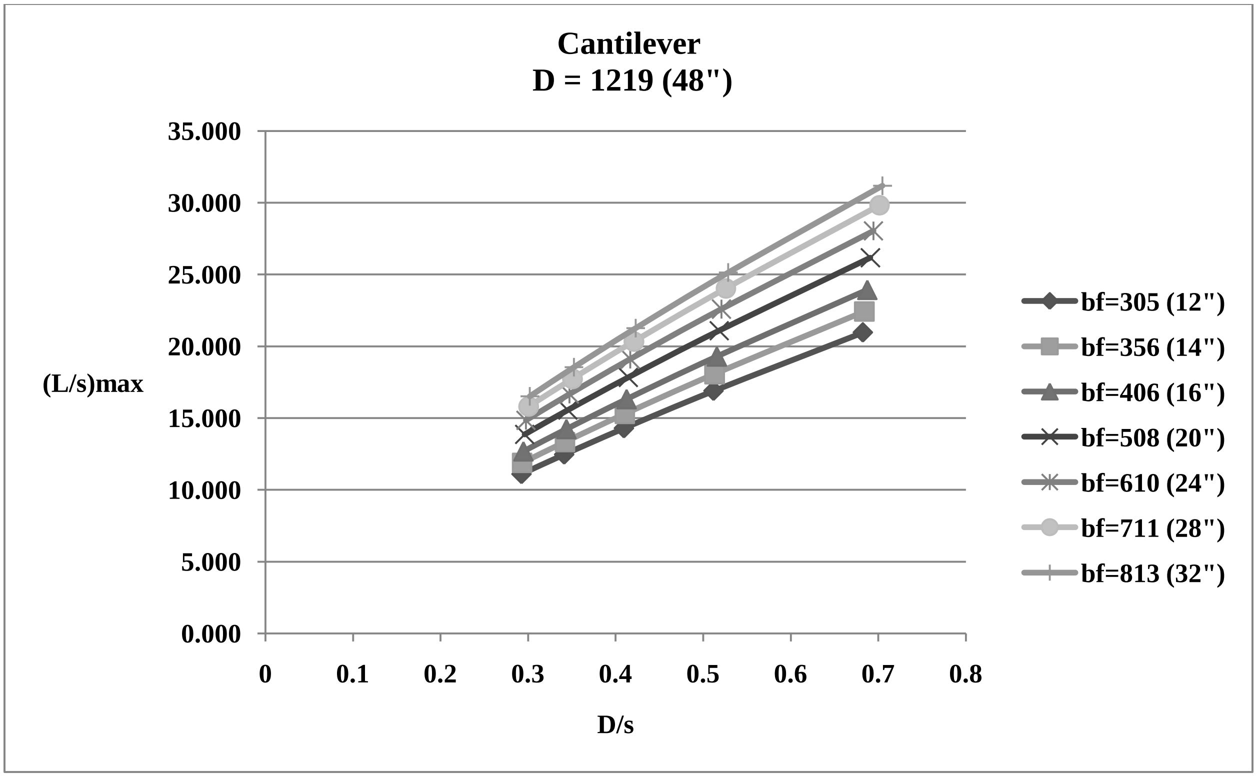
Cantilever
D = 1219 (48")
35.000
30.000
25.000
20.000
15.000
10.000
5.000
0.000
(L/s)max
0
0.1
0.2
0.3
0.4
0.5
0.6
0.7
0.8
D/s
bf=305 (12")
bf=356 (14")
bf=406 (16")
bf=508 (20")
bf=610 (24")
bf=711 (28")
bf=813 (32")

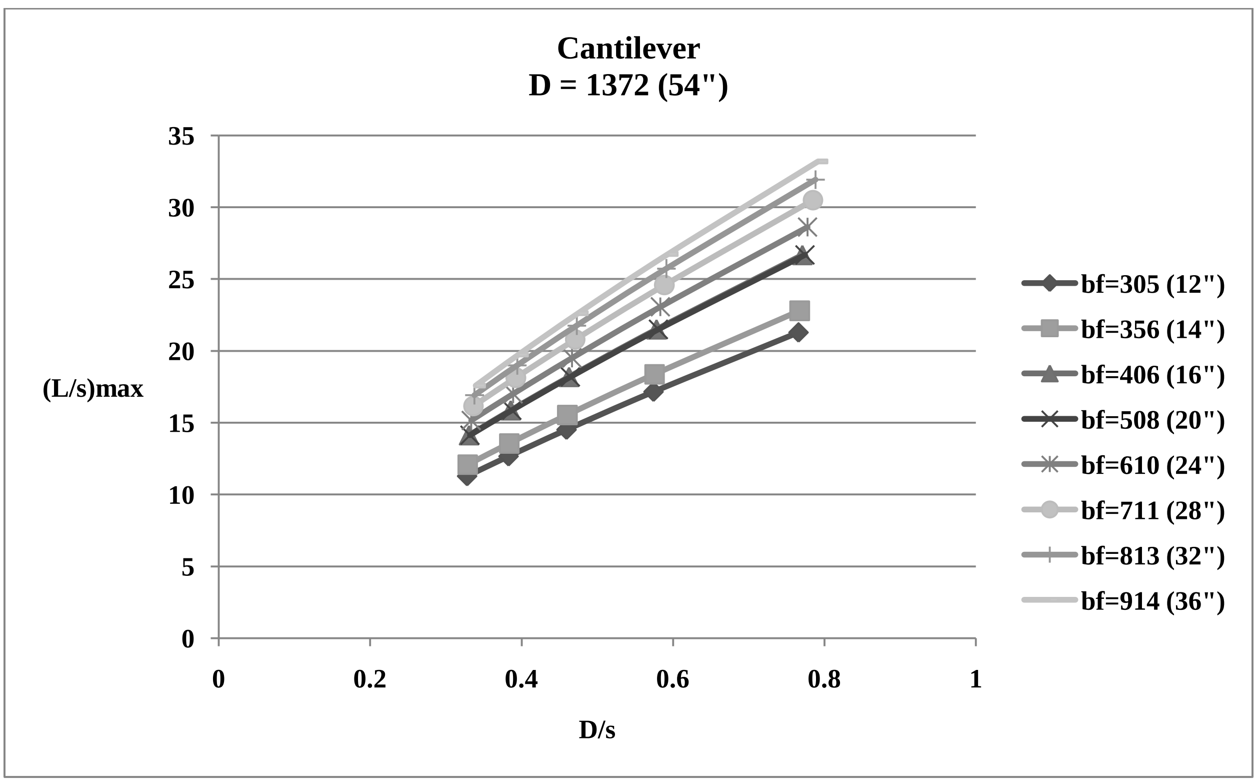
Cantilever
D = 1372 (54")
35
30
25
20
15
10
5
0
(L/s)max
0
0.2
0.4
0.6
0.8
1
D/s
bf=305 (12")
bf=356 (14")
bf=406 (16")
bf=508 (20")
bf=610 (24")
bf=711 (28")
bf=813 (32")
bf=914 (36")

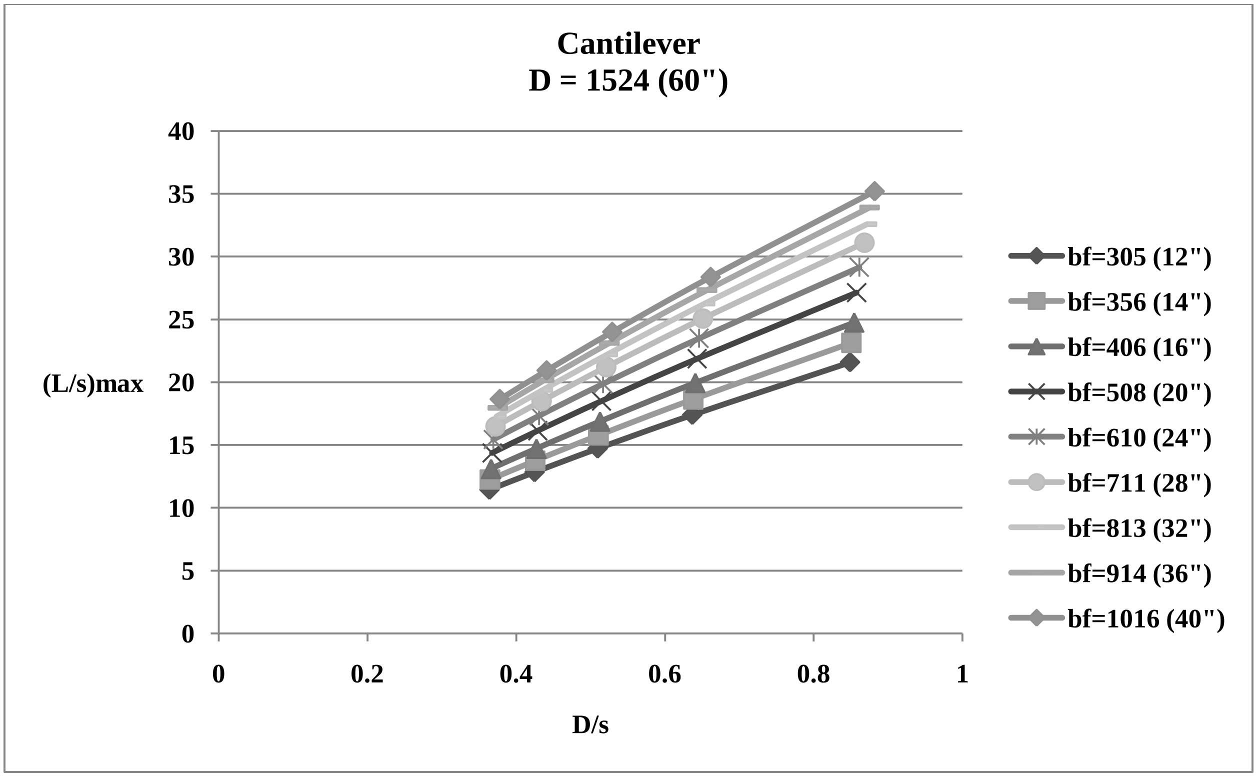
Cantilever
D = 1524 (60")
(L/s)max
D/s
0
5
10
15
20
25
30
35
40
0
0.2
0.4
0.6
0.8
1
bf=305 (12")
bf=356 (14")
bf=406 (16")
bf=508 (20")
bf=610 (24")
bf=711 (28")
bf=813 (32")
bf=914 (36")
bf=1016 (40")

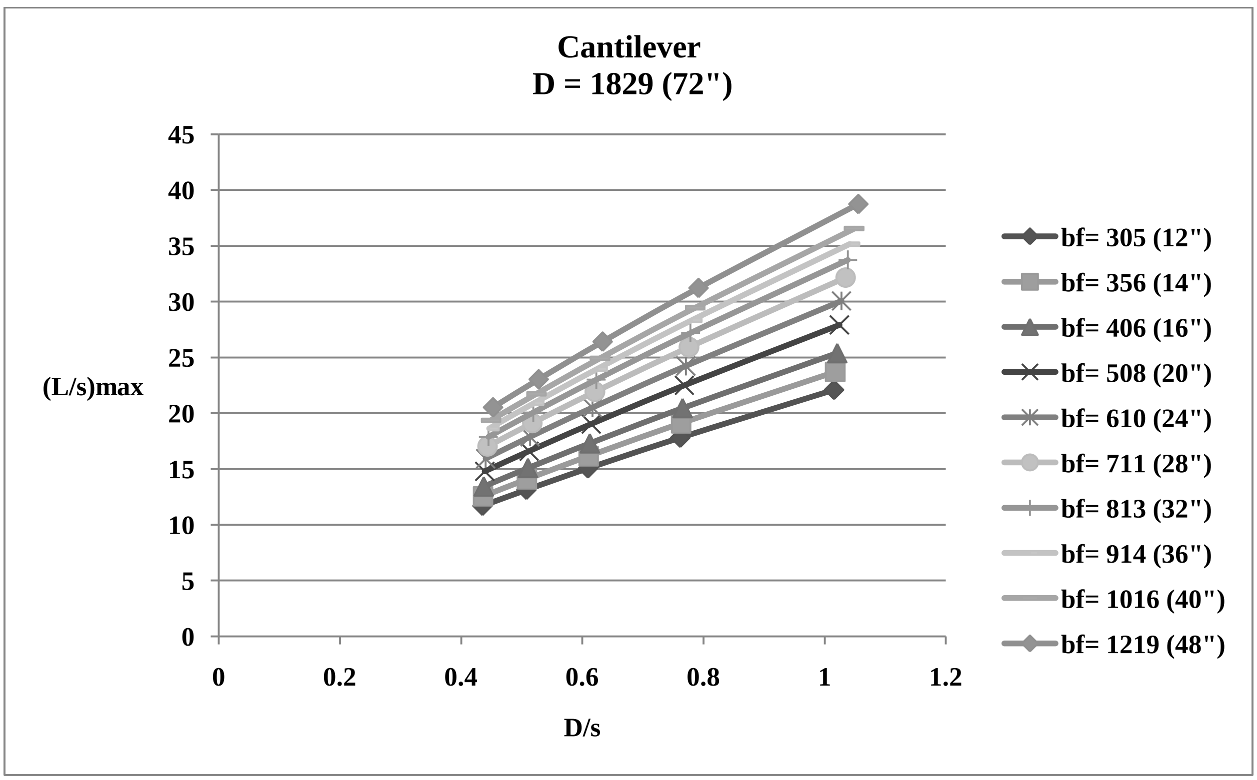
Cantilever
D = 1829 (72")
(L/s)max
D/s
0
5
10
15
20
25
30
35
40
45
0
0.2
0.4
0.6
0.8
1
1.2
bf= 305 (12")
bf= 356 (14")
bf= 406 (16")
bf= 508 (20")
bf= 610 (24")
bf= 711 (28")
bf= 813 (32")
bf= 914 (36")
bf= 1016 (40")
bf= 1219 (48")

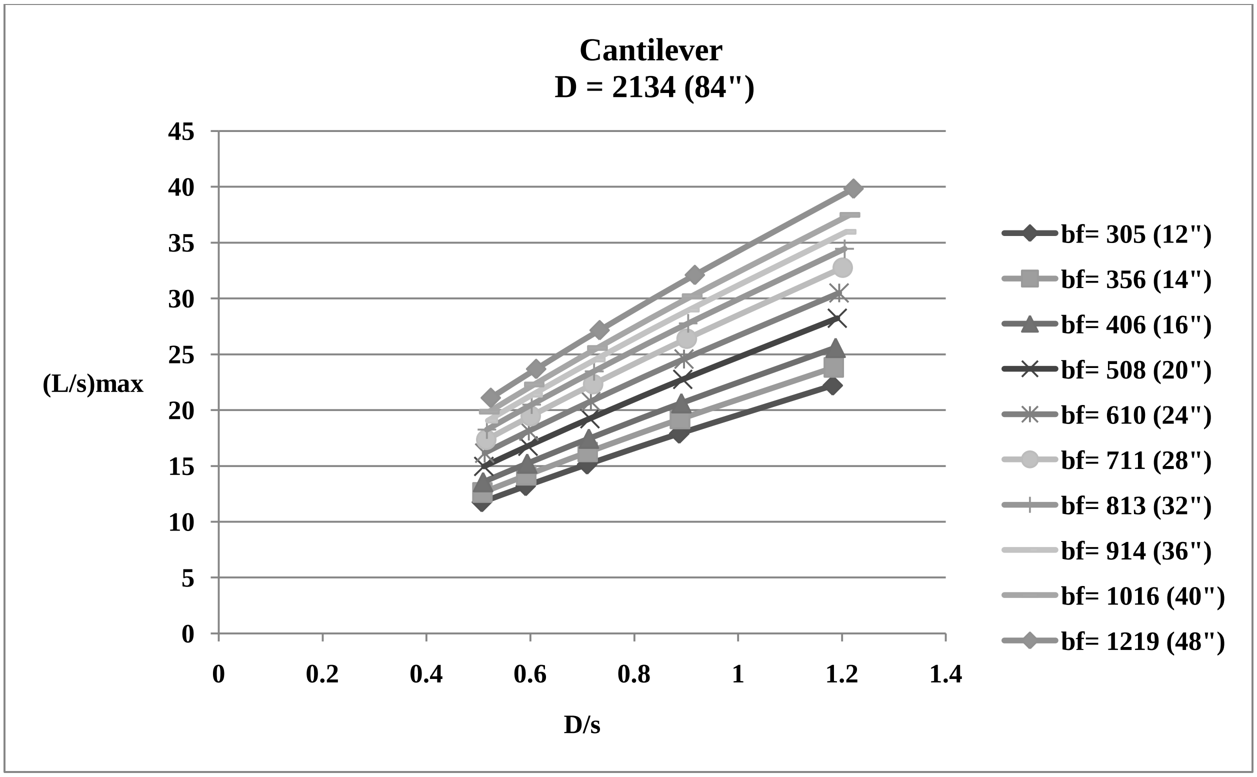

Cantilever
D = 2134 (84")
(L/s)max
D/s
0
5
10
15
20
25
30
35
40
45
0
0.2
0.4
0.6
0.8
1
1.2
1.4
bf= 305 (12")
bf= 356 (14")
bf= 406 (16")
bf= 508 (20")
bf= 610 (24")
bf= 711 (28")
bf= 813 (32")
bf= 914 (36")
bf= 1016 (40")
bf= 1219 (48")

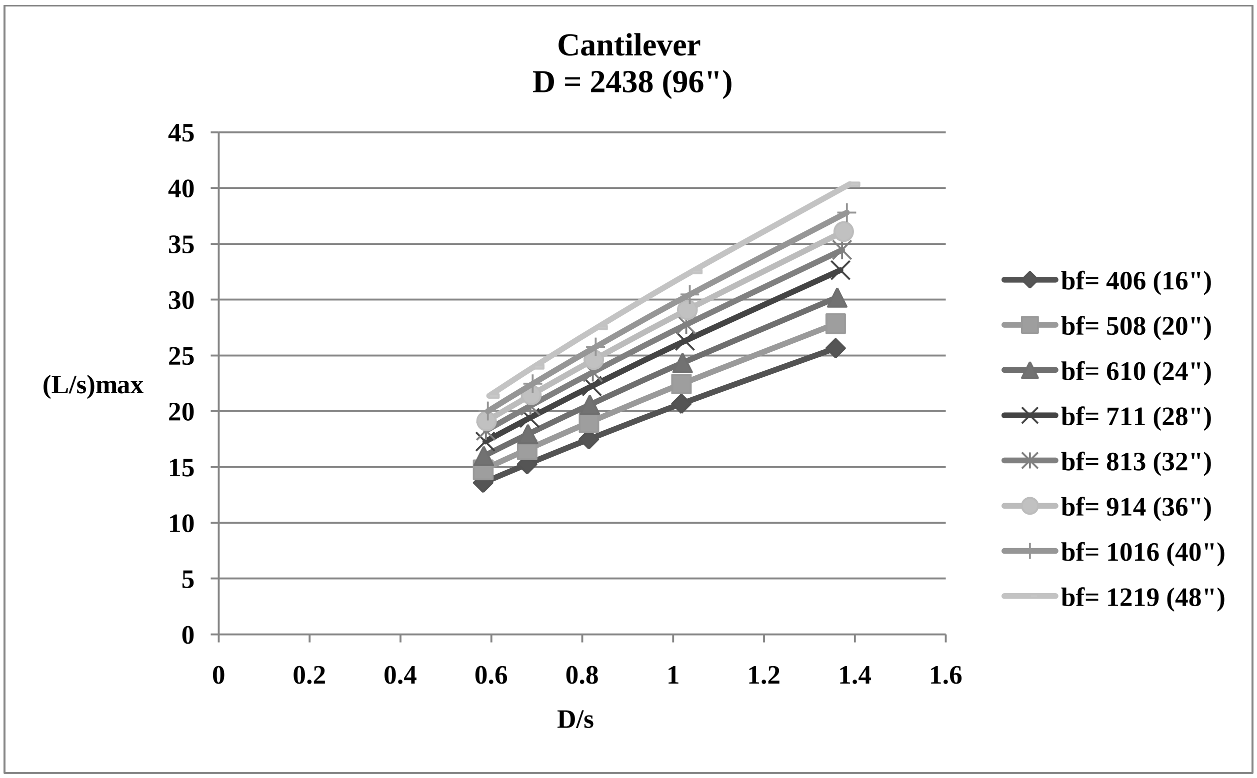

Cantilever
D = 2438 (96")
(L/s)max
D/s
0
5
10
15
20
25
30
35
40
45
0
0.2
0.4
0.6
0.8
1
1.2
1.4
1.6
bf= 406 (16")
bf= 508 (20")
bf= 610 (24")
bf= 711 (28")
bf= 813 (32")
bf= 914 (36")
bf= 1016 (40")
bf= 1219 (48")

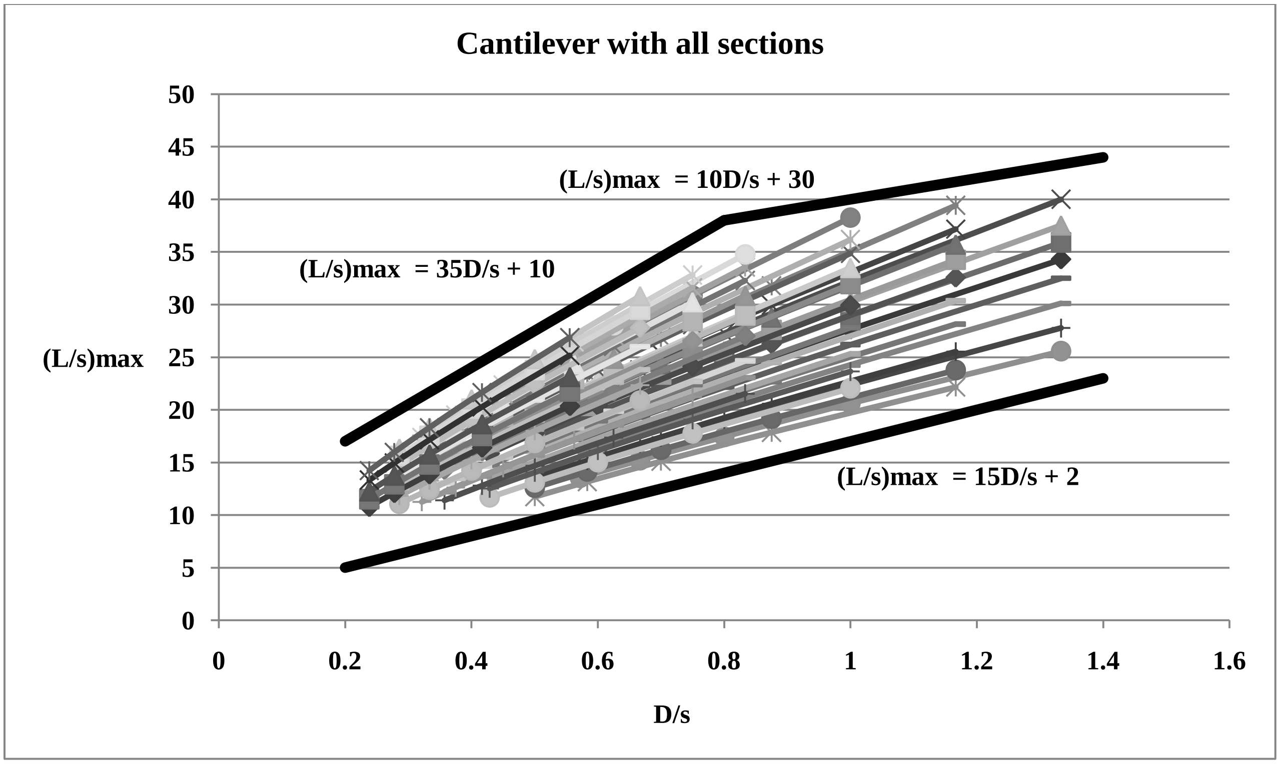
Cantilever with all sections
(L/s)max = 10D/s + 30
(L/s)max = 35D/s + 10
(L/s)max = 15D/s + 2
(L/s)max
D/s
0
5
10
15
20
25
30
35
40
45
50
0
0.2
0.4
0.6
0.8
1
1.2
1.4
1.6

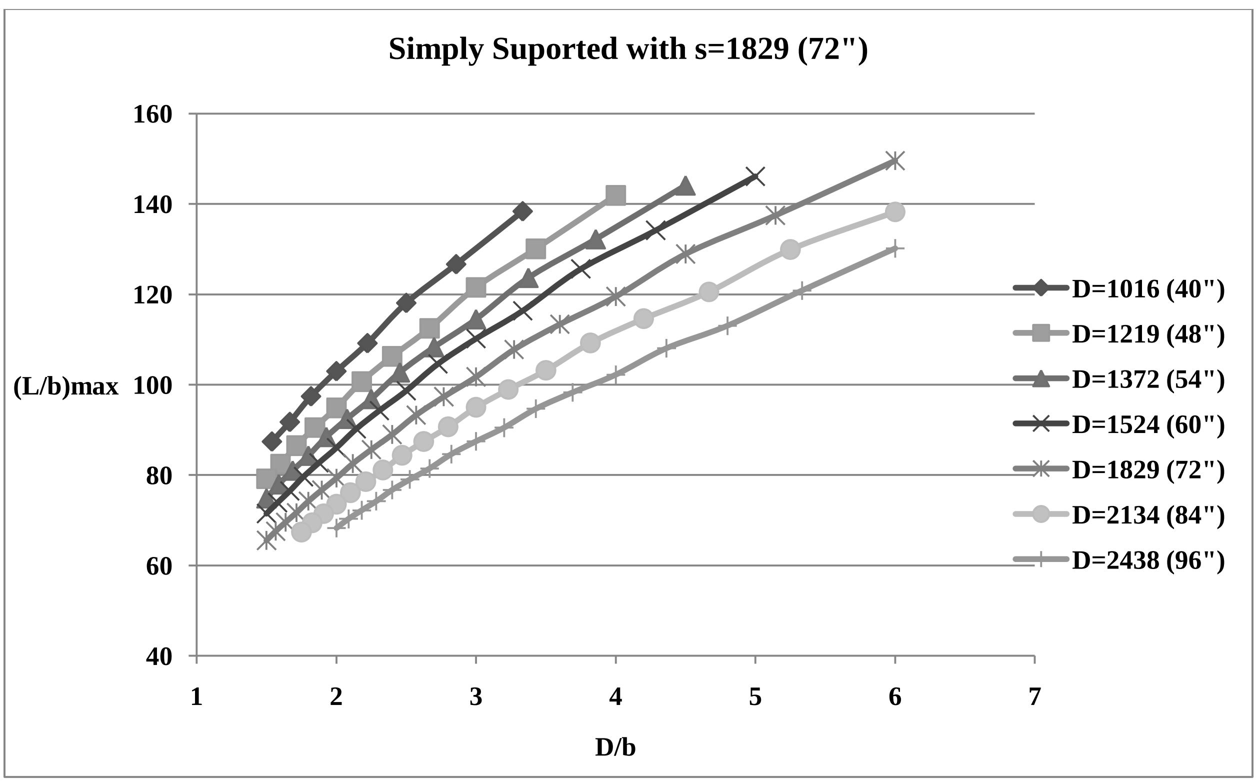
Simply Suported with s=1829 (72")
(L/b)max
D/b
40
60
80
100
120
140
160
1
2
3
4
5
6
7
D=1016 (40")
D=1219 (48")
D=1372 (54")
D=1524 (60")
D=1829 (72")
D=2134 (84")
D=2438 (96")

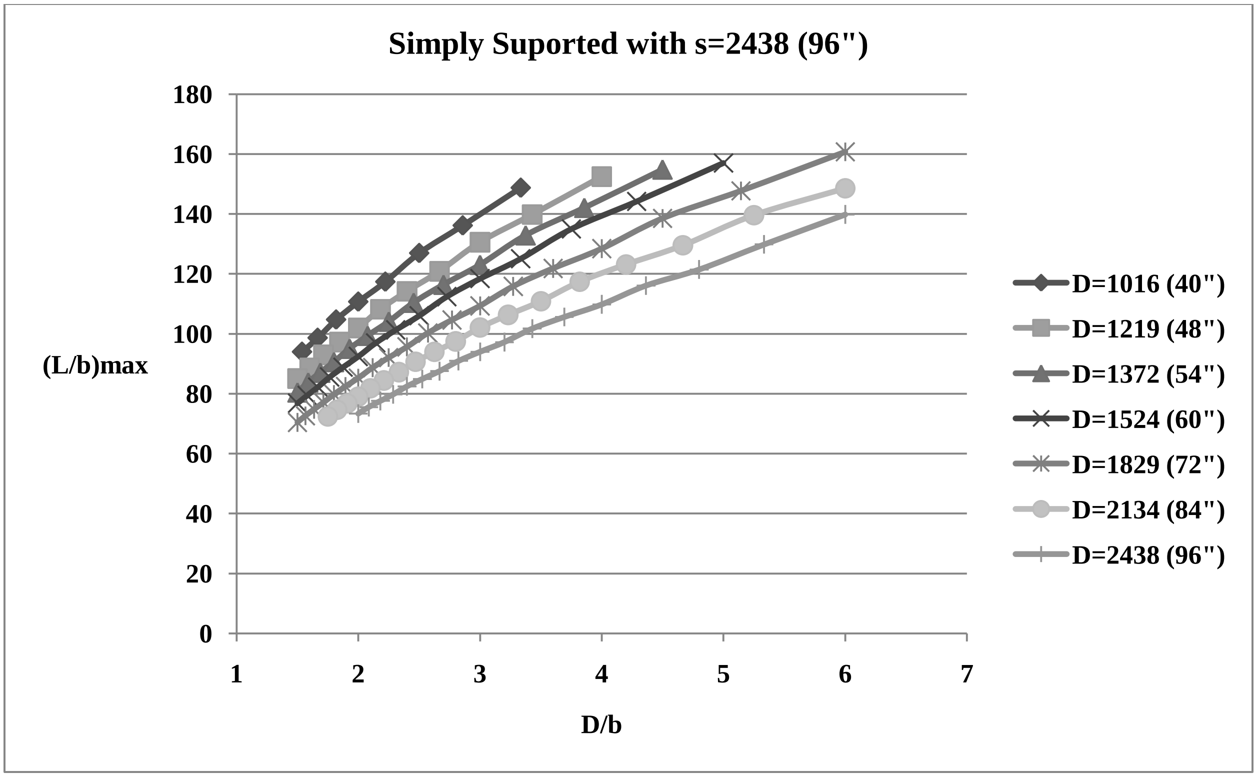
Simply Suported with s=2438 (96")
(L/b)max
D/b
D=1016 (40")
D=1219 (48")
D=1372 (54")
D=1524 (60")
D=1829 (72")
D=2134 (84")
D=2438 (96")

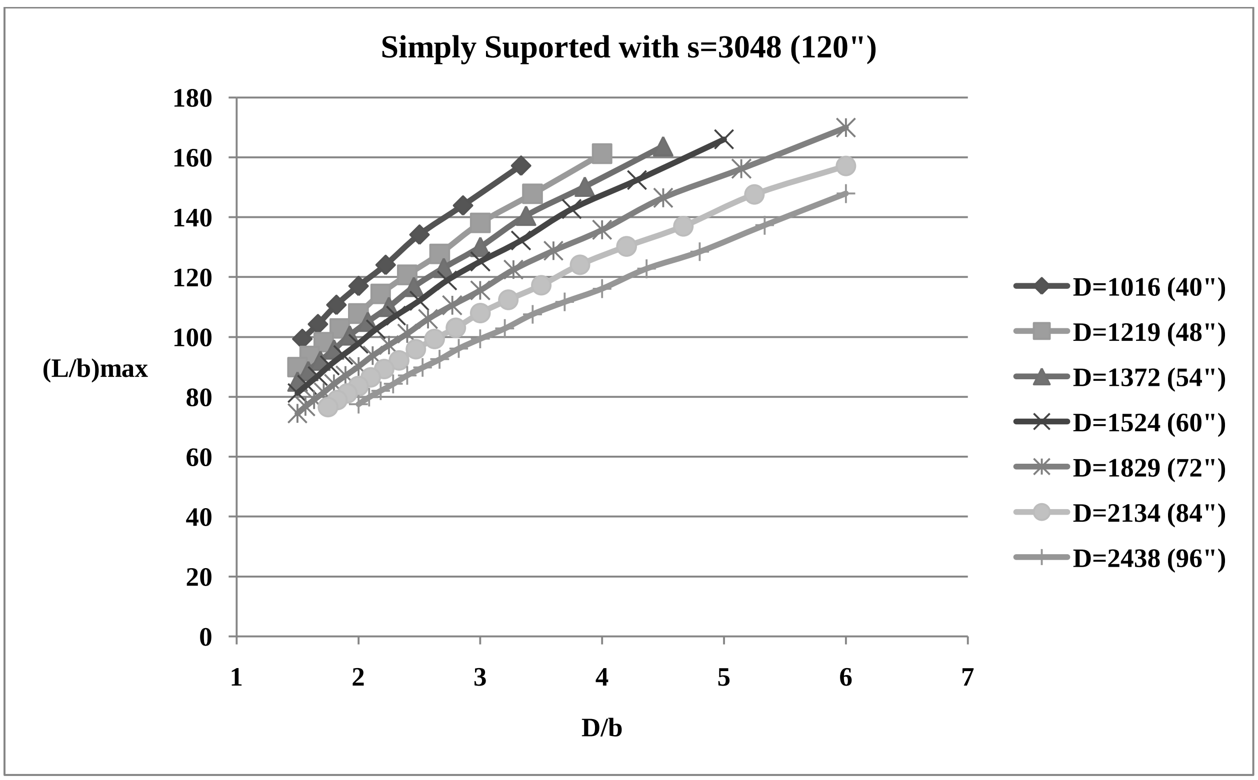
Simply Suported with s=3048 (120")
(L/b)max
D/b
D=1016 (40")
D=1219 (48")
D=1372 (54")
D=1524 (60")
D=1829 (72")
D=2134 (84")
D=2438 (96")

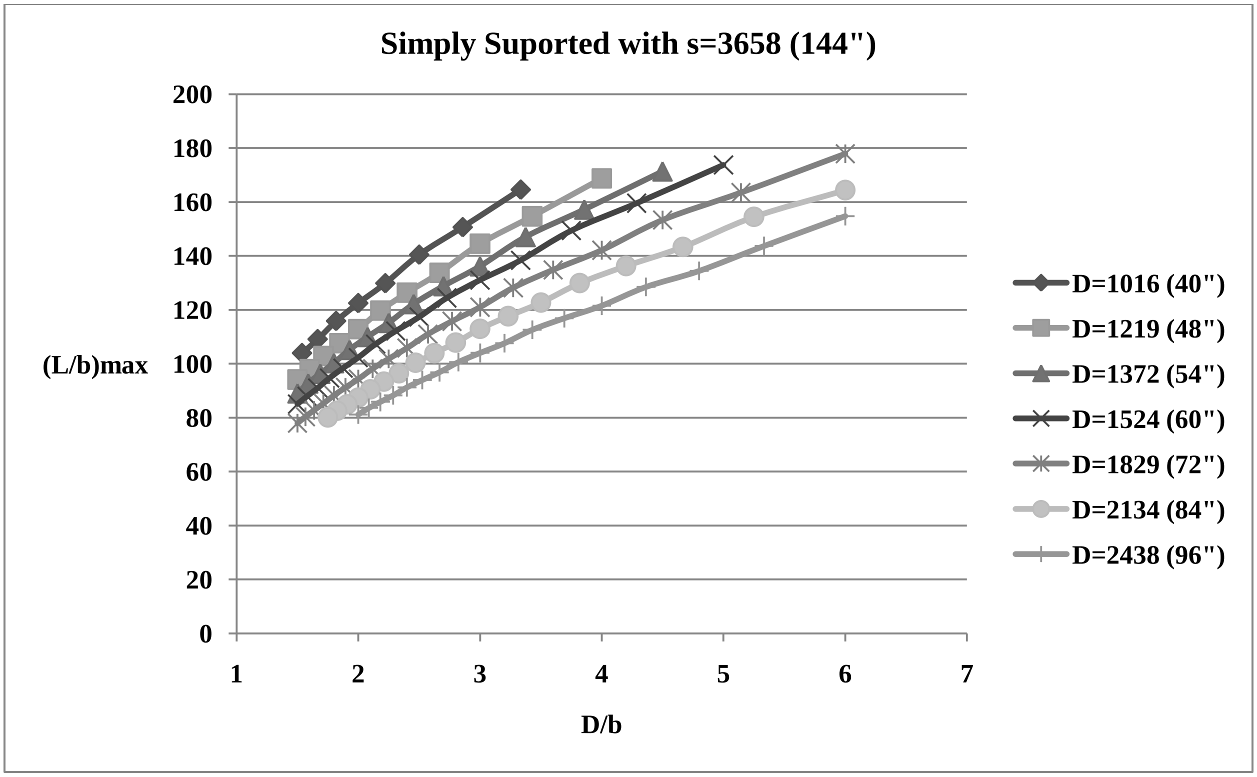
Simply Suported with s=3658 (144")
(L/b)max
200
180
160
140
120
100
80
60
40
20
0
1
2
3
4
5
6
7
D/b
D=1016 (40")
D=1219 (48")
D=1372 (54")
D=1524 (60")
D=1829 (72")
D=2134 (84")
D=2438 (96")

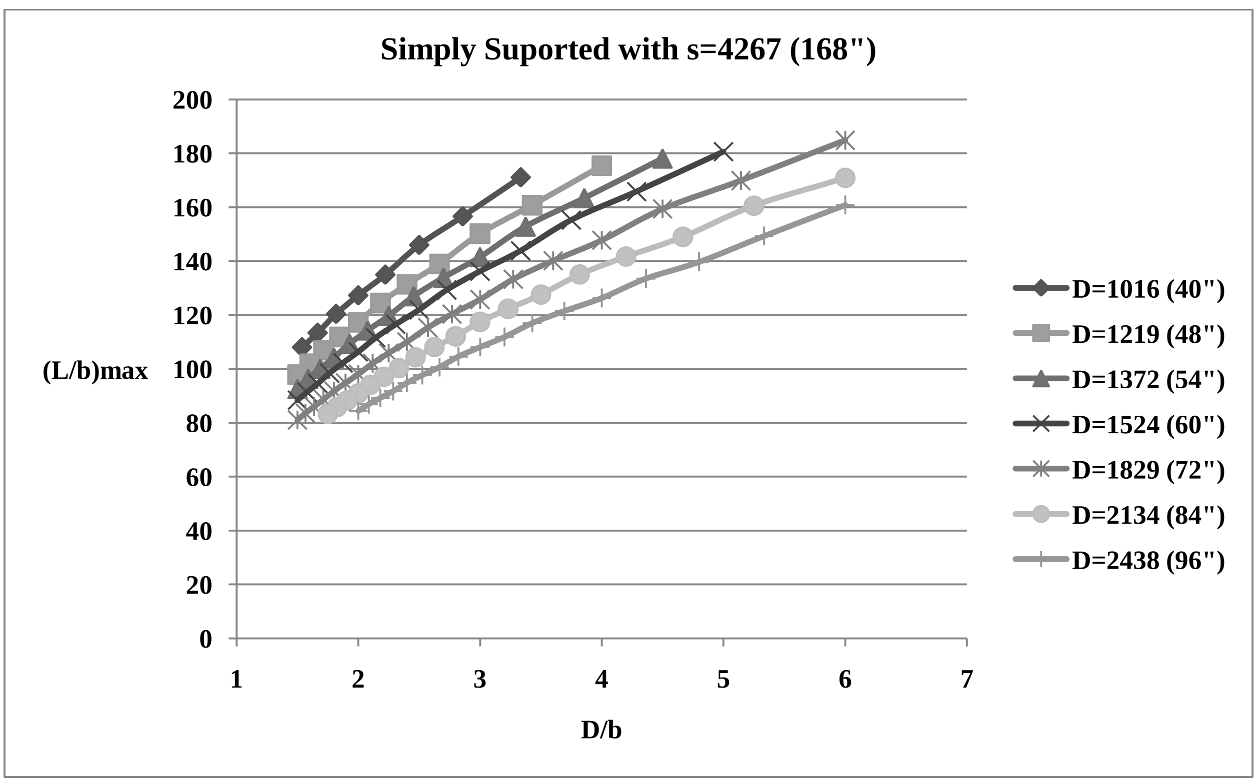
Simply Suported with s=4267 (168")
(L/b)max
200
180
160
140
120
100
80
60
40
20
0
1
2
3
4
5
6
7
D/b
D=1016 (40")
D=1219 (48")
D=1372 (54")
D=1524 (60")
D=1829 (72")
D=2134 (84")
D=2438 (96")

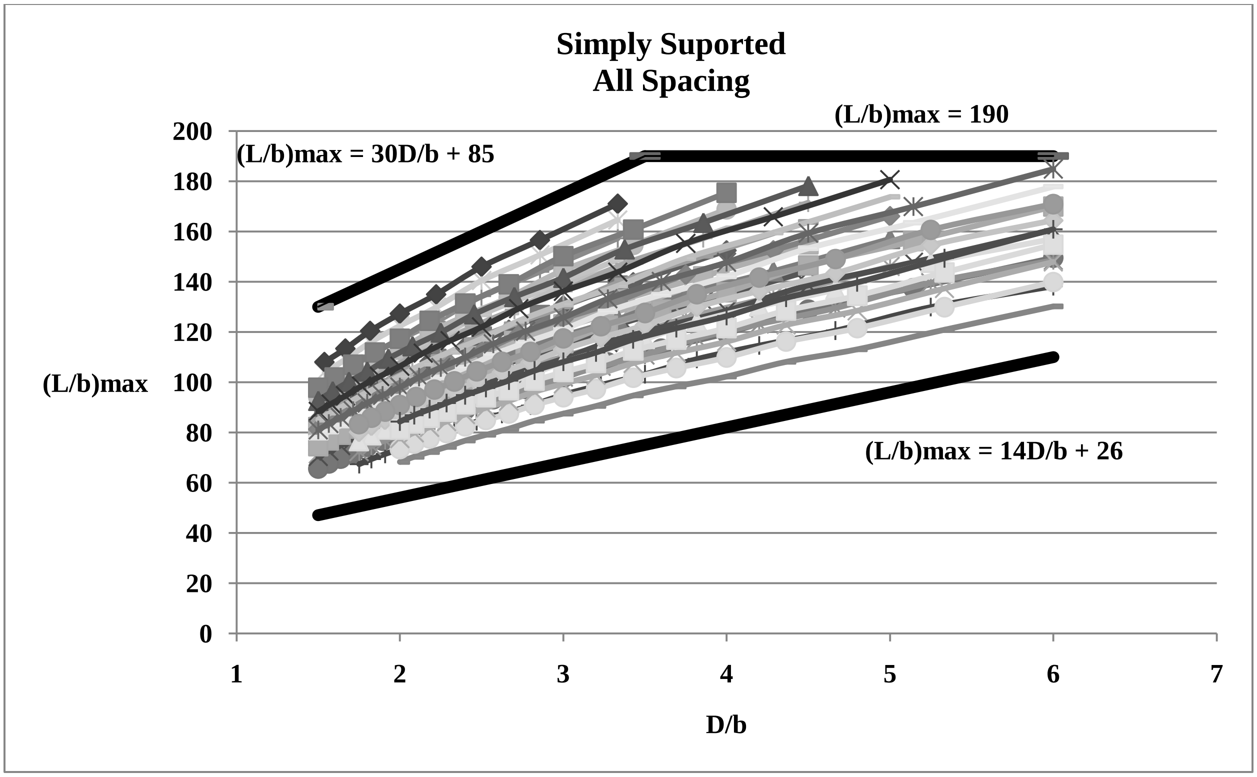
Simply Suported
All Spacing
(L/b)max = 190
(L/b)max = 30D/b + 85
(L/b)max = 14D/b + 26
(L/b)max
D/b
200
180
160
140
120
100
80
60
40
20
0
1
2
3
4
5
6
7

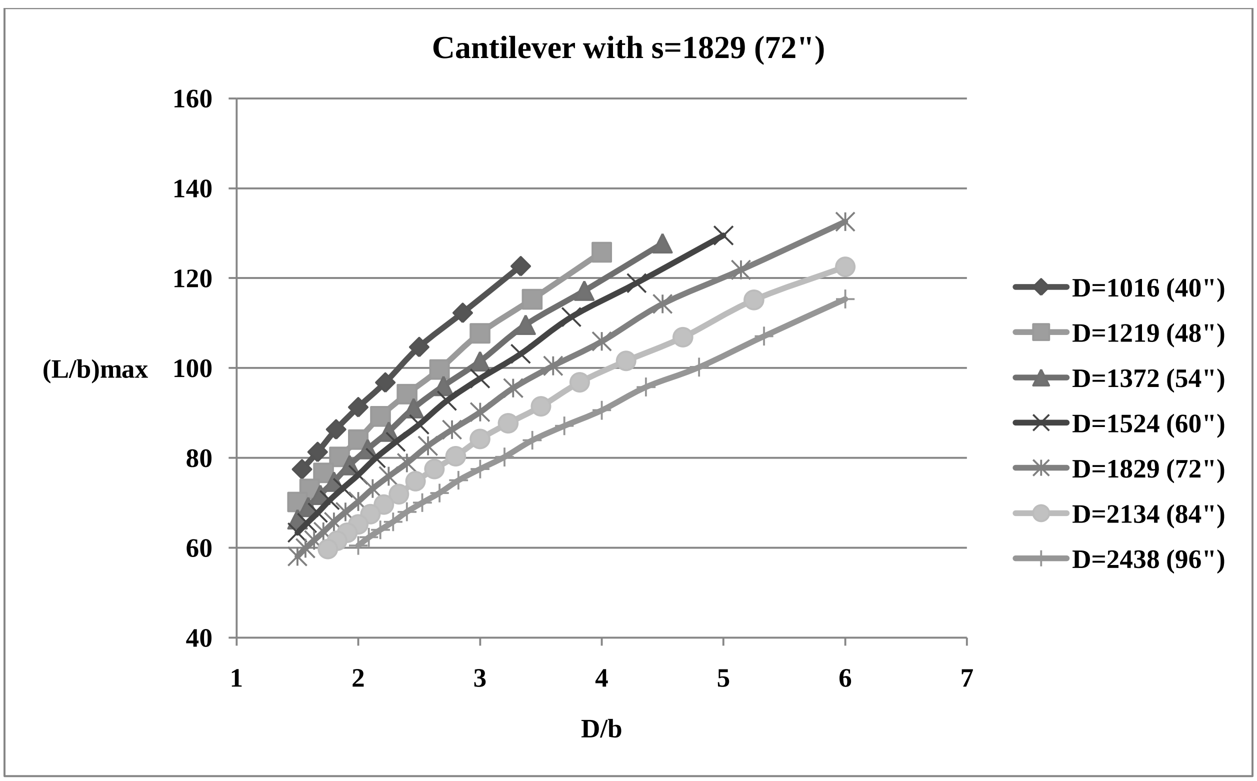
Cantilever with s=1829 (72")
(L/b)max
D/b
160
140
120
100
80
60
40
1
2
3
4
5
6
7
D=1016 (40")
D=1219 (48")
D=1372 (54")
D=1524 (60")
D=1829 (72")
D=2134 (84")
D=2438 (96")

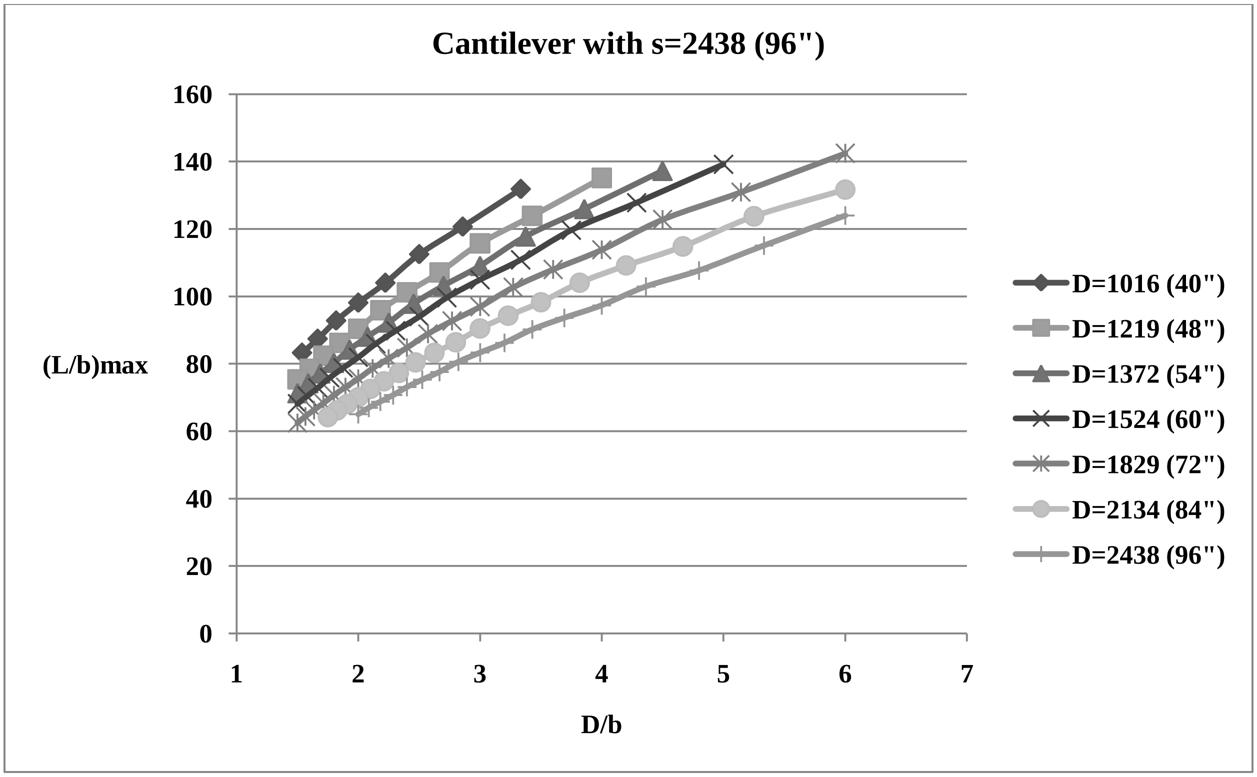
Cantilever with s=2438 (96")
(L/b)max
0
20
40
60
80
100
120
140
160
D/b
1
2
3
4
5
6
7
D=1016 (40")
D=1219 (48")
D=1372 (54")
D=1524 (60")
D=1829 (72")
D=2134 (84")
D=2438 (96")

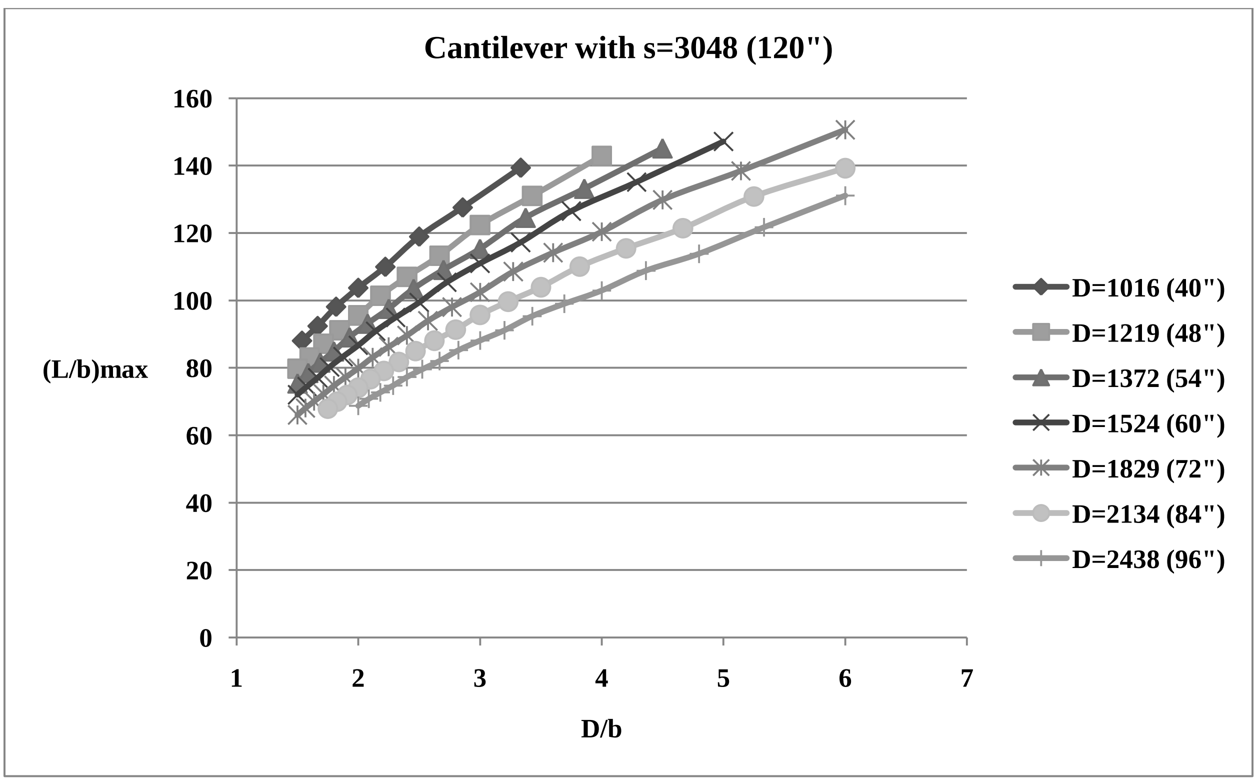
Cantilever with s=3048 (120")
(L/b)max
0
20
40
60
80
100
120
140
160
D/b
1
2
3
4
5
6
7
D=1016 (40")
D=1219 (48")
D=1372 (54")
D=1524 (60")
D=1829 (72")
D=2134 (84")
D=2438 (96")

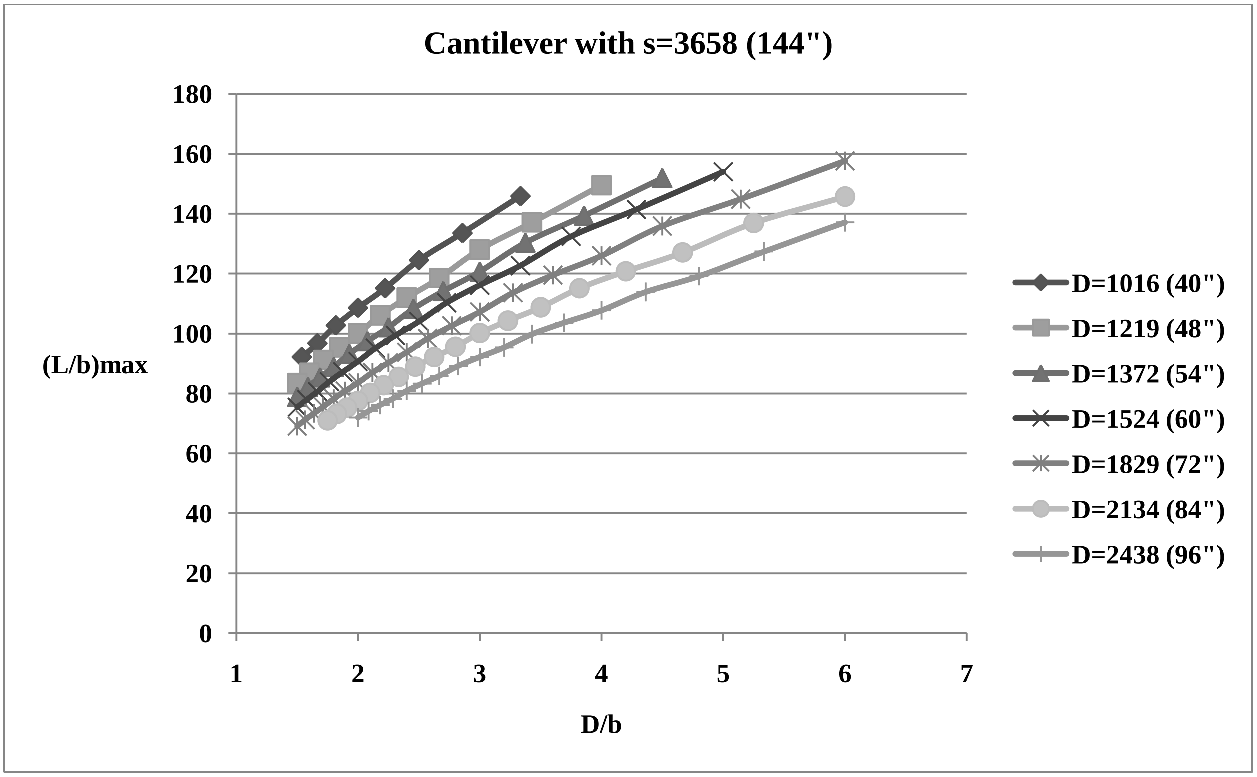
Cantilever with s=3658 (144")
(L/b)max
D/b
0
20
40
60
80
100
120
140
160
180
1
2
3
4
5
6
7
D=1016 (40")
D=1219 (48")
D=1372 (54")
D=1524 (60")
D=1829 (72")
D=2134 (84")
D=2438 (96")

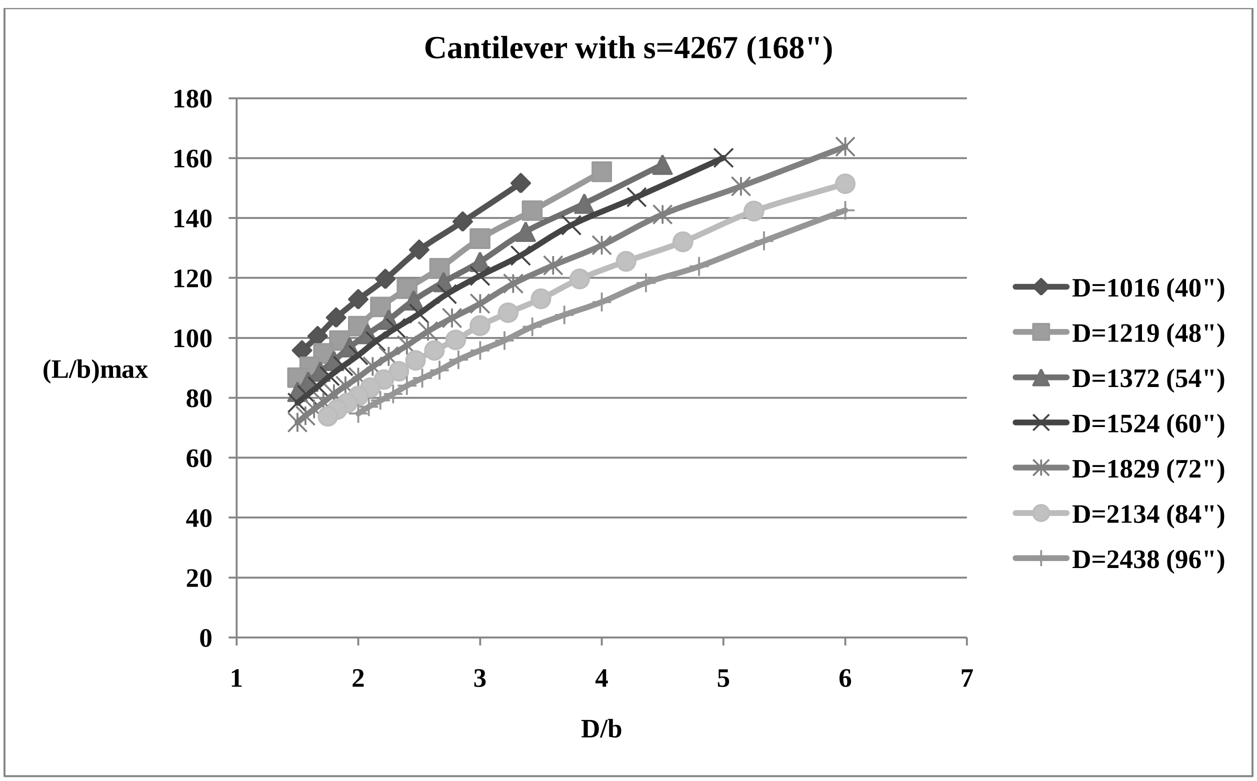
Cantilever with s=4267 (168")
(L/b)max
D/b
0
20
40
60
80
100
120
140
160
180
1
2
3
4
5
6
7
D=1016 (40")
D=1219 (48")
D=1372 (54")
D=1524 (60")
D=1829 (72")
D=2134 (84")
D=2438 (96")

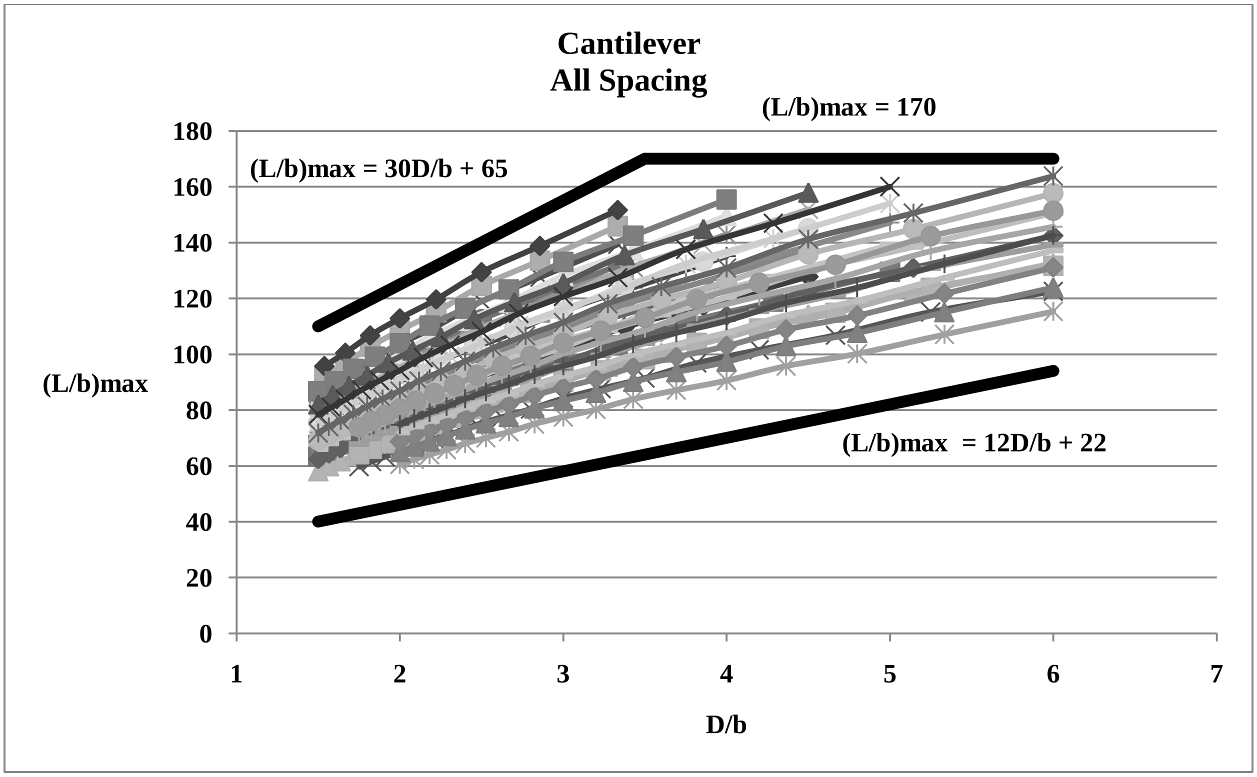
Cantilever
All Spacing
(L/b)max = 170
(L/b)max = 30D/b + 65
(L/b)max = 12D/b + 22
(L/b)max
D/b
180
160
140
120
100
80
60
40
20
0
1
2
3
4
5
6
7

APPENDIX D: SINGLE SYMMETRIC DOUBLE GIRDERS

Appendix D shows L/s vs. D/s, and L/b vs. D/b plots for single symmetric double girders with various spacings between girders. Simply supported and cantilever are investigated with dead load only.

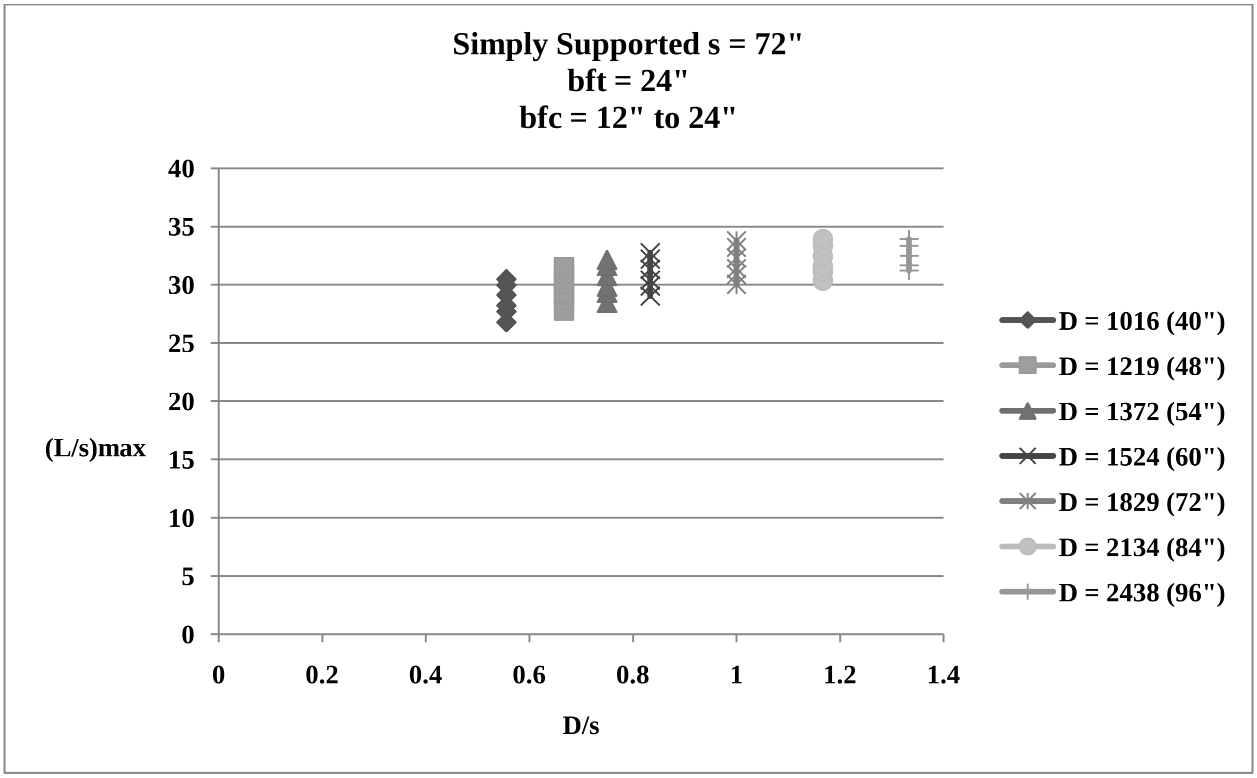

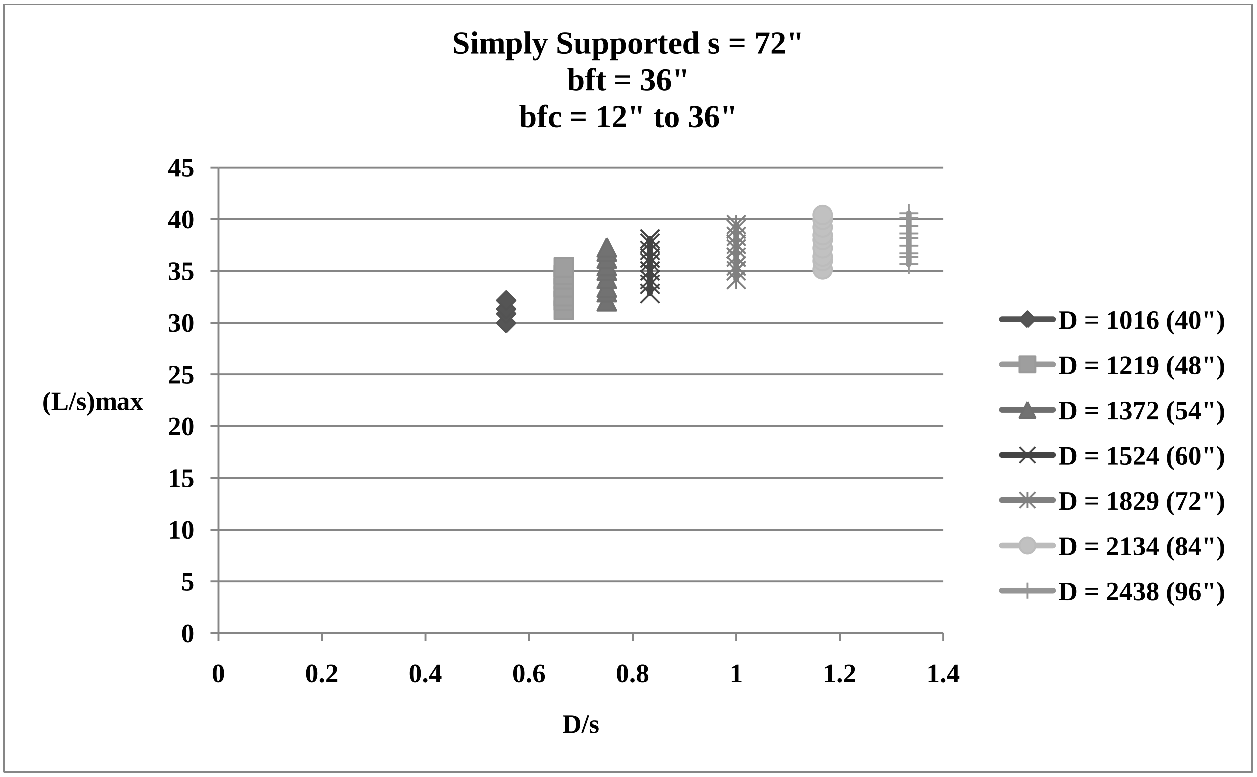
Simply Supported s = 72"
bft = 36"
bfc = 12" to 36"
45
40
35
30
25
20
15
10
5
0
(L/s)max
0
0.2
0.4
0.6
0.8
1
1.2
1.4
D/s
D = 1016 (40")
D = 1219 (48")
D = 1372 (54")
D = 1524 (60")
D = 1829 (72")
D = 2134 (84")
D = 2438 (96")

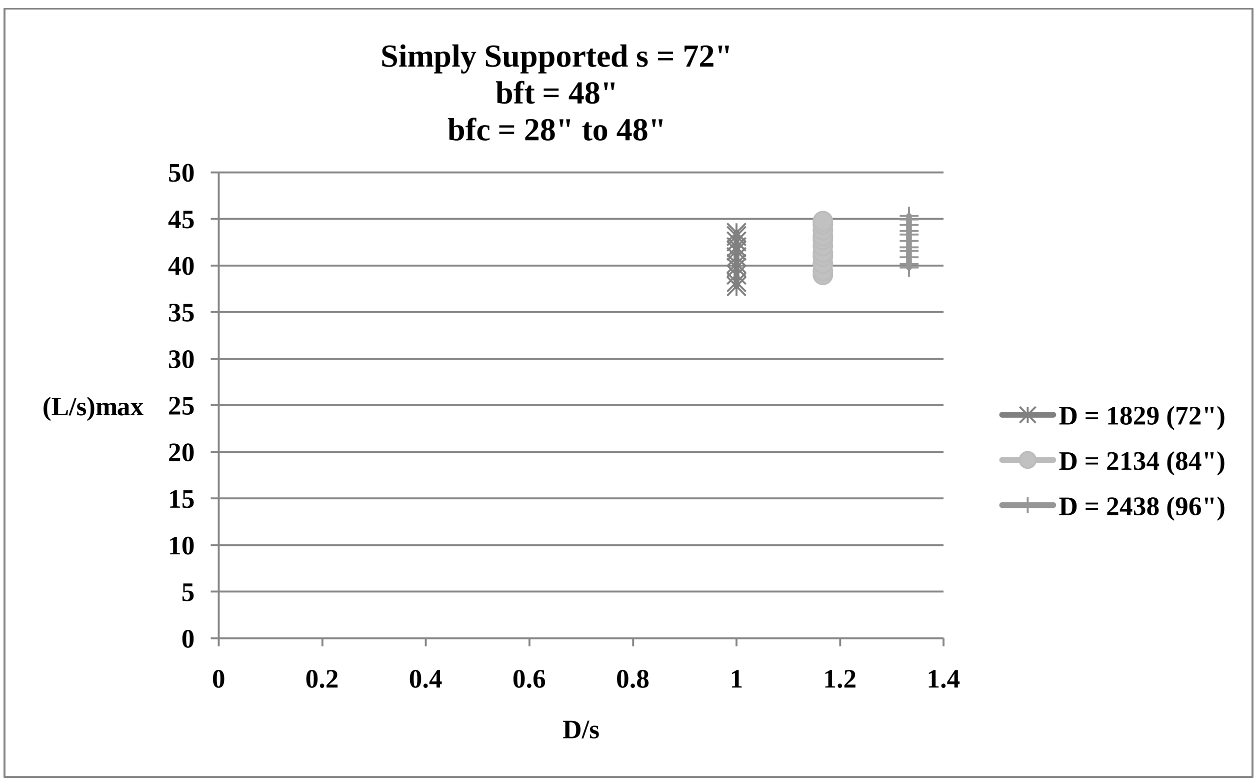
Simply Supported s = 72"
bft = 48"
bfc = 28" to 48"
50
45
40
35
30
25
20
15
10
5
0
(L/s)max
0
0.2
0.4
0.6
0.8
1
1.2
1.4
D/s
D = 1829 (72")
D = 2134 (84")
D = 2438 (96")

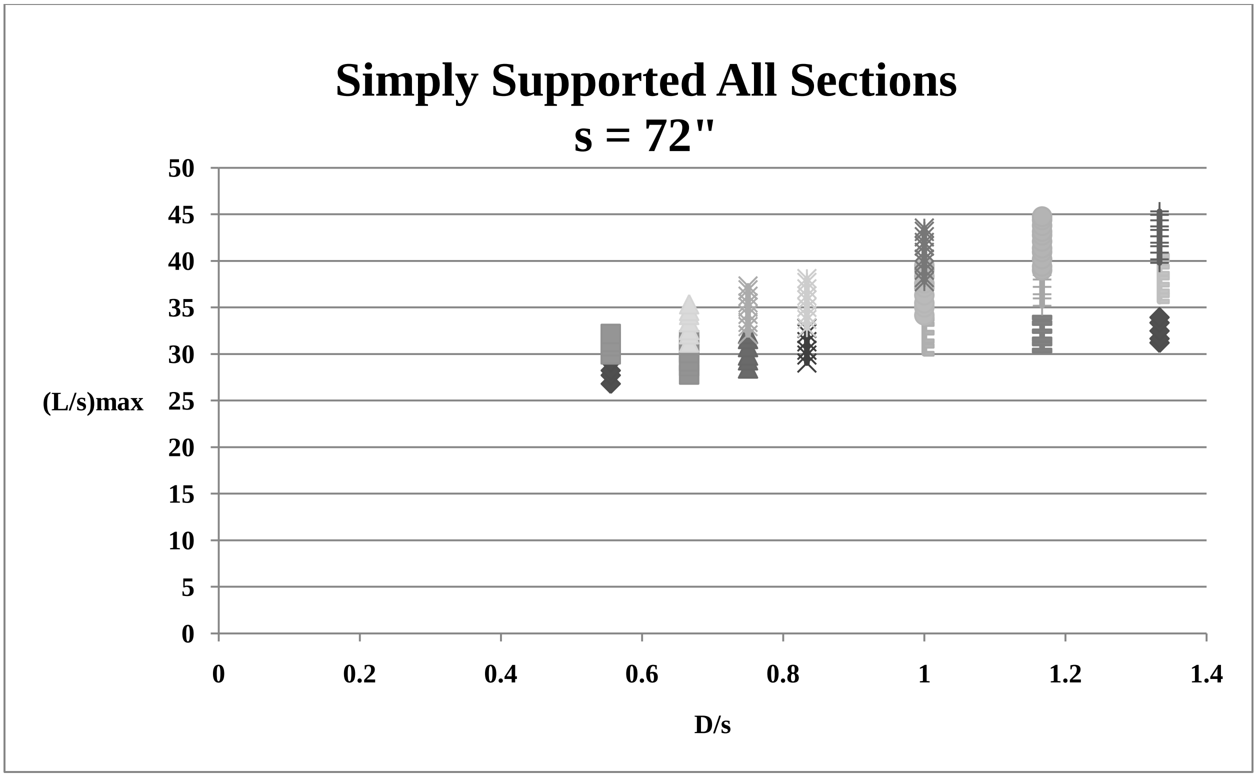
Simply Supported All Sections
s = 72"
(L/s)max
0
5
10
15
20
25
30
35
40
45
50
0
0.2
0.4
0.6
0.8
1
1.2
1.4
D/s

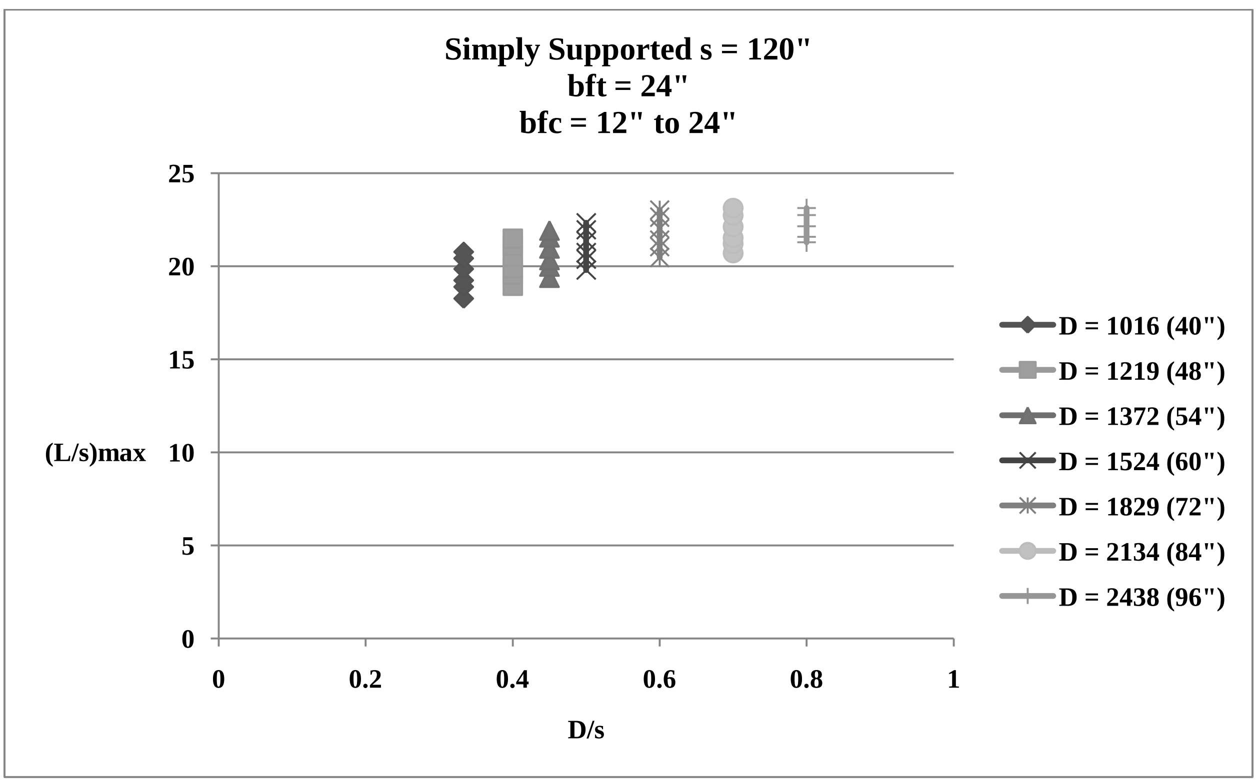
Simply Supported s = 120"
bft = 24"
bfc = 12" to 24"
(L/s)max
0
5
10
15
20
25
0
0.2
0.4
0.6
0.8
1
D/s
D = 1016 (40")
D = 1219 (48")
D = 1372 (54")
D = 1524 (60")
D = 1829 (72")
D = 2134 (84")
D = 2438 (96")

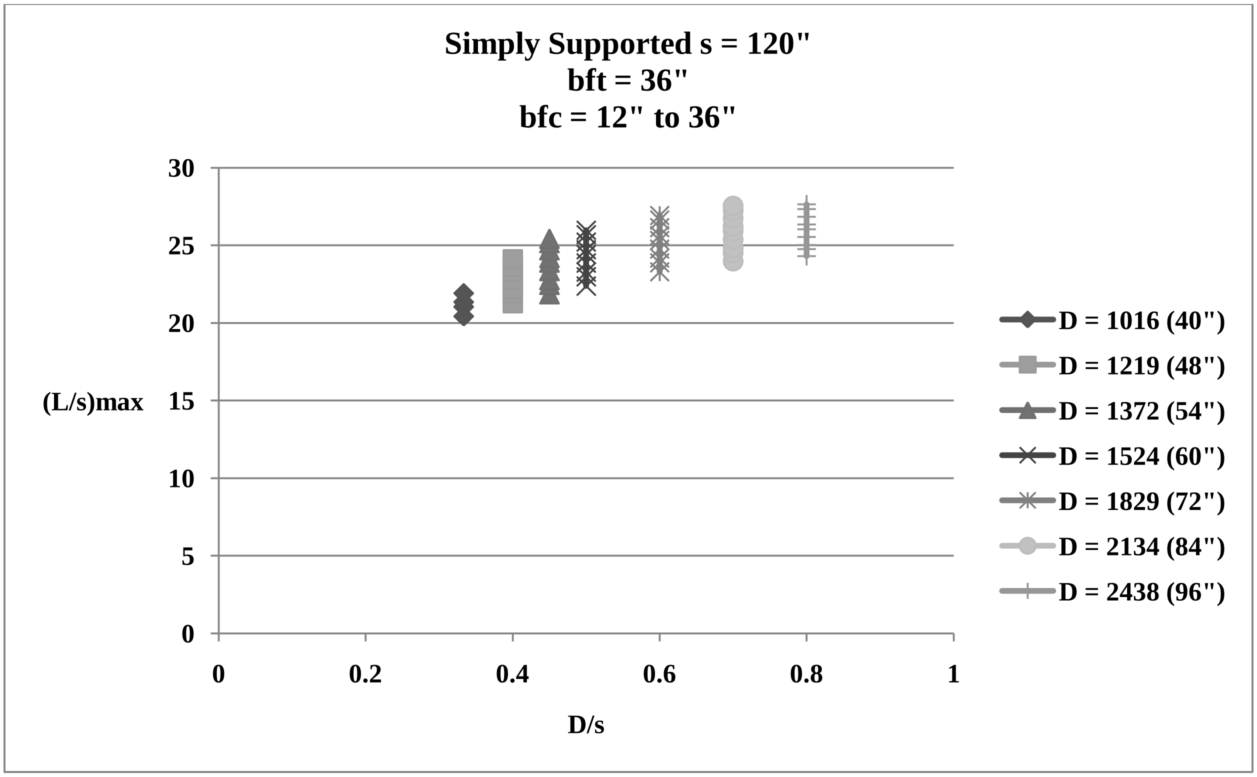
Simply Supported s = 120"
bft = 36"
bfc = 12" to 36"
(L/s)max
30
25
20
15
10
5
0
0
0.2
0.4
0.6
0.8
1
D/s
D = 1016 (40")
D = 1219 (48")
D = 1372 (54")
D = 1524 (60")
D = 1829 (72")
D = 2134 (84")
D = 2438 (96")

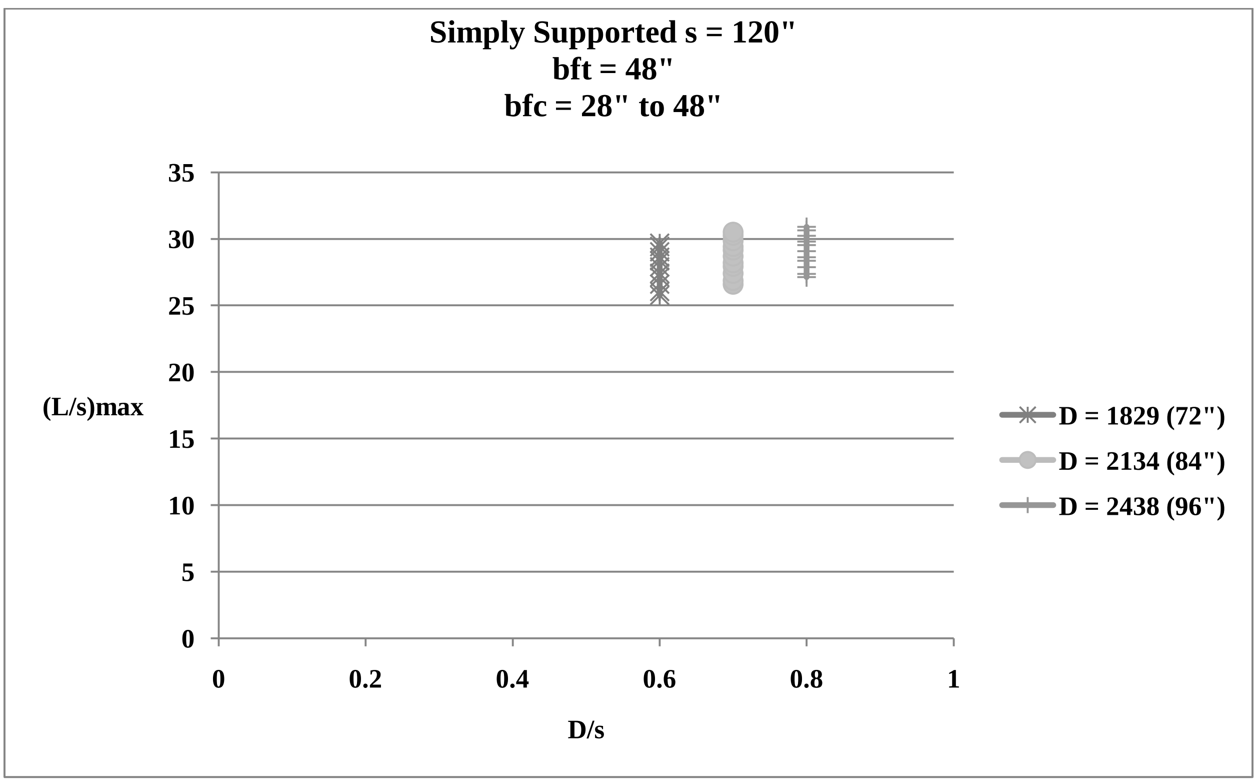
Simply Supported s = 120"
bft = 48"
bfc = 28" to 48"
(L/s)max
35
30
25
20
15
10
5
0
0
0.2
0.4
0.6
0.8
1
D/s
D = 1829 (72")
D = 2134 (84")
D = 2438 (96")

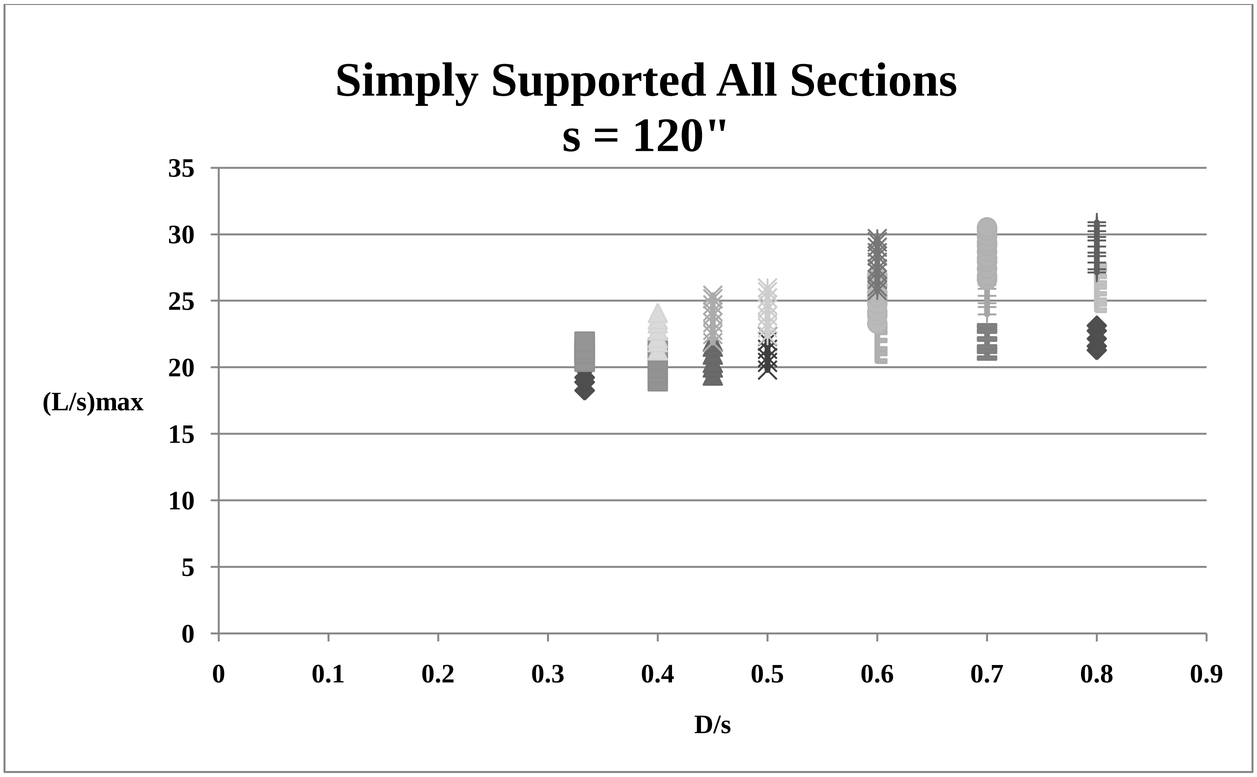

Simply Supported All Sections
s = 120"
(L/s)max
D/s
0
5
10
15
20
25
30
35
0
0.1
0.2
0.3
0.4
0.5
0.6
0.7
0.8
0.9

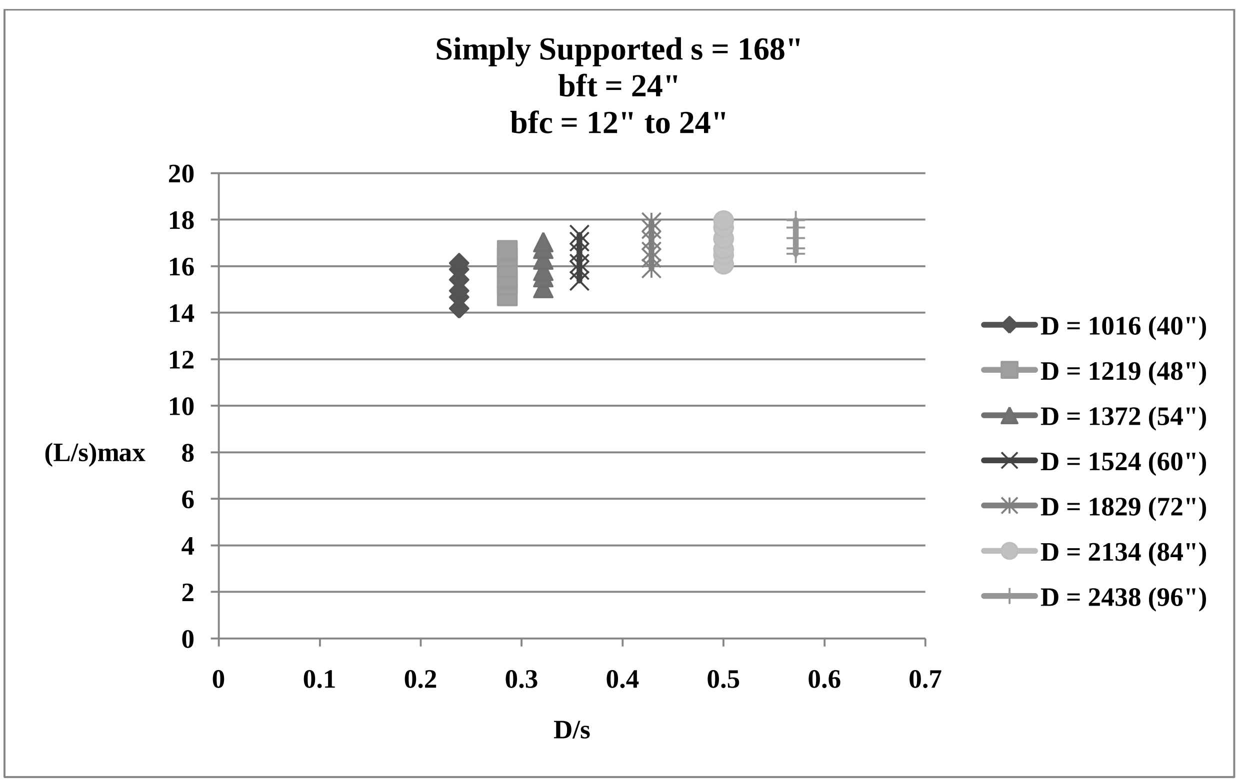

Simply Supported s = 168"
bft = 24"
bfc = 12" to 24"
(L/s)max
D/s
0
2
4
6
8
10
12
14
16
18
20
0
0.1
0.2
0.3
0.4
0.5
0.6
0.7
D = 1016 (40")
D = 1219 (48")
D = 1372 (54")
D = 1524 (60")
D = 1829 (72")
D = 2134 (84")
D = 2438 (96")

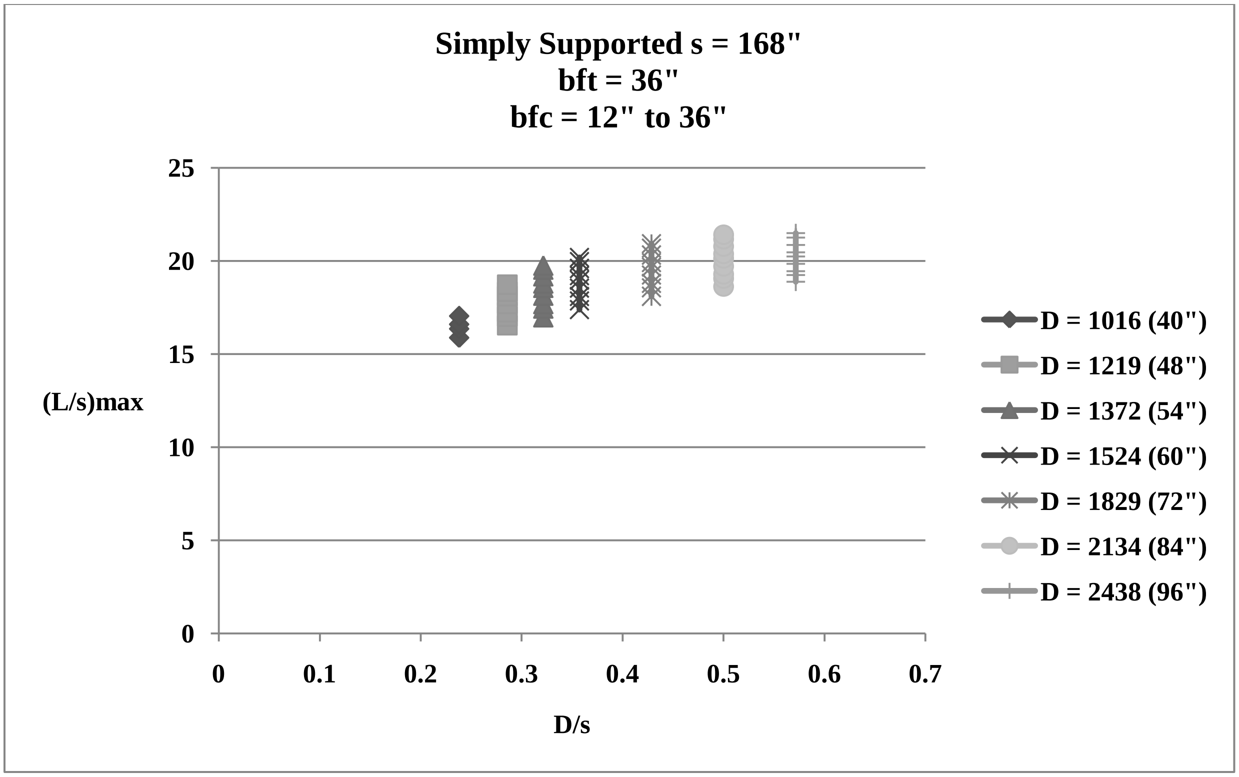
Simply Supported s = 168"
bft = 36"
bfc = 12" to 36"
25
20
15
10
5
0
(L/s)max
0
0.1
0.2
0.3
0.4
0.5
0.6
0.7
D/s
D = 1016 (40")
D = 1219 (48")
D = 1372 (54")
D = 1524 (60")
D = 1829 (72")
D = 2134 (84")
D = 2438 (96")

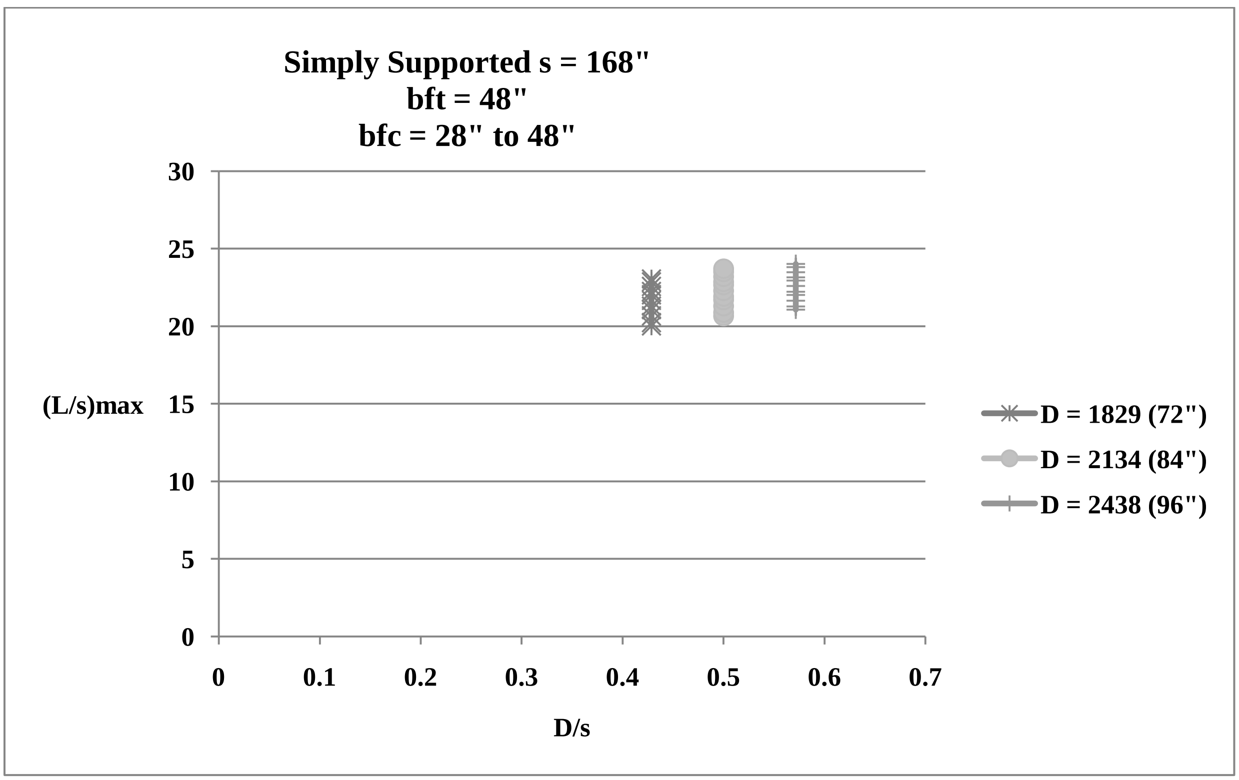
Simply Supported s = 168"
bft = 48"
bfc = 28" to 48"
30
25
20
15
10
5
0
(L/s)max
0
0.1
0.2
0.3
0.4
0.5
0.6
0.7
D/s
D = 1829 (72")
D = 2134 (84")
D = 2438 (96")

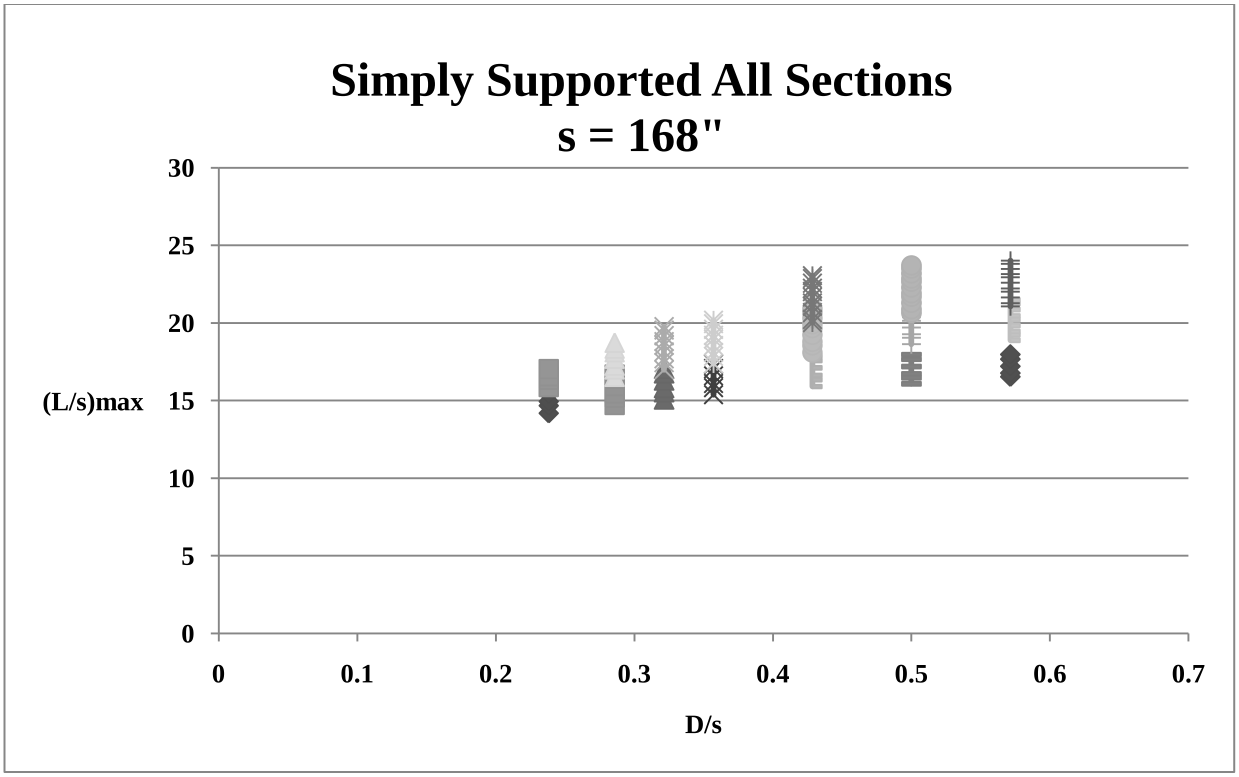

Simply Supported All Sections
s = 168"
30
25
20
15
10
5
0
(L/s)max
0
0.1
0.2
0.3
0.4
0.5
0.6
0.7
D/s

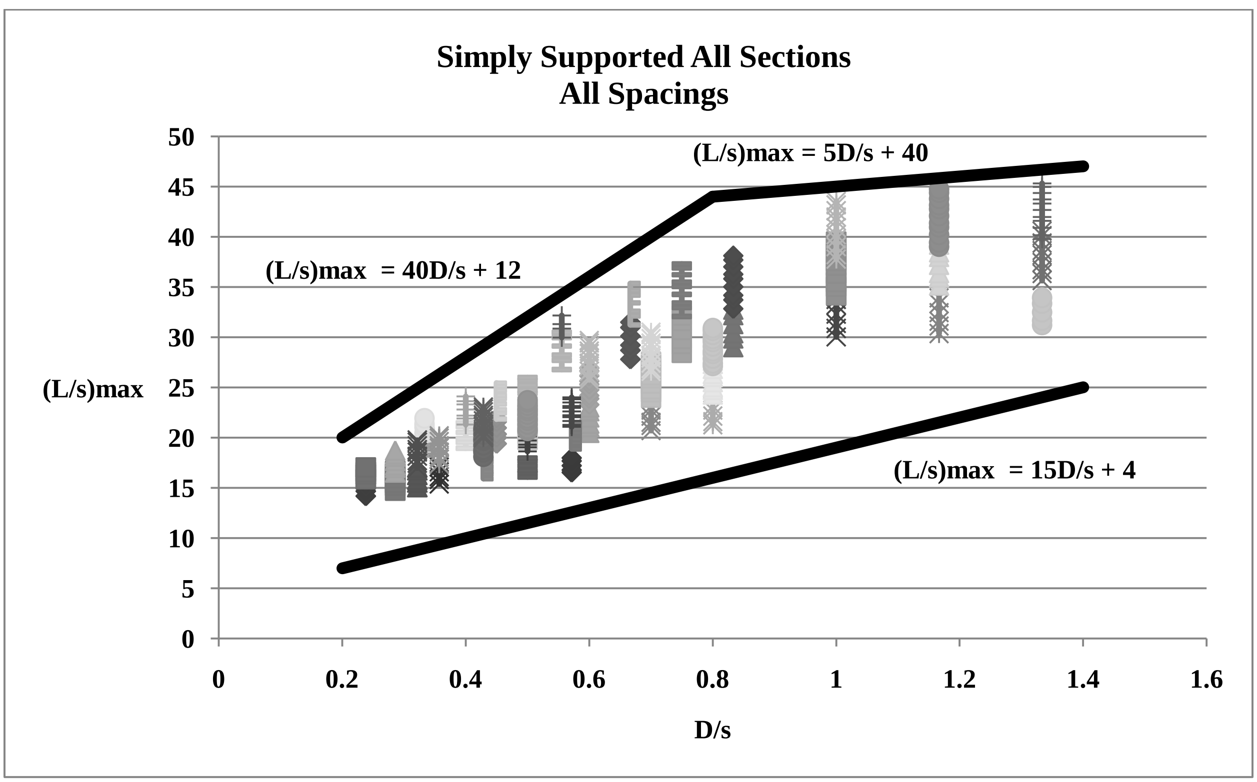

Simply Supported All Sections
All Spacings
50
45
40
35
30
25
20
15
10
5
0
(L/s)max
(L/s)max = 5D/s + 40
(L/s)max = 40D/s + 12
(L/s)max = 15D/s + 4
0
0.2
0.4
0.6
0.8
1
1.2
1.4
1.6
D/s

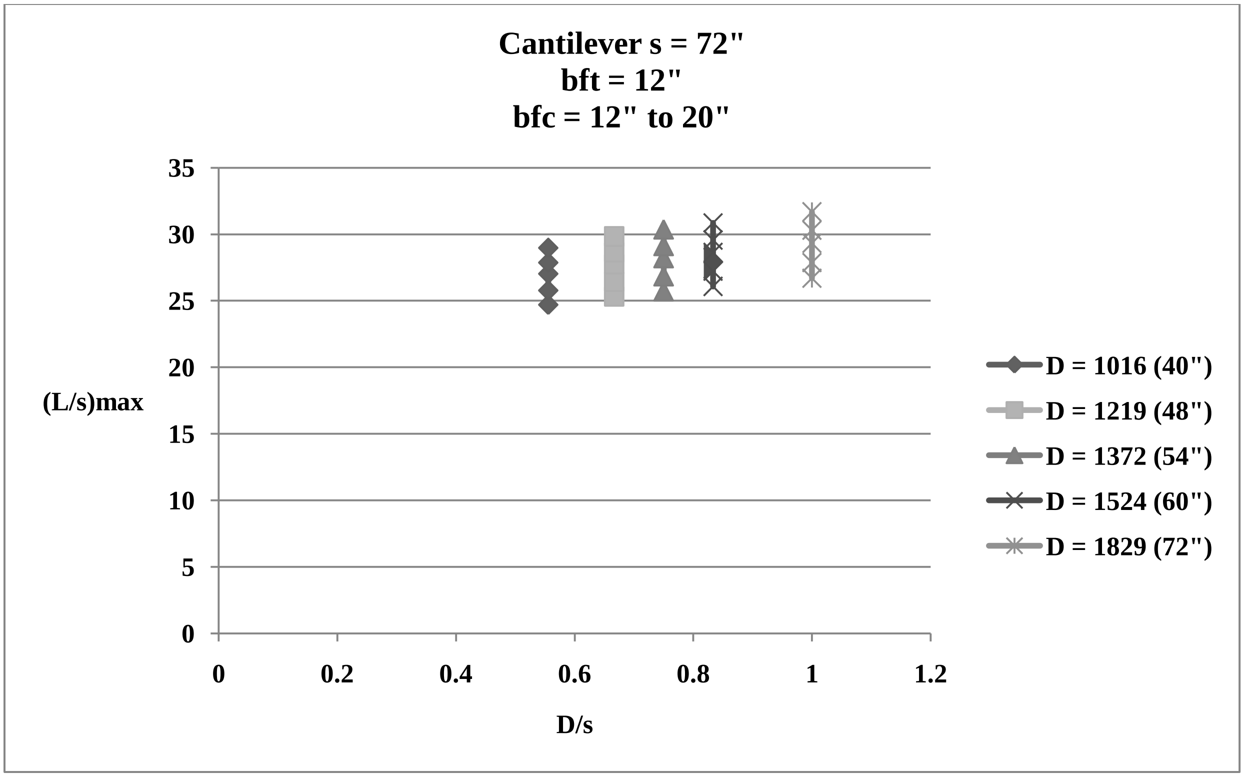
Cantilever s = 72"
bft = 12"
bfc = 12" to 20"
35
30
25
20
15
10
5
0
(L/s)max
0
0.2
0.4
0.6
0.8
1
1.2
D/s
D = 1016 (40")
D = 1219 (48")
D = 1372 (54")
D = 1524 (60")
D = 1829 (72")

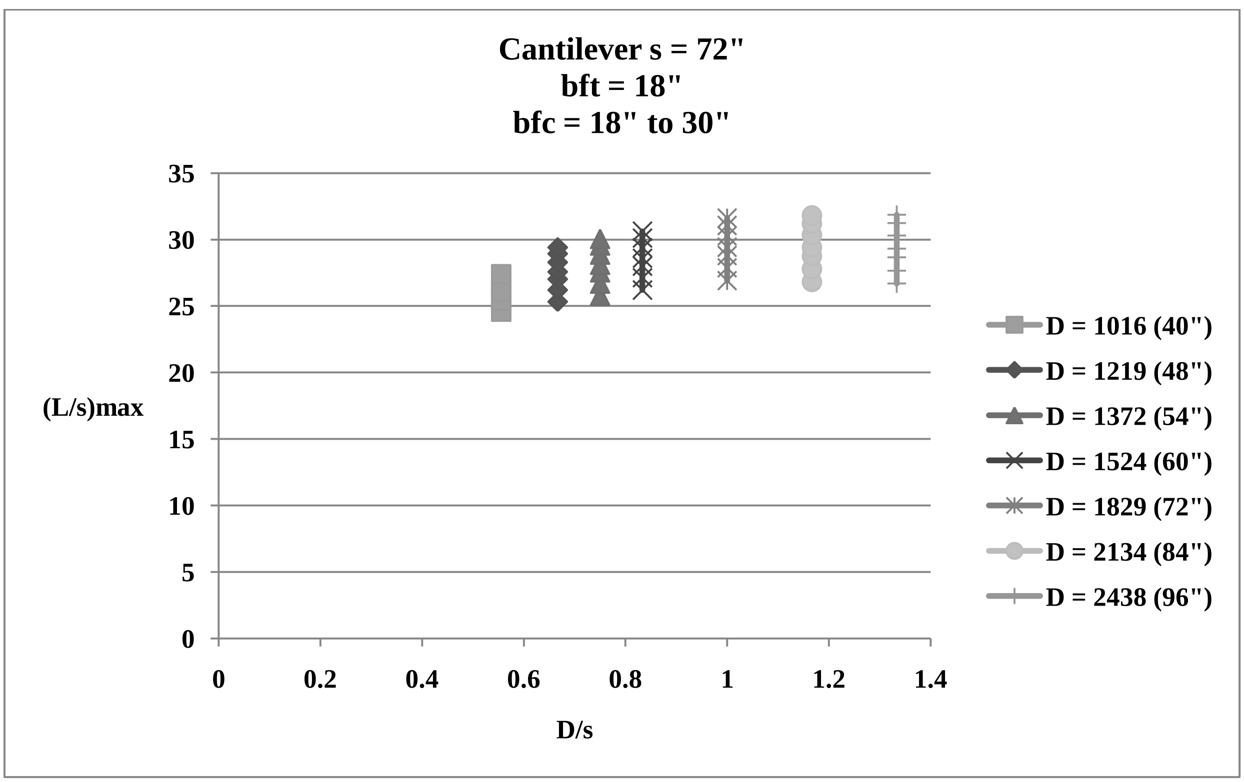
Cantilever s = 72"
bft = 18"
bfc = 18" to 30"
35
30
25
20
15
10
5
0
(L/s)max
0
0.2
0.4
0.6
0.8
1
1.2
1.4
D/s
D = 1016 (40")
D = 1219 (48")
D = 1372 (54")
D = 1524 (60")
D = 1829 (72")
D = 2134 (84")
D = 2438 (96")

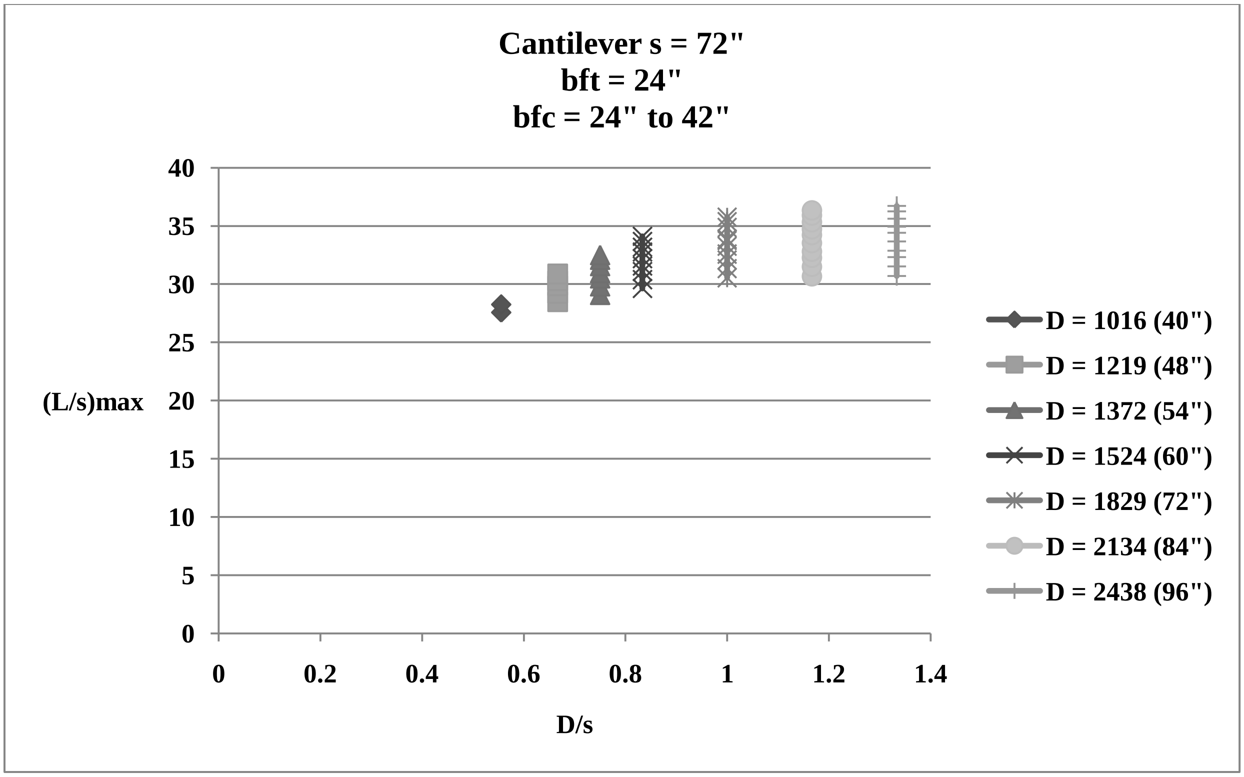
Cantilever s = 72"
bft = 24"
bfc = 24" to 42"
(L/s)max
D/s
0
5
10
15
20
25
30
35
40
0
0.2
0.4
0.6
0.8
1
1.2
1.4
D = 1016 (40")
D = 1219 (48")
D = 1372 (54")
D = 1524 (60")
D = 1829 (72")
D = 2134 (84")
D = 2438 (96")

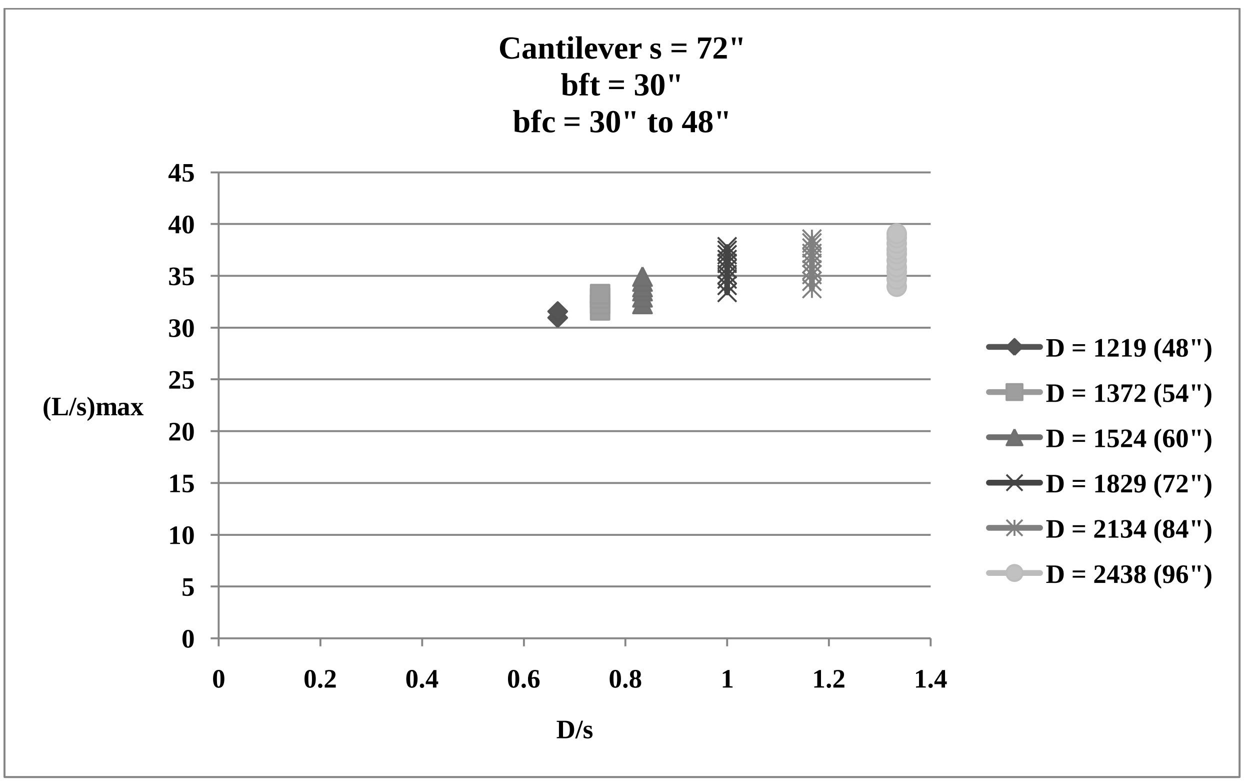
Cantilever s = 72"
bft = 30"
bfc = 30" to 48"
(L/s)max
D/s
0
5
10
15
20
25
30
35
40
45
0
0.2
0.4
0.6
0.8
1
1.2
1.4
D = 1219 (48")
D = 1372 (54")
D = 1524 (60")
D = 1829 (72")
D = 2134 (84")
D = 2438 (96")

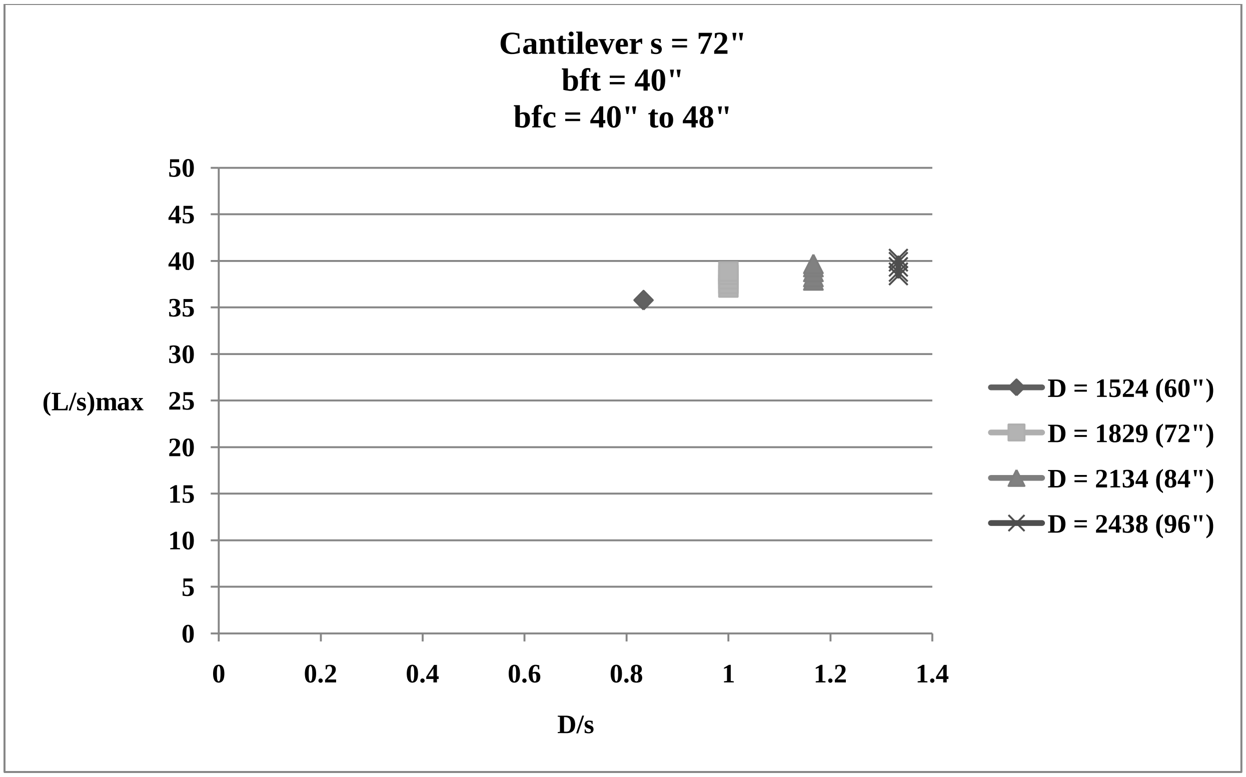
Cantilever s = 72"
bft = 40"
bfc = 40" to 48"
50
45
40
35
30
25
20
15
10
5
0
(L/s)max
0
0.2
0.4
0.6
0.8
1
1.2
1.4
D/s
D = 1524 (60")
D = 1829 (72")
D = 2134 (84")
D = 2438 (96")

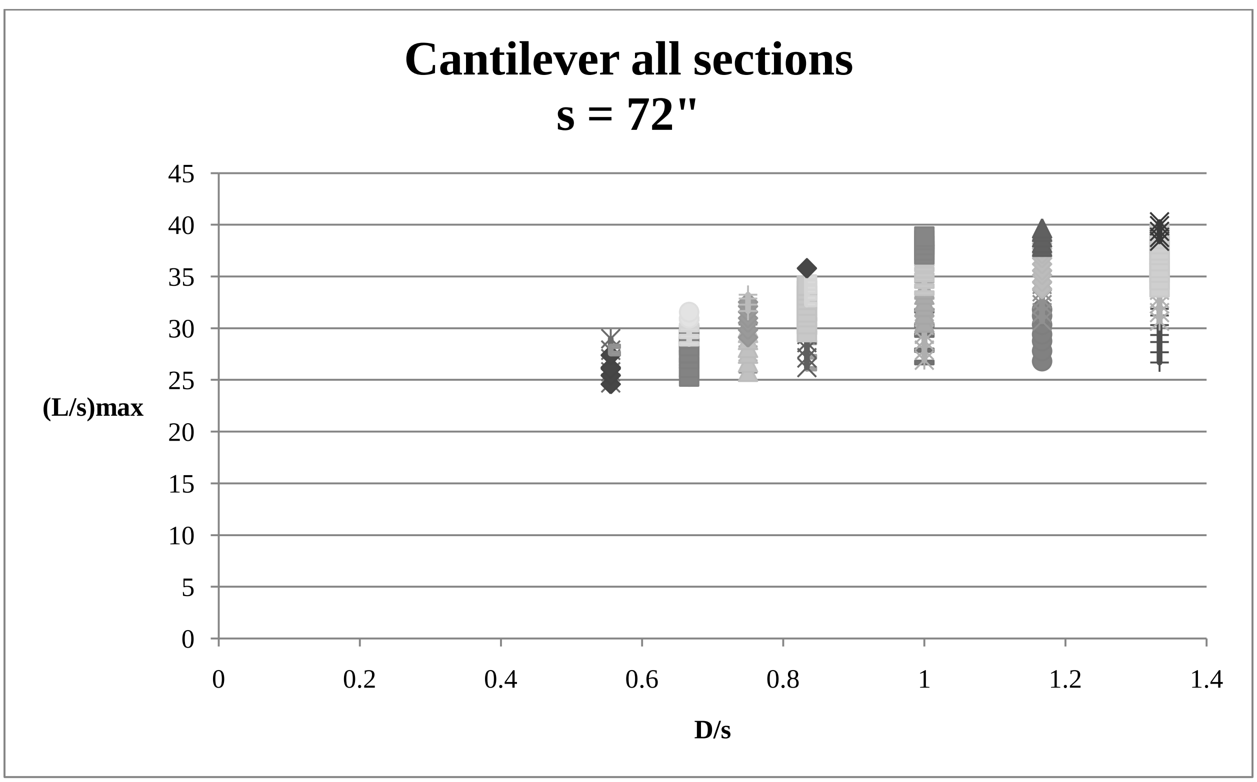
Cantilever all sections
s = 72"
45
40
35
30
25
20
15
10
5
0
(L/s)max
0
0.2
0.4
0.6
0.8
1
1.2
1.4
D/s

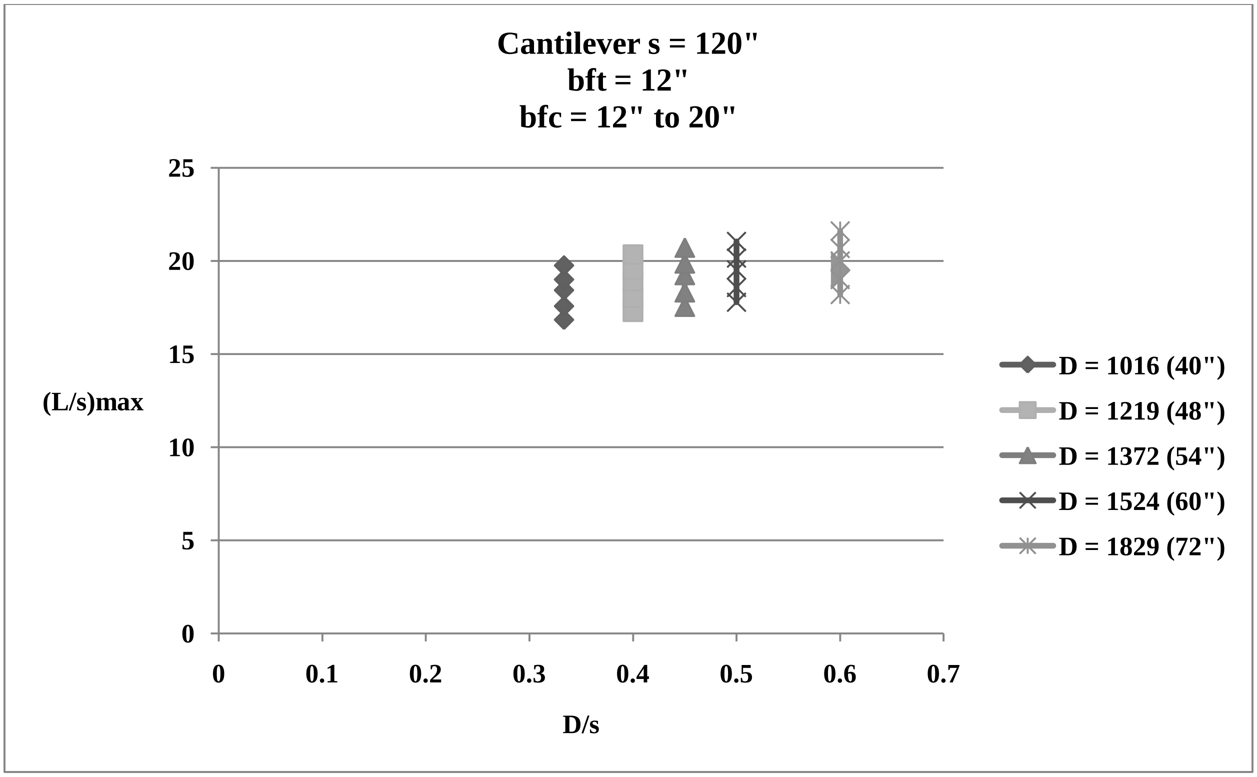
Cantilever s = 120"
bft = 12"
bfc = 12" to 20"
25
20
15
10
5
0
(L/s)max
0
0.1
0.2
0.3
0.4
0.5
0.6
0.7
D/s
D = 1016 (40")
D = 1219 (48")
D = 1372 (54")
D = 1524 (60")
D = 1829 (72")

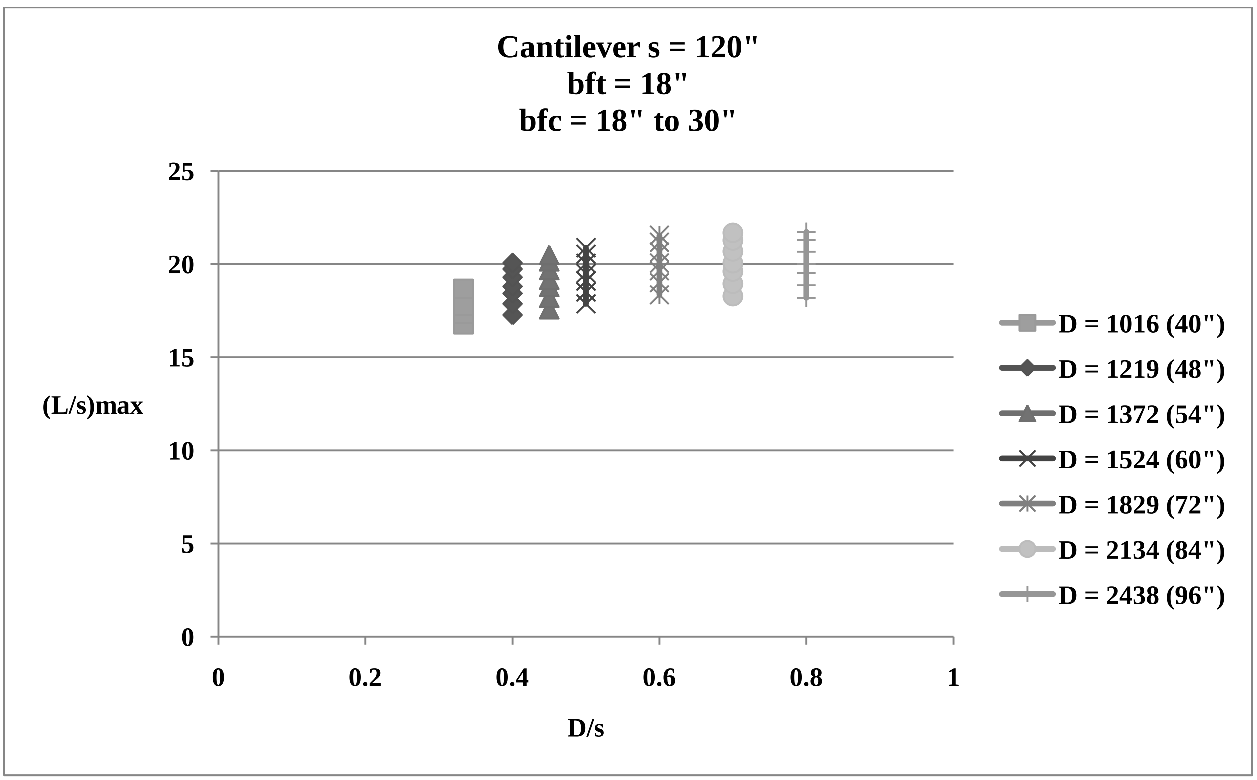
Cantilever s = 120"
bft = 18"
bfc = 18" to 30"
25
20
15
10
5
0
(L/s)max
0
0.2
0.4
0.6
0.8
1
D/s
D = 1016 (40")
D = 1219 (48")
D = 1372 (54")
D = 1524 (60")
D = 1829 (72")
D = 2134 (84")
D = 2438 (96")

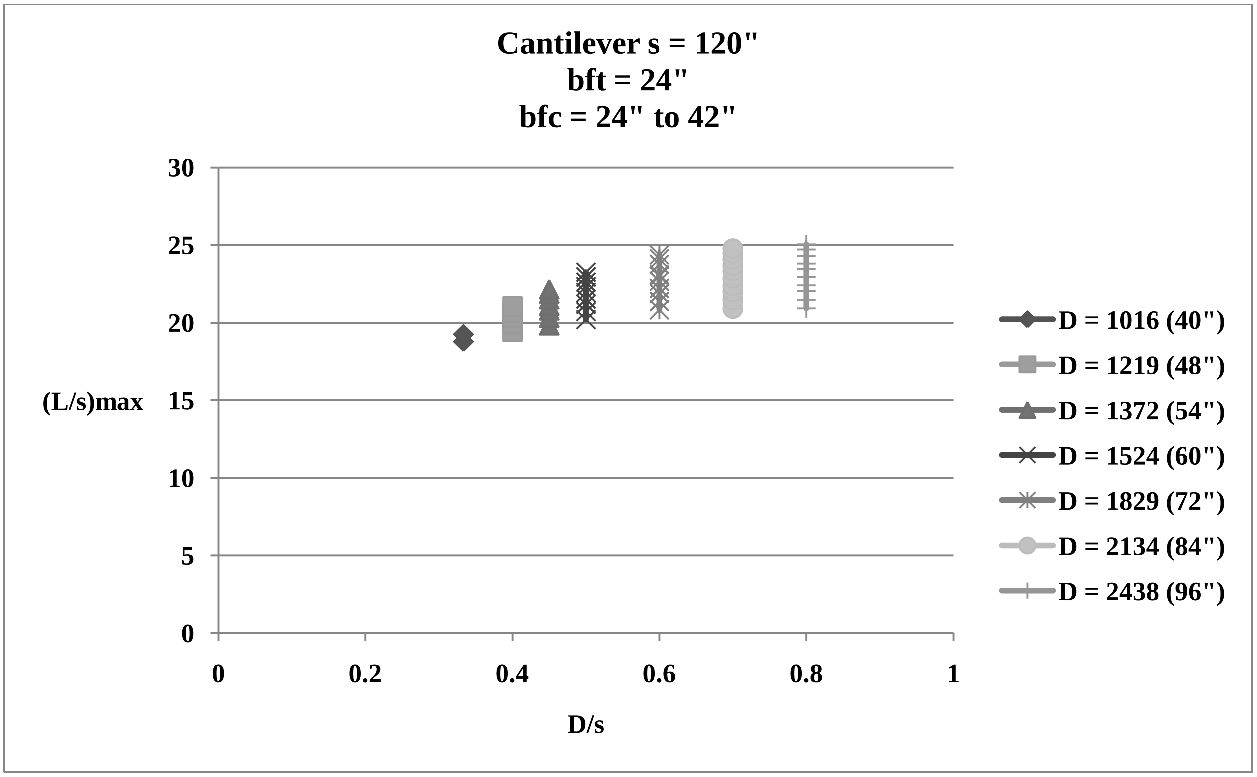
Cantilever s = 120"
bft = 24"
bfc = 24" to 42"
30
25
20
15
10
5
0
(L/s)max
0
0.2
0.4
0.6
0.8
1
D/s
D = 1016 (40")
D = 1219 (48")
D = 1372 (54")
D = 1524 (60")
D = 1829 (72")
D = 2134 (84")
D = 2438 (96")

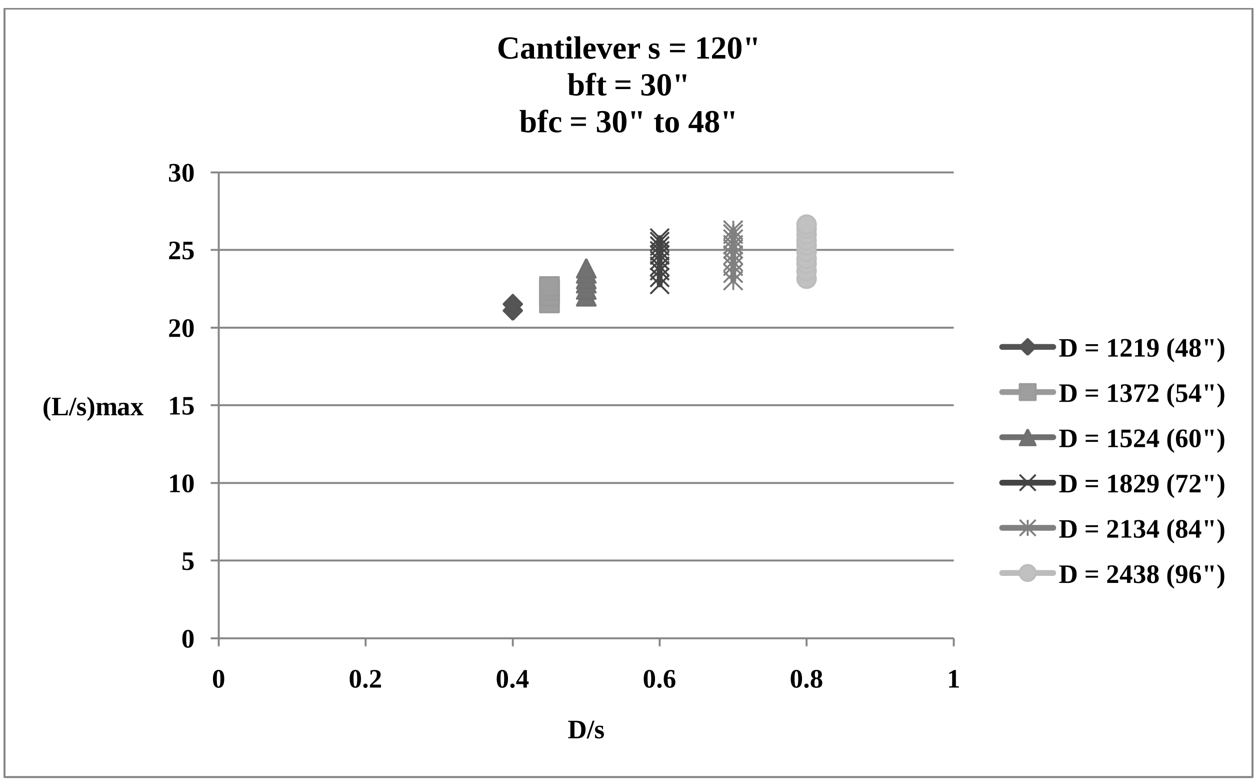
Cantilever s = 120"
bft = 30"
bfc = 30" to 48"
30
25
20
15
10
5
0
(L/s)max
0
0.2
0.4
0.6
0.8
1
D/s
D = 1219 (48")
D = 1372 (54")
D = 1524 (60")
D = 1829 (72")
D = 2134 (84")
D = 2438 (96")

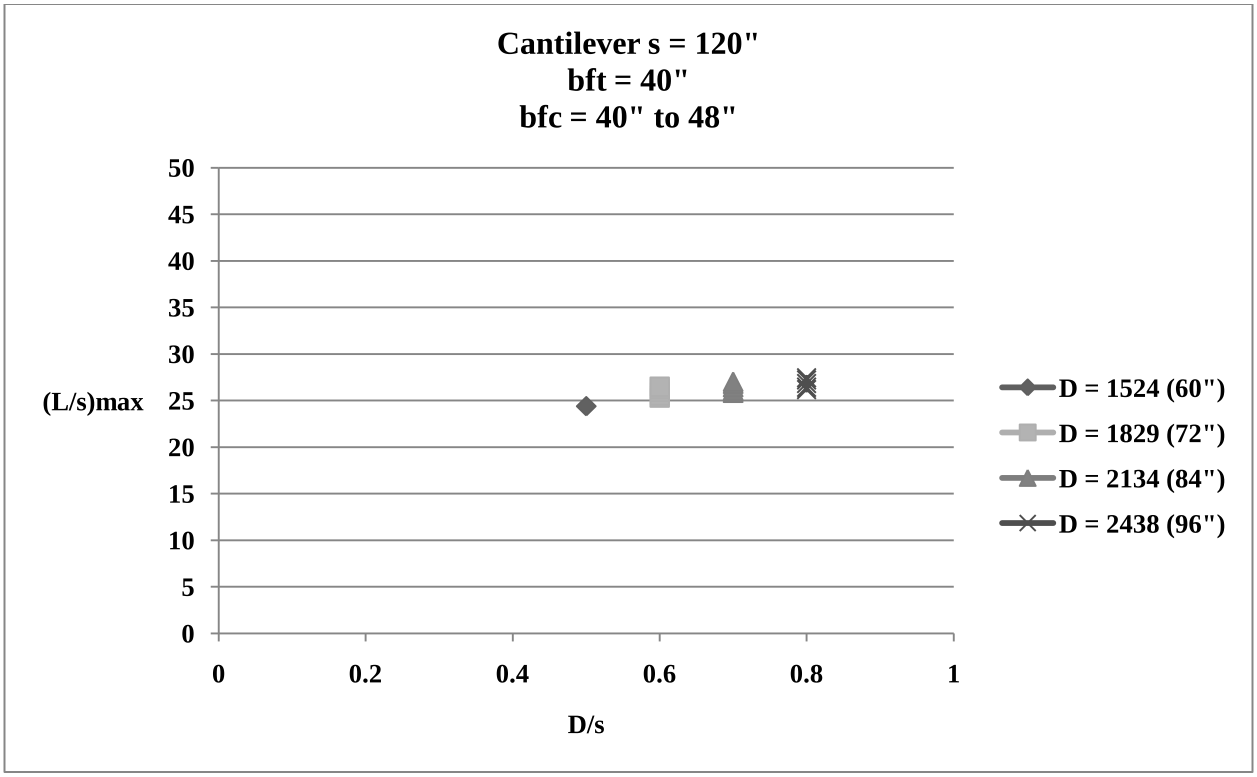
Cantilever s = 120"
bft = 40"
bfc = 40" to 48"
50
45
40
35
30
25
20
15
10
5
0
(L/s)max
0
0.2
0.4
0.6
0.8
1
D/s
D = 1524 (60")
D = 1829 (72")
D = 2134 (84")
D = 2438 (96")

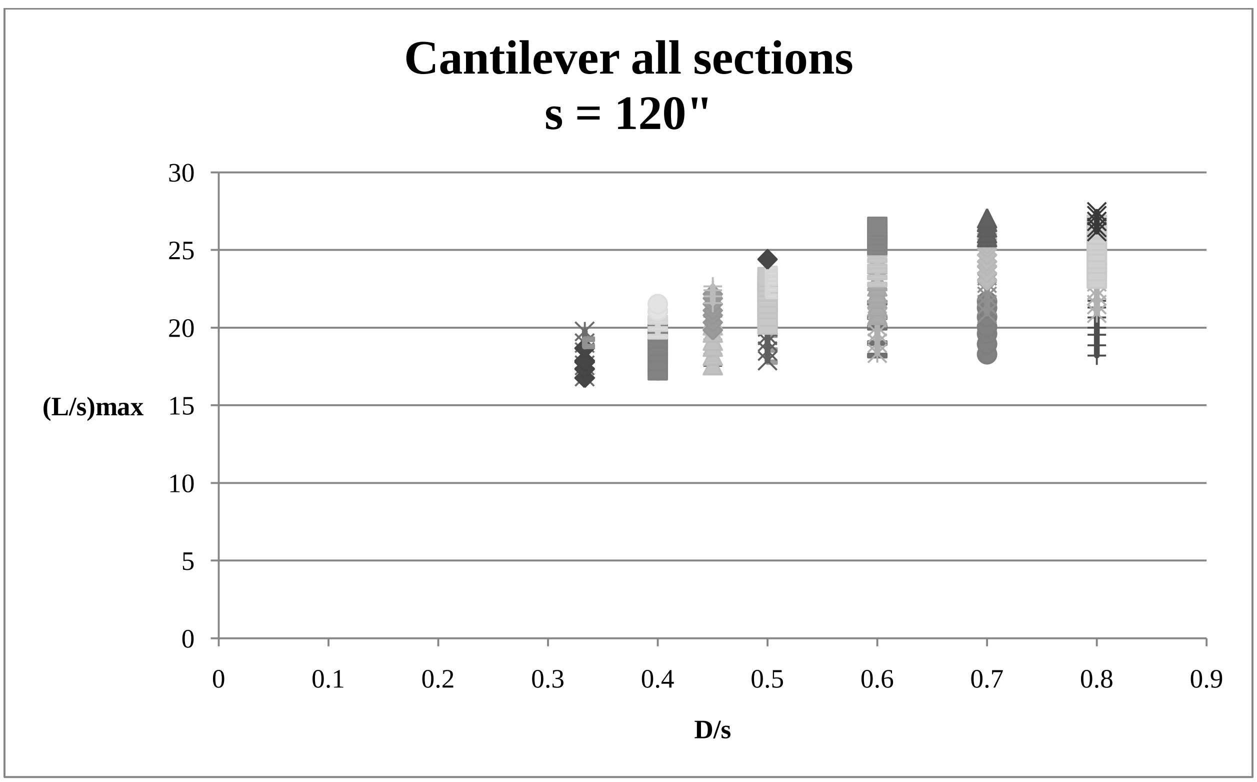
Cantilever all sections
s = 120"
30
25
20
15
10
5
0
(L/s)max
0
0.1
0.2
0.3
0.4
0.5
0.6
0.7
0.8
0.9
D/s

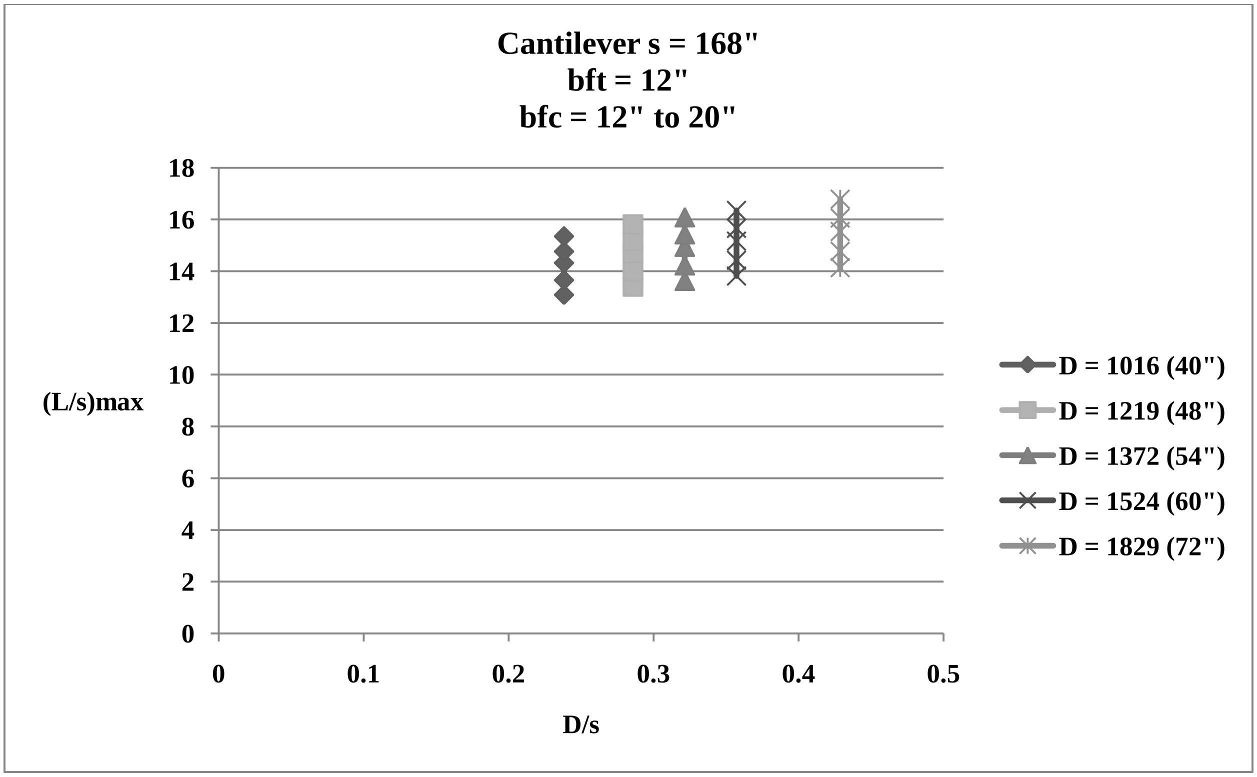
Cantilever s = 168"
bft = 12"
bfc = 12" to 20"
(L/s)max
D/s
D = 1016 (40")
D = 1219 (48")
D = 1372 (54")
D = 1524 (60")
D = 1829 (72")
0
2
4
6
8
10
12
14
16
18
0
0.1
0.2
0.3
0.4
0.5

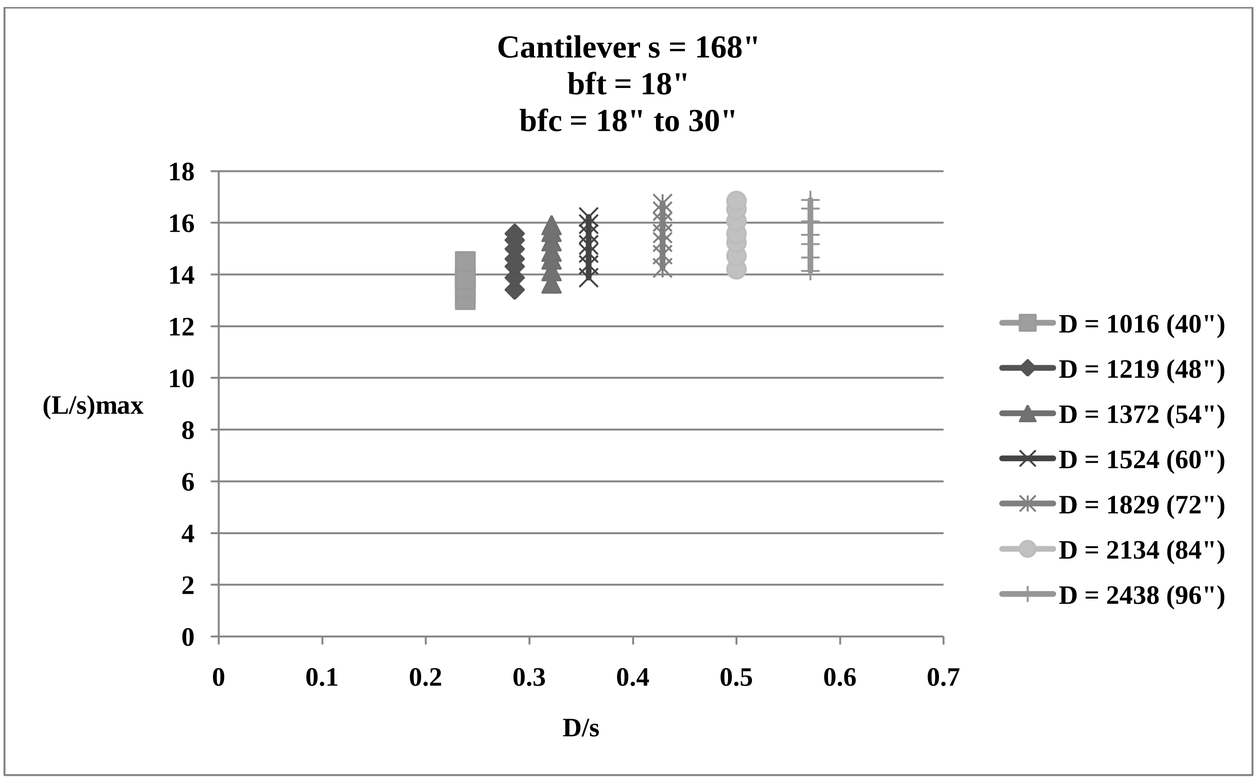
Cantilever s = 168"
bft = 18"
bfc = 18" to 30"
(L/s)max
D/s
D = 1016 (40")
D = 1219 (48")
D = 1372 (54")
D = 1524 (60")
D = 1829 (72")
D = 2134 (84")
D = 2438 (96")
0
2
4
6
8
10
12
14
16
18
0
0.1
0.2
0.3
0.4
0.5
0.6
0.7

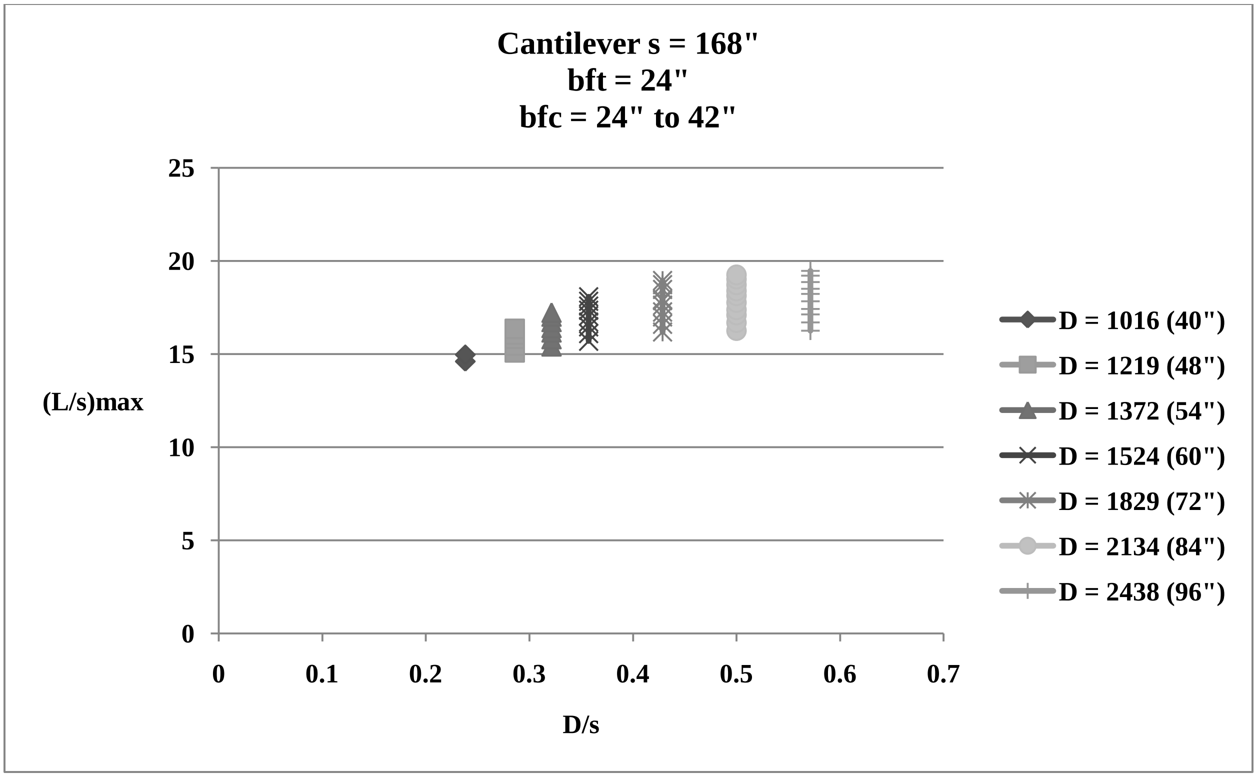
Cantilever s = 168"
bft = 24"
bfc = 24" to 42"
25
20
15
10
5
0
(L/s)max
0
0.1
0.2
0.3
0.4
0.5
0.6
0.7
D/s
D = 1016 (40")
D = 1219 (48")
D = 1372 (54")
D = 1524 (60")
D = 1829 (72")
D = 2134 (84")
D = 2438 (96")

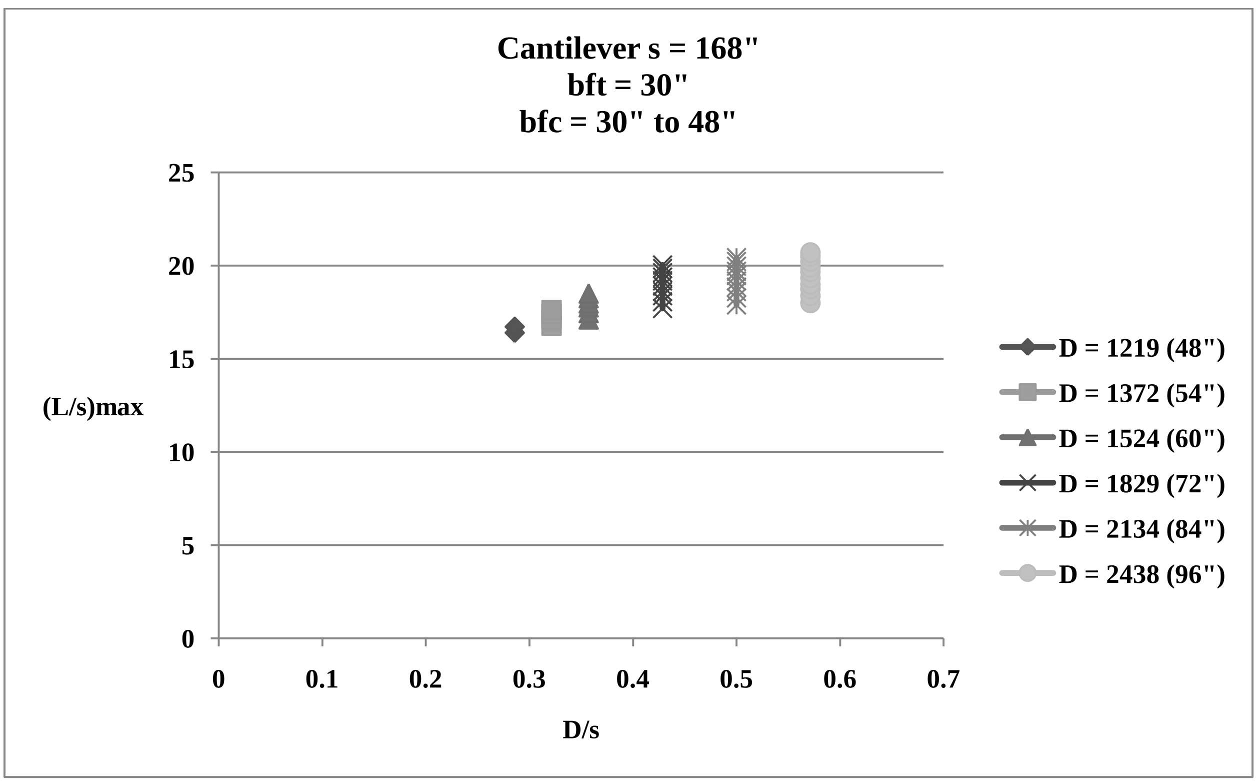
Cantilever s = 168"
bft = 30"
bfc = 30" to 48"
25
20
15
10
5
0
(L/s)max
0
0.1
0.2
0.3
0.4
0.5
0.6
0.7
D/s
D = 1219 (48")
D = 1372 (54")
D = 1524 (60")
D = 1829 (72")
D = 2134 (84")
D = 2438 (96")

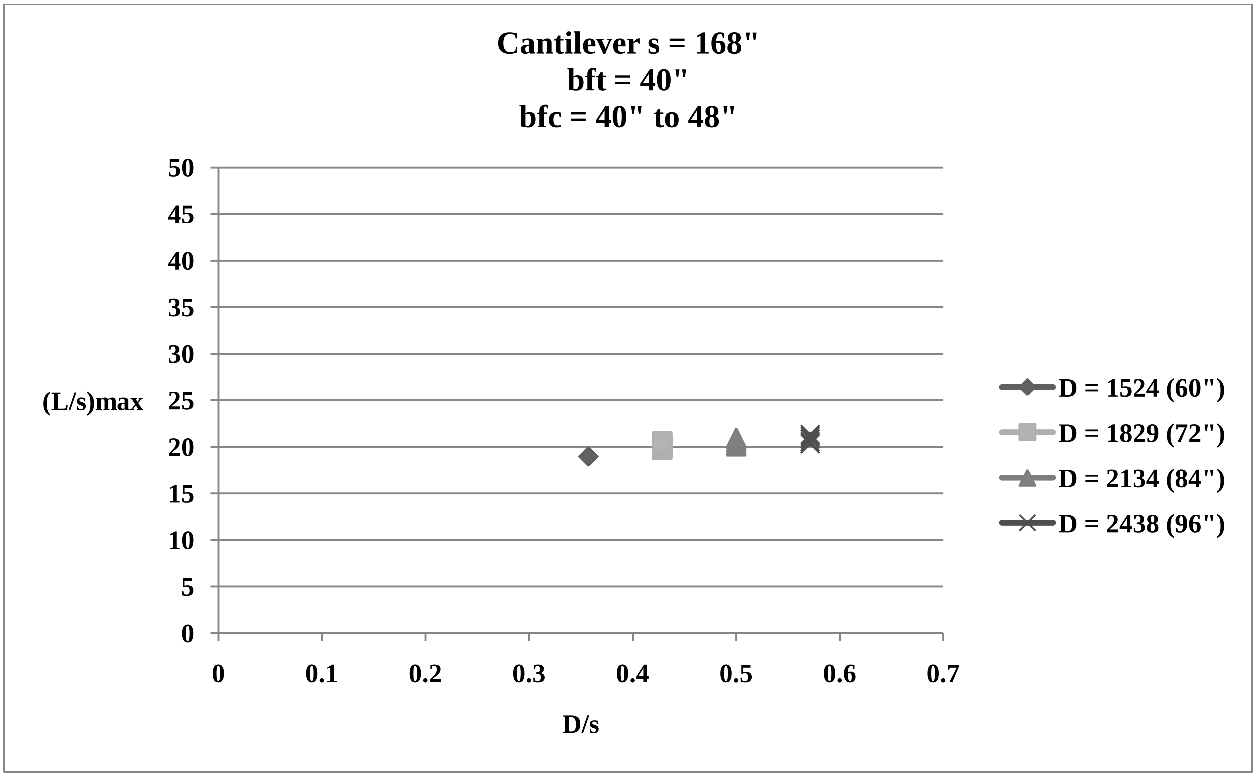
Cantilever s = 168"
bft = 40"
bfc = 40" to 48"
50
45
40
35
30
25
20
15
10
5
0
(L/s)max
0
0.1
0.2
0.3
0.4
0.5
0.6
0.7
D/s
D = 1524 (60")
D = 1829 (72")
D = 2134 (84")
D = 2438 (96")

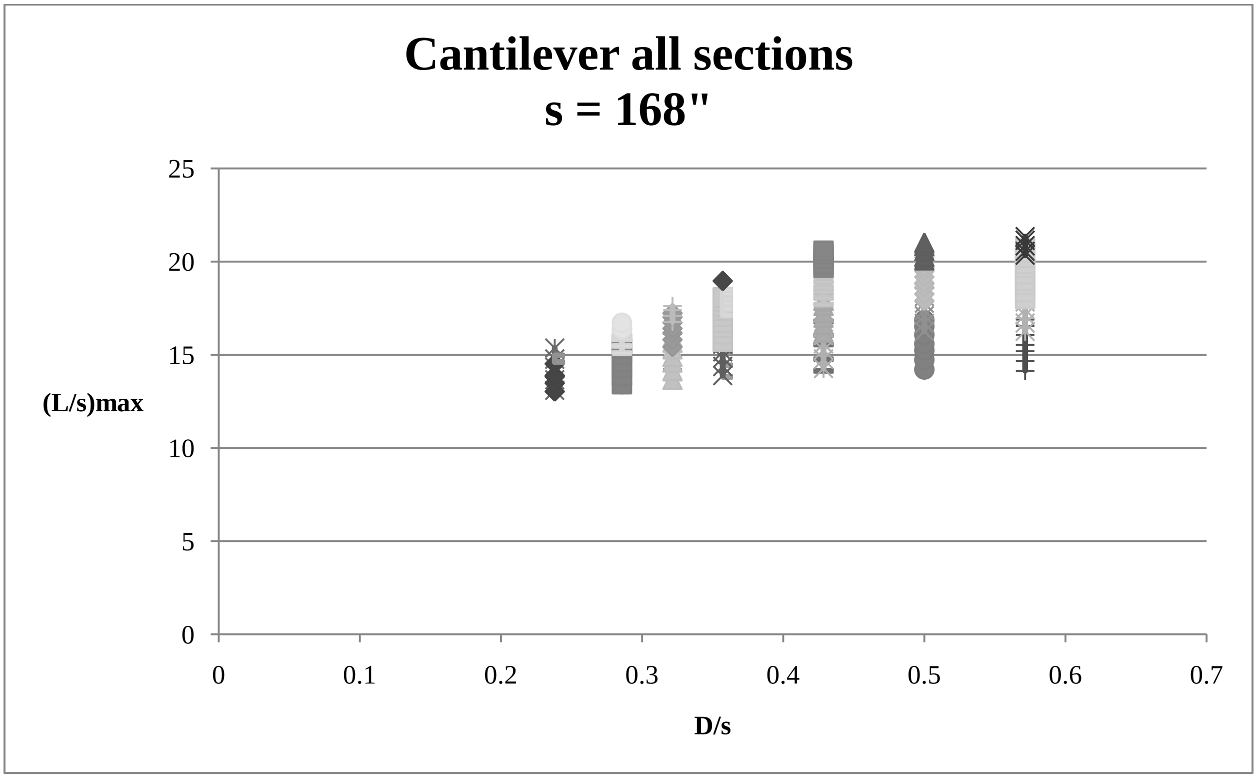
Cantilever all sections
s = 168"
25
20
15
10
5
0
(L/s)max
0
0.1
0.2
0.3
0.4
0.5
0.6
0.7
D/s

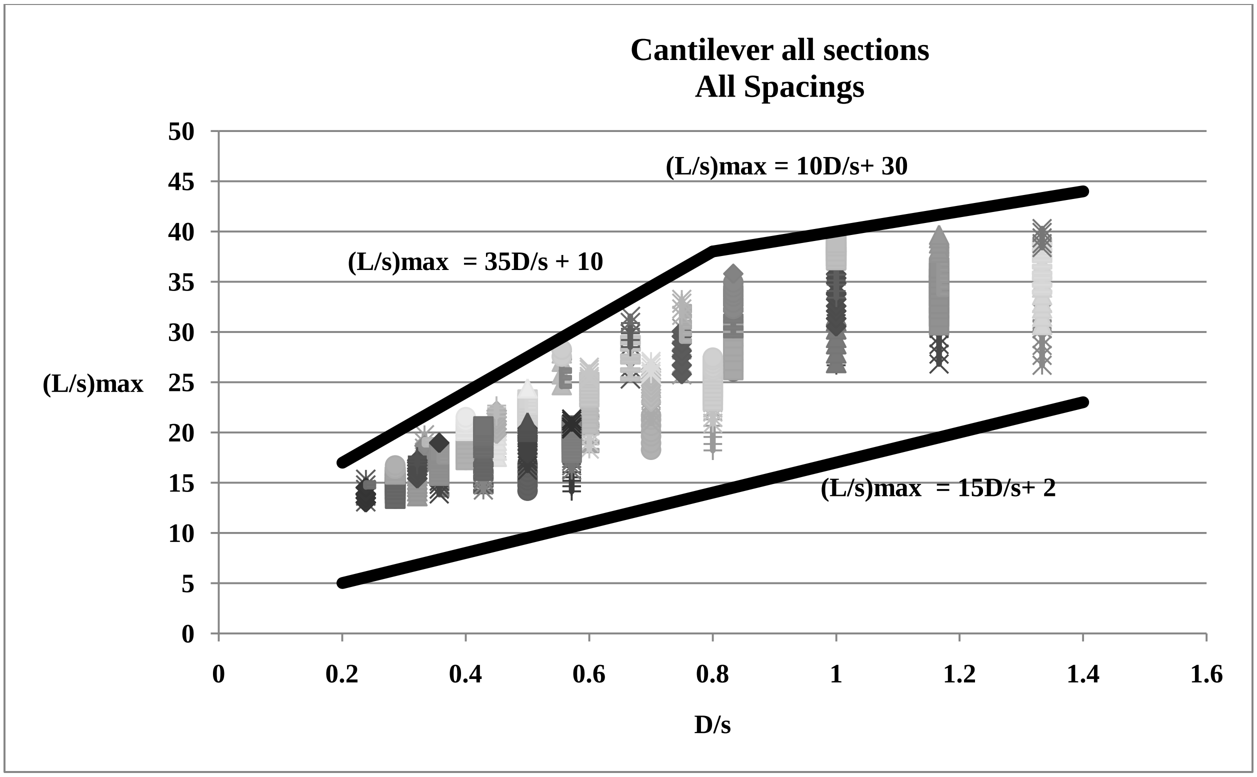
Cantilever all sections
All Spacings
(L/s)max = 10D/s+ 30
(L/s)max = 35D/s + 10
(L/s)max = 15D/s+ 2
(L/s)max
D/s
0
5
10
15
20
25
30
35
40
45
50
0
0.2
0.4
0.6
0.8
1
1.2
1.4
1.6

L/b plots for simply supported single symmetric double girders

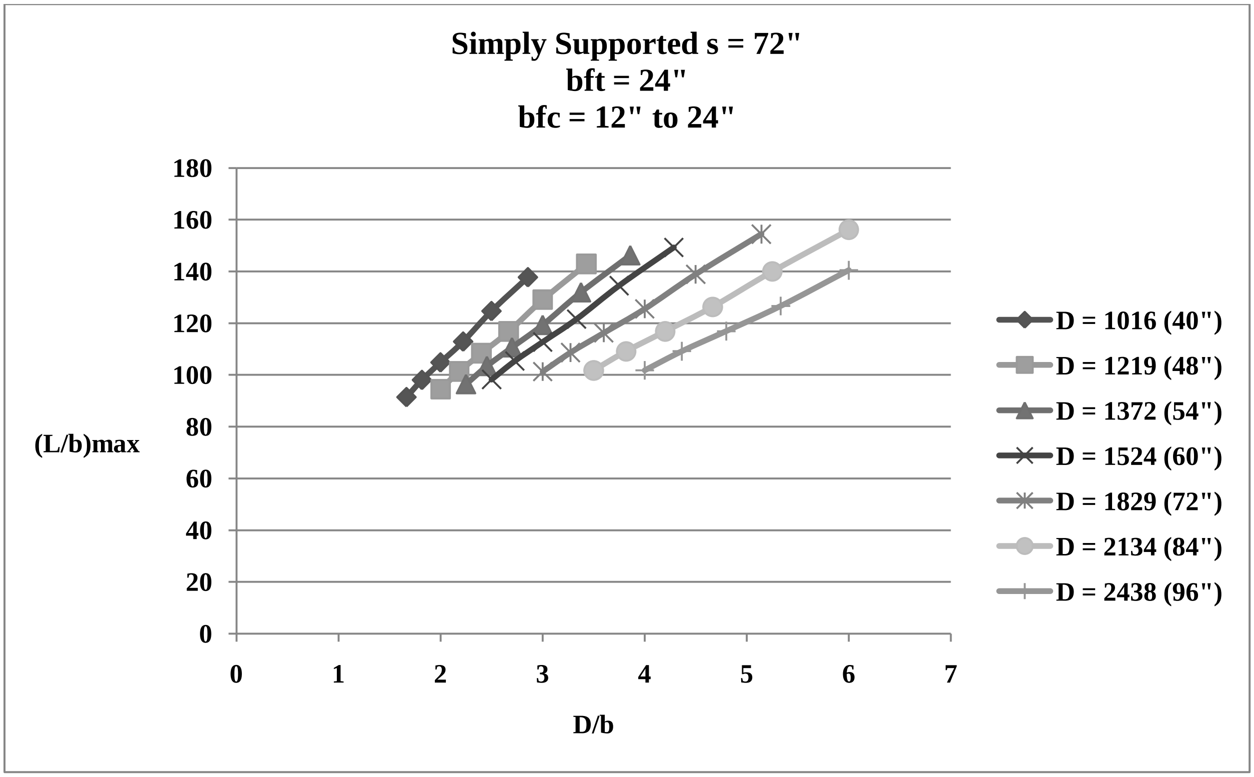

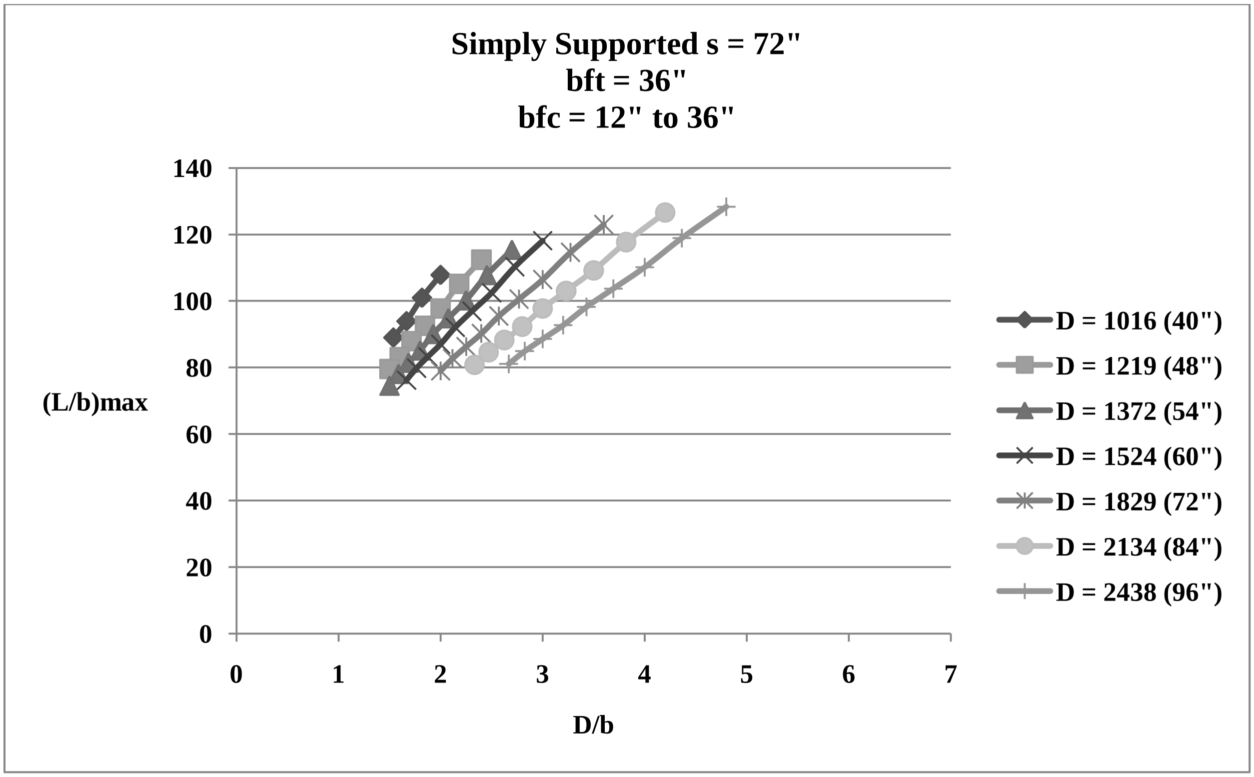

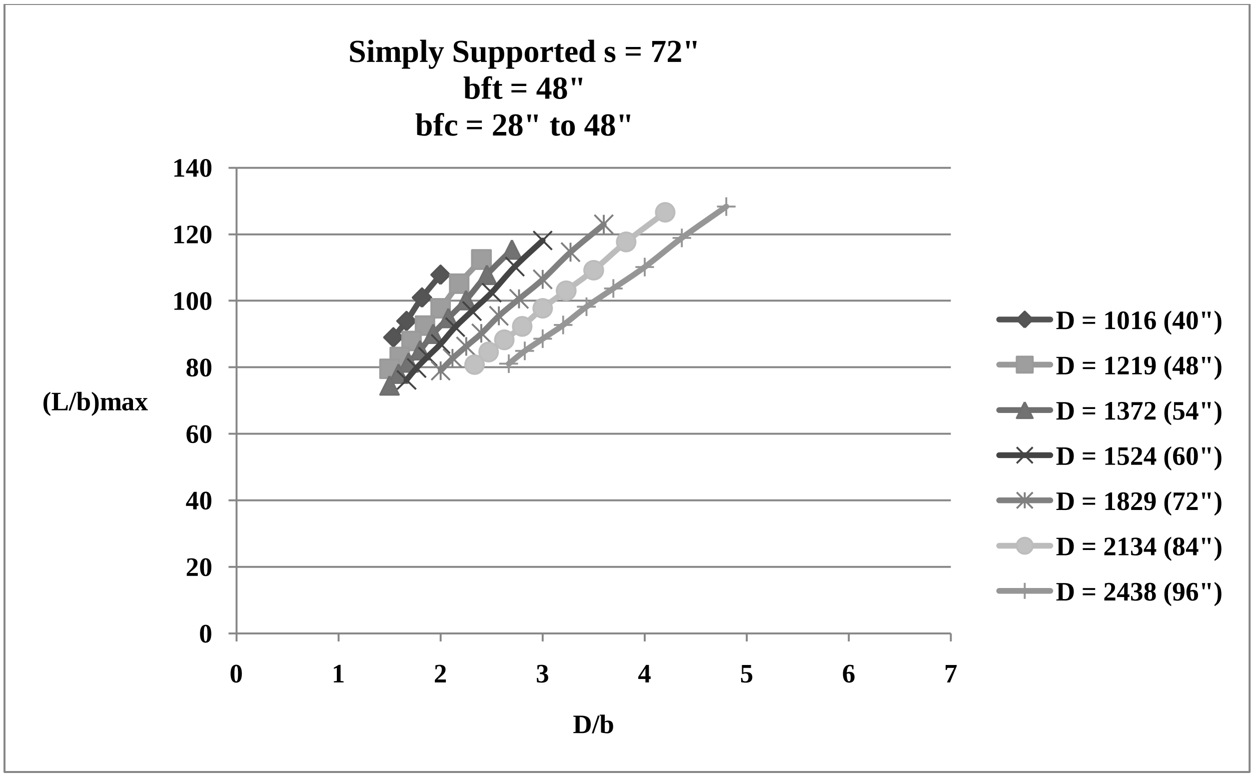
Simply Supported s = 72"
bft = 48"
bfc = 28" to 48"
140
120
100
80
60
40
20
0
(L/b)max
0
1
2
3
4
5
6
7
D/b
D = 1016 (40")
D = 1219 (48")
D = 1372 (54")
D = 1524 (60")
D = 1829 (72")
D = 2134 (84")
D = 2438 (96")

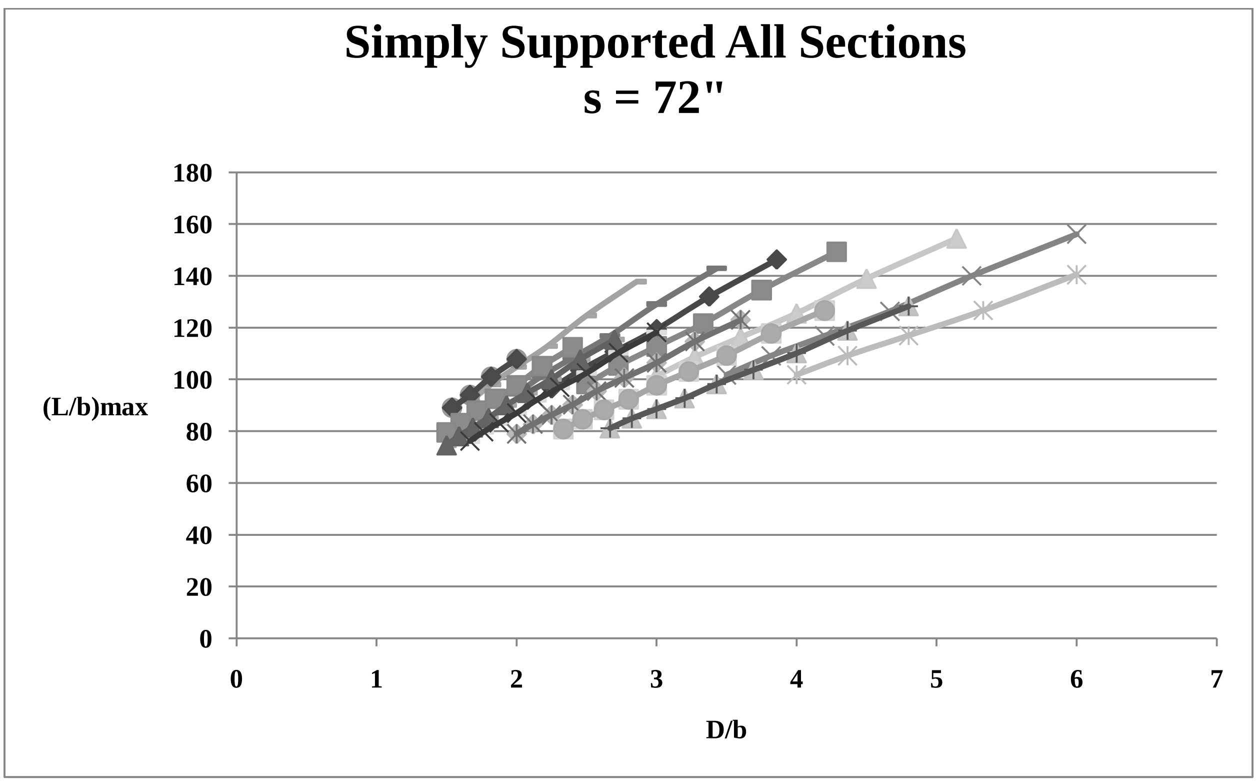
Simply Supported All Sections
s = 72"
180
160
140
120
100
80
60
40
20
0
(L/b)max
0
1
2
3
4
5
6
7
D/b

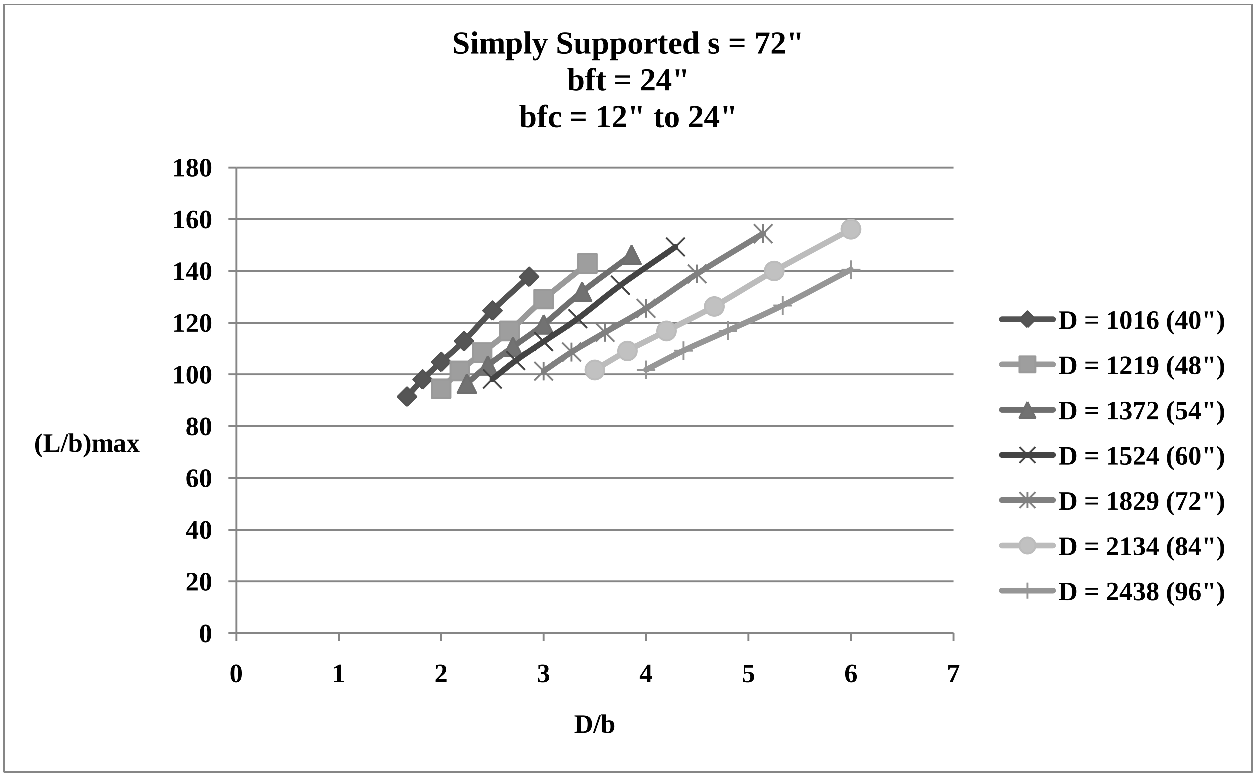
Simply Supported s = 72"
bft = 24"
bfc = 12" to 24"
(L/b)max
D/b
0
20
40
60
80
100
120
140
160
180
0
1
2
3
4
5
6
7
D = 1016 (40")
D = 1219 (48")
D = 1372 (54")
D = 1524 (60")
D = 1829 (72")
D = 2134 (84")
D = 2438 (96")

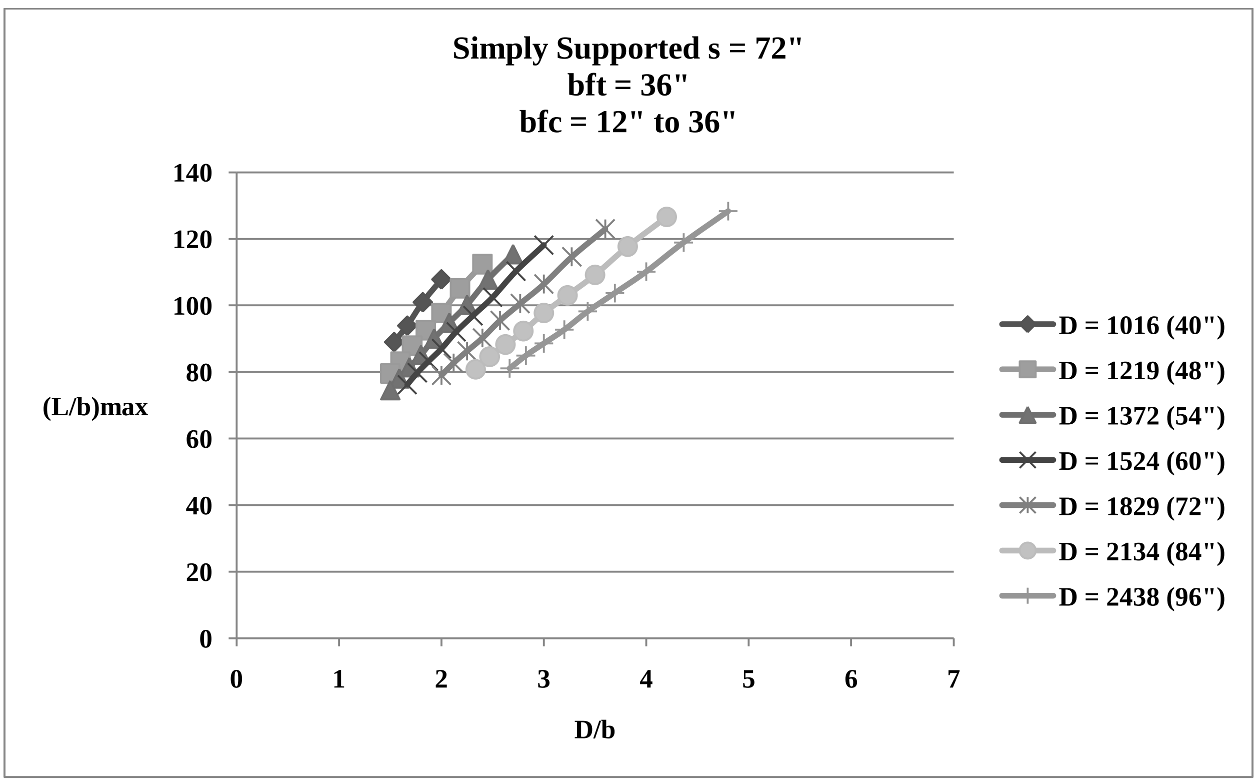
Simply Supported s = 72"
bft = 36"
bfc = 12" to 36"
(L/b)max
D/b
0
20
40
60
80
100
120
140
0
1
2
3
4
5
6
7
D = 1016 (40")
D = 1219 (48")
D = 1372 (54")
D = 1524 (60")
D = 1829 (72")
D = 2134 (84")
D = 2438 (96")

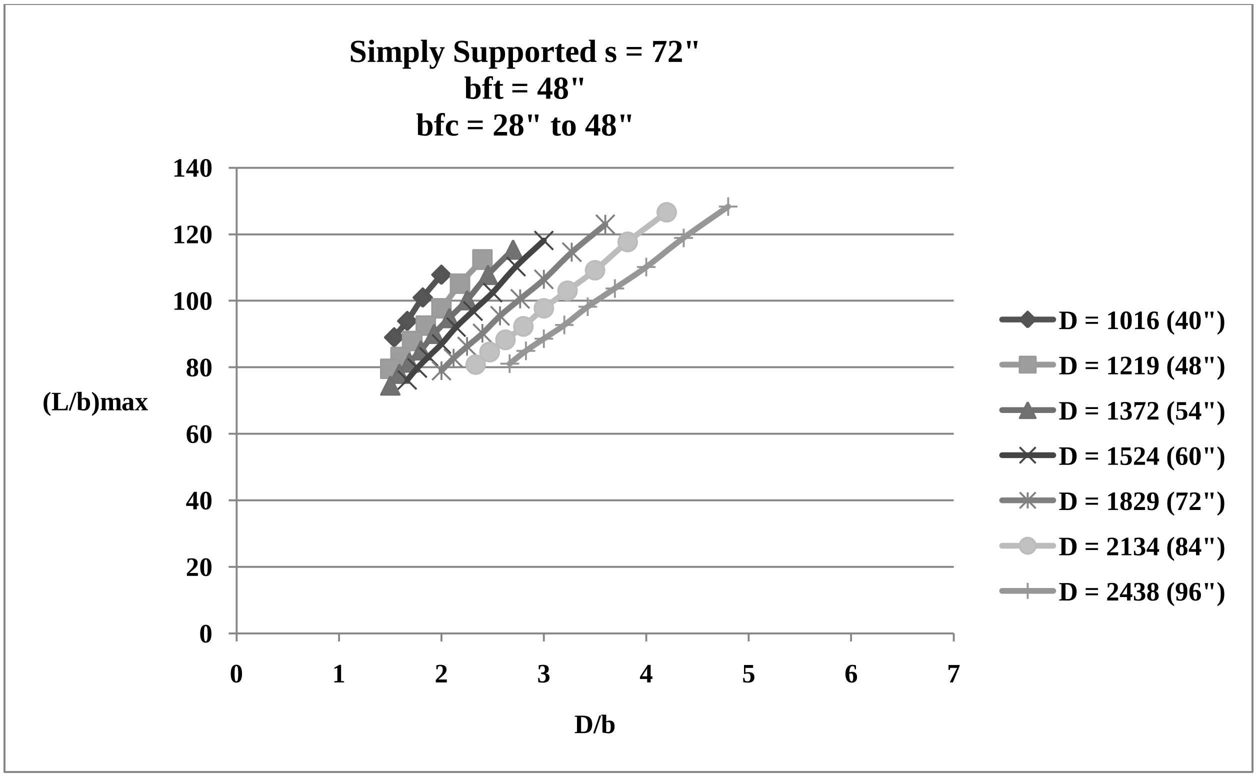
Simply Supported s = 72"
bft = 48"
bfc = 28" to 48"
(L/b)max
D/b
D = 1016 (40")
D = 1219 (48")
D = 1372 (54")
D = 1524 (60")
D = 1829 (72")
D = 2134 (84")
D = 2438 (96")

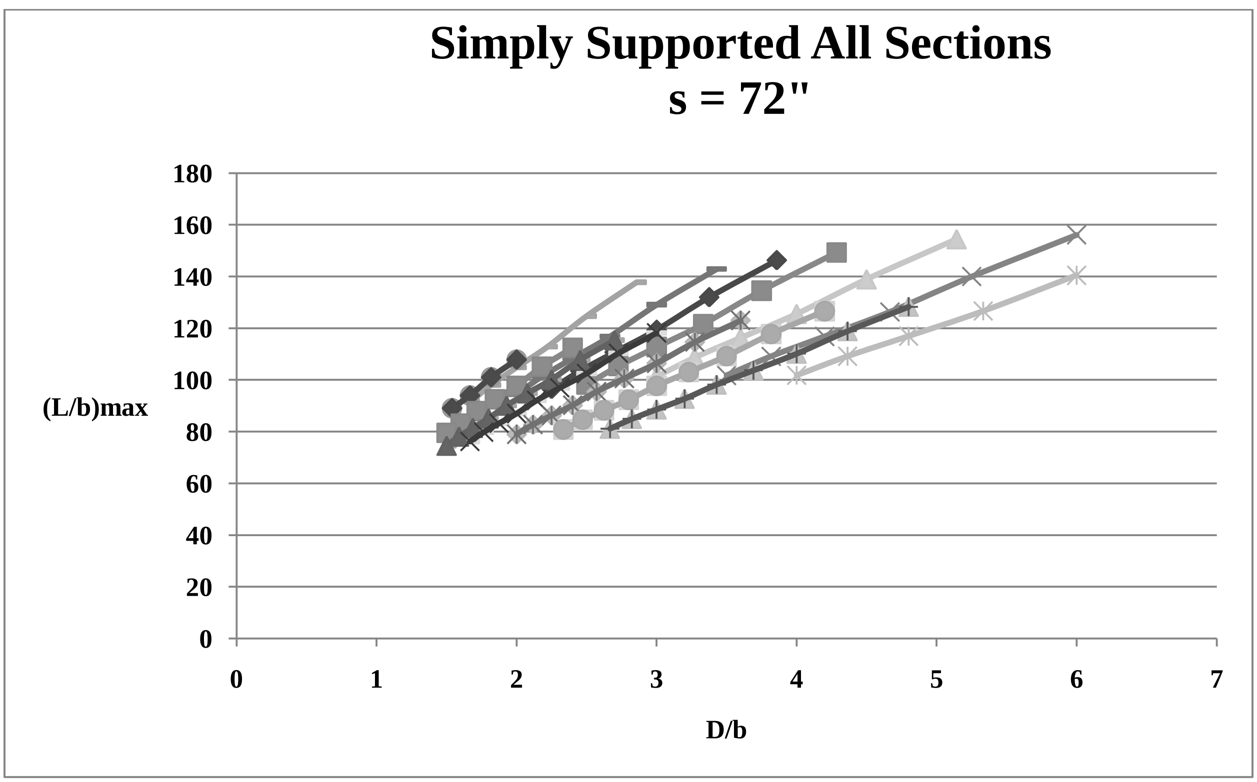
Simply Supported All Sections
s = 72"
(L/b)max
D/b

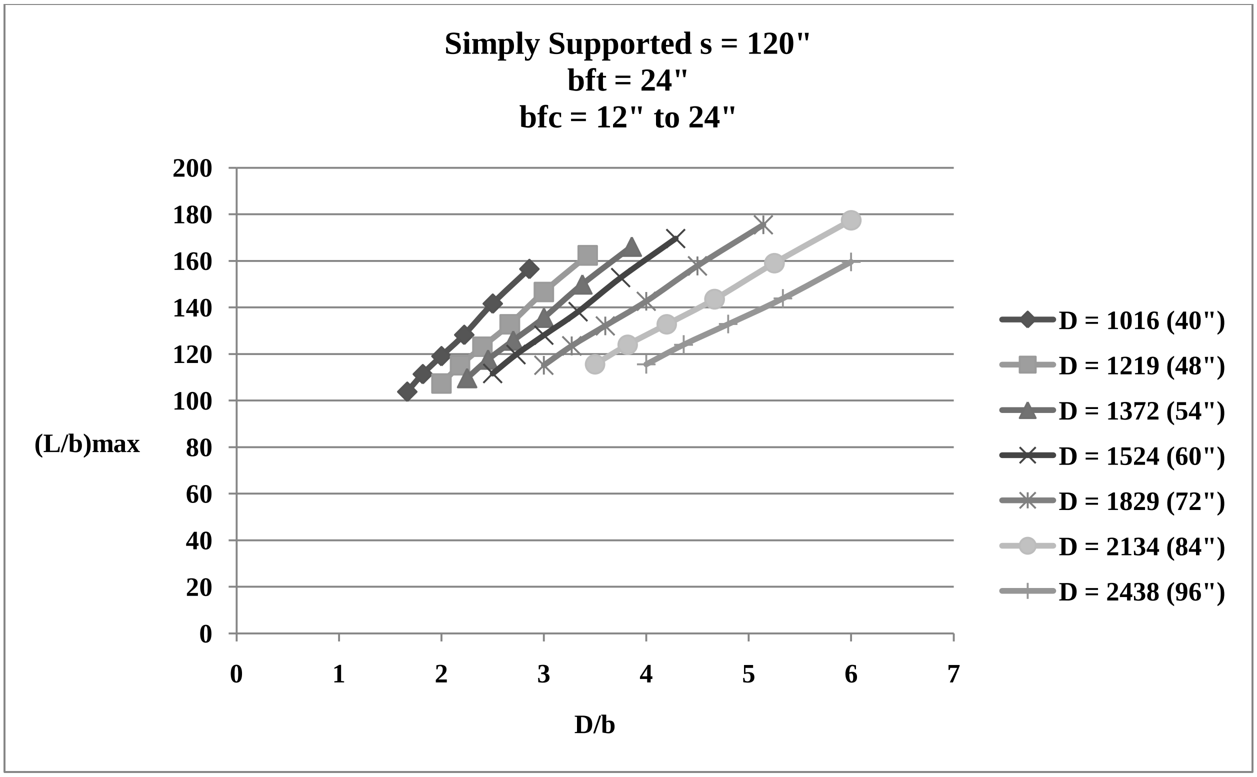
Simply Supported s = 120"
bft = 24"
bfc = 12" to 24"
(L/b)max
D/b
D = 1016 (40")
D = 1219 (48")
D = 1372 (54")
D = 1524 (60")
D = 1829 (72")
D = 2134 (84")
D = 2438 (96")

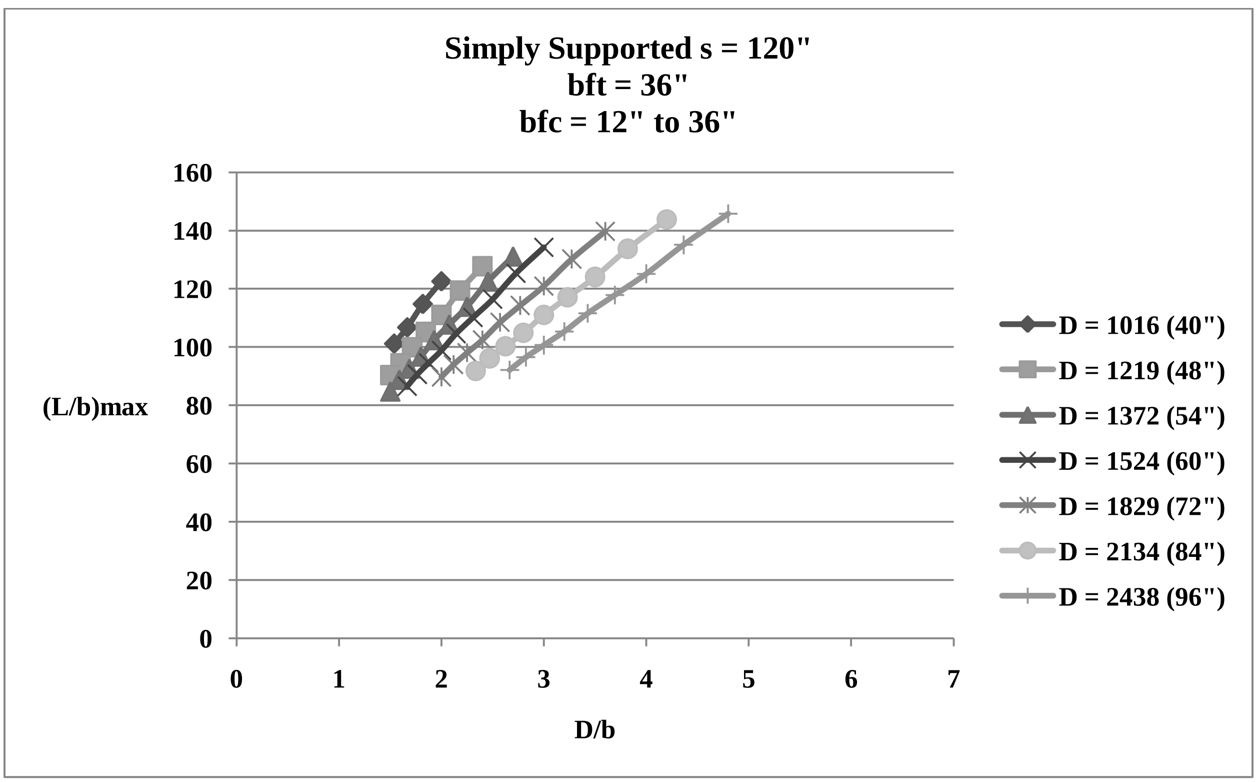
Simply Supported s = 120"
bft = 36"
bfc = 12" to 36"
(L/b)max
D/b
D = 1016 (40")
D = 1219 (48")
D = 1372 (54")
D = 1524 (60")
D = 1829 (72")
D = 2134 (84")
D = 2438 (96")

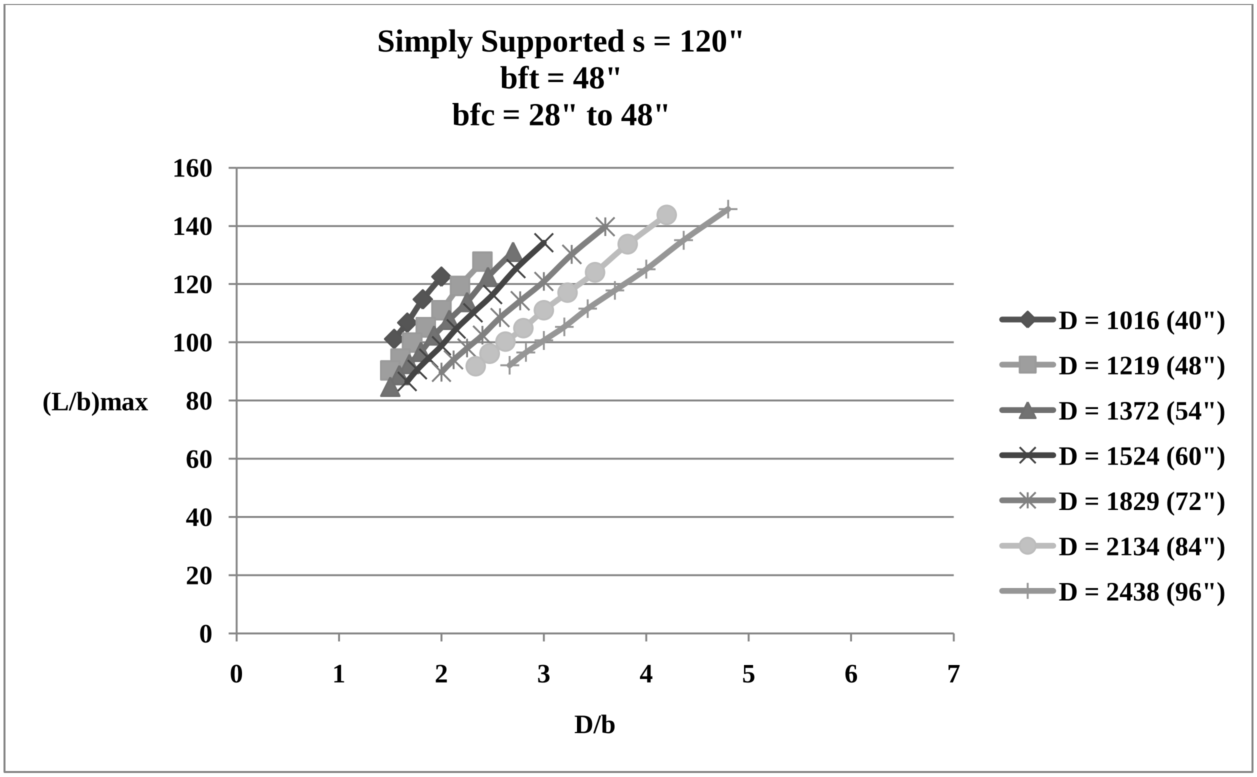
Simply Supported s = 120"
bft = 48"
bfc = 28" to 48"
160
140
120
100
80
60
40
20
0
(L/b)max
0
1
2
3
4
5
6
7
D/b
D = 1016 (40")
D = 1219 (48")
D = 1372 (54")
D = 1524 (60")
D = 1829 (72")
D = 2134 (84")
D = 2438 (96")

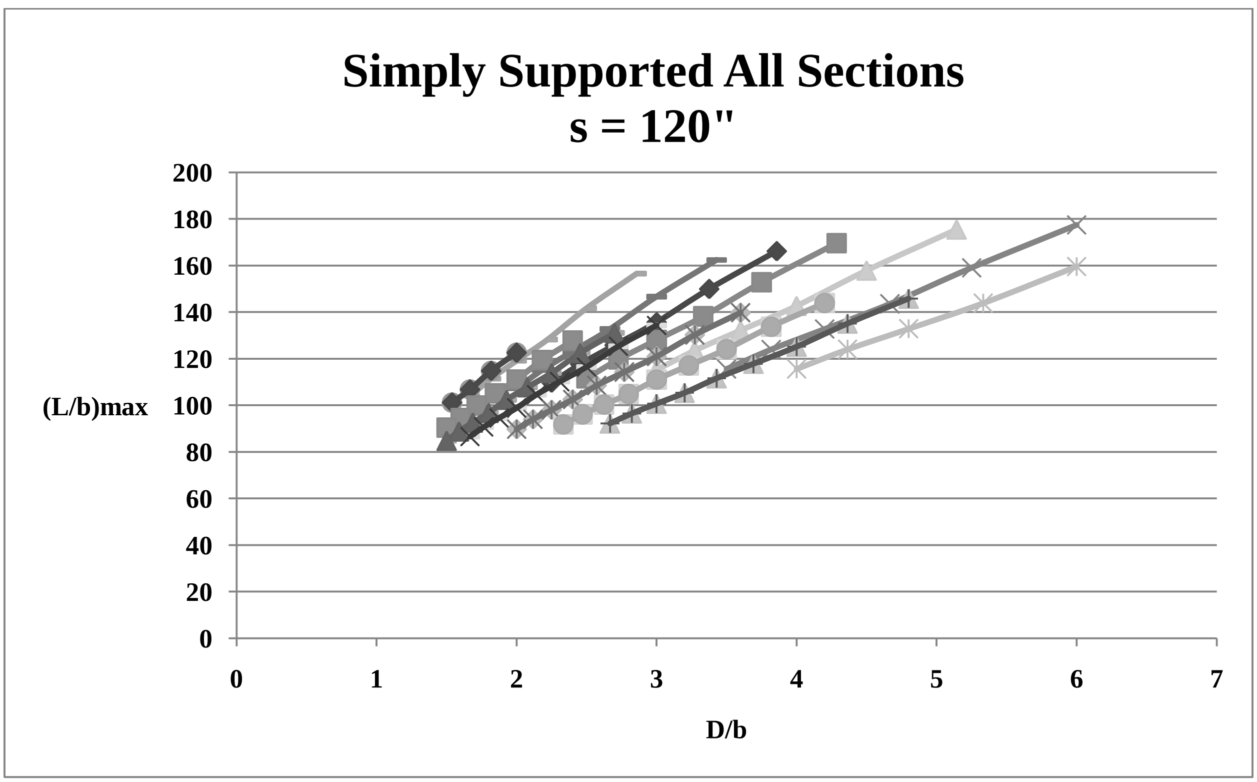
Simply Supported All Sections
s = 120"
200
180
160
140
120
100
80
60
40
20
0
(L/b)max
0
1
2
3
4
5
6
7
D/b

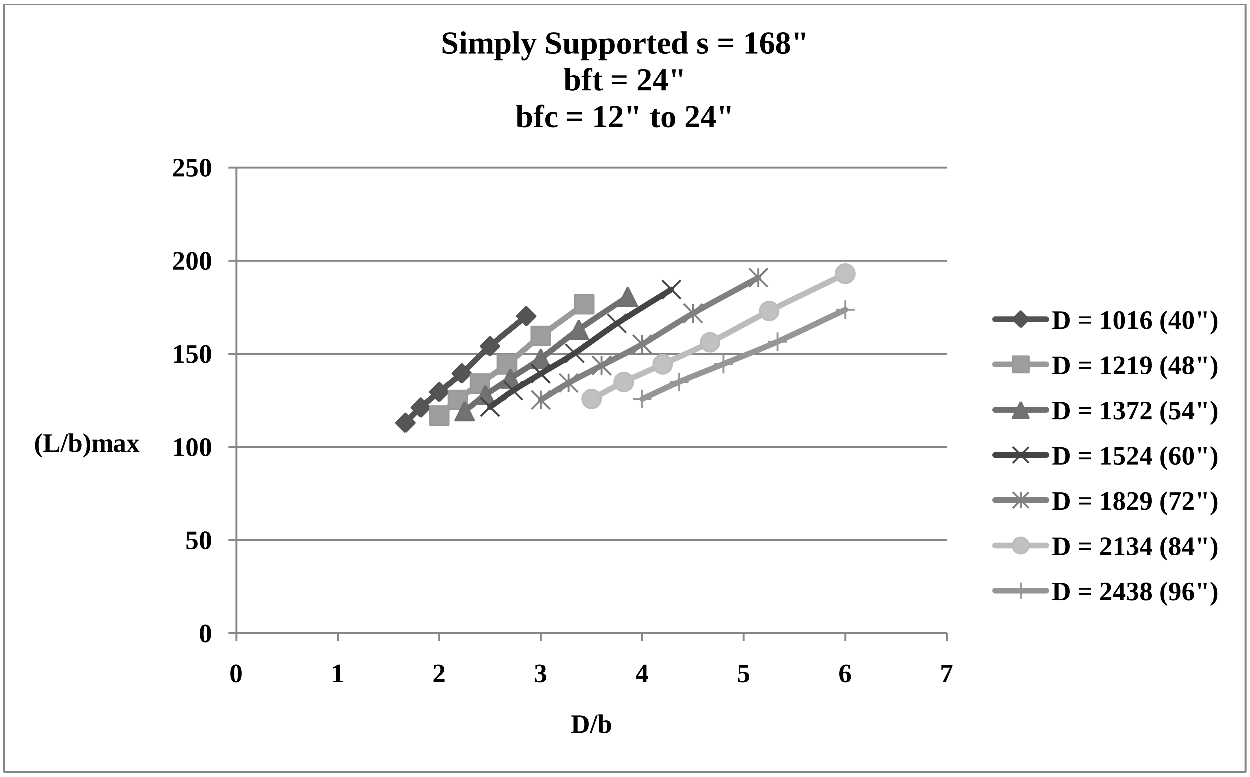
Simply Supported s = 168"
bft = 24"
bfc = 12" to 24"
(L/b)max
250
200
150
100
50
0
0
1
2
3
4
5
6
7
D/b
D = 1016 (40")
D = 1219 (48")
D = 1372 (54")
D = 1524 (60")
D = 1829 (72")
D = 2134 (84")
D = 2438 (96")

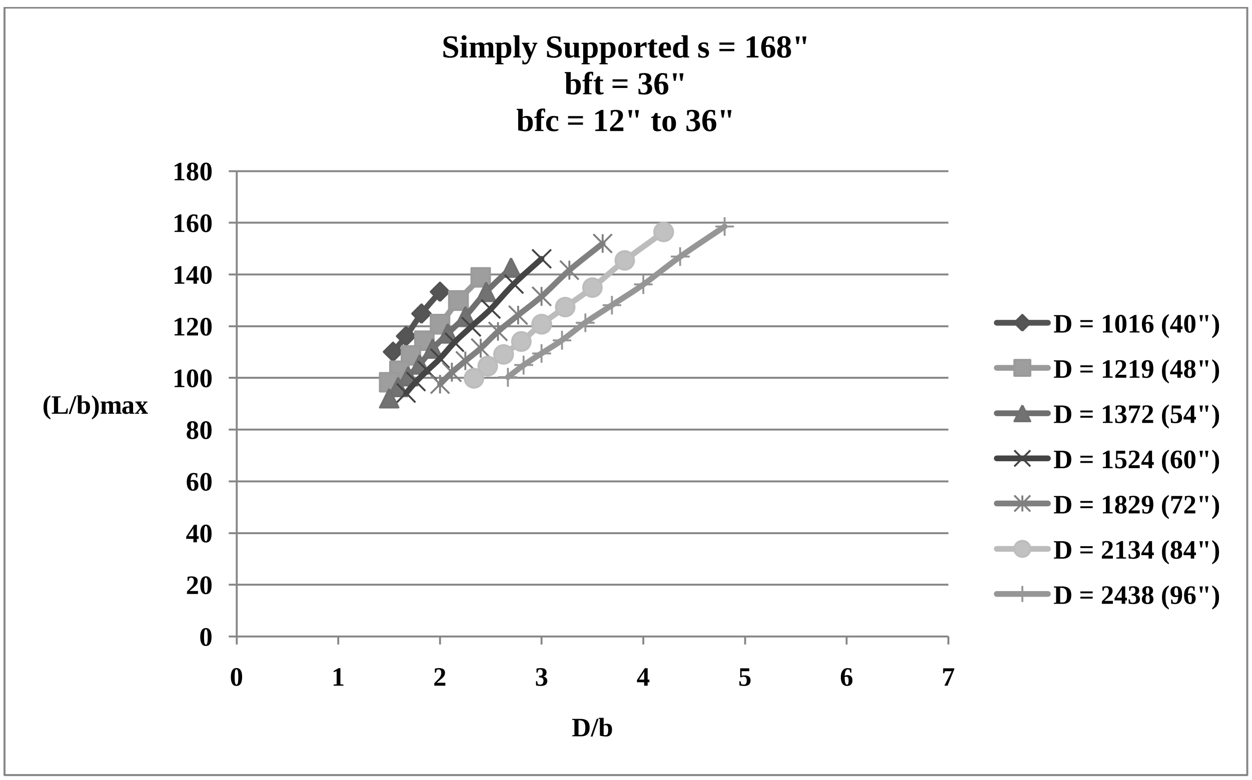
Simply Supported s = 168"
bft = 36"
bfc = 12" to 36"
(L/b)max
180
160
140
120
100
80
60
40
20
0
0
1
2
3
4
5
6
7
D/b
D = 1016 (40")
D = 1219 (48")
D = 1372 (54")
D = 1524 (60")
D = 1829 (72")
D = 2134 (84")
D = 2438 (96")

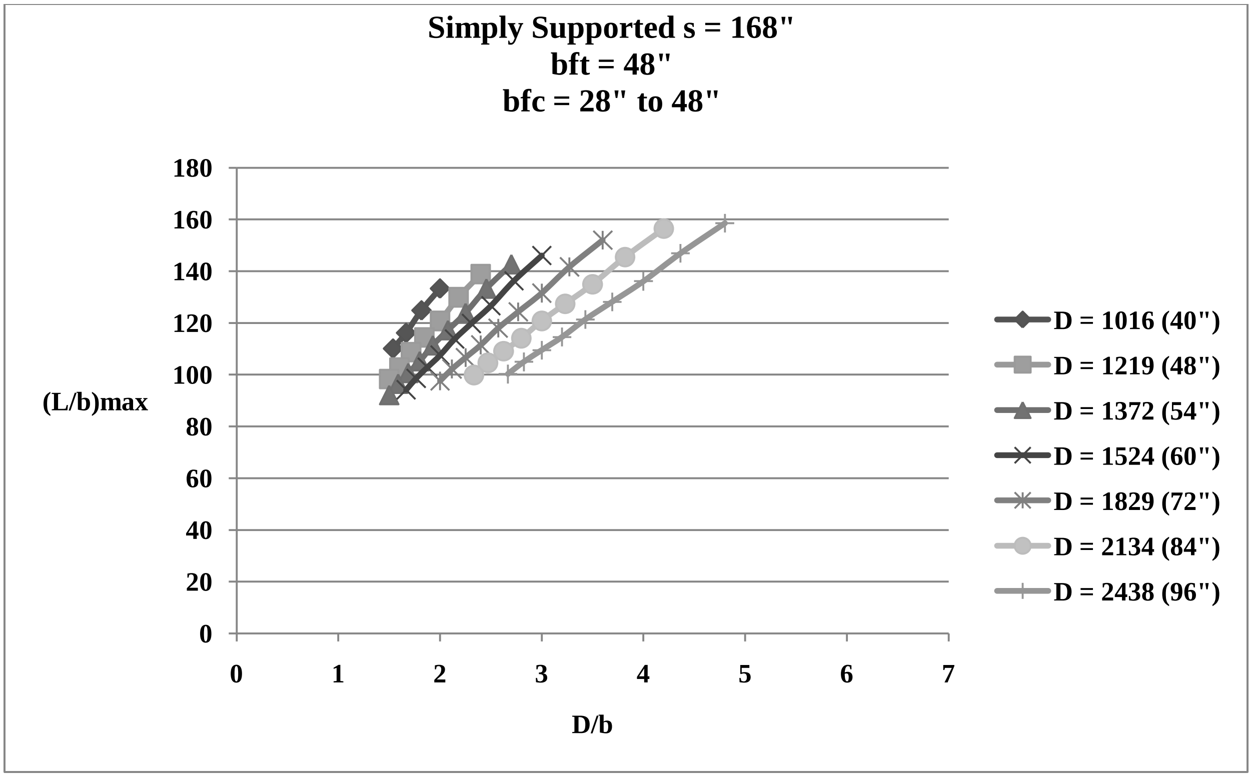
Simply Supported s = 168"
bft = 48"
bfc = 28" to 48"
(L/b)max
D/b
D = 1016 (40")
D = 1219 (48")
D = 1372 (54")
D = 1524 (60")
D = 1829 (72")
D = 2134 (84")
D = 2438 (96")

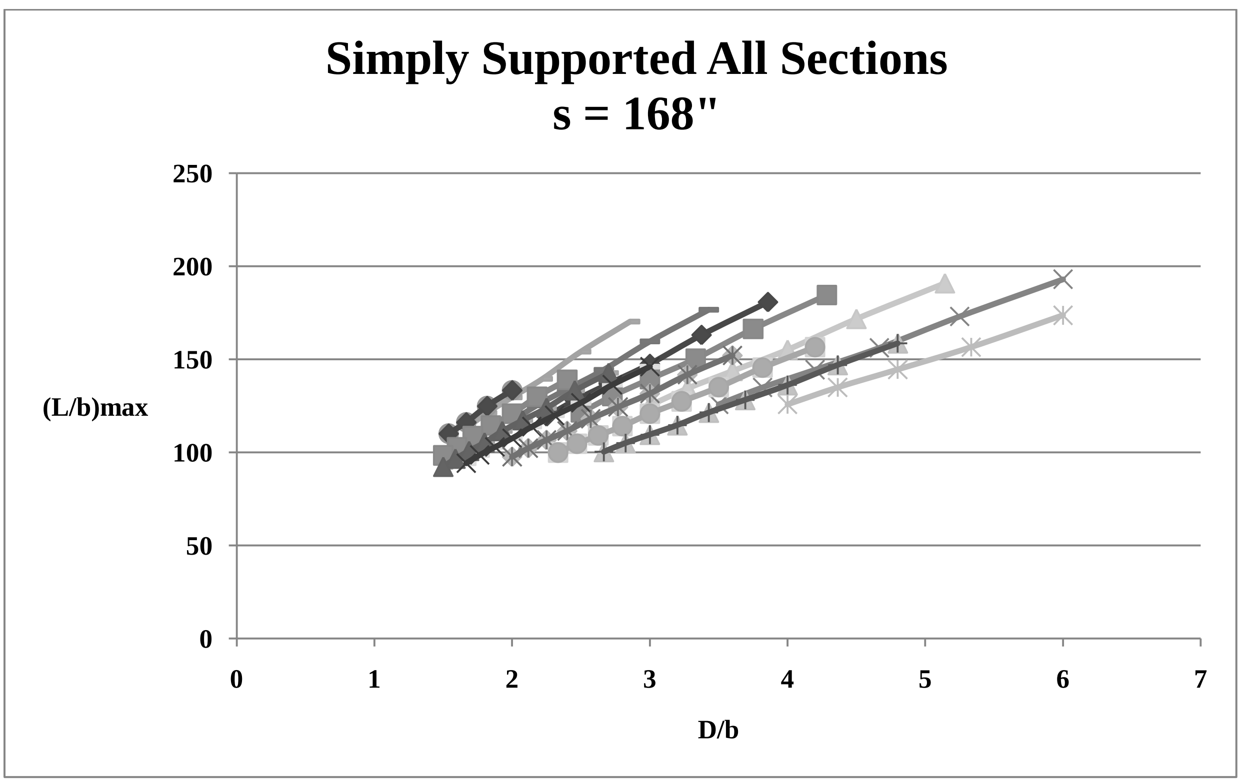
Simply Supported All Sections
s = 168"
(L/b)max
D/b

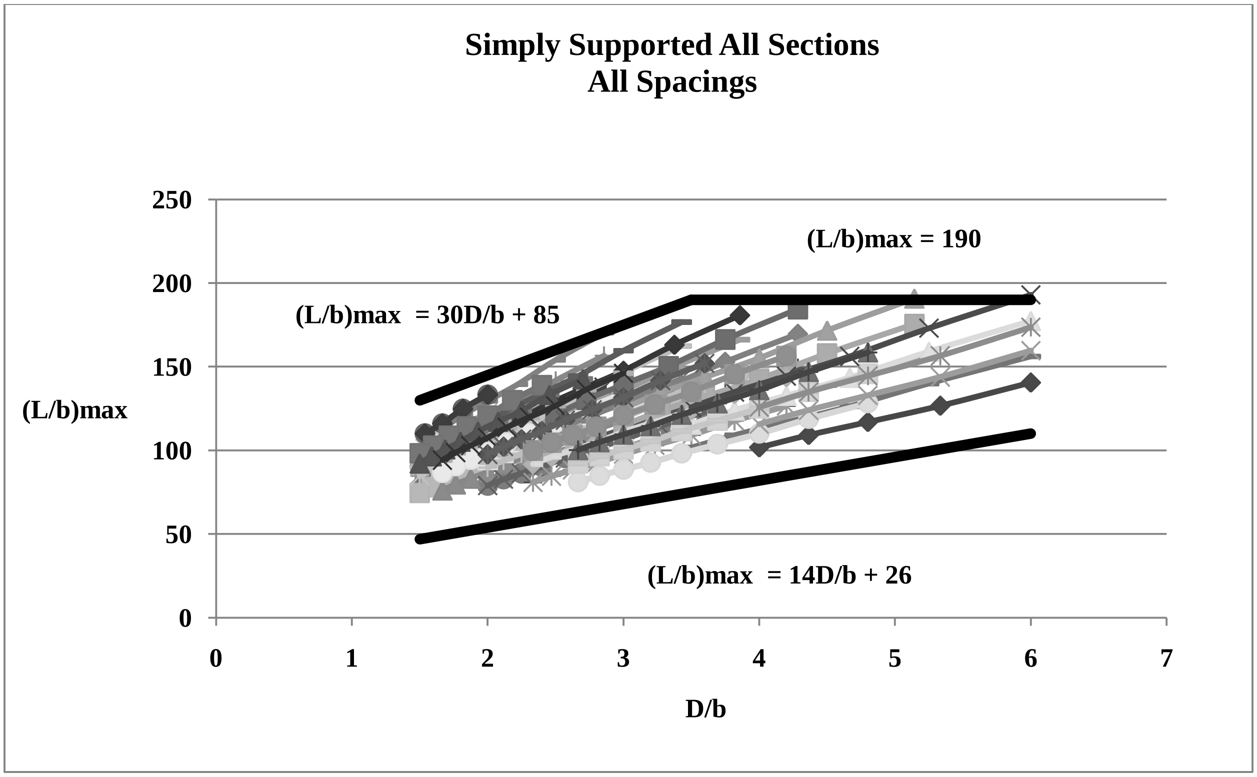

L/b plots for cantilever single symmetric double girders

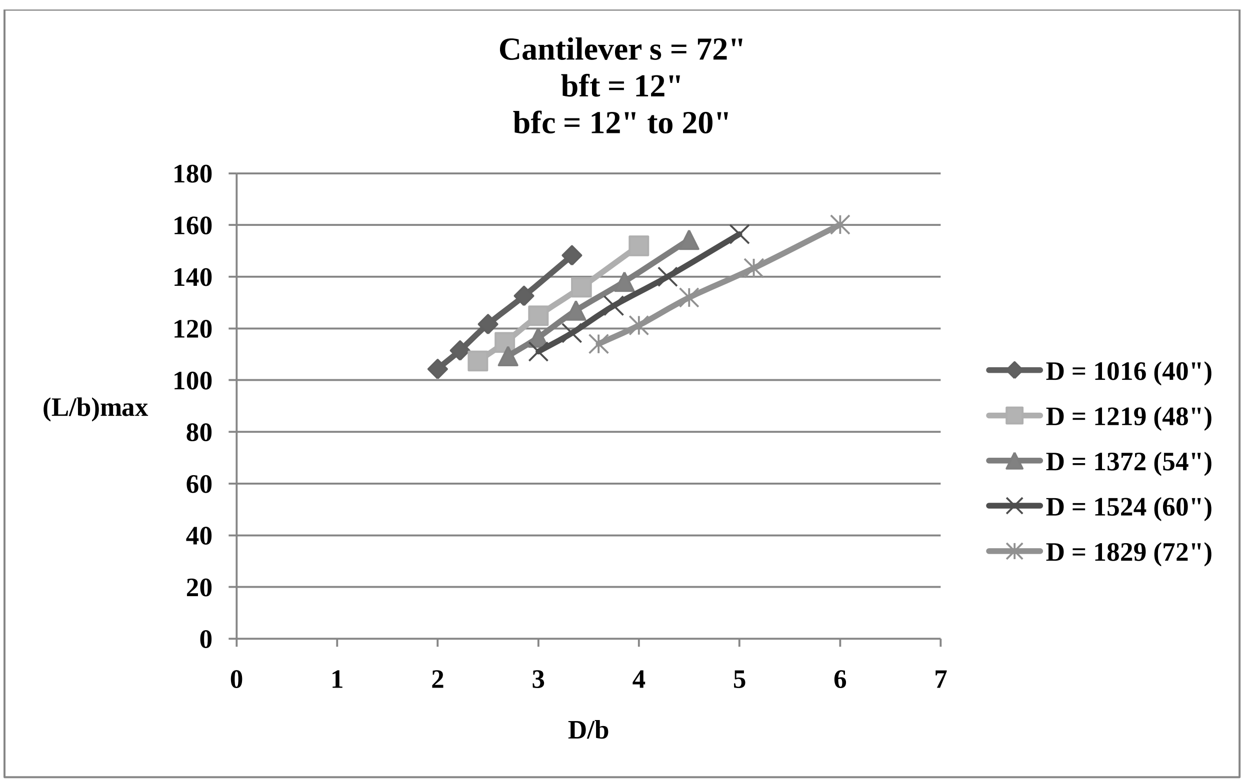

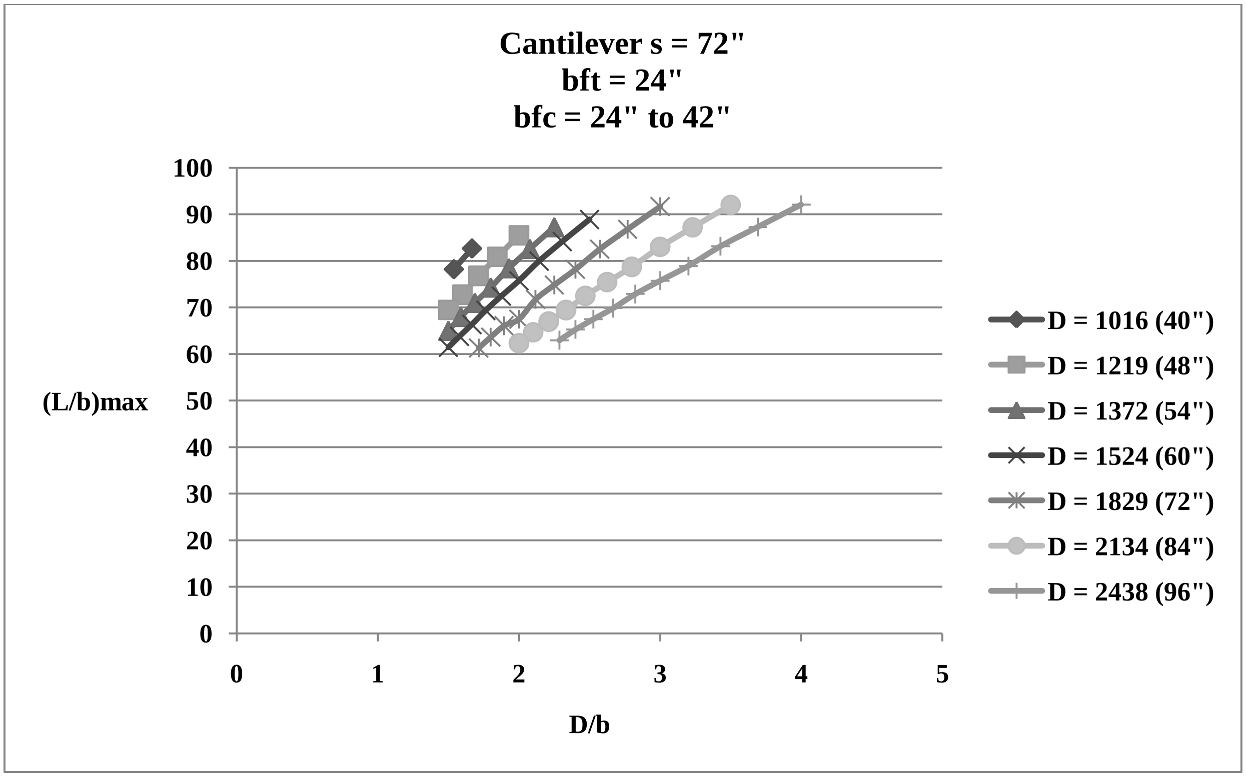
Cantilever s = 72"
bft = 24"
bfc = 24" to 42"
(L/b)max
100
90
80
70
60
50
40
30
20
10
0
0
1
2
3
4
5
D/b
D = 1016 (40")
D = 1219 (48")
D = 1372 (54")
D = 1524 (60")
D = 1829 (72")
D = 2134 (84")
D = 2438 (96")

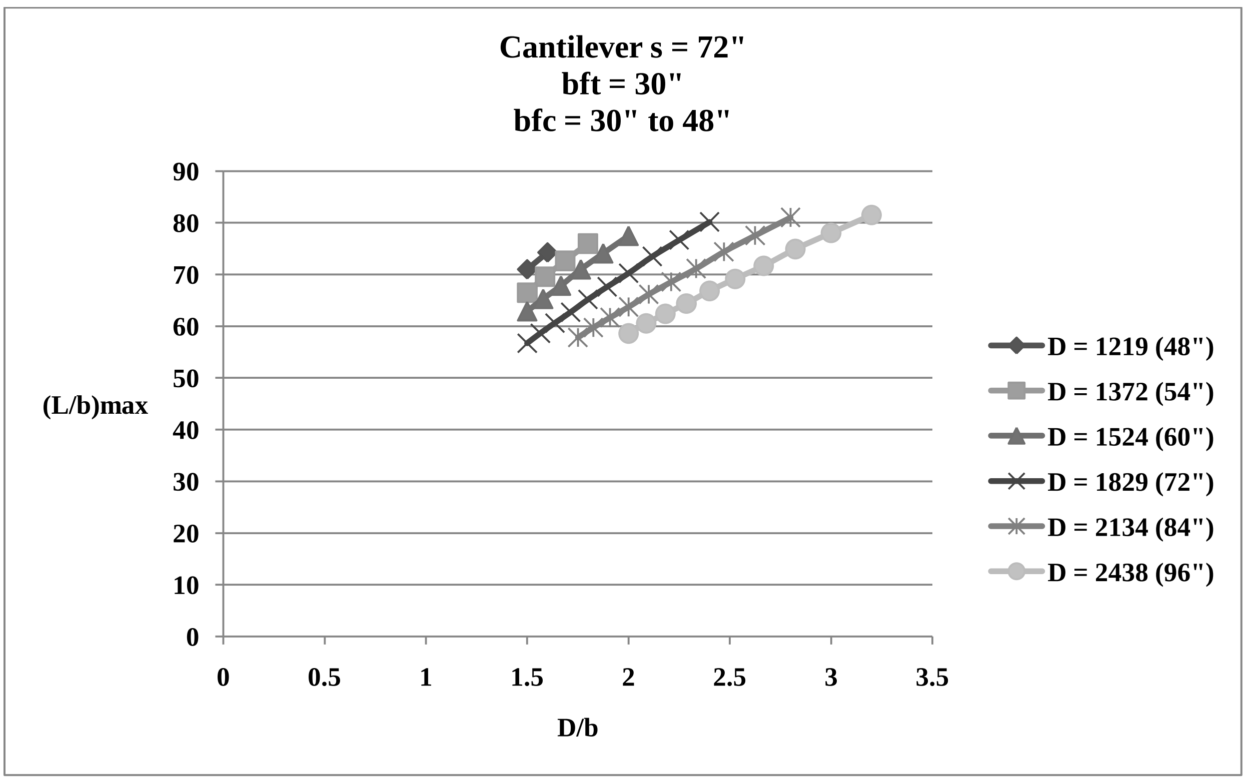
Cantilever s = 72"
bft = 30"
bfc = 30" to 48"
(L/b)max
90
80
70
60
50
40
30
20
10
0
0
0.5
1
1.5
2
2.5
3
3.5
D/b
D = 1219 (48")
D = 1372 (54")
D = 1524 (60")
D = 1829 (72")
D = 2134 (84")
D = 2438 (96")

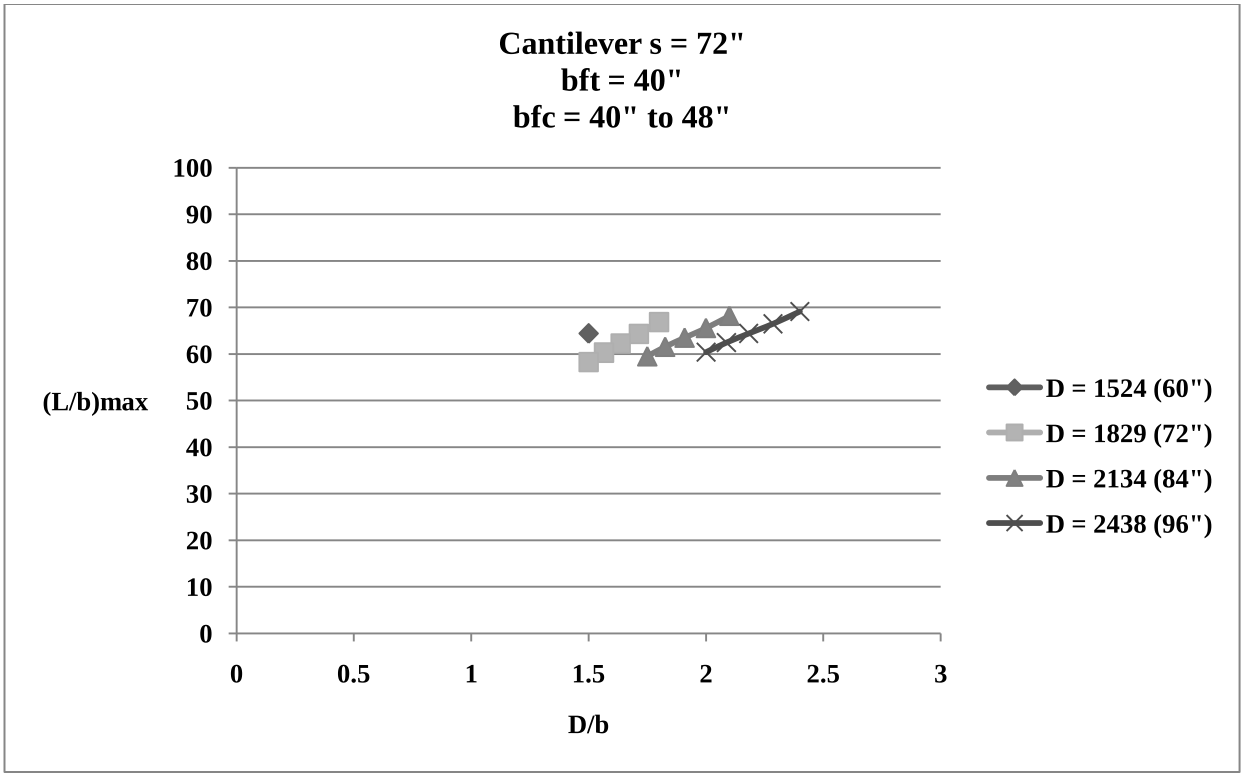
Cantilever s = 72"
bft = 40"
bfc = 40" to 48"
(L/b)max
D/b
0
10
20
30
40
50
60
70
80
90
100
0
0.5
1
1.5
2
2.5
3
D = 1524 (60")
D = 1829 (72")
D = 2134 (84")
D = 2438 (96")

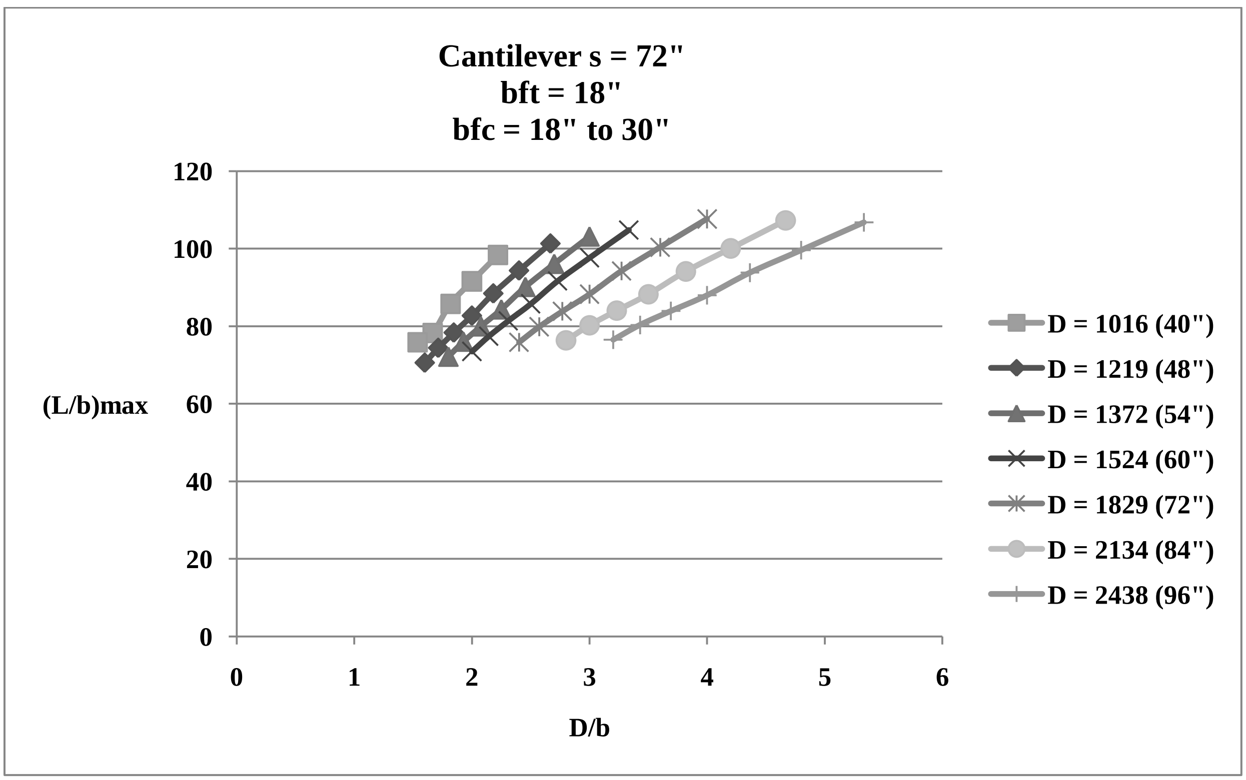
Cantilever s = 72"
bft = 18"
bfc = 18" to 30"
(L/b)max
D/b
0
20
40
60
80
100
120
0
1
2
3
4
5
6
D = 1016 (40")
D = 1219 (48")
D = 1372 (54")
D = 1524 (60")
D = 1829 (72")
D = 2134 (84")
D = 2438 (96")

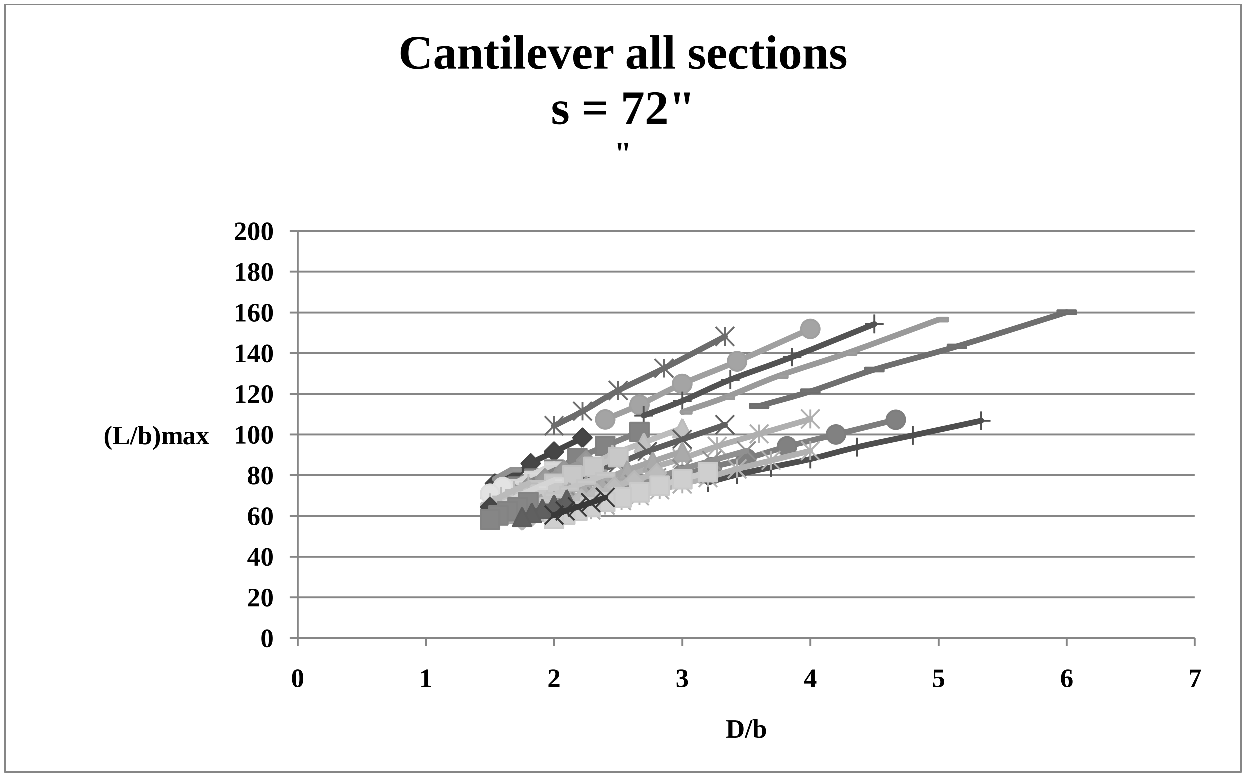
Cantilever all sections
s = 72"
"
(L/b)max
D/b

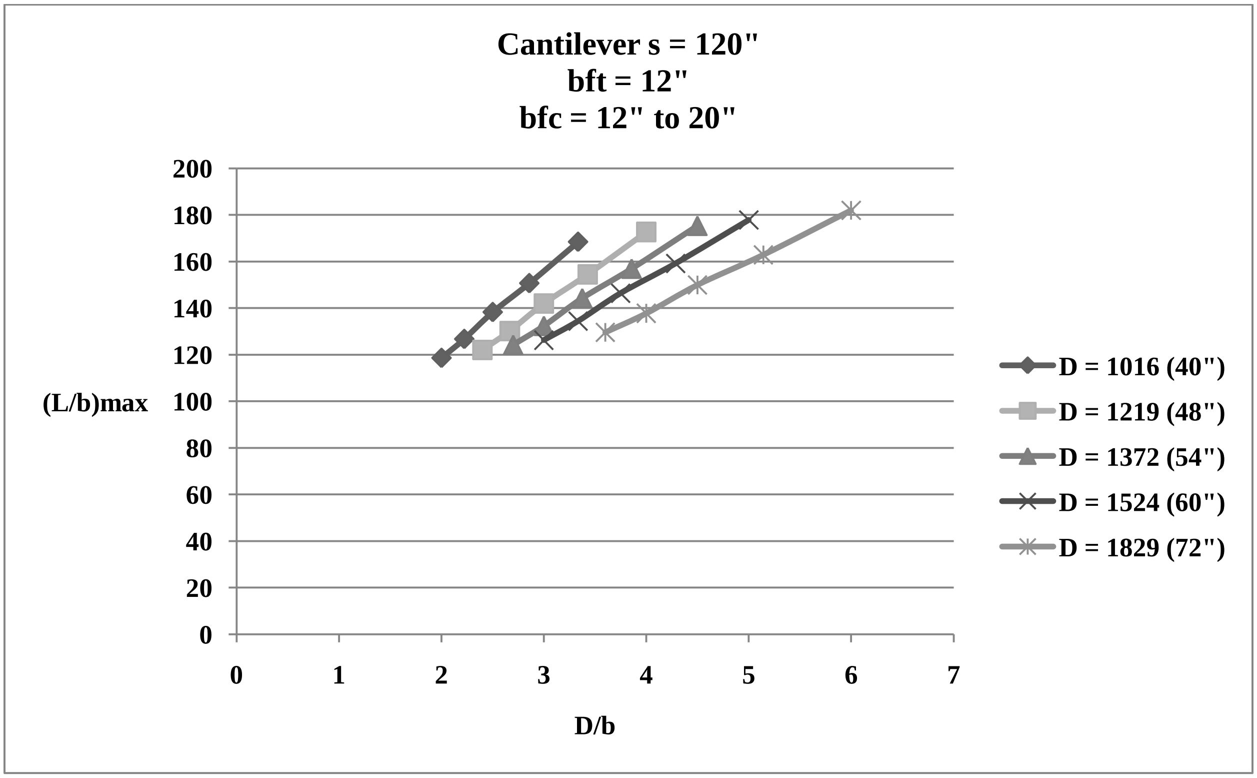
Cantilever s = 120"
bft = 12"
bfc = 12" to 20"
(L/b)max
D/b
D = 1016 (40")
D = 1219 (48")
D = 1372 (54")
D = 1524 (60")
D = 1829 (72")

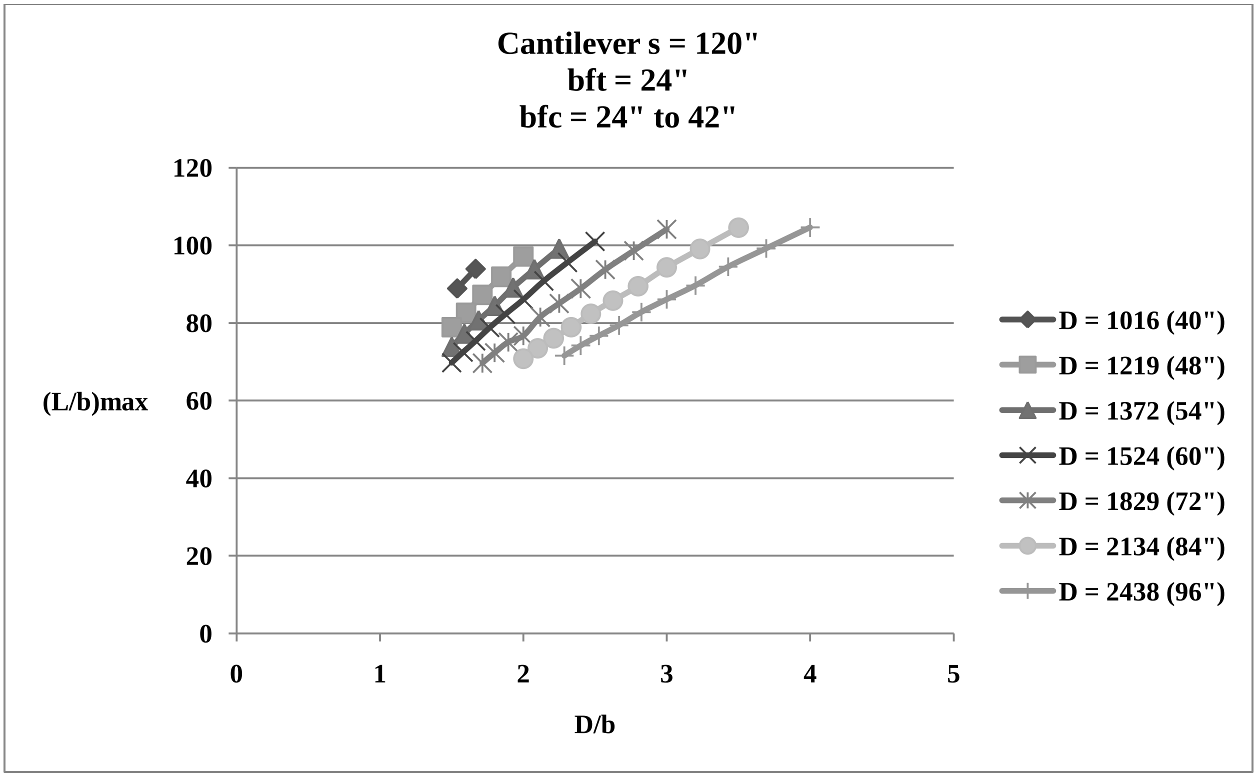
Cantilever s = 120"
bft = 24"
bfc = 24" to 42"
(L/b)max
D/b
D = 1016 (40")
D = 1219 (48")
D = 1372 (54")
D = 1524 (60")
D = 1829 (72")
D = 2134 (84")
D = 2438 (96")

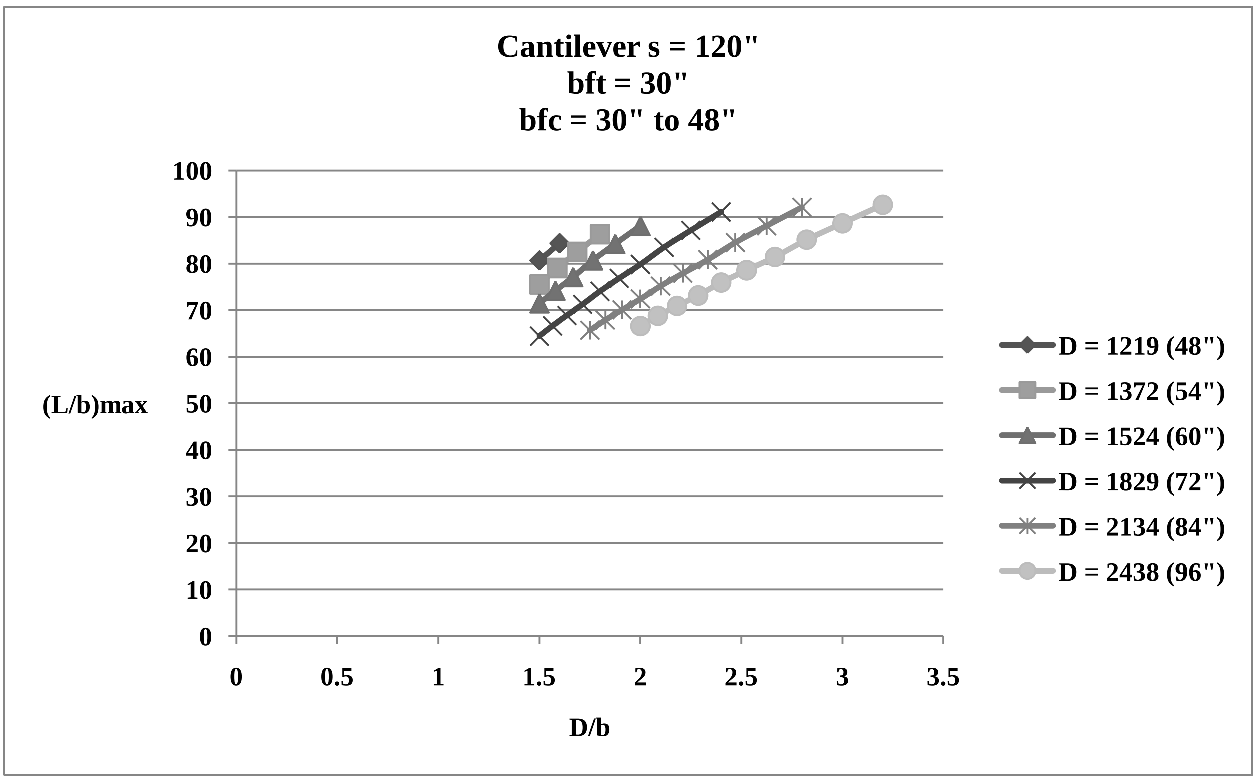
Cantilever s = 120"
bft = 30"
bfc = 30" to 48"
(L/b)max
D/b
D = 1219 (48")
D = 1372 (54")
D = 1524 (60")
D = 1829 (72")
D = 2134 (84")
D = 2438 (96")

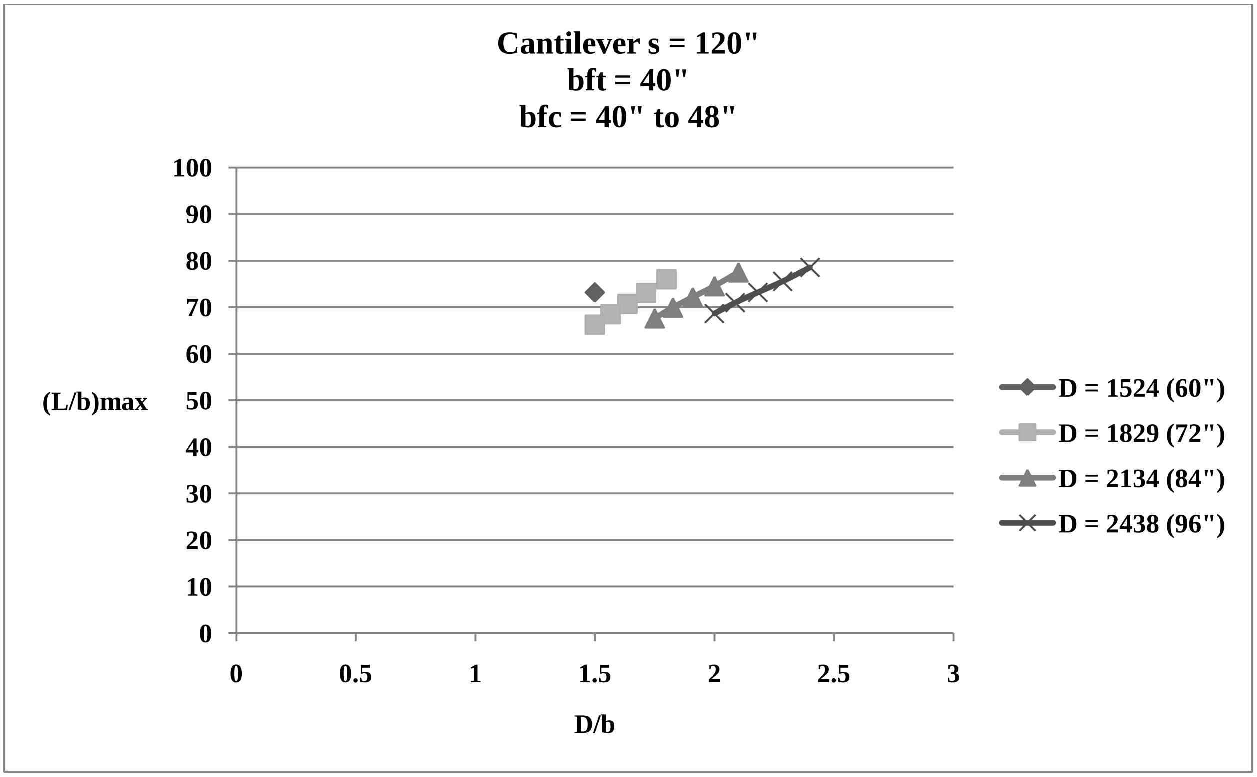
Cantilever s = 120"
bft = 40"
bfc = 40" to 48"
(L/b)max
D/b
D = 1524 (60")
D = 1829 (72")
D = 2134 (84")
D = 2438 (96")

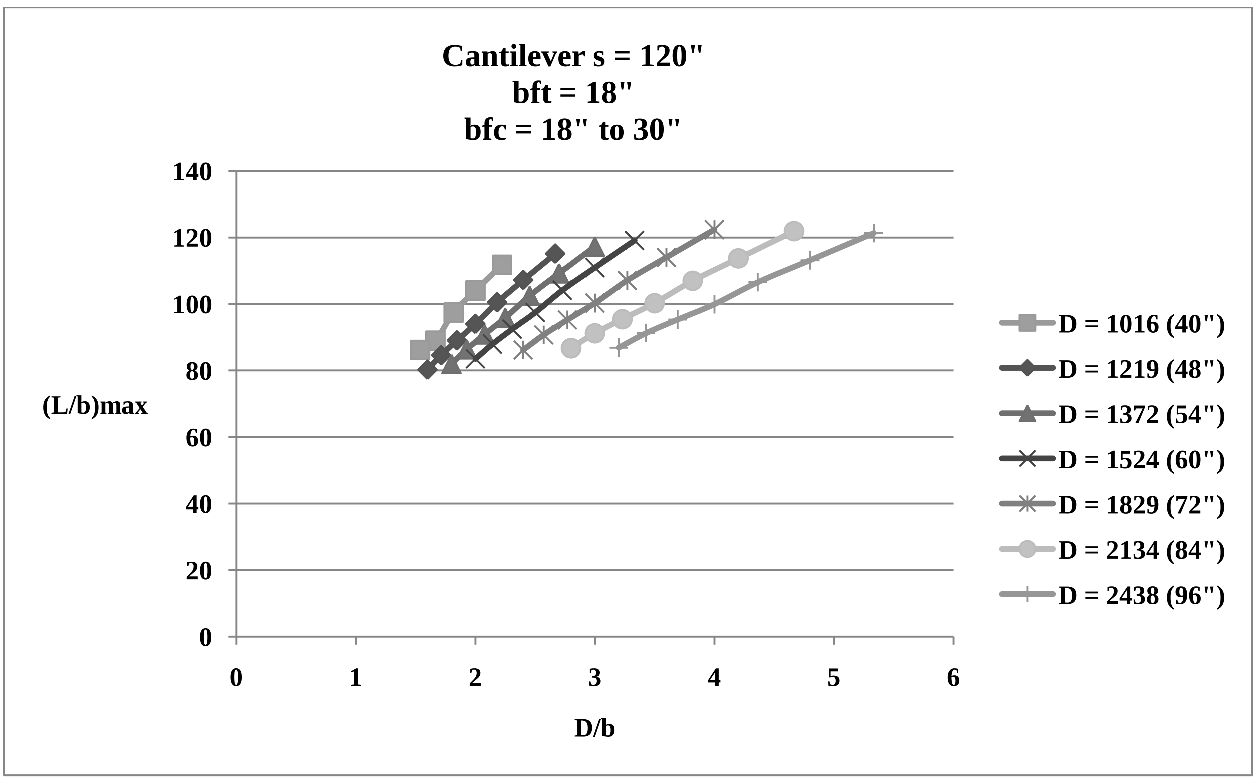
Cantilever s = 120"
bft = 18"
bfc = 18" to 30"
(L/b)max
D/b
D = 1016 (40")
D = 1219 (48")
D = 1372 (54")
D = 1524 (60")
D = 1829 (72")
D = 2134 (84")
D = 2438 (96")

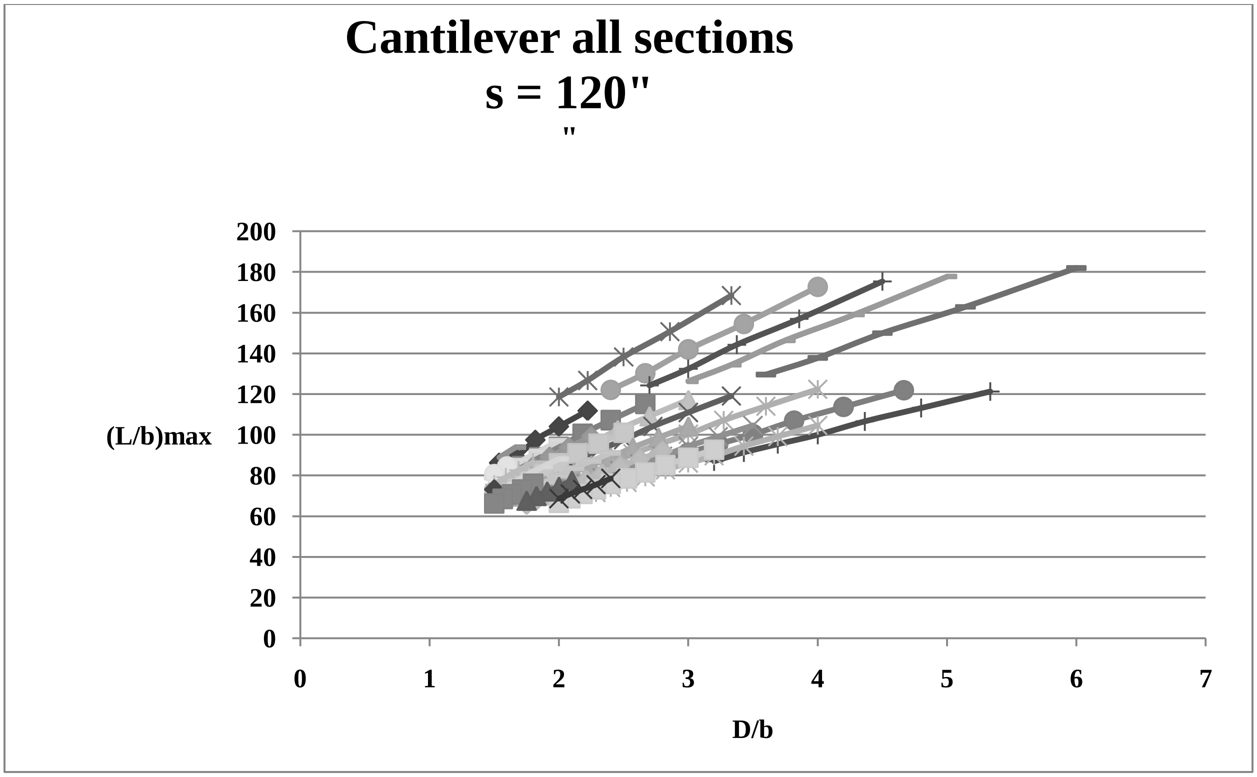

Cantilever all sections
s = 120"
"
200
180
160
140
120
100
80
60
40
20
0
(L/b)max
0
1
2
3
4
5
6
7
D/b

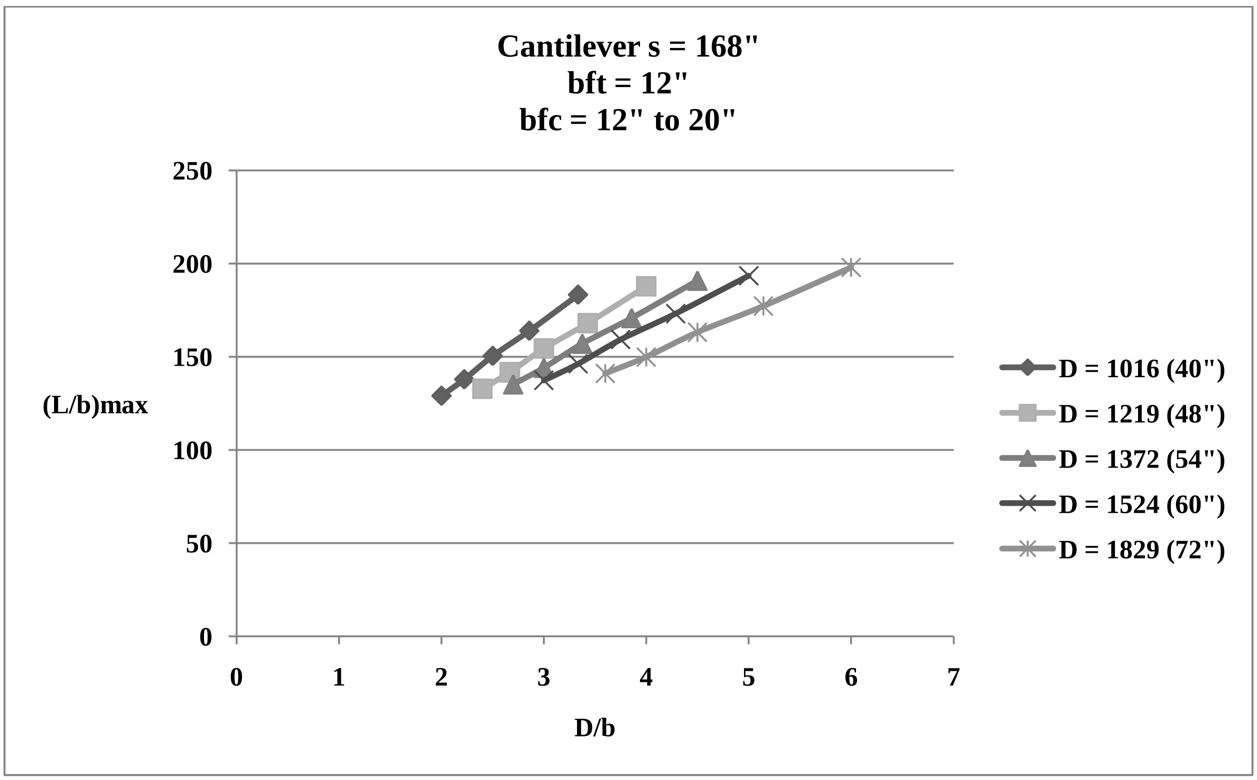

Cantilever s = 168"
bft = 12"
bfc = 12" to 20"
250
200
150
100
50
0
(L/b)max
0
1
2
3
4
5
6
7
D/b
D = 1016 (40")
D = 1219 (48")
D = 1372 (54")
D = 1524 (60")
D = 1829 (72")

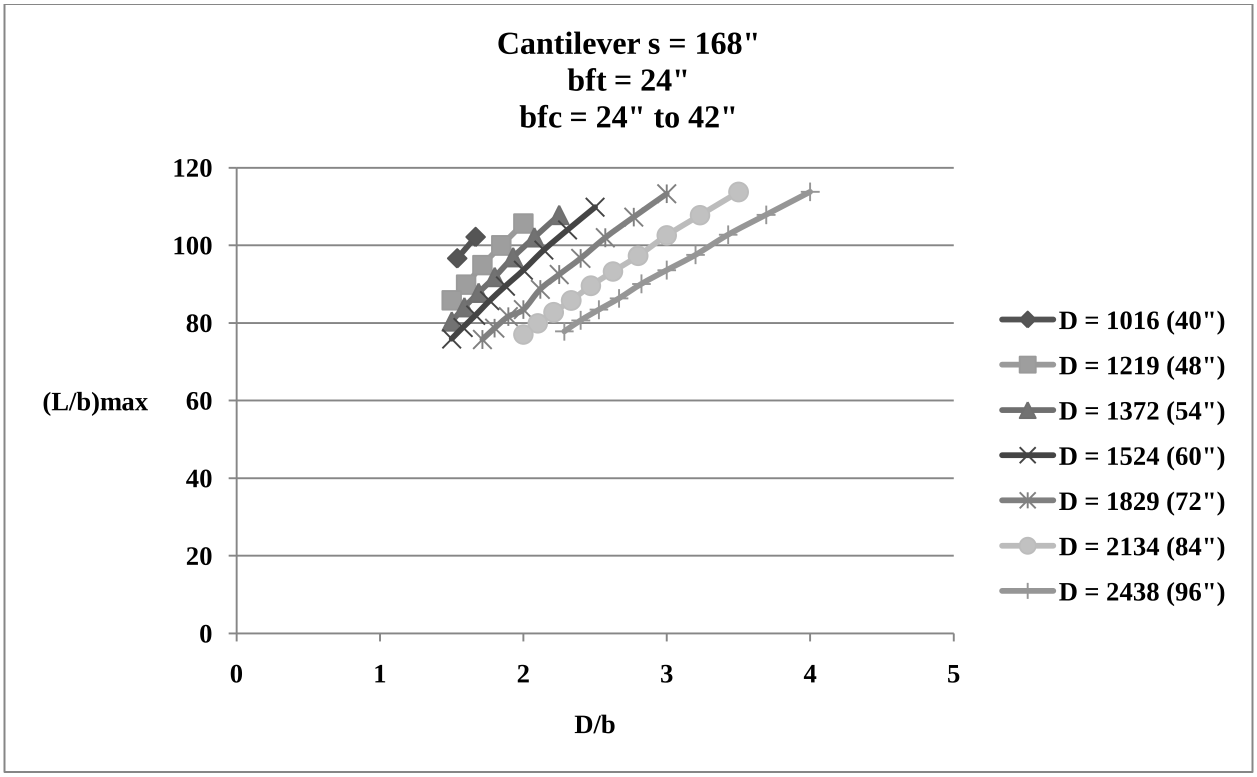

Cantilever s = 168"
bft = 24"
bfc = 24" to 42"
120
100
80
60
40
20
0
(L/b)max
0
1
2
3
4
5
D/b
D = 1016 (40")
D = 1219 (48")
D = 1372 (54")
D = 1524 (60")
D = 1829 (72")
D = 2134 (84")
D = 2438 (96")

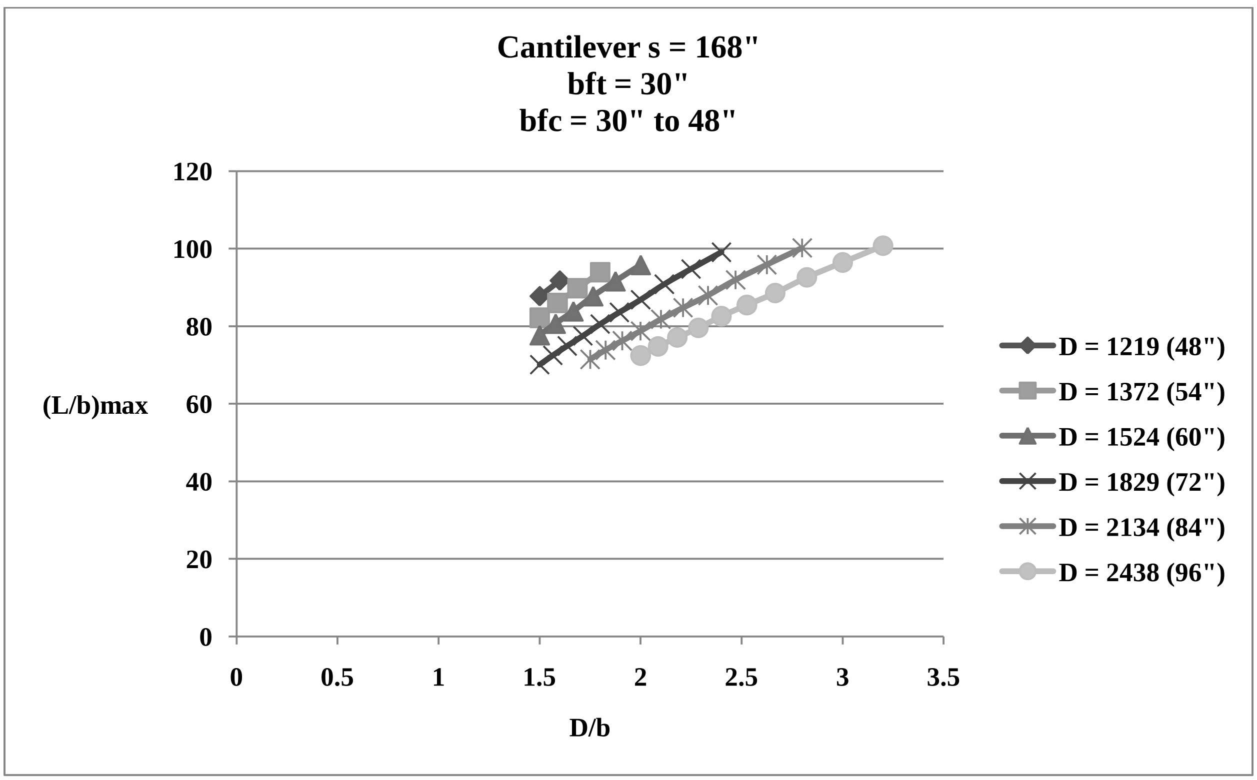

Cantilever s = 168"
bft = 30"
bfc = 30" to 48"
120
100
80
60
40
20
0
(L/b)max
0
0.5
1
1.5
2
2.5
3
3.5
D/b
D = 1219 (48")
D = 1372 (54")
D = 1524 (60")
D = 1829 (72")
D = 2134 (84")
D = 2438 (96")

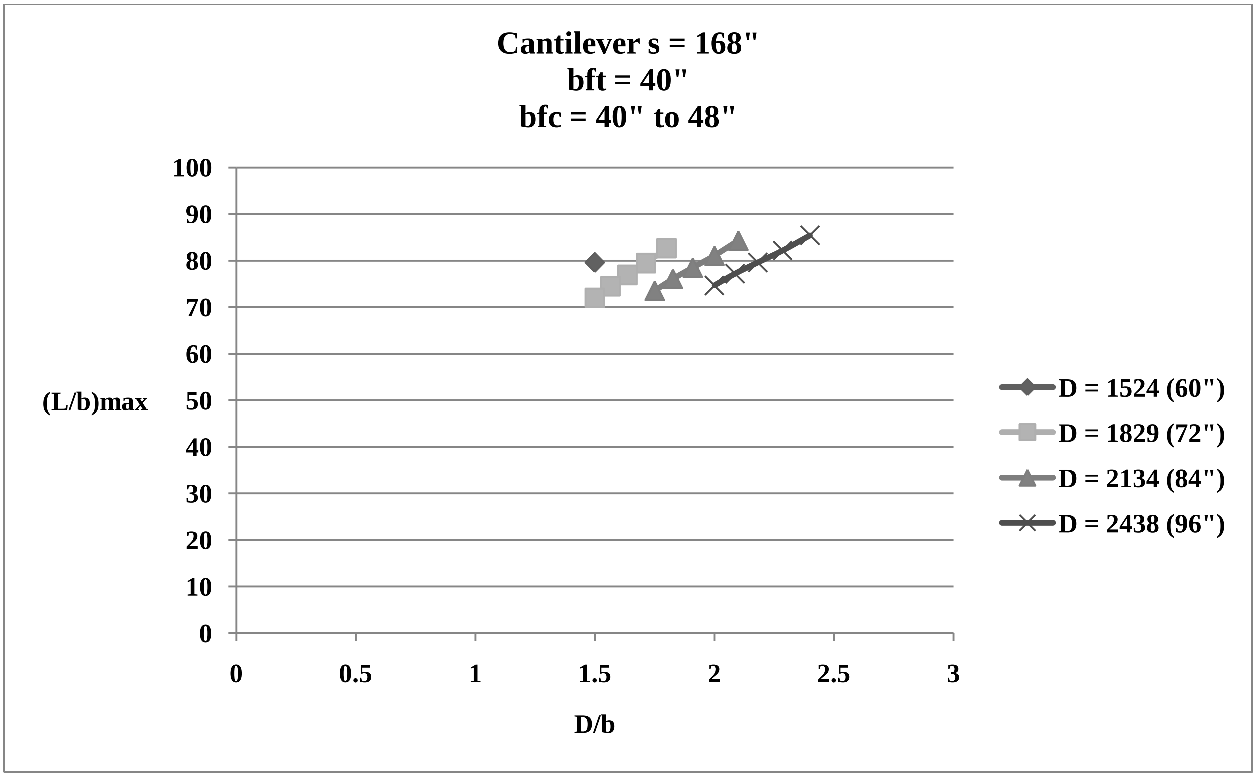
Cantilever s = 168"
bft = 40"
bfc = 40" to 48"
(L/b)max
D/b
D = 1524 (60")
D = 1829 (72")
D = 2134 (84")
D = 2438 (96")

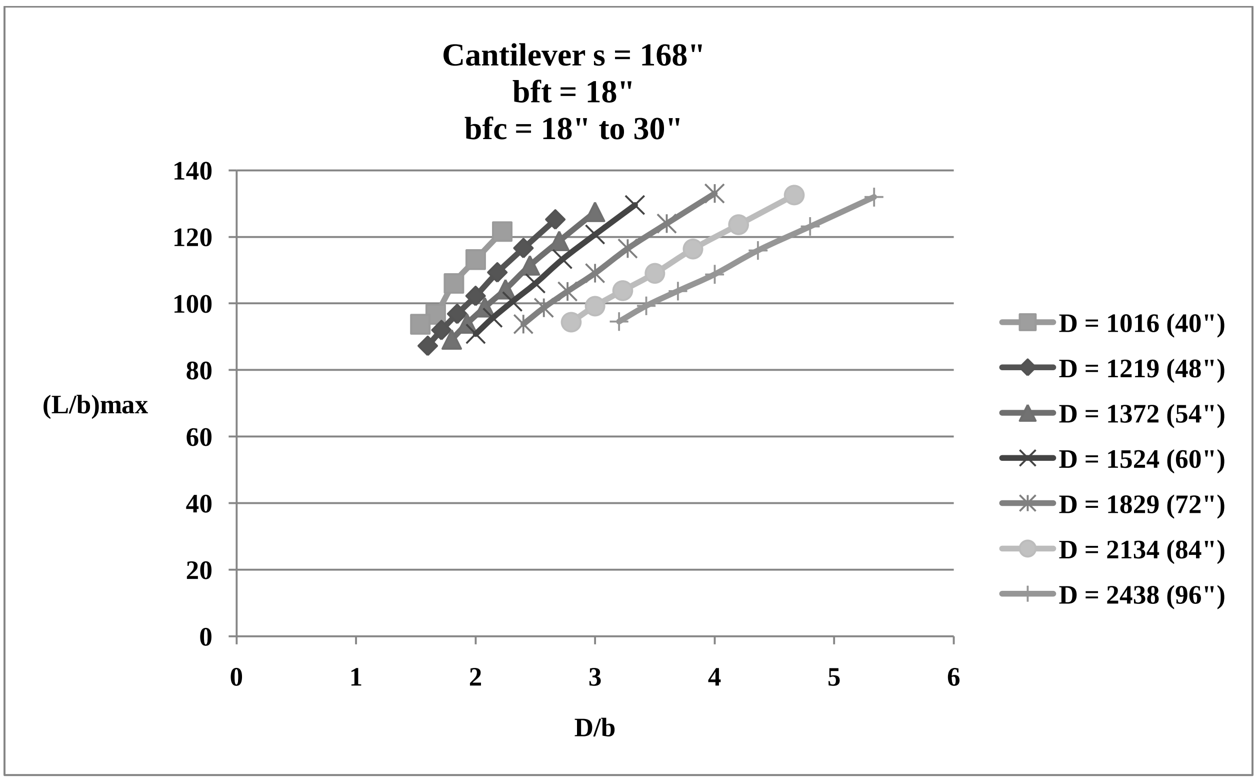
Cantilever s = 168"
bft = 18"
bfc = 18" to 30"
(L/b)max
D/b
D = 1016 (40")
D = 1219 (48")
D = 1372 (54")
D = 1524 (60")
D = 1829 (72")
D = 2134 (84")
D = 2438 (96")

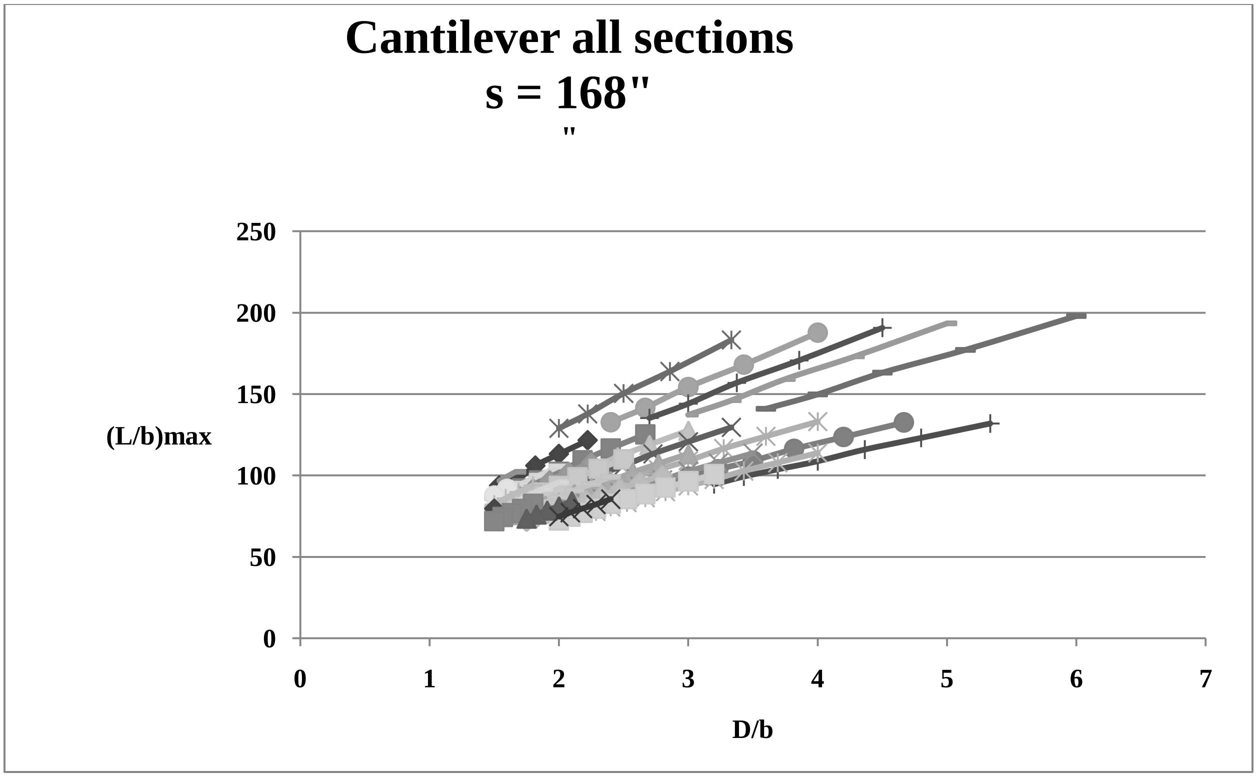

Cantilever all sections
s = 168"
"
(L/b)max
250
200
150
100
50
0
0
1
2
3
4
5
6
7
D/b

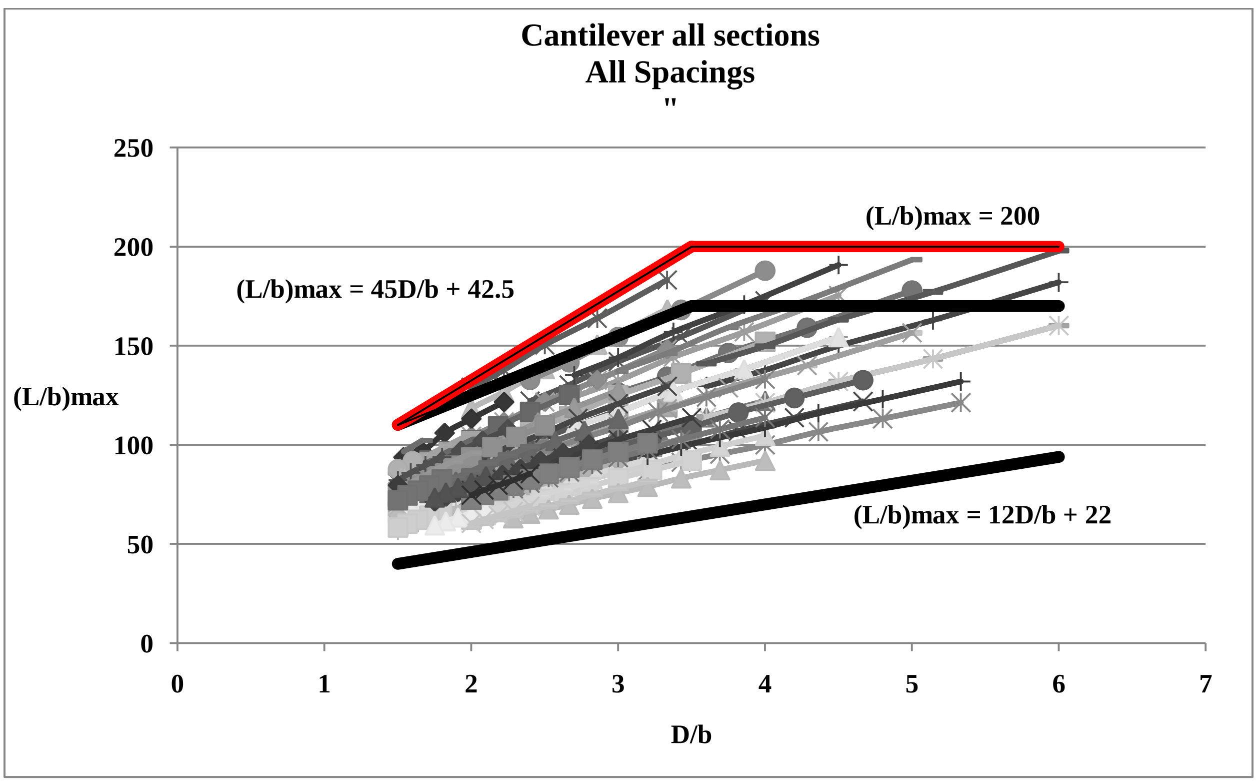

Cantilever all sections
All Spacings
"
(L/b)max
(L/b)max = 200
(L/b)max = 45D/b + 42.5
(L/b)max = 12D/b + 22
250
200
150
100
50
0
0
1
2
3
4
5
6
7
D/b

VITA

I was born November 18, 1985 in Chattanooga Tennessee. I grew up in Marion County and attended all schools in Jasper, TN. After graduating from Marion County High School, I attended Middle Tennessee State University for two years studying business and completing my general education courses. In 2006, I decided to move to Knoxville to pursue a degree in engineering at UTK. After the first semester, I decided that Civil Engineering would be my focus and received my B.S. in Spring of 2009. A M.S. Degree in Structural Engineering would be my next goal, accomplished Fall of 2010 at UTK. I am now ready to move on, but will miss all of my professors and friends and wish the best for them all.